“THIS INFORMATION IS DISTRIBUTED SOLELY FOR THE PURPOSE OF PRE-DISSEMINATION PEER REVIEW UNDER APPLICABLE INFORMATION QUALITY GUIDELINES. IT HAS NOT BEEN FORMALLY DISSEMINATED BY BSEE. IT DOES NOT REPRESENT AND SHOULD NOT BE CONSTRUED TO REPRESENT ANY BSEE DETERMINATION OR POLICY.”

COASTAL

FRONTIERS

Grounded Pile-Up Anchoring Landfast Ice off Icy Cape (June 15, 2020)

2020 BREAK-UP STUDY OF ARCTIC SEA ICE IN THE ALASKAN BEAUFORT AND CHUKCHI SEAS

Coastal Frontiers Corporation
882A Patriot Drive
Moorpark, CA 93021-3544
(818) 341-8133

Vaudrey & Associates, Inc.
1685 El Caserio Court
San Luis Obispo, CA 93401
(805) 544-9399

"THIS INFORMATION IS DISTRIBUTED SOLELY FOR THE PURPOSE OF PRE-DISSEMINATION PEER REVIEW UNDER APPLICABLE INFORMATION QUALITY GUIDELINES. IT HAS NOT BEEN FORMALLY DISSEMINATED BY BSEE. IT DOES NOT REPRESENT AND SHOULD NOT BE CONSTRUED TO REPRESENT ANY BSEE DETERMINATION OR POLICY."

CFC-1070

2020 BREAK-UP STUDY OF ARCTIC SEA ICE IN THE ALASKAN BEAUFORT AND CHUKCHI SEAS

FINAL REPORT

Prepared for:

U.S. Department of the Interior, Bureau of Safety and Environmental Enforcement
Washington, D.C.

Prepared by:

Coastal Frontiers Corporation
Moorpark, California

Vaudrey & Associates, Inc.
San Luis Obispo, California

February 2021

Funding was provided by the U.S. Department of the Interior, Bureau of Safety and Environmental Enforcement (BSEE), Office of Offshore Regulatory Programs, Washington, DC under Contract Number ***140E0119C0011.*** *The opinions, findings, conclusions, and recommendations expressed in this report are those of the authors and they do not necessarily represent the views or policies of BSEE.*

This report was prepared as an account of work sponsored by an agency of the United States Government. Neither the United States Government nor any agency thereof, not any of their employees, makes any warranty, express or implied, or assumes any legal liability or responsibility for the accuracy, completeness, or usefulness of any information, apparatus, product, or process disclosed, or represents that its use would not infringe privately owned rights. Reference herein to any specific commercial product, process, or service by trade name, trademark, manufacturer, or otherwise, does not necessarily constitute or imply its endorsement, recommendation, or favoring by the United States Government or any agency thereof.

"THIS INFORMATION IS DISTRIBUTED SOLELY FOR THE PURPOSE OF PRE-DISSEMINATION PEER REVIEW UNDER APPLICABLE INFORMATION QUALITY GUIDELINES. IT HAS NOT BEEN FORMALLY DISSEMINATED BY BSEE. IT DOES NOT REPRESENT AND SHOULD NOT BE CONSTRUED TO REPRESENT ANY BSEE DETERMINATION OR POLICY."

EXECUTIVE SUMMARY

This report describes an investigation of the ice conditions that prevailed in the Alaskan Beaufort and Chukchi Seas during the 2020 break-up season. The study was performed for the U.S. Department of the Interior, Bureau of Safety and Environmental Enforcement (BSEE), by Coastal Frontiers Corporation and Vaudrey & Associates, Inc.

The 2020 break-up study represents the second such study undertaken by BSEE in recent years, with the first conducted in 2017. It is designed to address five specific objectives:

1. Describe the ice conditions that evolve during break-up, including the deterioration of the landfast ice;
2. Locate and map features of potential importance for offshore exploration and production activities, including ice movement lines, substantial leads and polynyas, first-year ridges and rubble fields, and multi-year ice floes;
3. Locate, map, and characterize ice pile-ups and ride-ups on natural shorelines and man-made structures;
4. Correlate significant changes in the ice canopy with the corresponding meteorological conditions;
5. Compare the break-up processes observed in 2017 and 2020 with those that occurred in the past.

The study was conducted using a combination of publicly-available data, proprietary data, and aerial reconnaissance missions. The acquisition of open-source meteorological data, ice charts, drift buoy data, and satellite imagery began in May and continued through July. These data were supplemented with ten high-resolution, proprietary RADARSAT-2 images purchased from MDA Geospatial Services Inc., for the period from mid-May through mid-July.

Two sets of aerial reconnaissance missions were conducted to document the ice conditions near the end of the break-up season. The missions consisted of two fixed-wing flights in the Chukchi in mid-June followed by two such flights in the Beaufort in early July.

The principal study findings are summarized below:

"THIS INFORMATION IS DISTRIBUTED SOLELY FOR THE PURPOSE OF PRE-DISSEMINATION PEER REVIEW UNDER APPLICABLE INFORMATION QUALITY GUIDELINES. IT HAS NOT BEEN FORMALLY DISSEMINATED BY BSEE. IT DOES NOT REPRESENT AND SHOULD NOT BE CONSTRUED TO REPRESENT ANY BSEE DETERMINATION OR POLICY."

Methods

1. ***Reconnaissance Flights:*** Reconnaissance flights provide invaluable opportunities to confirm and refine the data derived from remote sensing, and to identify small-scale features and processes that otherwise would escape detection. Conducting the flights in the Chukchi several weeks before those in the Beaufort, with the timing dictated by the progress of break-up in each basin, represented a substantial improvement over 2017, when all of the break-up flights were undertaken in rapid succession.

Chukchi Sea

1. ***Air Temperatures:*** The daily average air temperatures at Utqiagvik Airport remained within or close to the normal range throughout May, June, and July. Over the entire three-month period, the daily average values exceeded the normal range on 13 days (14% frequency) and fell below on six days (7% frequency). Although six of the ten warmest break-up seasons occurred during the past decade, 2020 was relatively cold, ranking 35th out of the past 51 years in terms of the number of thawing-degree days.

2. ***Wind Regime:*** Easterlies outnumbered westerlies by substantial margins in each of the three months from May through July. Over the entire period, easterlies occurred 77% of the time versus 23% for westerlies. The monthly average speeds were nearly constant, with values of 11 kt (6 m/s) in May and July, and 10 kt (5 m/s) in June.

3. ***Storm Events:*** The 2020 break-up season was relatively storm-free, in that storm events with daily average wind speeds exceeding 15 kt (8 m/s) occurred on only four occasions encompassing 11 days. Three of the storms were easterlies, with an average duration of 2.7 days/event, while one was a westerly with a duration of three days.

4. ***Ice Thickness:*** Thawing-degree days began to accumulate on May 29th, when the daily average air temperature at Utqiagvik Airport reached 33°F (1°C). The computed thickness of undeformed first-year ice at the end of the winter season, 148 cm, decreased to zero during the 59 day period that began on that date and ended with the accumulation of 297 thawing degree days on July 26th.

5. ***Coastal Flaw Lead:*** A narrow flaw lead that existed off the Chukchi Sea coast at the end of April expanded throughout May, evolving into a large expanse of open water that was approximately 15 nm (37 km) wide off Point Barrow and 85 nm (158 km) wide off Point Lay at month-end. It continued to expand in June and July.

6. ***River Overflood:*** Of the seven rivers that discharge in or adjacent to the Chukchi Sea study area, the first began overflooding the sea ice on May 12th and the last on June 1st. Most of the flood water was contained in the receiving lagoons, with minimal penetration onto the landfast ice farther offshore.

"THIS INFORMATION IS DISTRIBUTED SOLELY FOR THE PURPOSE OF PRE-DISSEMINATION PEER REVIEW UNDER APPLICABLE INFORMATION QUALITY GUIDELINES. IT HAS NOT BEEN FORMALLY DISSEMINATED BY BSEE. IT DOES NOT REPRESENT AND SHOULD NOT BE CONSTRUED TO REPRESENT ANY BSEE DETERMINATION OR POLICY."

7. ***Lagoon Ice:*** Break-up in the semi-protected lagoon areas began with South Kasegaluk Lagoon on May 23rd, continued with North Kasegaluk Lagoon and the Kuk River Entrance on June 10th, and concluded with Peard Bay on June 14th. Open water followed in South Kasegaluk Lagoon on June 20th, North Kasegaluk Lagoon on June 27th or 28th, the Kuk River Entrance between June 25th and 30th, and Peard Bay on July 7th.

8. ***Landfast Ice:*** Break-up of the landfast ice occurred on May 13th when an easterly storm dislodged a large piece from the region between Wainwright and Icy Cape, and smaller pieces from the region between Icy Cape and Point Lay. Intermittent losses followed during the remainder of May and first half of June, including a massive piece measuring 74 km long and 19 km wide that broke free from the region between Point Franklin and Utqiagvik. The rate of loss increased in mid-June in response to moderate northeasterly winds and warm air temperatures. At the beginning of July, the landfast ice that remained consisted of intermittent patches spanning the entire length of the study area. The last remnant, grounded off the base of the Point Franklin Spit, disappeared on July 16th or 17th.

9. ***Pack Ice:*** The pack ice retreated to the northwest at a relatively rapid rate in May, causing the southern edge to lie approximately 15 nm (37 km) off Point Barrow and 85 nm (158 km) off Point Lay at month-end. Although the retreat continued in June, it proceeded at a slower pace that reflected occasional reversals. The ice continued to dissipate in July, vacating the Siberian coast during the third week of the month. At the end of July, the southern edge trended northwest from the vicinity of Utqiagvik with the exception of a 50-nm (93-km) wide tongue that extended southwest as far as the Devil's Paw Prospects.

10. ***Ice Pile-Ups and Ride-Ups:*** Of the 57 ice pile-ups observed on the Chukchi Sea coast in late February, 53 were evident at the time of the break-up flights in mid-June. In addition to these relict features, five new pile-ups that had formed during break-up were identified. Two were located on the barrier islands between Point Lay and Icy Cape, while three were located on the mainland shore near the base of the Point Franklin Spit. The heights of the new pile-ups ranged from 2 to 5 m above sea level, the encroachment distances from 3 to 5 m onto the subaerial beach, and the alongshore lengths from 600 to 2,800 m.

11. ***Multi-Year Ice:*** Multi-year ice was present in the Chukchi Sea study area throughout the break-up study period. At the beginning of May, relatively small floes were embedded in the landfast ice at concentrations ranging from negligible to 20%. The dispersal of these floes mirrored the break-up of the landfast ice, commencing in mid-

"THIS INFORMATION IS DISTRIBUTED SOLELY FOR THE PURPOSE OF PRE-DISSEMINATION PEER REVIEW UNDER APPLICABLE INFORMATION QUALITY GUIDELINES. IT HAS NOT BEEN FORMALLY DISSEMINATED BY BSEE. IT DOES NOT REPRESENT AND SHOULD NOT BE CONSTRUED TO REPRESENT ANY BSEE DETERMINATION OR POLICY."

May and continuing through mid-July. Multi-year ice also was present in the pack ice, at concentrations ranging from negligible to 30%. The maximum horizontal dimensions of these floes varied from less than 10 m to more than 10 km.

12. ***Ice Drift:*** Two drift buoys embedded in the pack ice attained monthly average speeds of 7.8 and 8.5 nm/day (14.5 and 15.8 km/day) in July. The highest daily average speed, 13.8 nm/day (25.6 km/day), occurred on July 8th.

Beaufort Sea

1. ***Air Temperatures:*** The daily average air temperatures at Deadhorse Airport tended to fall within the normal range throughout the three-month study period, rising above on ten occasions (11% frequency) and dropping below on four (4% frequency). When excursions outside the normal range did occur, they were of limited extent and duration.

2. ***Wind Regime:*** As in the case of the Chukchi, easterly winds predominated by a substantial margin in each of the three months from May through July. Over the entire period, they outnumbered westerlies by a margin of 79% to 21%. The average monthly speeds decreased from 13 kt (7 m/s) in May to 12 kt (6 m/s) in June and 9 kt (5 m/s) in July.

3. ***Storm Events:*** Only four storm events took place during the study period, all of which were easterlies. They produced 18 storm-days, resulting in an average duration of 4.5 days/event.

4. ***Ice Thickness:*** Thawing-degree days began to accumulate on May 23rd, when the daily average air temperature reached 33°F (1°C) at Deadhorse Airport. The computed thickness of undeformed first-year ice at the end of the winter season, 162 cm, decreased to zero during the 47-day period that began on that date and ended with the accumulation of 319 thawing-degree days on July 8th.

5. ***River Overflood:*** The Canning and Sagavanirktok began overflooding the sea ice on May 19th, the Colville on May 22nd, the Kuparuk on May 27th, and the Ikpikpuk on May 29th. Most of the flood water remained in the receiving bays and lagoons. The sole exceptions consisted of the discharge of the Canning River onto the sea ice east of Brownlow Point, and small tongues of water from the Kuparuk that pushed past the barrier islands off Gwydyr Bay.

6. ***Lagoon Ice:*** Break-up of the lagoon ice began on or about June 4th when flood water from the Sagavanirktok River melted through the ice in Prudhoe Bay. Through-ice melting followed in Stefansson Sound, South Harrison Bay, South Camden Bay, Gwydyr Bay, and Smith Bay between June 8th and 11th. In Simpson Lagoon, break-up took place on or about June 26th in response to the heat emanating from the mainland coast. Open

"THIS INFORMATION IS DISTRIBUTED SOLELY FOR THE PURPOSE OF PRE-DISSEMINATION PEER REVIEW UNDER APPLICABLE INFORMATION QUALITY GUIDELINES. IT HAS NOT BEEN FORMALLY DISSEMINATED BY BSEE. IT DOES NOT REPRESENT AND SHOULD NOT BE CONSTRUED TO REPRESENT ANY BSEE DETERMINATION OR POLICY."

water in the lagoon areas occurred over a period of several weeks that began with Gwydyr Bay between June 20th and 26th and ended with Stefansson Sound on July 10th. All of the lagoon sites were ice-free by the end of July.

7. ***Landfast Ice:*** Break-up of the landfast ice between Point Barrow and Cross Island occurred on May 23rd when a small loss occurred off Cape Halkett at the end of a six-day easterly storm. Farther east, between Cross Island and Barter Island, break-up began with modest losses off Stefansson Sound and Camden Bay on May 27th. In early June, the landfast ice edge tended to lie between the 18- and 11-m isobaths from Point Barrow to Flaxman Island, and to protrude seaward of the 18-m isobath in Camden Bay. In the absence of westerly storms, losses were minimal until the last week of the month. At that time, warm air temperatures, increased wind speeds, and warm sea surface temperatures resulting both from river overflood and from the arrival of warm-water plumes from the Alaska Coastal Current to the west and Mackenzie River to the east, caused substantial losses off Smith Bay and in Harrison and Camden Bays. The accelerated rate of deterioration continued during the first half of July. By mid-month, landfast ice was confined to a patch in Elson Lagoon, narrow strips on both sides of Smith Bay, small patches on the west side of Harrison Bay, and a narrow, discontinuous strip fronting the barrier islands from Cross to Flaxman. At the end of the month, small patches persisted between Pole and Flaxman Islands.

8. ***Pack Ice:*** The pack ice remained compact during the first three weeks of May. At month-end, however, warm water from the Alaska Coastal Current produced patches of open water adjacent to the landfast ice as far east as Harrison Bay. In analogous fashion, warm water from the Mackenzie River created a patch of open water adjacent to the landfast ice in Camden Bay. In June, unrelenting easterly winds propelled the Mackenzie plume to the west while impeding the easterly progress of the plume from the Alaska Coastal Current. During the final week, the pack ice concentrations in the nearshore region declined markedly in response to the westward progression of the Mackenzie plume to Harrison Bay and the eastern progression of the Alaska Coastal Current plume to Smith Bay. At the end of the month, the only two areas in which dense tongues of pack ice extended as far south as the landfast ice were located off western Harrison Bay and off Admiralty Bay. The deterioration continued in July, with the dense tongues dispersing by mid-month.

9. ***Ice Pile-Ups and Ride-Ups:*** Of the 32 ice pile-ups observed in the central portion of the Alaskan Beaufort Sea in late February, 16 were evident at the time of the break-up flights in early July. In all cases, the dimensions of the relict pile-ups had been diminished by melting. No new pile-ups or ride-ups were discovered in July.

"THIS INFORMATION IS DISTRIBUTED SOLELY FOR THE PURPOSE OF PRE-DISSEMINATION PEER REVIEW UNDER APPLICABLE INFORMATION QUALITY GUIDELINES. IT HAS NOT BEEN FORMALLY DISSEMINATED BY BSEE. IT DOES NOT REPRESENT AND SHOULD NOT BE CONSTRUED TO REPRESENT ANY BSEE DETERMINATION OR POLICY."

10. ***Multi-Year Ice:*** Multi-year ice was present in the Beaufort Sea study area throughout the break-up study period. At the beginning of May, the concentration tended to be less than 10% in the landfast ice and to range from less than 10% to 50% in the pack ice. The only region lacking multi-year ice was a tongue of first-year ice that extended from the U.S.-Canadian border to the eastern edge of Harrison Bay just offshore of the landfast ice. The multi-year ice embedded in the landfast ice remained in place until late May, when losses began to occur in conjunction with the disintegration of the latter. The dispersal of the embedded multi-year ice paralleled that of the landfast ice, which continued through the end of the study period. With the exception of the nearshore tongue of first-year ice, which closed during the first week in June, multi-year ice remained omnipresent in the pack ice through the end of July. The concentrations ranged from less than 10% to a maximum of 70%. The floe sizes varied over a wide range, from brash ice to maximum horizontal dimensions exceeding 25 km.

11. ***Ice Drift:*** Drift buoys embedded in the pack ice attained monthly average speeds that averaged 5.4 nm/day (10.0 km/day) in May, 4.3 nm/day (8.0 km/day) in June, and 2.9 nm/day (5.4 km/day) in July. The highest daily average speed, 15.4 nm/day (28.5 km/day), occurred on both May 12th and July 28th.

Trends

1. ***Air Temperatures:*** Since the 1970s, progressively warmer break-up seasons have caused the number of accumulated thawing-degree days at Utqiagvik to increase at an average rate of 4.2 per year. The rate of warming has varied widely, however, on time scales ranging from interannual to interdecadal.

2. ***Storms:*** Since the early 1980s, the frequency of storm events during break-up has nearly doubled, from 3.2 to 5.8 storms per year.

3. ***River Overflood:*** The limited data available suggest that the initiation of river overflood onto the sea ice in the Chukchi and Beaufort Seas has been trending earlier at rates ranging from negligible to less than one day per year.

4. ***Timing of Break-Up in the Chukchi Sea:*** The occurrence of break-up appears to be trending earlier, but the rate of change cannot be quantified due to the variability inherent in the timing coupled with a paucity of both historical and recent data.

5. ***Timing of Break-Up in the Beaufort Sea:*** The data acquired in 2017 and 2020, when compared with those from 1953 through 1975, suggest that both break-up and open water are trending earlier, with the occurrence of open water advancing more rapidly than that of break-up. As a result, the duration of the break-up season appears to be decreasing. The rates of change in the timing of break-up and open water appear to be highest for

"THIS INFORMATION IS DISTRIBUTED SOLELY FOR THE PURPOSE OF PRE-DISSEMINATION PEER REVIEW UNDER APPLICABLE INFORMATION QUALITY GUIDELINES. IT HAS NOT BEEN FORMALLY DISSEMINATED BY BSEE. IT DOES NOT REPRESENT AND SHOULD NOT BE CONSTRUED TO REPRESENT ANY BSEE DETERMINATION OR POLICY."

pack ice, intermediate for landfast ice, and insignificant for lagoon ice. It is cautioned, however, that additional data will be required to substantiate and refine these preliminary findings.

6. ***Length of Open-Water Season:*** Trends toward an earlier occurrence of break-up and a later occurrence of freeze-up are causing the length of the open-water season to increase at rapid rates in both the Chukchi and Beaufort Seas.

7. ***Multi-Year Ice:*** The probability of multi-year ice residing in the Chukchi Sea and nearshore portion of the Beaufort Sea during break-up appears to have decreased since the 1980s. Nevertheless, the possibility of encountering such ice cannot be dismissed.

"THIS INFORMATION IS DISTRIBUTED SOLELY FOR THE PURPOSE OF PRE-DISSEMINATION PEER REVIEW UNDER APPLICABLE INFORMATION QUALITY GUIDELINES. IT HAS NOT BEEN FORMALLY DISSEMINATED BY BSEE. IT DOES NOT REPRESENT AND SHOULD NOT BE CONSTRUED TO REPRESENT ANY BSEE DETERMINATION OR POLICY."

TABLE OF CONTENTS

(continued)

"THIS INFORMATION IS DISTRIBUTED SOLELY FOR THE PURPOSE OF PRE-DISSEMINATION PEER REVIEW UNDER APPLICABLE INFORMATION QUALITY GUIDELINES. IT HAS NOT BEEN FORMALLY DISSEMINATED BY BSEE. IT DOES NOT REPRESENT AND SHOULD NOT BE CONSTRUED TO REPRESENT ANY BSEE DETERMINATION OR POLICY."

TABLE OF CONTENTS
(continued)

"THIS INFORMATION IS DISTRIBUTED SOLELY FOR THE PURPOSE OF PRE-DISSEMINATION PEER REVIEW UNDER APPLICABLE INFORMATION QUALITY GUIDELINES. IT HAS NOT BEEN FORMALLY DISSEMINATED BY BSEE. IT DOES NOT REPRESENT AND SHOULD NOT BE CONSTRUED TO REPRESENT ANY BSEE DETERMINATION OR POLICY."

LIST OF TABLES

(continued)

"THIS INFORMATION IS DISTRIBUTED SOLELY FOR THE PURPOSE OF PRE-DISSEMINATION PEER REVIEW UNDER APPLICABLE INFORMATION QUALITY GUIDELINES. IT HAS NOT BEEN FORMALLY DISSEMINATED BY BSEE. IT DOES NOT REPRESENT AND SHOULD NOT BE CONSTRUED TO REPRESENT ANY BSEE DETERMINATION OR POLICY."

LIST OF TABLES
(continued)

"THIS INFORMATION IS DISTRIBUTED SOLELY FOR THE PURPOSE OF PRE-DISSEMINATION PEER REVIEW UNDER APPLICABLE INFORMATION QUALITY GUIDELINES. IT HAS NOT BEEN FORMALLY DISSEMINATED BY BSEE. IT DOES NOT REPRESENT AND SHOULD NOT BE CONSTRUED TO REPRESENT ANY BSEE DETERMINATION OR POLICY."

LIST OF FIGURES

(continued)

"THIS INFORMATION IS DISTRIBUTED SOLELY FOR THE PURPOSE OF PRE-DISSEMINATION PEER REVIEW UNDER APPLICABLE INFORMATION QUALITY GUIDELINES. IT HAS NOT BEEN FORMALLY DISSEMINATED BY BSEE. IT DOES NOT REPRESENT AND SHOULD NOT BE CONSTRUED TO REPRESENT ANY BSEE DETERMINATION OR POLICY."

LIST OF FIGURES
(continued)

Title — Page No.

(continued)

"THIS INFORMATION IS DISTRIBUTED SOLELY FOR THE PURPOSE OF PRE-DISSEMINATION PEER REVIEW UNDER APPLICABLE INFORMATION QUALITY GUIDELINES. IT HAS NOT BEEN FORMALLY DISSEMINATED BY BSEE. IT DOES NOT REPRESENT AND SHOULD NOT BE CONSTRUED TO REPRESENT ANY BSEE DETERMINATION OR POLICY."

LIST OF FIGURES
(continued)

Title — Page No.

(continued)

"THIS INFORMATION IS DISTRIBUTED SOLELY FOR THE PURPOSE OF PRE-DISSEMINATION PEER REVIEW UNDER APPLICABLE INFORMATION QUALITY GUIDELINES. IT HAS NOT BEEN FORMALLY DISSEMINATED BY BSEE. IT DOES NOT REPRESENT AND SHOULD NOT BE CONSTRUED TO REPRESENT ANY BSEE DETERMINATION OR POLICY."

LIST OF FIGURES
(continued)

Title — Page No.

"THIS INFORMATION IS DISTRIBUTED SOLELY FOR THE PURPOSE OF PRE-DISSEMINATION PEER REVIEW UNDER APPLICABLE INFORMATION QUALITY GUIDELINES. IT HAS NOT BEEN FORMALLY DISSEMINATED BY BSEE. IT DOES NOT REPRESENT AND SHOULD NOT BE CONSTRUED TO REPRESENT ANY BSEE DETERMINATION OR POLICY."

LIST OF PLATES

(continued)

"THIS INFORMATION IS DISTRIBUTED SOLELY FOR THE PURPOSE OF PRE-DISSEMINATION PEER REVIEW UNDER APPLICABLE INFORMATION QUALITY GUIDELINES. IT HAS NOT BEEN FORMALLY DISSEMINATED BY BSEE. IT DOES NOT REPRESENT AND SHOULD NOT BE CONSTRUED TO REPRESENT ANY BSEE DETERMINATION OR POLICY."

LIST OF PLATES
(continued)

"THIS INFORMATION IS DISTRIBUTED SOLELY FOR THE PURPOSE OF PRE-DISSEMINATION PEER REVIEW UNDER APPLICABLE INFORMATION QUALITY GUIDELINES. IT HAS NOT BEEN FORMALLY DISSEMINATED BY BSEE. IT DOES NOT REPRESENT AND SHOULD NOT BE CONSTRUED TO REPRESENT ANY BSEE DETERMINATION OR POLICY."

2020 BREAK-UP STUDY OF ARCTIC SEA ICE IN THE ALASKAN BEAUFORT AND CHUKCHI SEAS

1. INTRODUCTION

This report describes an investigation of the ice conditions that prevailed in the Alaskan Beaufort and Chukchi Seas during the 2020 break-up season. The study was performed on behalf of the U.S. Department of the Interior, Bureau of Safety and Environmental Enforcement (BSEE), by Coastal Frontiers Corporation and Vaudrey & Associates, Inc.

As shown in Figure 1-1, the study area includes the southern portion of the Beaufort Sea from Barter Island on the east to Point Barrow on the west, and the northeastern portion of the Chukchi Sea bounded by the shoreline between Point Barrow and Point Lay, the 74°N parallel, and the 168°W meridian. The boundaries in the Beaufort Sea were selected to encompass all existing oil and gas developments, while those in the Chukchi were selected to encompass Hanna Shoal and lease tracts of recent interest, including the Burger and Crackerjack prospects.

Despite their proximity, the ice regimes in the Beaufort and Chukchi Seas differ markedly due to factors that include geography, meteorology, and oceanography. Whereas the Beaufort Sea coast trends east-southeast to west-northwest, the Chukchi coast is oriented northeast-southwest (Figure 1-1). As a result, the easterly winds that occur frequently in both basins tend to push the ice along the Beaufort Sea coast but away from the Chukchi coast. In the Beaufort, the alongshore winds coupled with flat nearshore slopes produce an extensive zone of grounded, landfast ice bordered by a compact, well-consolidated ice canopy farther offshore. In the Chukchi, the growth of landfast ice is limited not only by the prevalence of offshore winds but also by the relatively steep slopes that exist off the coast. As a result, the landfast ice zone typically consists of a narrow strip of grounded ice that clings to the shoreline. A flaw lead frequently opens offshore of the landfast ice, and the ice canopy tends to be less consolidated and more mobile than in the Beaufort.

The pronounced difference in ice regimes that exists during the freeze-up and winter seasons also prevails during break-up and summer. Whereas the Beaufort Gyre transports pack ice from east to west in the Beaufort Sea, the Alaska Coastal Current carries warm water north from the Bering Sea and contributes to the retreat of the pack ice in the Chukchi (Figure 1-1).

"THIS INFORMATION IS DISTRIBUTED SOLELY FOR THE PURPOSE OF PRE-DISSEMINATION PEER REVIEW UNDER APPLICABLE INFORMATION QUALITY GUIDELINES. IT HAS NOT BEEN FORMALLY DISSEMINATED BY BSEE. IT DOES NOT REPRESENT AND SHOULD NOT BE CONSTRUED TO REPRESENT ANY BSEE DETERMINATION OR POLICY."

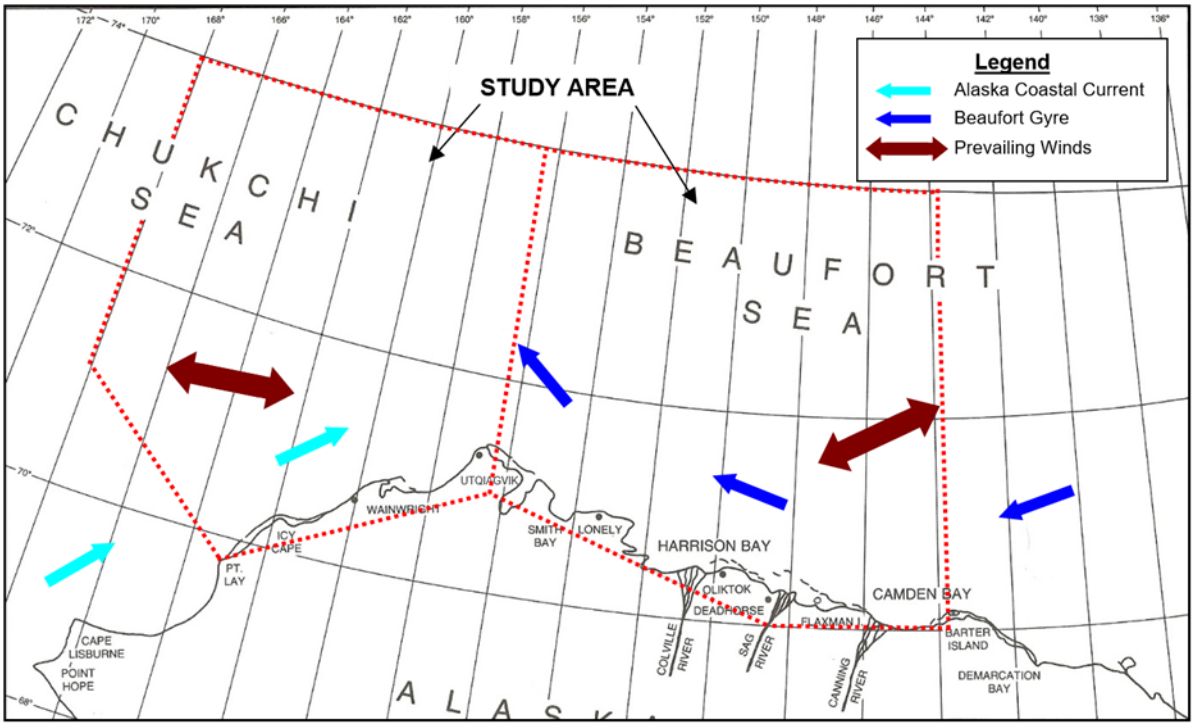

Figure 1-1. Study Area

During break-up, the deteriorating landfast ice in the study area fractures into progressively smaller floes. Farther offshore, the pack ice also begins to deteriorate, but at a slower rate. The ice canopy in this region typically contains numerous first-year ridges and rubble fields that were created by ice movement during the freeze-up and winter seasons, as well as multi-year floes that have survived at least one melt season. The relatively thick, strong multi-year floes become more mobile as the surrounding first-year ice degrades and can move long distances at high speeds in the absence of substantial confinement. Potential concerns for oil and gas facilities include impact loads on fixed structures such as man-made islands and platforms, displacement of floating structures such as drillships, and ice gouging of the sea bottom on the routes of subsea pipelines.

In addition to large ice movements, the storms that occur during break-up can cause significant deformation of the first-year ice, leading to the formation of ridges and rubble fields. Such storms also can cause substantial ride-up and pile-up events if the moving ice encounters natural shorelines, shoals, or man-made islands.

The foregoing phenomena, along with the end of the season for on-ice transportation and construction and the beginning of the season for open-water vessel navigation, suggest that an understanding of break-up is essential for the safe design and efficient operation of offshore oil and gas facilities.

"THIS INFORMATION IS DISTRIBUTED SOLELY FOR THE PURPOSE OF PRE-DISSEMINATION PEER REVIEW UNDER APPLICABLE INFORMATION QUALITY GUIDELINES. IT HAS NOT BEEN FORMALLY DISSEMINATED BY BSEE. IT DOES NOT REPRESENT AND SHOULD NOT BE CONSTRUED TO REPRESENT ANY BSEE DETERMINATION OR POLICY."

To this end, five break-up studies were conducted as joint-industry projects from 1981 through 1985 (Vaudrey, 1982; 1983; 1984a; 1984b; 1985a; 1985b; 1986). Each was largely observational in nature and included a series of aerial surveys typically undertaken between early June and late July. The primary objectives of these annual studies were as follows: (1) document the locations and characteristics of strudel drainage features in the ice sheet; (2) document the locations and characteristics of ice ride-ups and pile-ups; (3) identify specific storms that produced the ride-ups and pile-ups; and (4) document nearshore ice conditions, including the locations and characteristics of multi-year floes.

Since 1986, break-up processes in the Alaskan Beaufort and Chukchi Seas have been investigated primarily through the analysis of satellite imagery (Vaudrey, 1988; 1989; 1990; 1991; 1992; Eicken, *et al*., 2006; Mahoney, *et al*., 2007; Mahoney, *et al*., 2012; Bureau of Ocean Energy Management, 2020). The resulting information, although useful in its own right, lacks some of the detail provided by the earlier observational studies. Specifically, items such as the characteristics of multi-year ice floes and the locations and dimensions of ice pile-ups cannot be extracted from the remotely-sensed data. To address this shortcoming, a break-up study that combined remote sensing with on-site observations was undertaken in 2017 (Coastal Frontiers and Vaudrey, 2018).

An investigation similar to that in 2017 was conducted in 2020 to expand the database on the nature and interannual variability of present-day break-up processes. The scope of work was designed to address five specific objectives:

1. Describe the ice conditions that evolve during break-up, including the deterioration of the landfast ice;
2. Locate and map features of potential importance for offshore exploration and production activities, including ice movement lines, substantial leads and polynyas, first-year ridges and rubble fields, and multi-year ice floes;
3. Locate, map, and characterize ice pile-ups and ride-ups on natural shorelines and man-made structures;
4. Correlate significant changes in the ice canopy with the corresponding meteorological conditions;
5. Compare the break-up processes observed in 2017 and 2020 with those that occurred in the past.

It should be noted that strudel drainage, which typically occurs in late May and early June when river discharge floods the sea ice (Leidersdorf, *et al*., 2007), received only secondary consideration in this study. Although it exerts a significant influence on break-up

"THIS INFORMATION IS DISTRIBUTED SOLELY FOR THE PURPOSE OF PRE-DISSEMINATION PEER REVIEW UNDER APPLICABLE INFORMATION QUALITY GUIDELINES. IT HAS NOT BEEN FORMALLY DISSEMINATED BY BSEE. IT DOES NOT REPRESENT AND SHOULD NOT BE CONSTRUED TO REPRESENT ANY BSEE DETERMINATION OR POLICY."

in the Alaskan Beaufort Sea by weakening the sea ice off river deltas, this uniquely-Arctic phenomenon was investigated in detail in a project undertaken for the Minerals Management Service by Hearon, *et al*. (2009). As a result, strudel drainage was excluded from primary consideration in the current study in the interest of economy.

The acquisition of publicly-available meteorological data, ice charts, drift buoy data, and satellite imagery began in May 2020 and continued through July 2020. These data were supplemented with ten high-resolution, proprietary RADARSAT-2 images acquired from mid-May through mid-July.

Two sets of aerial reconnaissance missions were conducted to document the ice conditions near the end of the break-up season. The missions consisted of two fixed-wing flights in the Chukchi in mid-June, followed by two such flights in the Beaufort in early July.

The remainder of this report presents a detailed account of the 2020 Break-Up Study. The conventions and definitions adopted for the study are discussed in Section 2. To provide historical context, the findings of the five studies conducted from 1981 through 1985 as well as the study conducted in 2017 are summarized in Section 3. Data acquisition and analysis in 2020 are discussed in Section 4, which covers the aerial reconnaissance missions as well as the data obtained from all other sources. Section 5 describes the ice conditions that prevailed at the end of the 2019-20 winter season. Section 6 chronicles the progression of break-up that occurred in the Alaskan Chukchi Sea in 2020, while Section 7 provides analogous information for the Alaskan Beaufort. In Section 8, the break-up processes observed in 2017 and 2020 are compared with those in the past, including those observed in the 1980s. Conclusions are presented in Section 9, followed by references in Section 10.

Figures, tables, and plates are interspersed with the text, while three large-format drawings that display the observations made during the reconnaissance flights are provided in Appendix A. Image acquisition reports pertaining to the RADARSAT-2 images are provided in Appendix B, while post-observation reports describing the reconnaissance flights are provided in Appendix C. A technical summary of the study appears in Appendix D. The digital data files that were used to conduct the study are compiled on a DVD that constitutes Appendix E.

Throughout this report, the locations of ice features are referenced to geographic features that include bays, rivers, lagoons, points of land, natural and man-made islands, and coastal villages. For ease of reference, these geographic features are shown in Figures 1-2 (Central Beaufort Sea), 1-3 (Western Beaufort Sea), and 1-4 (Chukchi Sea).

"THIS INFORMATION IS DISTRIBUTED SOLELY FOR THE PURPOSE OF PRE-DISSEMINATION PEER REVIEW UNDER APPLICABLE INFORMATION QUALITY GUIDELINES. IT HAS NOT BEEN FORMALLY DISSEMINATED BY BSEE. IT DOES NOT REPRESENT AND SHOULD NOT BE CONSTRUED TO REPRESENT ANY BSEE DETERMINATION OR POLICY."

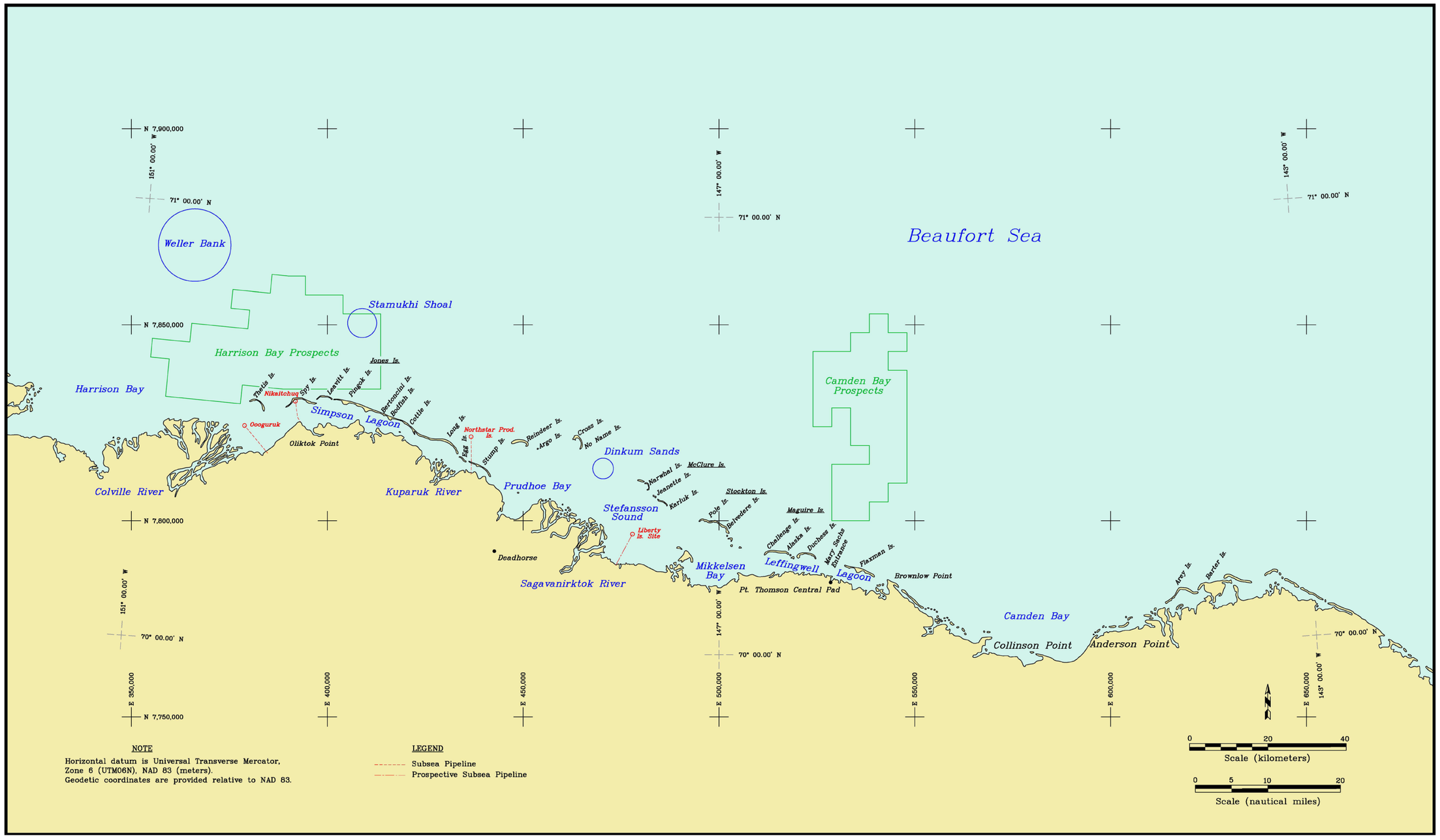

Figure 1-2. Geographic Points of Interest in Central Beaufort Sea

"THIS INFORMATION IS DISTRIBUTED SOLELY FOR THE PURPOSE OF PRE-DISSEMINATION PEER REVIEW UNDER APPLICABLE INFORMATION QUALITY GUIDELINES. IT HAS NOT BEEN FORMALLY DISSEMINATED BY BSEE. IT DOES NOT REPRESENT AND SHOULD NOT BE CONSTRUED TO REPRESENT ANY BSEE DETERMINATION OR POLICY."

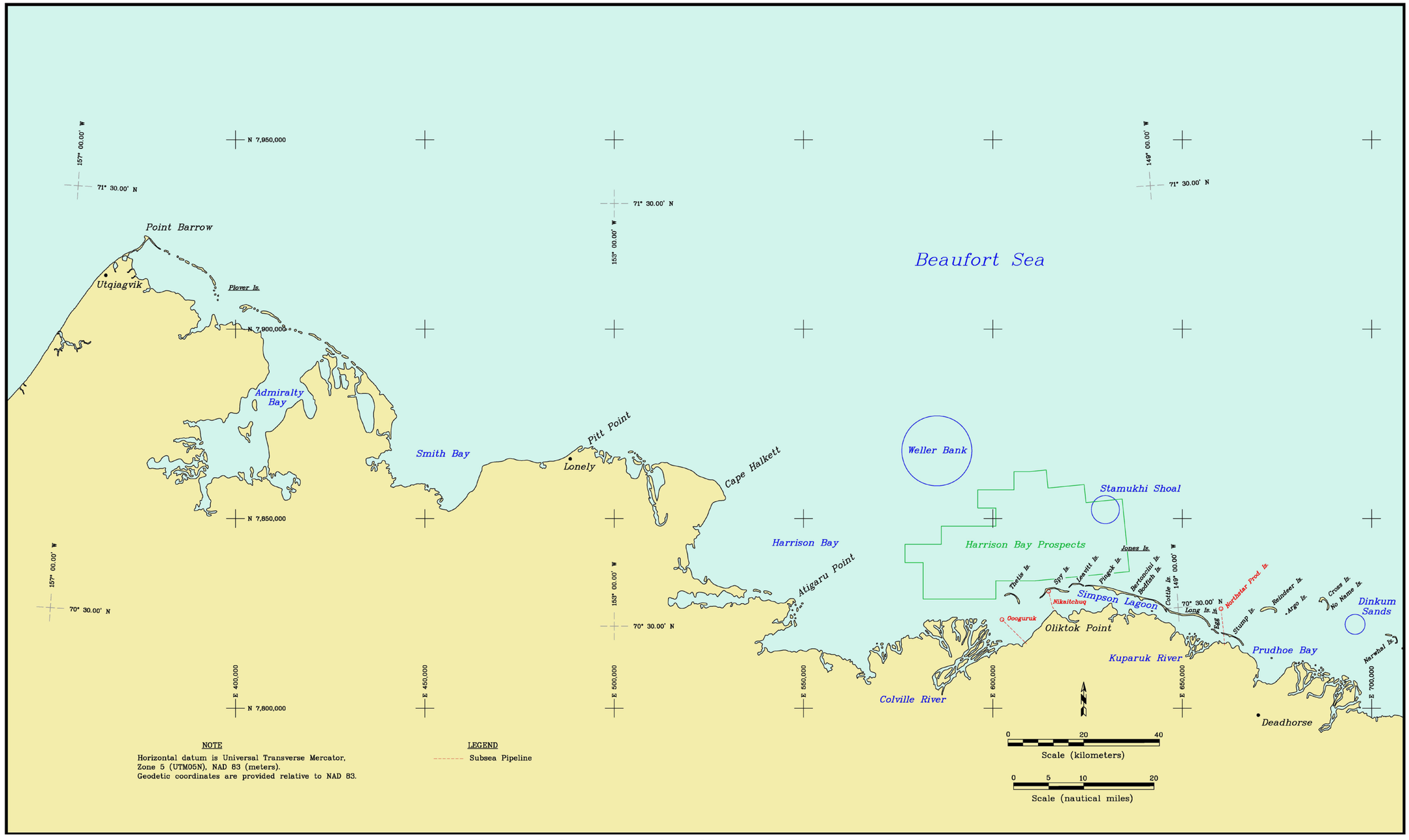

Figure 1-3. Geographic Points of Interest in Western Beaufort Sea

“THIS INFORMATION IS DISTRIBUTED SOLELY FOR THE PURPOSE OF PRE-DISSEMINATION PEER REVIEW UNDER APPLICABLE INFORMATION QUALITY GUIDELINES. IT HAS NOT BEEN FORMALLY DISSEMINATED BY BSEE. IT DOES NOT REPRESENT AND SHOULD NOT BE CONSTRUED TO REPRESENT ANY BSEE DETERMINATION OR POLICY.”

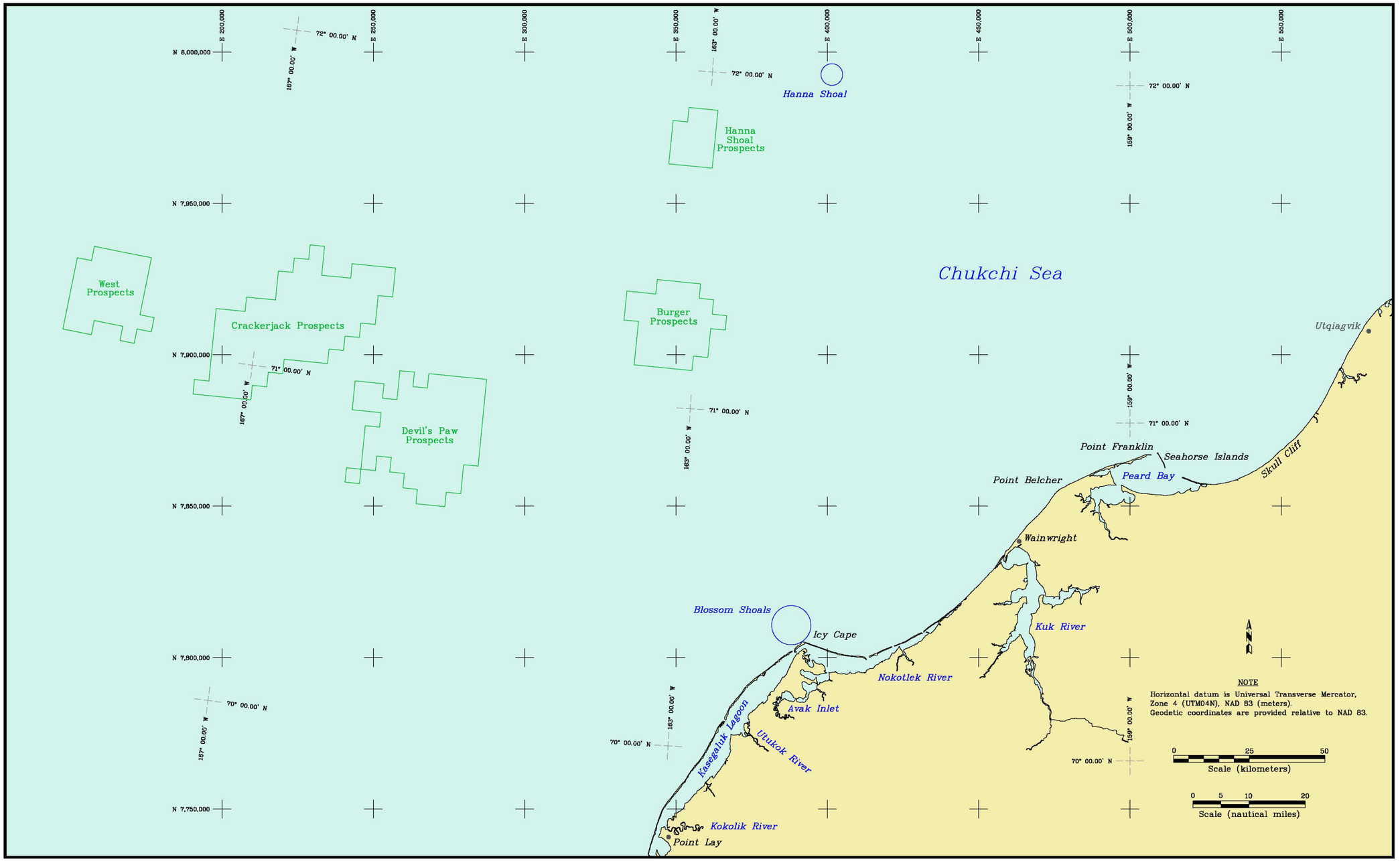

Figure 1-4. Geographic Points of Interest in Chukchi Sea

"THIS INFORMATION IS DISTRIBUTED SOLELY FOR THE PURPOSE OF PRE-DISSEMINATION PEER REVIEW UNDER APPLICABLE INFORMATION QUALITY GUIDELINES. IT HAS NOT BEEN FORMALLY DISSEMINATED BY BSEE. IT DOES NOT REPRESENT AND SHOULD NOT BE CONSTRUED TO REPRESENT ANY BSEE DETERMINATION OR POLICY."

2. CONVENTIONS, DEFINITIONS, AND ACCESSIBILITY

The conventions and definitions adopted for this study are presented in Sections 2.1 and 2.2, respectively. Comments related to accessibility follow in Section 2.3.

2.1 Conventions

- **Horizontal Datum:** The horizontal datum for all geographic coordinates is the North American Datum of 1983 (NAD 83). Many of the graphical products also include a grid referenced to the Universal Transverse Mercator (UTM) Datum, NAD 83, with units of meters. UTM Zone 6N is used in the central Beaufort Sea, UTM Zone 5N in the western Beaufort Sea, and UTM Zone 4N in the Chukchi Sea.
- **Vertical Datum:** The vertical datum is Mean Sea Level (MSL). MSL lies only 11 cm above Mean Lower Low Water (MLLW) at Prudhoe Bay, 9 cm at Utqiagvik, and 10 cm at Point Hope (National Ocean Service, 2020). For purposes of this report, the difference between MSL and MLLW (which represents the vertical datum for all National Ocean Service nautical charts of the region) is assumed to be negligible.
- **Units:** The International System of Units (SI) is used throughout this report, with three exceptions: (1) distances are provided in nautical miles (nm) to maintain consistency with the use of geographic coordinates; (2) wind speeds are provided in knots (kt), again to maintain consistency with the use of geographic coordinates; and (3) temperatures are provided in degrees Fahrenheit (°F), and both freezing-degree days (FDD) and thawing-degree days (TDD) are computed using the Fahrenheit rather than Celsius scale to provide greater resolution and to maintain consistency with past freeze-up reports. In the case of nautical miles, knots, and degrees Fahrenheit, the corresponding values in SI units are provided in parentheses.
- **Winds:** Unless stated otherwise, the wind speeds discussed in the text refer to the daily average values (rather than the daily maximum values or hourly values). The wind directions indicate the orientations **from which** the wind is blowing (*i.e.*, an "easterly wind" is directed from east to west).
- **Ice Drift:** The ice drift speeds discussed in the text refer to the daily average values. The drift directions indicate the orientations **to which** the ice is moving (*i.e.*, an "easterly drift" is directed from west to east).

"THIS INFORMATION IS DISTRIBUTED SOLELY FOR THE PURPOSE OF PRE-DISSEMINATION PEER REVIEW UNDER APPLICABLE INFORMATION QUALITY GUIDELINES. IT HAS NOT BEEN FORMALLY DISSEMINATED BY BSEE. IT DOES NOT REPRESENT AND SHOULD NOT BE CONSTRUED TO REPRESENT ANY BSEE DETERMINATION OR POLICY."

2.2 Definitions

The following definitions borrow heavily from, but are not identical to, those adopted by the World Meteorological Organization (WMO; 2014).

Ice Types by Location

- **Lagoon Ice:** Ice that forms in semi-protected basins adjacent to the coast, including bays, lagoons, and river entrances. Although lagoon ice typically constitutes a subset of the landfast ice, it is accounted for separately in this report.

- **Landfast Ice:** Ice that remains attached to land (either the mainland, one or more barrier islands, or both, for an extended period of time (typically exceeding one week).

- **Landfast Ice Edge:** The seaward boundary of the landfast ice.

- **Pack Ice:** Sea ice that is susceptible to advection by meteorologic and oceanographic influences, other than lagoon ice or landfast ice.

Ice Types by Stage of Development

- **First-Year Ice:** Sea ice of not more than one winter's growth that is at least 30 cm thick.

- **Multi-Year Ice:** Sea ice that has survived at least one summer melt season, including both true multi-year floes from the permanent polar pack ("pack floes") and second-year floes that develop when grounded pieces of thick first-year ice survive the summer melt season.

- **Second-Year Ice:** Multi-year ice that has survived only one summer melt season.

- **Ice-Free:** Water in which no ice of any kind is present.

Ice Types by Size

- **Brash Ice**: An accumulation of floating ice fragments not more than 2 m across.

- **Ice Cake:** A relatively flat piece of ice between 2 and 20 m across.

- **Small Ice Floe:** A relatively flat piece of ice between 20 and 100 m across.

- **Medium Ice Floe:** A relatively flat piece of ice between 100 and 500 m across.

"THIS INFORMATION IS DISTRIBUTED SOLELY FOR THE PURPOSE OF PRE-DISSEMINATION PEER REVIEW UNDER APPLICABLE INFORMATION QUALITY GUIDELINES. IT HAS NOT BEEN FORMALLY DISSEMINATED BY BSEE. IT DOES NOT REPRESENT AND SHOULD NOT BE CONSTRUED TO REPRESENT ANY BSEE DETERMINATION OR POLICY."

- **Big Ice Floe:** A relatively flat piece of ice between 500 m and 2 km across.
- **Vast Ice Floe:** A relatively flat piece of ice between 2 and 10 km across.

Ice Movement

- **Wind Factor:** The ratio of wind speed to ice drift speed, expressed as a percent.

Features

- **Ice Pile-Up:** A feature formed when an advancing ice sheet breaks into discrete blocks while encountering a natural shoreline, shoal, or man-made structure.
- **Ice Ride-Up:** A feature formed when an advancing ice sheet remains substantially intact while moving onto a natural shoreline, shoal, or man-made structure.
- **Ice Ridge:** A line or wall of deformed sea ice created by pressure. A pressure ridge is formed when one ice feature pushes against a second feature while moving perpendicular to their common boundary. A shear ridge is formed when one ice feature grinds past the other while moving parallel to their common boundary.
- **Ice Rubble:** An area of deformed sea ice created by pressure. A rubble pile is a grounded feature composed of ice broken into discrete blocks. A rubble field is a continuous body or region of floating (rather than grounded) ice blocks or closely-spaced ice ridges.
- **Lead:** A linear or quasi-linear opening in the sea ice that exposes sea water to the atmosphere.
- **Flaw Lead:** A lead that exists at the boundary between landfast ice and pack ice.
- **Melt Pond:** A pool of melted snow and/or ice that forms on the surface of the sea ice.
- **Polynya:** A non-linear opening in the sea ice that exposes sea water to the atmosphere.
- **River Overflood:** River discharge that floods the sea ice adjacent to a river mouth due to the presence of bottomfast ice (ice that occupies the entire extent of the water column).

"THIS INFORMATION IS DISTRIBUTED SOLELY FOR THE PURPOSE OF PRE-DISSEMINATION PEER REVIEW UNDER APPLICABLE INFORMATION QUALITY GUIDELINES. IT HAS NOT BEEN FORMALLY DISSEMINATED BY BSEE. IT DOES NOT REPRESENT AND SHOULD NOT BE CONSTRUED TO REPRESENT ANY BSEE DETERMINATION OR POLICY."

- **Shear Line:** A linear boundary that forms between two ice features when one grinds past the other while moving parallel to their common boundary. Shear lines typically contain shear ridges on one or both sides of the boundary.

- **Strudel Drainage:** The drainage of river overflood through the sea ice at discontinuities that can include seal breathing holes, tidal cracks, thermal cracks, and stress cracks.

- **Thermal Crack:** A crack that forms in the sea ice in response to a rapid drop in air temperature. The drop causes contraction and cracking of the ice sheet while an ensuing rise can cause compression and extrusion of the refreezing slush in the crack, creating a ridge.

Freezing and Thawing

- **Freezing-Degree Day (FDD):** The difference between the daily average air temperature and the freezing point of seawater (29°F; -2°C).

- **Thawing-Degree Day (TDD):** The difference between the daily average air temperature and the melting point of freshwater ice (32°F; 0°C).

Dates

- **Break-Up:** The first occasion on which the ice coverage in a specified region falls below 10/10s (100%).

- **Open Water:** The first occasion on which the ice coverage in a specified region falls below 1/10 (10%).

- **First Ice:** The first occasion on which ice begins to form in protected or semi-protected waters at the outset of freeze-up (excluding ice that forms but subsequently melts before freeze-up begins in earnest).

- **Nearshore Freeze-Up:** The first occasion on which complete (10/10s) ice coverage occurs in the region typically occupied by landfast ice.

Lagoon Extents

- **North Kasegaluk Lagoon:** That portion of Kasegaluk Lagoon that lies to the east of Icy Cape.

"THIS INFORMATION IS DISTRIBUTED SOLELY FOR THE PURPOSE OF PRE-DISSEMINATION PEER REVIEW UNDER APPLICABLE INFORMATION QUALITY GUIDELINES. IT HAS NOT BEEN FORMALLY DISSEMINATED BY BSEE. IT DOES NOT REPRESENT AND SHOULD NOT BE CONSTRUED TO REPRESENT ANY BSEE DETERMINATION OR POLICY."

- **South Kasegaluk Lagoon:** That portion of Kasegaluk Lagoon that lies to the south of Icy Cape.
- **South Camden Bay:** That portion of Camden Bay that lies to the south of a line between the mouth of the Canning River and Anderson Point.
- **South Harrison Bay:** That portion of Harrison Bay that lies to the south of a line between Atigaru Point and Spy Island.

2.3 Accessibility

Although this report passes all checks for Section 508 compliance in Adobe Acrobat, the software incorrectly verbalizes the abbreviations for the units displayed in Table 2-1:

Table 2-1. Units Incorrectly Verbalized by Adobe Acrobat

Abbreviation	Correct Verbalization	Incorrect Verbalization by Acrobat
km^2	square kilometers	"k-m-2"
kt	knots	"k-t"
m	meters	"m"
m/s	meters per second	"m-slash-s"
nm	nautical miles	"nanometers"

Adobe Acrobat also struggles with the pronunciation of the Inupiat names shown in Table 2-2. Phonetic pronunciations are provided in this table.

“THIS INFORMATION IS DISTRIBUTED SOLELY FOR THE PURPOSE OF PRE-DISSEMINATION PEER REVIEW UNDER APPLICABLE INFORMATION QUALITY GUIDELINES. IT HAS NOT BEEN FORMALLY DISSEMINATED BY BSEE. IT DOES NOT REPRESENT AND SHOULD NOT BE CONSTRUED TO REPRESENT ANY BSEE DETERMINATION OR POLICY.”

Table 2-2. Phonetic Pronunciations of Inupiat Names

Name	Phonetic Pronunciation
Avak	AH-vak
Chukchi	CHOOK-chee
Kasegaluk	Ca-SEE-ga-luk
Kokolik	KO-ko-lik
Kuk	KOOK
Nokotlek	No-KOT-lek
Oliktok	O-LIK-tok
Oooguruk	OO-gu-ruk
Sagavanirktok	Sag-a-va-NIRK-tok
Stamukhi	Stah-MOOK-ee
Utqiagvik	OOK-key-ag-vik
Utukok	OO-too-kok

"THIS INFORMATION IS DISTRIBUTED SOLELY FOR THE PURPOSE OF PRE-DISSEMINATION PEER REVIEW UNDER APPLICABLE INFORMATION QUALITY GUIDELINES. IT HAS NOT BEEN FORMALLY DISSEMINATED BY BSEE. IT DOES NOT REPRESENT AND SHOULD NOT BE CONSTRUED TO REPRESENT ANY BSEE DETERMINATION OR POLICY."

3. PRIOR STUDIES

3.1 1980s Break-Up Studies

As indicated in Section 1, five annual break-up studies were conducted from 1981 through 1985 by Vaudrey & Associates, Inc. (Vaudrey, 1982; 1983; 1984a; 1984b; 1985a; 1985b; 1986). The methods employed and results obtained in these prior studies are summarized below.

Each of the studies conducted was undertaken on a joint industry basis with a confidentiality period that continued for five years after the date of report issuance. As a result, all currently reside in the public domain, and may be used to provide historical context for the present study.

The primary objectives of each of the five studies were as follows: (1) document the locations and characteristics of strudel drainage features formed in the ice sheet during river overflood; (2) document the locations and characteristics of ice ride-ups and pile-ups on man-made islands, natural barrier islands, and the mainland coast; (3) identify specific storms that produced the individual ride-ups and pile-ups; and (4) document nearshore ice conditions, including the locations and characteristics of multi-year ice floes. Each study included a series of aerial surveys that began in early June and ended in late July to monitor the progression of break-up.

The first two studies were limited to the central portion of the Alaskan Beaufort Sea, while the last three were expanded to cover more of the Alaskan Beaufort as well as the northeast Chukchi. The geographic extent of each study is summarized below:

1981	Flaxman Island to Cape Halkett (west of Harrison Bay)
1982	Flaxman Island to Drew Point (east of Smith Bay)
1983	U.S.-Canadian Border to Point Lay
1984	Barter Island to Icy Cape
1985	Griffin Point (east of Barter Island) to Wainwright

The progress of break-up was documented by reporting the ice conditions observed during each successive trip. Meteorological data, including wind speed and direction, air temperature, and cloud cover (which affects insolation) were acquired from the Federal Aviation Administration (FAA) for Deadhorse Airport (1981-84), and the U.S. Weather Bureau for coastal weather stations at Utqiagvik (1983-85) and Barter Island (1985).

Key findings from the five studies are summarized below.

"THIS INFORMATION IS DISTRIBUTED SOLELY FOR THE PURPOSE OF PRE-DISSEMINATION PEER REVIEW UNDER APPLICABLE INFORMATION QUALITY GUIDELINES. IT HAS NOT BEEN FORMALLY DISSEMINATED BY BSEE. IT DOES NOT REPRESENT AND SHOULD NOT BE CONSTRUED TO REPRESENT ANY BSEE DETERMINATION OR POLICY."

Beaufort Sea: 1981-1985

- **River Overflood:** The transition from winter to break-up began with thawing of the upland rivers and overflooding of the nearshore sea ice in late May and early June. Strudel drainage holes, typically to 5 m in diameter, were concentrated in the region between the 1.8-m isobath and the seaward limit of the overflood. Drainage also occurred through tidal cracks, thermal cracks, and stress cracks in the ice sheet.
- **Melt Ponds:** Melt ponds began to form on the surface of the ice in late May and could extend completely through the ice by late June. They accelerated the break-up process not only by weakening the ice sheet, but also by increasing the rate of melting through exposure to sea water and warm air.
- **Mechanisms of Break-Up:** Break-up was governed by two primary mechanisms: (1) *in-situ* deterioration of the ice sheet, and (2) lines of weakness that developed through melt ponds and/or along old thermal cracks and stress cracks. The former caused a loss of confinement, predisposing the lines of weakness to failure under wind stress. The relative importance of the two mechanisms varied from year to year, with warm air temperatures, vigorous overfloods, and cloud-free skies favoring the former, and wind shifts that included strong winds with southerly components favoring the latter.
- **Timing of Break-Up:** From 1981 through 1985, break-up of the lagoon ice occurred as early as June 27th and as late as July 9th. The average was July 3rd. It should be noted, however, that these dates do not include the earlier break-up noted at river mouths in response to overflooding. Farther offshore, in the region typically occupied by landfast ice, break-up varied between July 4th and 28th, with an average value of July 11th. The standard deviation was 4 days for the lagoons and 10 days for the landfast ice zone.
- **Ice Ride-Ups and Pile-Ups on Natural Beaches:** Ride-up and pile-up events occurred on the natural beaches of the barrier islands and mainland coast in each of the five break-up seasons, with the dates ranging from June 24th to July 21st and the encroachment distances (onto the subaerial beach) from negligible to 45 m. The largest encroachment distances were associated with ride-ups, which take place when the sheet ice remains intact while moving onshore – a circumstance more likely to occur during break-up than freeze-up due to the ductility of the relatively warm ice. Once the ice broke up into relatively small individual floes, ride-ups occurred less frequently due to the attendant decrease in the driving force.

"THIS INFORMATION IS DISTRIBUTED SOLELY FOR THE PURPOSE OF PRE-DISSEMINATION PEER REVIEW UNDER APPLICABLE INFORMATION QUALITY GUIDELINES. IT HAS NOT BEEN FORMALLY DISSEMINATED BY BSEE. IT DOES NOT REPRESENT AND SHOULD NOT BE CONSTRUED TO REPRESENT ANY BSEE DETERMINATION OR POLICY."

- **Man-Made Gravel Islands:** The impacts of break-up on man-made gravel islands were investigated at nine exploratory drillsites, consisting of Resolution, Endeavor, Duck 3, and BF-37 Islands in the Sagavanirktok ("Sag") River Delta; Tern Island in Foggy Island Bay; Mukluk Island in Harrison Bay; and Seal Island, Northstar Exploration Island, and Sandpiper Island in the exposed waters northwest of Prudhoe Bay. Break-up in the Sagavanirktok River Delta proved to be relatively benign, due in large part to *in-situ* melting of the ice sheet that occurred in response to the influx of river overflood water at the outset of the break-up period. Only three ice pile-up events were noted in this region during the five years of observation, with two located on Duck Island and one on Endeavor. All three were prompted by easterly winds in late June or early July. The pile-up heights ranged from 2 to 3 m, while the encroachment distances ranged from 6 to 13 m.

  Both the frequency and severity of encroachment tended to be higher at the other island sites. Such events were documented on both Tern and Seal Islands in three of the four years in which observations were made, and on both Northstar Exploration and Sandpiper Islands shortly after their construction in 1985. Encroachment did not take place on Mukluk Island during the two-year observation period (1984 and 1985), due in large part to the presence of ice rubble that became grounded during the previous freeze-up. The most substantial pile-up was recorded on Tern Island, where the ice attained a maximum height of 8 m and encroached 14 m beyond the waterline onto the gravel bag armor in response to a westerly storm in early July, 1984. The most substantial ride-up occurred on Northstar Exploration Island in early July, 1985, when a northwesterly wind drove the 1- to 1½-m thick ice sheet 21 m up the armored side slope.

- **Multi-Year Ice:** Multi-year ice floes were present in the nearshore region of the Alaskan Beaufort Sea in each of the five break-up seasons. Some of the floes were grounded, while others remained adrift. They tended to occur in localized bands and patches, with concentrations varying from less than 10% to 80%, and diameters from tens of meters to more than 3 km. The floes deteriorated rapidly through the formation of melt ponds. Once they lost the confinement imposed by the surrounding sheet ice, collisions with other floes caused them to split into smaller fragments.

- **Ice Island Fragments:** During the 1981 Break-Up Study, 14 grounded ice island fragments that had broken off the ice shelves on Ellesmere Island were discovered in water depths of 20 to 25 m. Eleven were located in eastern Harrison Bay, while the other three were located off Belvedere Island to the north of Mikkelsen Bay

"THIS INFORMATION IS DISTRIBUTED SOLELY FOR THE PURPOSE OF PRE-DISSEMINATION PEER REVIEW UNDER APPLICABLE INFORMATION QUALITY GUIDELINES. IT HAS NOT BEEN FORMALLY DISSEMINATED BY BSEE. IT DOES NOT REPRESENT AND SHOULD NOT BE CONSTRUED TO REPRESENT ANY BSEE DETERMINATION OR POLICY."

(Figure 1-2). All of the fragments were roughly rectangular in plan form, with maximum horizontal dimensions ranging from 30 to 60 m and freeboards from 4 to 8 m. Nine of those in Harrison Bay appeared to have been derived from a single, larger ice island with an area of at least 18,000 m^2 and an approximate thickness of 28 m. It is noteworthy that the next documented sighting of ice islands or icebergs in Alaskan Arctic waters occurred more than 30 years later, when several icebergs were discovered in the Chukchi Sea during the 2011-12 Freeze-Up Study (Coastal Frontiers and Vaudrey, 2012).

Chukchi Sea: 1983-1985

- **Contrast with Beaufort Sea:** Break-up in the northeast Chukchi Sea is inherently different than that in the Alaskan Beaufort due to the northeast-southwest orientation of the coastline (which results in a predominance of onshore-offshore winds), the existence of steeper slopes in the nearshore region, and a paucity of major rivers that overflood the sea ice.
- **Mechanism of Break-Up:** Reflecting the greatly-diminished role of river overflood, break-up was governed primarily by wind speed and direction. Strong easterly winds tended to dislodge the landfast ice from the relatively steep nearshore slopes, particularly if they occurred in concert with a flaw lead farther offshore.
- **Timing of Break-Up:** Break-up of the landfast ice occurred prior to June 25th in 1983, on or about July 2nd in 1984, and between July 6th and 25th in 1985.
- **Ice Ride-Ups and Pile-Ups:** Ride-up and pile-up events occurred in each of the three break-up seasons, triggered by westerly (onshore) winds. The dates of the six events ranged from June 21st to July 8th, while the encroachment distances onto the subaerial beaches ranged from 6 to 30 m.
- **Multi-Year Ice:** Multi-year ice floes were present in the nearshore region of the northeast Chukchi Sea in each of the three break-up seasons. As in the Beaufort, some were grounded or trapped in the landfast ice zone, while others remained adrift. The concentrations typically varied from less than 10% to 50%, but grounded fragments attained local concentrations as high as 80% in 1985. The largest floes, with diameters to 1.5 km, were observed off Icy Cape in 1983.

"THIS INFORMATION IS DISTRIBUTED SOLELY FOR THE PURPOSE OF PRE-DISSEMINATION PEER REVIEW UNDER APPLICABLE INFORMATION QUALITY GUIDELINES. IT HAS NOT BEEN FORMALLY DISSEMINATED BY BSEE. IT DOES NOT REPRESENT AND SHOULD NOT BE CONSTRUED TO REPRESENT ANY BSEE DETERMINATION OR POLICY."

3.2 2017 Break-Up Study

The scope and methods of the 2017 Freeze-Up Study, which were adopted with only minor modifications for the 2020 study, are described in detail by Coastal Frontiers and Vaudrey (2018). Significant findings are as follows:

Beaufort Sea

- **River Overflood:** The Canning River began overflooding the sea ice on May 20th, the Sagavanirktok on May 21st, the Colville on May 23rd, the Kuparuk on May 28th, and the Ikpikpuk on June 1st. Most of the flood water remained in the receiving bays and lagoons.
- **Lagoon Ice:** Break-up of the lagoon ice began on or about June 8th, when flood water from the Colville River melted through the ice in South Harrison Bay. Open water in the lagoon areas occurred over a 12-day period that began with South Camden Bay and Gwydyr Bay on June 27th and ended with Stefansson Sound on July 8th.
- **Landfast Ice:** Break-up of the landfast ice occurred on May 26th in response to a one-day southeasterly storm. The ice edge then remained stable until June 21st, when a wind shift from easterly to southwesterly and a substantial rise in the air temperature initiated rapid deterioration that continued through month-end. The last remnants of landfast ice disappeared between July 4th and 14th.
- **Pack Ice:** Commencing in the second half of May, fracturing of the ice canopy produced progressively smaller floes in the pack ice. In mid-June, warm water moving to the west from the Mackenzie River began to reduce the ice concentration off Camden Bay while warm water from the Alaska Coastal Current began to reduce the ice concentration to the east of Point Barrow. The two melt zones converged in mid-July, producing pack ice concentrations that ranged from negligible in most areas to as much as 50% in the region of convergence between Harrison and Prudhoe Bays.
- **Ice Pile-Ups and Ride-Ups:** Of the 38 ice pile-ups observed in the central Beaufort Sea in late February, 16 remained in early July. Four new pile-ups and six new ride-ups also were observed on that date. The heights of the new features ranged from 2 to 4 m above sea level, the encroachment distances from negligible to 3 m onto the subaerial beach, and the alongshore lengths from 20 to 1,100 m.
- **Multi-Year Ice:** Multi-year ice remained absent from the nearshore region of the Alaskan Beaufort Sea throughout the three-month study period.

"THIS INFORMATION IS DISTRIBUTED SOLELY FOR THE PURPOSE OF PRE-DISSEMINATION PEER REVIEW UNDER APPLICABLE INFORMATION QUALITY GUIDELINES. IT HAS NOT BEEN FORMALLY DISSEMINATED BY BSEE. IT DOES NOT REPRESENT AND SHOULD NOT BE CONSTRUED TO REPRESENT ANY BSEE DETERMINATION OR POLICY."

- **Ice Drift:** Drift buoys embedded in the pack ice attained monthly average speeds that ranged from a high of 6.7 nm per day (12.4 km per day) in June to a low of 2.6 nm per day (4.8 km per day) in July. The highest daily average speed, 20 nm per day (38.7 km per day), occurred during an easterly storm in early July.

Chukchi Sea

- **River Overflood:** Of the seven rivers that discharge in or adjacent to the Chukchi Sea study area, the Kukpowruk was the first to begin overflooding the sea ice, on May 16th, and the Kugrua was the last, on June 22nd. Virtually all of the flood water was contained in the receiving lagoons.
- **Lagoon Ice:** Break-up of the lagoon ice took place in June, starting with South Kasegaluk Lagoon on or about June 3rd and progressing north to Peard Bay on June 22nd. Open water occurred in South Kasegaluk Lagoon, North Kasegaluk Lagoon, and the Kuk River Entrance on June 24th, and in Peard Bay between July 7th and 10th.
- **Landfast Ice:** Break-up of the landfast ice occurred on June 3rd, when easterly winds dislodged a large piece between Icy Cape and Wainwright. Intermittent losses continued throughout June and early July, causing the last vestiges of landfast ice to disappear on July 5th.
- **Pack Ice:** The pack ice retreated to the north and west throughout the study period, leaving the region between Alaska and Siberia nearly ice-free in late July. The southern edge of the ice was located approximately 40 nm (74 km) off Point Barrow at that time.
- **Ice Ride-Ups and Pile-Ups:** Of the 63 ice pile-ups observed on the Chukchi Sea coast in early March, only four remained on July 6th. In addition to these relict features, four small ride-ups that had formed during break-up were discovered in the vicinity of Point Franklin. The heights of the ride-ups ranged from 1 to 3 m, the encroachment distances from 5 to 20 m onto the subaerial beach, and the alongshore lengths from 15 to 200 m.
- **Multi-Year Ice:** Multi-year ice remained absent from the Chukchi Sea study area throughout the three-month study period.

"THIS INFORMATION IS DISTRIBUTED SOLELY FOR THE PURPOSE OF PRE-DISSEMINATION PEER REVIEW UNDER APPLICABLE INFORMATION QUALITY GUIDELINES. IT HAS NOT BEEN FORMALLY DISSEMINATED BY BSEE. IT DOES NOT REPRESENT AND SHOULD NOT BE CONSTRUED TO REPRESENT ANY BSEE DETERMINATION OR POLICY."

4. DATA ACQUISITION AND ANALYSIS

As outlined in Section 1, the 2020 Break-Up Study was conducted using a combination of remotely-sensed data and on-site observations. This section describes the sources of data and methods of analysis in terms of the following five categories: meteorological data (Section 4.1), ice charts (Section 4.2), satellite imagery (Section 4.3), drift buoy data (Section 4.4), and aerial reconnaissance missions (Section 4.5). The underlying digital data are provided in Appendix E.

4.1 Meteorological Data

Meteorological conditions during the three-month period from May through July 2020 were derived from the *Local Climatological Data* (LCD) for the Deadhorse and Utqiagvik Airport Automated Surface Observing System stations compiled by the National Oceanographic and Oceanic Administration (NOAA, 2020a). The LCD includes hourly observations and daily summaries of temperature, pressure, humidity, precipitation, and winds. Raw daily and hourly data are provided in Appendix E in PDF format. Excel spreadsheets with monthly summaries of the meteorological conditions also are included in Appendix E.

The wind data were used to identify storms and changes in wind direction that could impact the ice canopy. Such impacts included the loss of landfast ice, changes in ice drift, the opening and closing of the Chukchi Sea flaw lead, and the generation of ice pile-ups and ride-ups. The air temperature data were used to derive thawing-degree days (TDD), which were computed for each day as the difference between the air temperature and the melting point of freshwater ice (32°F; 0°C). The melting point of freshwater ice was adopted for the computation rather than that of sea ice (29°F; -2°C) to reflect the substantial reduction in the salinity of first-year sea ice that occurs over the course of the winter season. As discussed by Kovacs (1996), brine drainage typically causes the salinity of first-year sea ice to decrease to about five parts per thousand at the time of break-up. Days in which the air temperature remained below 32°F produced negative TDD. TDD were accumulated at each site starting on the date after which the sum remained positive (May 29th at Utqiagvik Airport and May 23rd at Deadhorse Airport) and continuing through the end of July. The results are shown in Table 4-1.

To provide historical perspective, the normal range of daily air temperatures at each weather station defined by the average values of the daily highs and lows from 1980-81 through 2009-10 was obtained from NOAA (Arguez, *et al.*, 2010). The appropriate range is included in each plot of daily average air temperature that appears in Sections 6 and 7.

"THIS INFORMATION IS DISTRIBUTED SOLELY FOR THE PURPOSE OF PRE-DISSEMINATION PEER REVIEW UNDER APPLICABLE INFORMATION QUALITY GUIDELINES. IT HAS NOT BEEN FORMALLY DISSEMINATED BY BSEE. IT DOES NOT REPRESENT AND SHOULD NOT BE CONSTRUED TO REPRESENT ANY BSEE DETERMINATION OR POLICY."

Table 4-1. Accumulated Thawing-Degree Days (>32°F) at Month-End at Utqiagvik and Deadhorse Airports, May-July 2020

Site	*May*	*June*	*July*
Utqiagvik	2[1]	149	322
Deadhorse	12[2]	233	586

Notes:
[1] TDD began accumulating at Utqiagvik Airport on May 29th.
[2] TDD began accumulating at Deadhorse Airport on May 23rd.

As in each of the nine freeze-up studies undertaken between 2009-10 and 2019-20 (Coastal Frontiers and Vaudrey, 2010; 2011; 2012; 2013; 2014; 2015; 2016; 2017; 2020) as well as the break-up study undertaken in 2017 (Coastal Frontiers and Vaudrey, 2018), Utqiagvik Airport was adopted as the primary source of weather data for the Chukchi Sea. Although the data from Wainwright Airport have become sufficiently reliable to warrant consideration, a comparison with the Utqiagvik data for the 2014-15 freeze-up season indicated that the differences were relatively minor (Coastal Frontiers and Vaudrey, 2015). As a result, to maintain continuity with the prior studies, all of the wind and temperature data pertaining to the Chukchi were obtained from Utqiagvik.

To supplement the data from Deadhorse Airport, monthly plots of wind speed, wind direction, air temperature and barometric pressure measured at the Prudhoe Bay West Dock Seawater Treatment Plant (STP) were downloaded from the National Ocean Service website (2020) for the period from May through July 2020. These plots are included as PNG files in Appendix E.

4.2 Ice Charts

Weekly ice charts pertaining to the study area were downloaded from two government sources: the Canadian Ice Service (CIS; 2020) and the National Ice Center (NIC; 2020). Daily ice charts prepared by the National Weather Service (NWS; 2020) also were acquired. Although the charts from all three organizations provide similar information, the CIS products tend to incorporate greater detail. However, coverage is limited to the Beaufort Sea and extreme northeast portion of the Chukchi Sea whereas the NIC and NWS charts encompass the entire Chukchi as well as the Beaufort.

Thirteen weekly ice charts were obtained from the CIS covering the period from May 4 through July 27, 2020. The charts are provided in Appendix E in shapefile and image (GIF) format. For clarity, the CIS provides two versions of each ice chart, with one showing the ice

"THIS INFORMATION IS DISTRIBUTED SOLELY FOR THE PURPOSE OF PRE-DISSEMINATION PEER REVIEW UNDER APPLICABLE INFORMATION QUALITY GUIDELINES. IT HAS NOT BEEN FORMALLY DISSEMINATED BY BSEE. IT DOES NOT REPRESENT AND SHOULD NOT BE CONSTRUED TO REPRESENT ANY BSEE DETERMINATION OR POLICY."

concentration and the other the stage of development. Figure 4-1 presents the CIS ice concentration chart for May 4, 2020, shortly after the start of the study period.

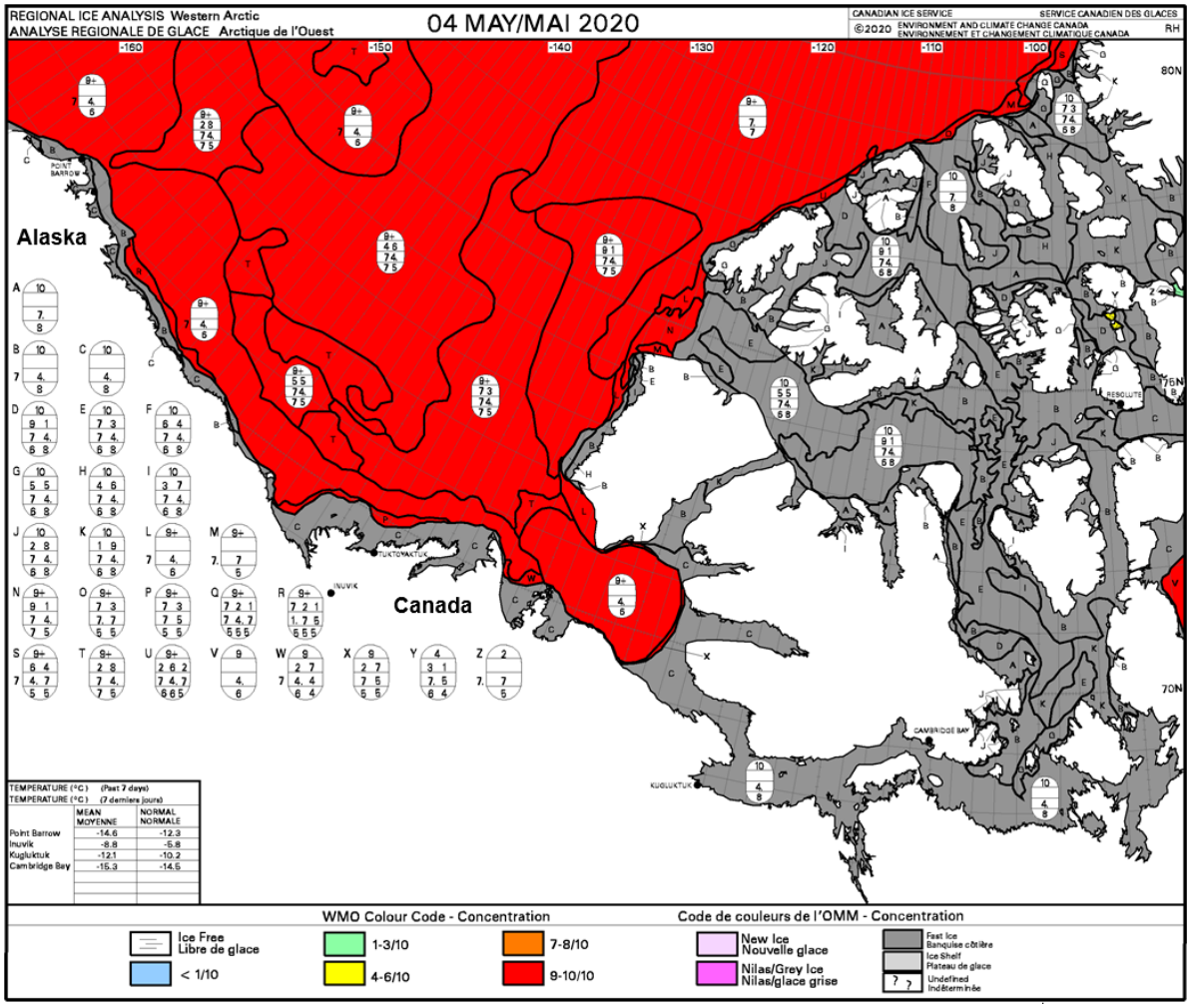

After: Canadian Ice Service, 2020

Figure 4-1. CIS Ice Concentration Chart of Beaufort Sea for May 4, 2020

Fourteen weekly ice charts covering the period from May 1 through July 30, 2020 were obtained from the NIC. As in the case of the CIS charts, the NIC charts are available in shapefile and image format, and in two versions that display concentration and stage of development. The NIC charts are included in Appendix E. Figure 4-2 presents the NIC stage of development chart for July 30, 2020, at the end of the study period.

Background information on the progression of break-up in the entire Arctic region was obtained from the NIC Arctic Marginal Ice Zone charts, which depict the extent of the pack ice and marginal ice zone. For the purpose of preparing these charts, pack ice is assumed to occupy the region with eight tenths or more coverage, while the marginal ice zone represents

"THIS INFORMATION IS DISTRIBUTED SOLELY FOR THE PURPOSE OF PRE-DISSEMINATION PEER REVIEW UNDER APPLICABLE INFORMATION QUALITY GUIDELINES. IT HAS NOT BEEN FORMALLY DISSEMINATED BY BSEE. IT DOES NOT REPRESENT AND SHOULD NOT BE CONSTRUED TO REPRESENT ANY BSEE DETERMINATION OR POLICY."

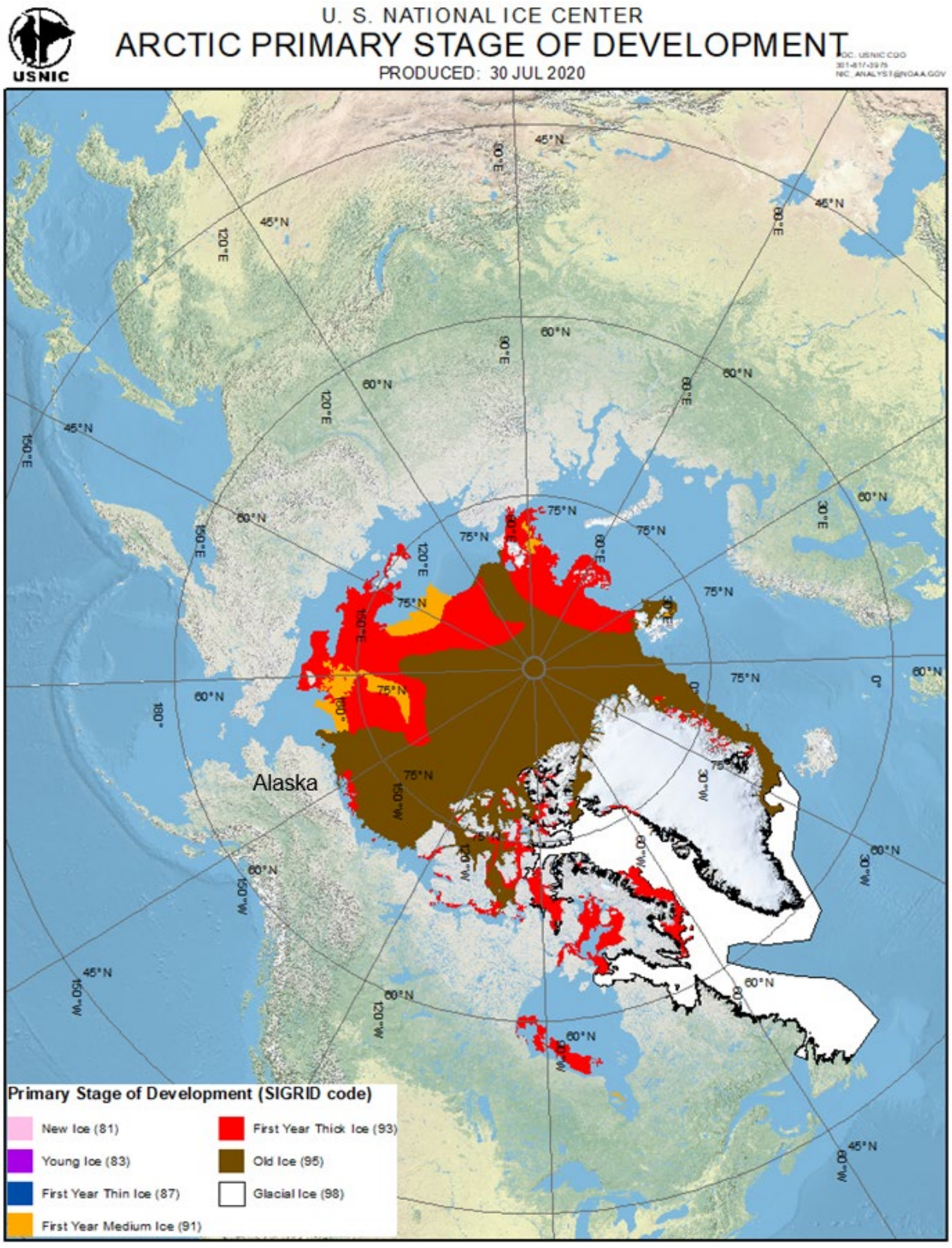

After: National Ice Center, 2020

Figure 4-2. NIC Arctic Ice Stage of Development Chart for July 30, 2020

"THIS INFORMATION IS DISTRIBUTED SOLELY FOR THE PURPOSE OF PRE-DISSEMINATION PEER REVIEW UNDER APPLICABLE INFORMATION QUALITY GUIDELINES. IT HAS NOT BEEN FORMALLY DISSEMINATED BY BSEE. IT DOES NOT REPRESENT AND SHOULD NOT BE CONSTRUED TO REPRESENT ANY BSEE DETERMINATION OR POLICY."

the transition between ice-free water and pack ice (NIC, 2020). A representative example corresponding to July 17, 2020, when the region between Alaska and Siberia was nearly free of pack ice, is provided as Figure 4-3. Fourteen Arctic Marginal Ice Zone charts covering the period from May 1 through July 31, 2020 on a weekly basis are included as image (PNG) files in Appendix E.

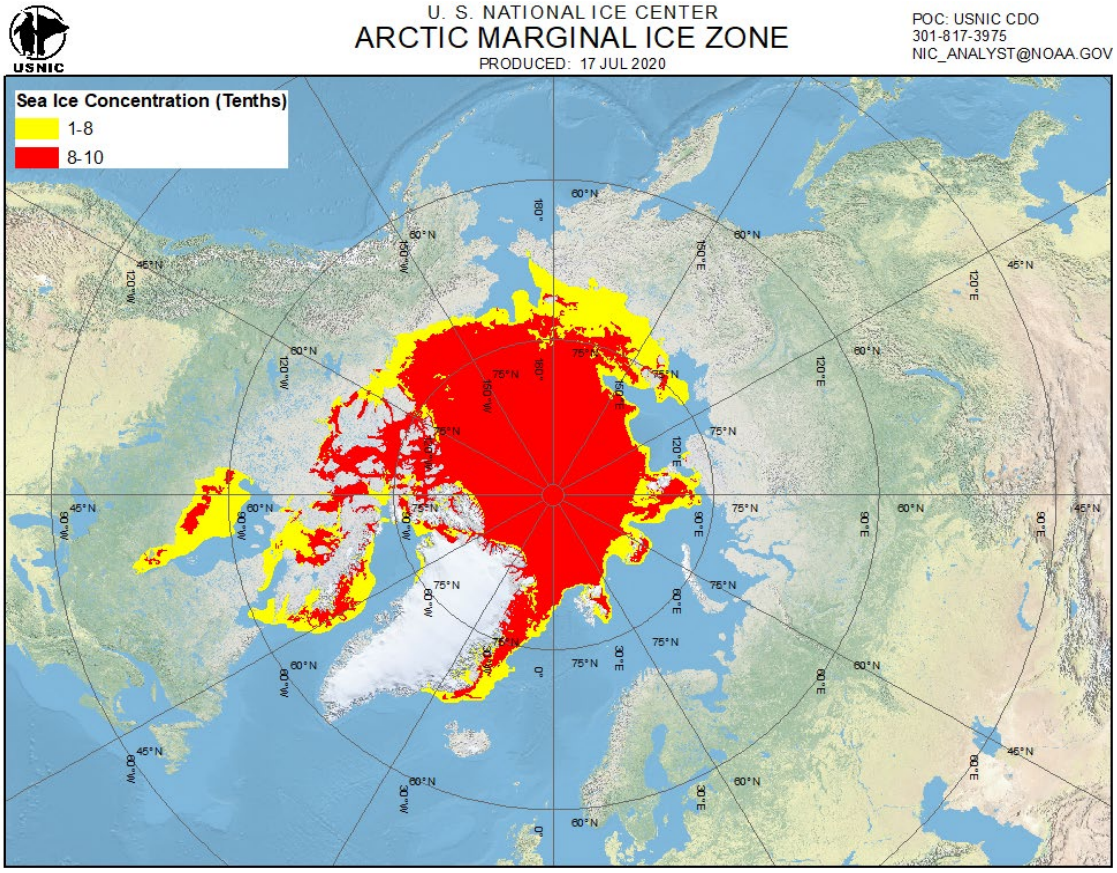

Source: National Ice Center, 2020

Figure 4-3. NIC Arctic Marginal Ice Zone Chart for July 17, 2020

The data obtained from the CIS and NIC were supplemented with daily ice charts produced by the National Weather Service for the months of May, June, and July 2020. Because the NWS charts often differed from the corresponding CIS and NIC charts as well as from the satellite images obtained for this project, they were used only sparingly. They are included in image (JPG) and shapefile format in Appendix E.

The ice charts described above were used to track the evolution of break-up on a coarse scale, particularly during the early stages of the process. They were not sufficiently detailed to support the investigation of fine-scale features such as individual ice floes, rubble fields, and ice movement lines.

"THIS INFORMATION IS DISTRIBUTED SOLELY FOR THE PURPOSE OF PRE-DISSEMINATION PEER REVIEW UNDER APPLICABLE INFORMATION QUALITY GUIDELINES. IT HAS NOT BEEN FORMALLY DISSEMINATED BY BSEE. IT DOES NOT REPRESENT AND SHOULD NOT BE CONSTRUED TO REPRESENT ANY BSEE DETERMINATION OR POLICY."

4.3 Satellite Imagery

Three different types of satellite imagery were used to study the ice conditions that prevailed during the 2020 break-up season: RADARSAT-2, VIIRS (Visible Infrared Imaging Radiometer Suite), and MODIS (Moderate Resolution Imaging Spectro-radiometer). The RADARSAT-2 imagery served as the primary source of ice data, while the MODIS imagery played a supplemental role. The VIIRS imagery was used only sparingly.

General information about the progress of break-up was obtained from 13 publicly available RADARSAT-2 mosaics compiled by the CIS for the period from May 4 through July 27, 2020. The mosaics, which were produced on a weekly basis, are provided as GIF files in Appendix E. Although the resolution was inadequate to support detailed analysis, the composite images provided useful data on synoptic-scale ice conditions. A representative example from mid-July, 2020, is provided as Figure 4-4.

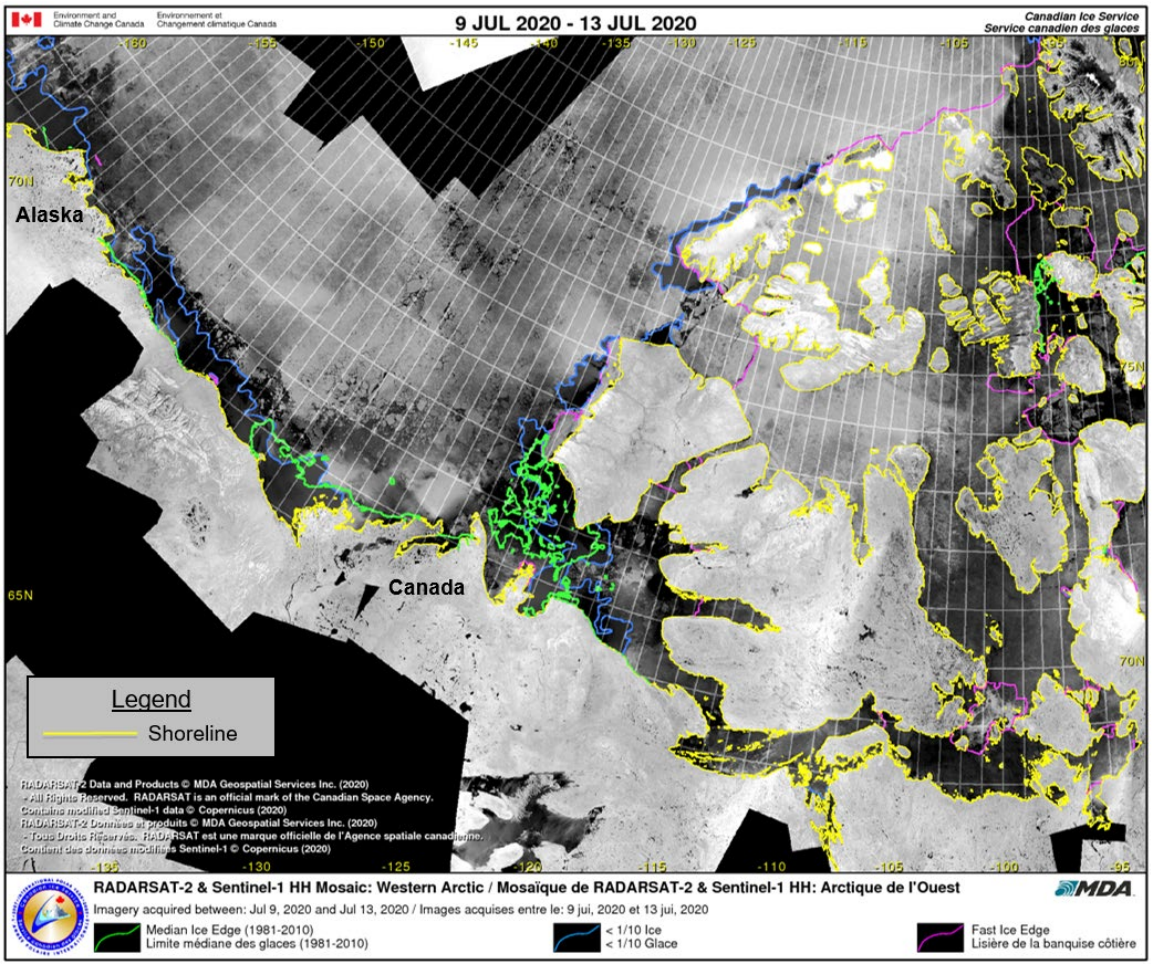

After: Canadian Ice Service, 2020

Figure 4-4. CIS RADARSAT-2 Mosaic for July 9-13, 2020

"THIS INFORMATION IS DISTRIBUTED SOLELY FOR THE PURPOSE OF PRE-DISSEMINATION PEER REVIEW UNDER APPLICABLE INFORMATION QUALITY GUIDELINES. IT HAS NOT BEEN FORMALLY DISSEMINATED BY BSEE. IT DOES NOT REPRESENT AND SHOULD NOT BE CONSTRUED TO REPRESENT ANY BSEE DETERMINATION OR POLICY."

The most useful RADARSAT-2 images were the ten high-resolution, georeferenced scenes captured using the ScanSAR Wide beam mode, which provides a nominal resolution of 100 m over a nominal area of 270 x 270 nm (500 x 500 km; MacDonald, Dettwiler and Associates, 2020). The data set consisted of five images of the Chukchi Sea obtained between May 14th and July 11th, and five images of the Beaufort Sea obtained between May 17th and July 14th. The image characteristics were sufficient not only to track the general evolution of the ice cover during break-up, but also to support detailed investigations of features that included the landfast ice zone, leads, and the southern edge of the pack ice.

As the licensing agreement for the RADARSAT-2 images prohibits the distribution of the original georeferenced TIFF files (MDA Geospatial Services, 2020), each scene is provided in Appendix E in PDF format. A sample image of the Beaufort Sea that was acquired on May 17, 2020, is provided as Figure 4-5. Image acquisition reports prepared following the receipt and processing of each pair of images (consisting of one image of the Beaufort and one of the Chukchi) are provided in Appendix B.

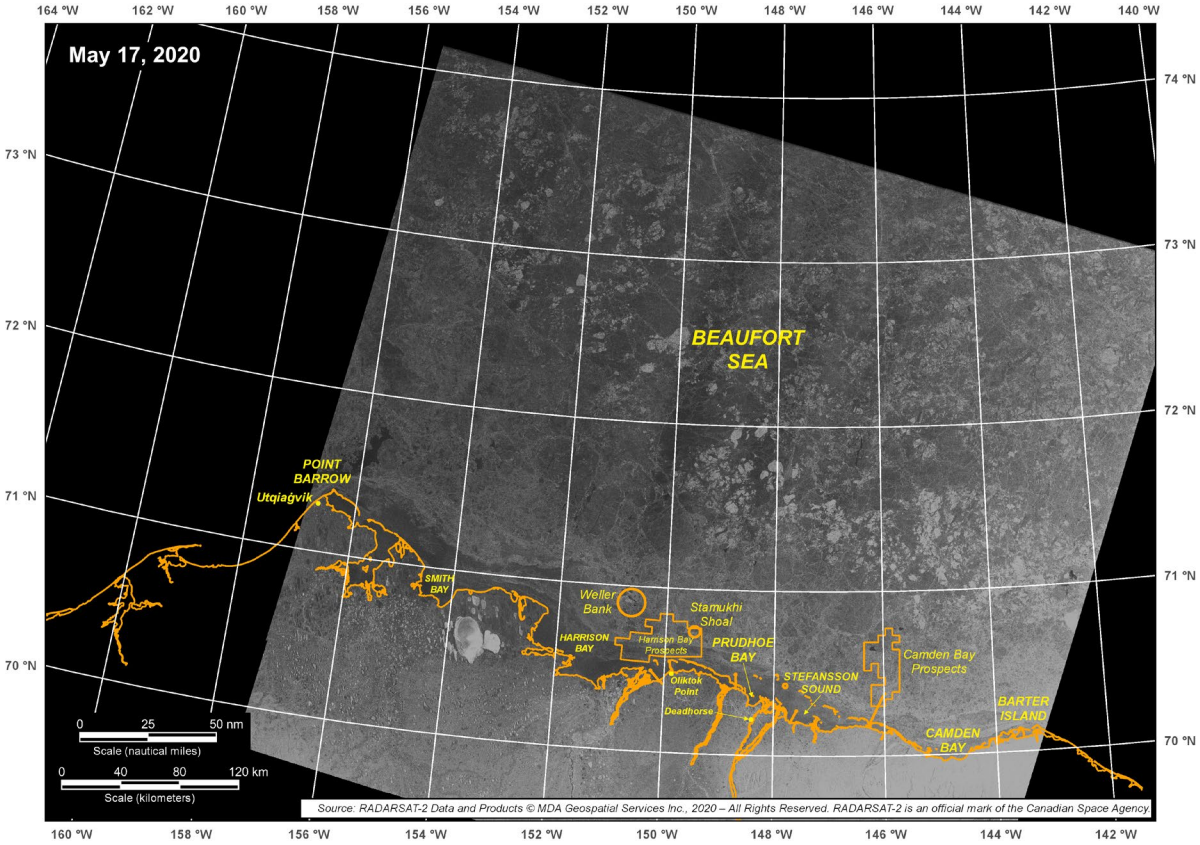

Figure 4-5. RADARSAT-2 Image of Beaufort Sea Acquired on May 17, 2020

"THIS INFORMATION IS DISTRIBUTED SOLELY FOR THE PURPOSE OF PRE-DISSEMINATION PEER REVIEW UNDER APPLICABLE INFORMATION QUALITY GUIDELINES. IT HAS NOT BEEN FORMALLY DISSEMINATED BY BSEE. IT DOES NOT REPRESENT AND SHOULD NOT BE CONSTRUED TO REPRESENT ANY BSEE DETERMINATION OR POLICY."

MODIS imagery was acquired to bridge the chronological gaps between RADARSAT-2 scenes. Key advantages of the MODIS platform include daily image capture and a maximum resolution of 250 m; the primary disadvantage is an inability to penetrate cloud cover. Notwithstanding this limitation, a relatively high percentage of clear skies during the 2020 break-up period allowed the acquisition of imagery that was particularly useful in identifying river overflood and break-up of the lagoon and landfast ice. The ninety-two images that were obtained between May 1st and July 31st from NASA Worldview Snapshots (NASA, 2020a) are provided as georeferenced JPG files in Appendix E.

Figure 4-6 presents a MODIS image acquired on June 3rd, the date on which a massive piece of landfast ice broke free from the region between Point Franklin and Utqiagvik in the Chukchi Sea.

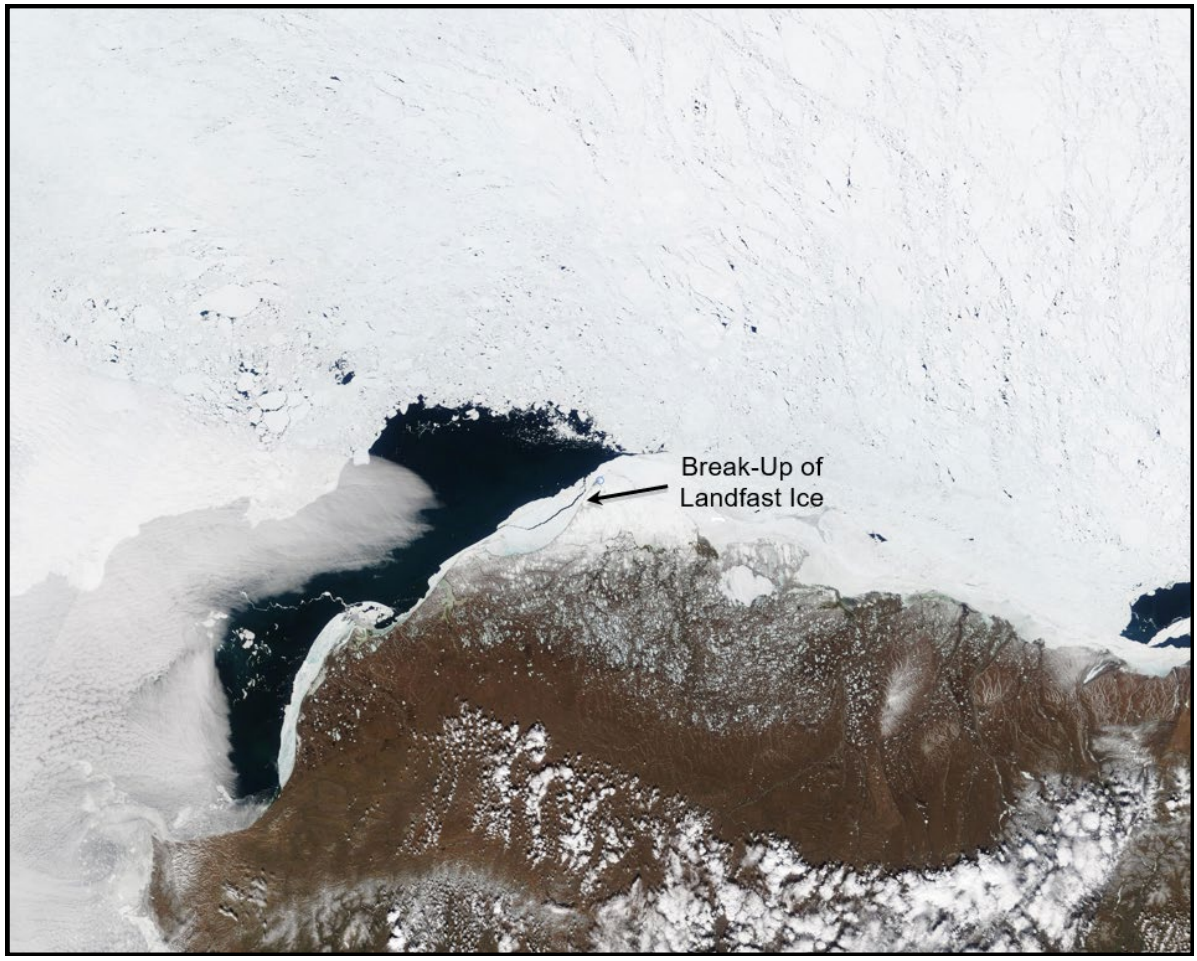

After: NASA, 2020a

Figure 4-6. MODIS Image Acquired on June 3, 2020

"THIS INFORMATION IS DISTRIBUTED SOLELY FOR THE PURPOSE OF PRE-DISSEMINATION PEER REVIEW UNDER APPLICABLE INFORMATION QUALITY GUIDELINES. IT HAS NOT BEEN FORMALLY DISSEMINATED BY BSEE. IT DOES NOT REPRESENT AND SHOULD NOT BE CONSTRUED TO REPRESENT ANY BSEE DETERMINATION OR POLICY."

VIIRS imagery, like MODIS imagery, was acquired to supplement the RADARSAT-2 scenes. Data were downloaded from the Geographic Information Network of Alaska (GINA, 2020) and from the Regional and Mesoscale Meteorology Branch of NOAA (2020).

The primary source of VIIRS imagery for this study was the Day-Night Band (DNB), which uses light in the visual spectrum. The utility of the imagery was limited by the sensor's resolution (750 m) and inability to penetrate cloud cover. Notwithstanding these drawbacks, the high frequency of image capture (multiple scenes per day subject to suitable weather conditions) allowed large-scale changes in the ice canopy to be tracked on a short-term basis. The imagery was particularly useful in assessing the status of the Chukchi Sea flaw lead. Most of the VIIRS images are provided as georeferenced TIFF files in Appendix E, but PNG files are provided in those cases where TIFF files were unavailable. A representative example in Figure 4-7 shows the flaw lead on May 27, 2020.

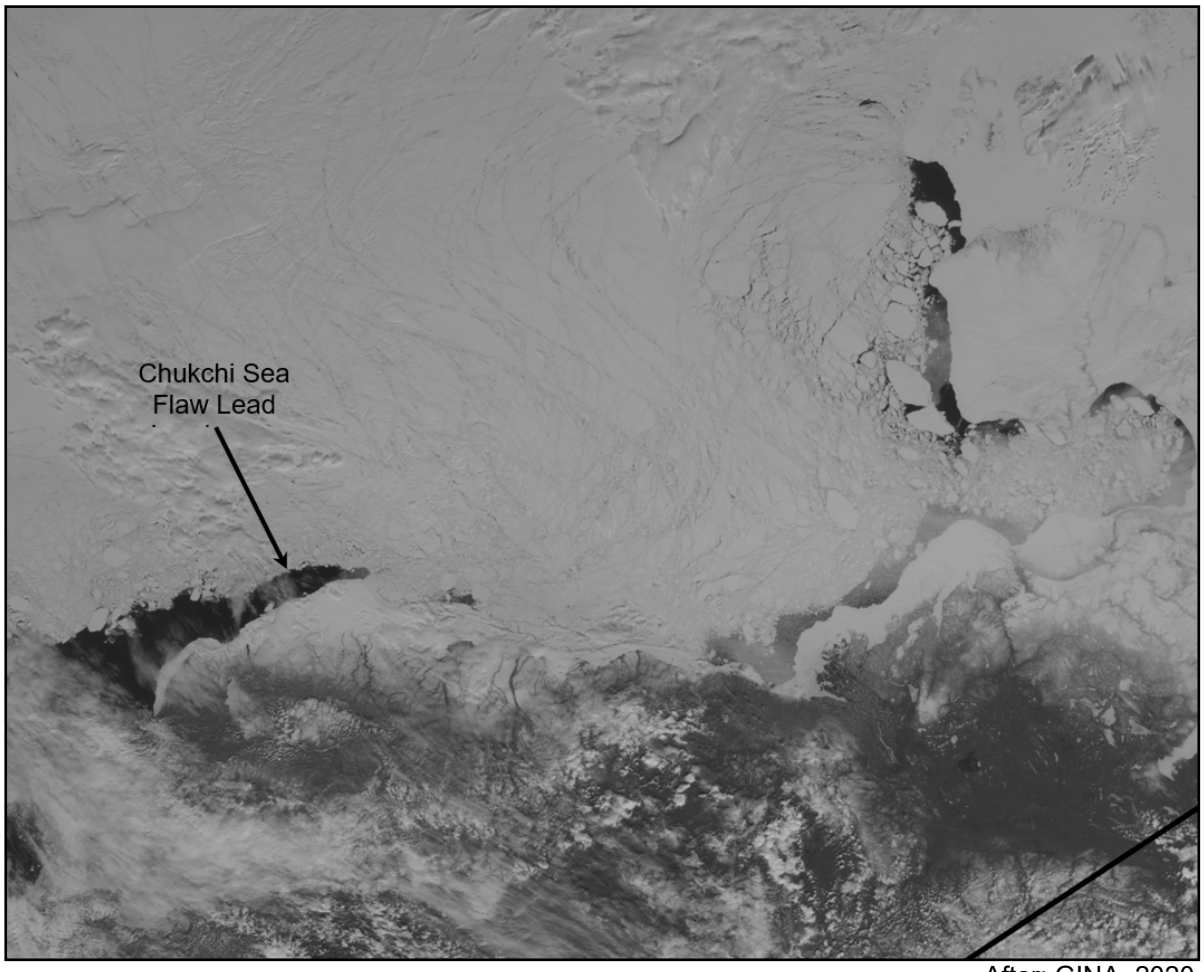

After: GINA, 2020

Figure 4-7. VIIRS Day Night Band Image Acquired on May 27, 2020

"THIS INFORMATION IS DISTRIBUTED SOLELY FOR THE PURPOSE OF PRE-DISSEMINATION PEER REVIEW UNDER APPLICABLE INFORMATION QUALITY GUIDELINES. IT HAS NOT BEEN FORMALLY DISSEMINATED BY BSEE. IT DOES NOT REPRESENT AND SHOULD NOT BE CONSTRUED TO REPRESENT ANY BSEE DETERMINATION OR POLICY."

4.4 Drift Buoys

As in recent freeze-up studies (Coastal Frontiers and Vaudrey, 2014; 2015; 2016; 2017; 2020) and in the 2017 break-up study (Coastal Frontiers and Vaudrey, 2018), information on ice drift was obtained from telemetry buoys monitored through the International Arctic Buoy Programme ("IABP"; Rigor, 2020). Six such buoys were present in the study area during portions of the break-up study period. Their characteristics are summarized in Table 4-2. Note that the lengthy buoy identification numbers used by the IABP have been replaced by one-letter designations in this study in the interest of simplicity.

Table 4-2. IABP Drift Buoy Characteristics

Buoy Identifier in this Report	IABP Buoy Identifier	Sponsor	Period of Ice Drift Data[1]	Basin
A	300234067523430	USIABP[2]	May 29 – June 13, 2020	Chukchi
B	300534060211310	JAMSTEC[3]	April 30 – July 20, 2020	Beaufort Chukchi
C	300234060834110	EC[4]	May 7 – July 20, 2020	Beaufort Chukchi
D	300234066699590	USIABP[2]	April 30 – July 16, 2020	Beaufort
E	900103	WHOI[5]	June 8 – July 10, 2020	Beaufort
F	900119	WHOI[5]	June 8 – July 31, 2020	Beaufort

Notes:

1 The period during which the movement of each buoy could be used to quantify ice drift was determined by superimposing its trajectory on available satellite imagery and ice charts.

2 U.S. Interagency Buoy Program (Polar Ice Center, 2020).

3 Japan Agency for Marine-Earth Science and Technology (JAMSTEC; 2020).

4 Environment and Climate Change Canada (EC; 2020).

5 Ice-Tethered Profiler data were collected and made available by the Ice-Tethered Profiler Program (Toole *et al.*, 2011; Krishfield *et al.*, 2008) conducted by Woods Hole Oceanographic Institution (http://www.whoi.edu/itp).

To determine the period in which the movement of a particular buoy could be used to quantify ice drift, its track was superimposed on the available RADARSAT-2, MODIS, and VIIRS images as well as on CIS ice concentration charts (Section 4.2). Those portions that corresponded to open water or partial ice cover were discarded, while those portions that corresponded to complete ice cover were retained. The resulting on-ice drift tracks are shown in Figure 4-8, which was constructed from the daily position of each buoy at midnight.

"THIS INFORMATION IS DISTRIBUTED SOLELY FOR THE PURPOSE OF PRE-DISSEMINATION PEER REVIEW UNDER APPLICABLE INFORMATION QUALITY GUIDELINES. IT HAS NOT BEEN FORMALLY DISSEMINATED BY BSEE. IT DOES NOT REPRESENT AND SHOULD NOT BE CONSTRUED TO REPRESENT ANY BSEE DETERMINATION OR POLICY."

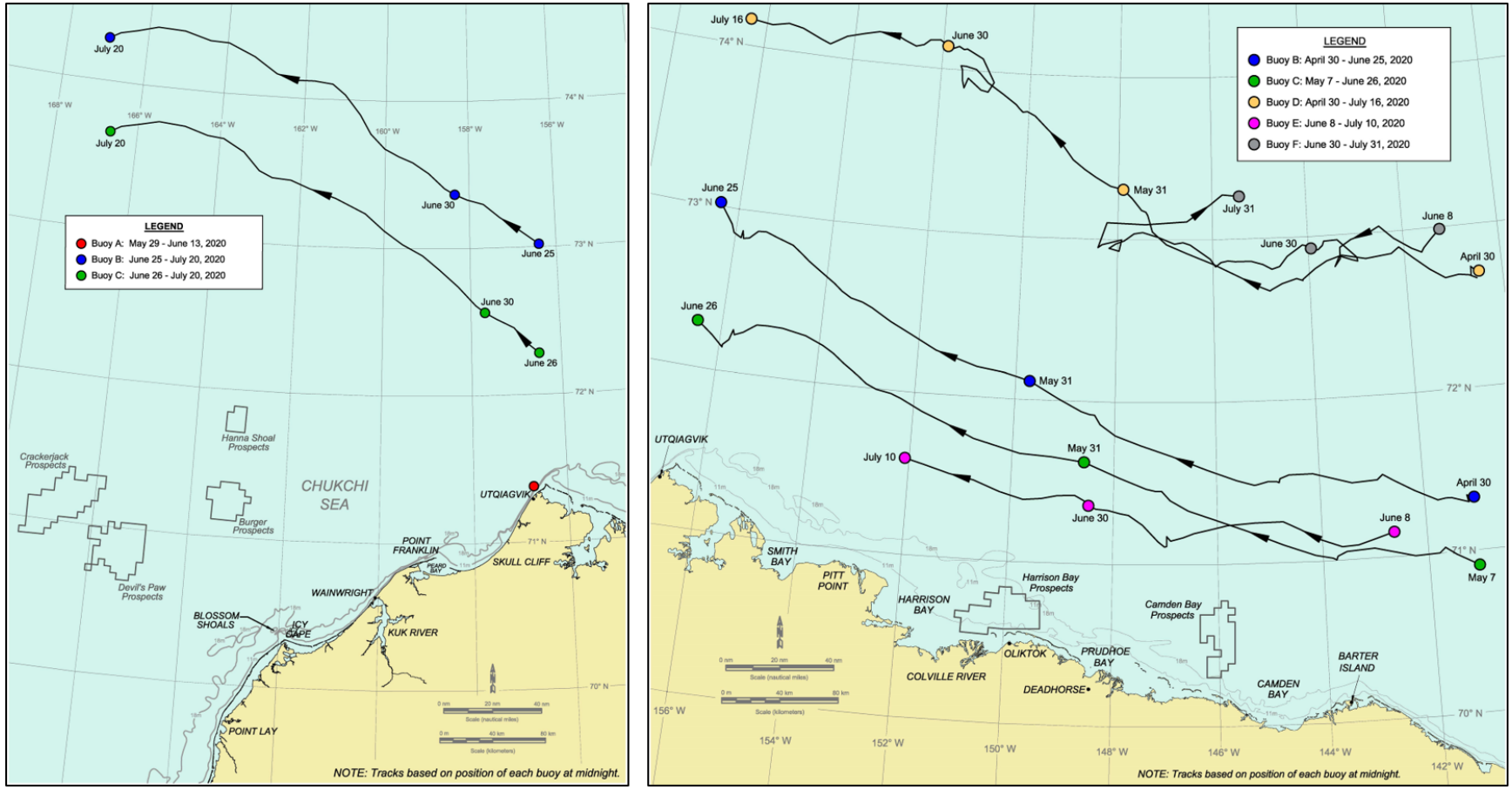

Data Source: Rigor, 2020

Figure 4-8. On-Ice Drift Buoy Tracks during 2020 Break-Up Season

"THIS INFORMATION IS DISTRIBUTED SOLELY FOR THE PURPOSE OF PRE-DISSEMINATION PEER REVIEW UNDER APPLICABLE INFORMATION QUALITY GUIDELINES. IT HAS NOT BEEN FORMALLY DISSEMINATED BY BSEE. IT DOES NOT REPRESENT AND SHOULD NOT BE CONSTRUED TO REPRESENT ANY BSEE DETERMINATION OR POLICY."
"THIS INFORMATION IS DISTRIBUTED SOLELY FOR THE PURPOSE OF PRE-DISSEMINATION PEER REVIEW UNDER APPLICABLE INFORMATION QUALITY GUIDELINES. IT HAS NOT BEEN FORMALLY DISSEMINATED BY BSEE. IT DOES NOT REPRESENT AND SHOULD NOT BE CONSTRUED TO REPRESENT ANY BSEE DETERMINATION OR POLICY."

4.5 Aerial Reconnaissance Missions

Two aerial reconnaissance missions were undertaken in the Chukchi Sea in mid-June followed by two in the Beaufort Seas in early July to observe the conditions that prevailed near the end of the break-up season. The specific objectives of the missions were as follows:

- Obtain ground truth information to confirm and expand upon the conclusions drawn from satellite imagery;
- Investigate significant features identified in the satellite imagery, such as large leads, the landfast ice edge, and well-developed shear lines;
- Detect, investigate, and document small-scale features that were beneath the resolution of the satellite imagery, including ridges, rubble piles, small multi-year ice floes, and shoreline pile-ups.

All of the flights were conducted using an Aero Commander 690 (Plate 4-1). This fixed-wing aircraft offers the benefits of an extended range, an ability to fly at relatively low speeds, a high wing that permitted unobstructed views of the ice below, and a moderate cost per flight hour.

Plate 4-1. Aero Commander 690 at Deadhorse Airport (July 10, 2020)

Each flight path was mapped using a Garmin GPSMap 196. To improve the accuracy of the position data, differential corrections broadcast in real time via satellite by the U.S. Government's Wide Area Augmentation System (WAAS) were received by the GPS unit

"THIS INFORMATION IS DISTRIBUTED SOLELY FOR THE PURPOSE OF PRE-DISSEMINATION PEER REVIEW UNDER APPLICABLE INFORMATION QUALITY GUIDELINES. IT HAS NOT BEEN FORMALLY DISSEMINATED BY BSEE. IT DOES NOT REPRESENT AND SHOULD NOT BE CONSTRUED TO REPRESENT ANY BSEE DETERMINATION OR POLICY."

when available. Static position checks conducted at North Slope survey monuments in the past have indicated that the accuracy attainable with WAAS is less than 1 m (*e.g.*, Coastal Frontiers, 2015). When operated in the stand-alone mode, the GPS accuracy typically is on the order of 10 m. The GPS position data were displayed on a base map of the study area in real time using a laptop computer and Hypack survey software. This arrangement allowed the field crew both to direct the aircraft to locations of interest identified in advance in the satellite imagery, and to record the positions of small-scale features noted during the flight.

The flight paths in the Chukchi are shown in Figure 4-9, while those in the Beaufort are show in Figure 4-10. Drawings CFC-1070-02-001, -002 and -003 (Appendix A) display the locations of ice features observed during the flights as well as those of photographs and videos taken during the flights. Each photo was assigned a unique identification code such as "B2-17" and each video a unique identification code such as "C1-V12". The first letter, "B" or "C", indicates whether the flight was conducted in the Beaufort or Chukchi; the number that follows indicates the order in which the flight was conducted in that basin. The number after the dash specifies the order in which the photo or video was acquired during that flight. Hence, C1-V12 designates the 12th video acquired during the first Chukchi Sea reconnaissance flight.

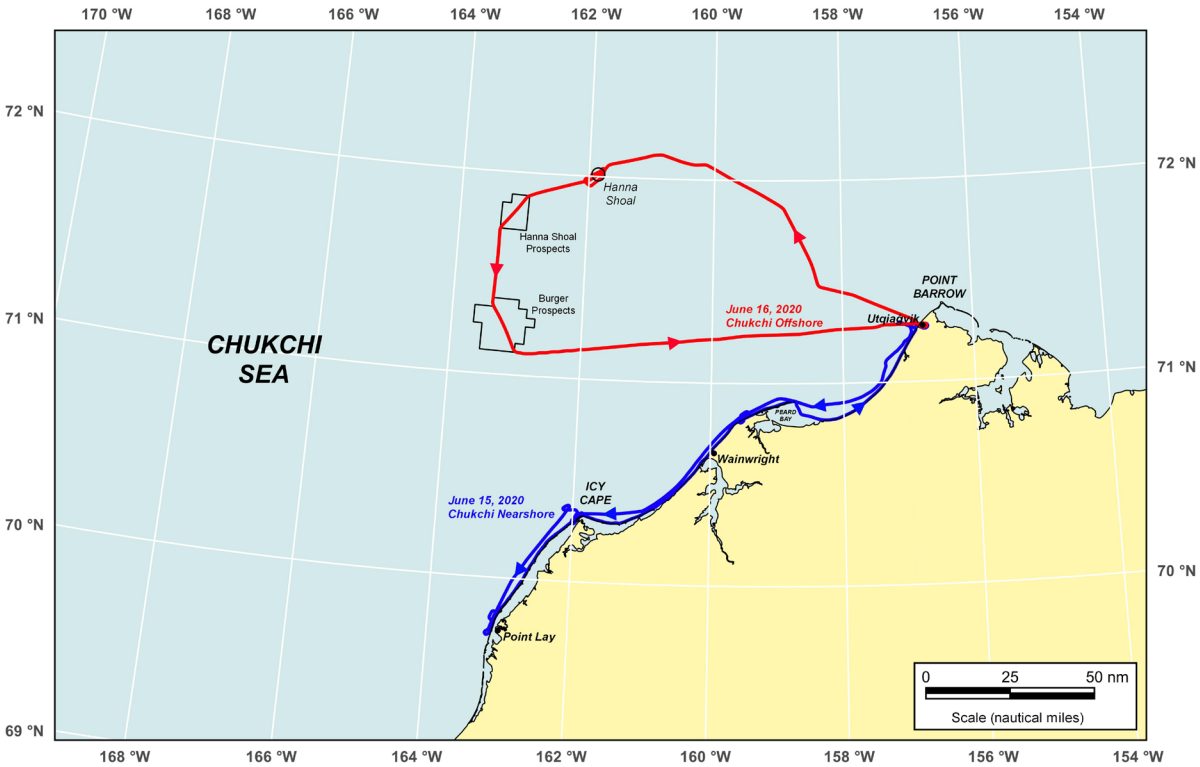

Figure 4-9. Flight Paths in Chukchi Sea

"THIS INFORMATION IS DISTRIBUTED SOLELY FOR THE PURPOSE OF PRE-DISSEMINATION PEER REVIEW UNDER APPLICABLE INFORMATION QUALITY GUIDELINES. IT HAS NOT BEEN FORMALLY DISSEMINATED BY BSEE. IT DOES NOT REPRESENT AND SHOULD NOT BE CONSTRUED TO REPRESENT ANY BSEE DETERMINATION OR POLICY."

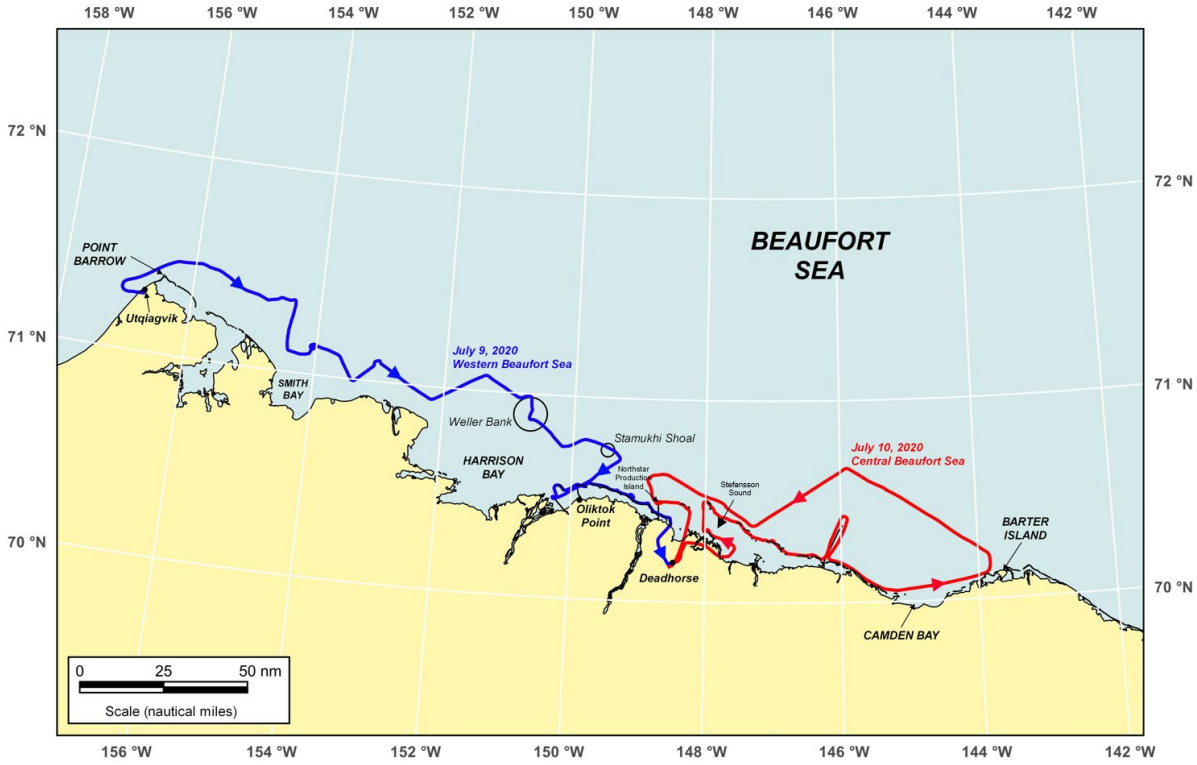

Figure 4-10. Flight Paths in Beaufort Sea

The photographs and videos are provided in digital form in Appendix E, with the file names corresponding to the identification codes shown on the drawings. The ice features and characteristics observed during the flights are denoted on the drawings using the abbreviations listed in Table 4-3. The objective and path of each flight are summarized below.

June 2020 Chukchi Sea Flight No. 1 ("C1" on Drawing CFC-1070-02-001)

The first reconnaissance flight in the Chukchi Sea was undertaken on June 15th to observe nearshore ice conditions and shoreline pile-ups between Utqiagvik and Point Lay. The flight, which was conducted under clear skies until fog was encountered just prior to landing, described the following path:

- Utqiagvik Airport
- Transit southwest to Point Lay at distances of 1 to 5 nm (2 to 9 km) offshore, altering course on several occasions to follow the landfast ice edge
- Barrier islands fronting South and North Kasegaluk Lagoon
- Shoreline from North Kasegaluk Lagoon to Point Franklin
- Seahorse Islands and Peard Bay
- Shoreline from Peard Bay to Utqiagvik
- Utqiagvik Airport
- Flight time = 2.6 hours.

"THIS INFORMATION IS DISTRIBUTED SOLELY FOR THE PURPOSE OF PRE-DISSEMINATION PEER REVIEW UNDER APPLICABLE INFORMATION QUALITY GUIDELINES. IT HAS NOT BEEN FORMALLY DISSEMINATED BY BSEE. IT DOES NOT REPRESENT AND SHOULD NOT BE CONSTRUED TO REPRESENT ANY BSEE DETERMINATION OR POLICY."

Table 4-3. Abbreviations for Ice Features

Ice Feature	Abbreviation
First-Year Ice (concentration in %)	FYI (_%)
Multiyear Ice (concentration in %)	MYI (_%)
Open Water	OW
Sea-Ice Free	SIF
Brash Ice	BSH
Ice Cake	CAK
Small Floe	SML
Medium Floe	MED
Big Floe	BIG
Compact Ice Edge	CIE
Diffuse Ice Edge	DIE
Landfast Ice Edge	LFI
Rotten Ice	RTN
Broken Ice	BKN
Inactive Shear Line	ISL
Small Melt Ponds	SMP
Medium Melt Ponds	MMP
Large Melt Ponds	LMP
Polynya	PLY
Through-Ice Holes	TIH
Ridges	RDG (_m)
Ruble	RBL (_m)
Pile-Up	P/U (_,_m)
Relict Pile-Up	P/U (relict)

Note: The prefixes "i" and "m" are used to indicate intermittent features and multiple features, respectively *(i.e.*, "iRBL" indicates intermittent rubble). The prefix "g" is used to indicate grounded features.

"THIS INFORMATION IS DISTRIBUTED SOLELY FOR THE PURPOSE OF PRE-DISSEMINATION PEER REVIEW UNDER APPLICABLE INFORMATION QUALITY GUIDELINES. IT HAS NOT BEEN FORMALLY DISSEMINATED BY BSEE. IT DOES NOT REPRESENT AND SHOULD NOT BE CONSTRUED TO REPRESENT ANY BSEE DETERMINATION OR POLICY."

June 2020 Chukchi Sea Flight No. 2 ("C2" on Drawing CFC-1070-02-001)

The second reconnaissance flight in the Chukchi Sea was undertaken on June 16th to observe the ice conditions in the offshore region to the northwest and west of Point Barrow. With the exception of the region north and west of the Burger Prospects, where fog was present, clear skies and excellent visibility prevailed. The flight proceeded in the following manner:

- Utqiagvik Airport
- Transit northwest, altering course as necessary to follow the edge of the pack ice
- Hanna Shoal
- Transit southwest
- Hanna Shoal Prospects
- Transit south
- Burger Prospects
- Transit east
- Utqiagvik Airport
- Flight time = 1.6 hours.

July 2020 Beaufort Sea Flight No. 1 ("B1" on Drawing CFC-1070-02-002)

The first reconnaissance flight in the Beaufort Sea was undertaken on July 9th to observe the ice conditions in the western portion. Dense fog prevailed at the beginning of the flight but diminished as the aircraft travelled east. Nevertheless, intermittent fog and poor visibility were encountered on numerous occasions. The flight path was as follows:

- Utqiagvik Airport
- Point Barrow
- Transit southeast at distances of 10 to 40 nm (19 to 74 km) offshore
- Weller Bank
- Harrison Bay Prospects, including Stamukhi Shoal
- Spy Island Drillsite (SID)
- Oooguruk Offshore Drillsite (ODS)
- Thetis Island
- Barrier islands from Spy to Stump (heading east)
- West Dock Causeway
- Deadhorse Airport
- Flight time = 2.2 hours.

"THIS INFORMATION IS DISTRIBUTED SOLELY FOR THE PURPOSE OF PRE-DISSEMINATION PEER REVIEW UNDER APPLICABLE INFORMATION QUALITY GUIDELINES. IT HAS NOT BEEN FORMALLY DISSEMINATED BY BSEE. IT DOES NOT REPRESENT AND SHOULD NOT BE CONSTRUED TO REPRESENT ANY BSEE DETERMINATION OR POLICY."

July 2020 Beaufort Sea Flight No. 2 ("B2" on Drawing CFC-1070-02-003)

The second reconnaissance flight in the Beaufort Sea was undertaken on July 10th to observe the ice conditions in the central portion. The route was as follows:

- Deadhorse Airport
- Stefansson Sound, including Endicott Development and Liberty Prospect
- Barrier islands from Cross to North Star (heading east-southeast)
- Sivulliq Development prospective pipeline route
- Flaxman Island, Brownlow Point, and adjacent spit
- Transit east across Camden Bay to Barter Island
- Barter Island
- Transit northwest
- Camden Bay Prospects
- Transit west at distances of 2 to 30 nm (4 to 56 km) off barrier islands
- Northstar Production Island
- Reindeer and Argo Islands
- Prudhoe Bay
- Deadhorse Airport
- Flight time = 2.0 hours.

"THIS INFORMATION IS DISTRIBUTED SOLELY FOR THE PURPOSE OF PRE-DISSEMINATION PEER REVIEW UNDER APPLICABLE INFORMATION QUALITY GUIDELINES. IT HAS NOT BEEN FORMALLY DISSEMINATED BY BSEE. IT DOES NOT REPRESENT AND SHOULD NOT BE CONSTRUED TO REPRESENT ANY BSEE DETERMINATION OR POLICY."

5. LATE WINTER

Arctic sea ice attained its maximum extent for the 2019-20 winter season on March 5th (NASA, 2020b; "extent" refers to the area in which ice covers at least 15% of the ocean surface). The total area, 15.05 million km^2, although the highest since 2013, was the eleventh lowest since the acquisition of satellite-based data began in 1979.

As shown in Figure 5-1, the maximum ice extent approached its median location for the 30-year period from 1981 through 2010 in the Bering Sea but fell short off the coasts of eastern Canada, Greenland, and western Russia. The net result was a deficiency of 590,000 km^2 relative to the average maximum extent over this 30-yr span.

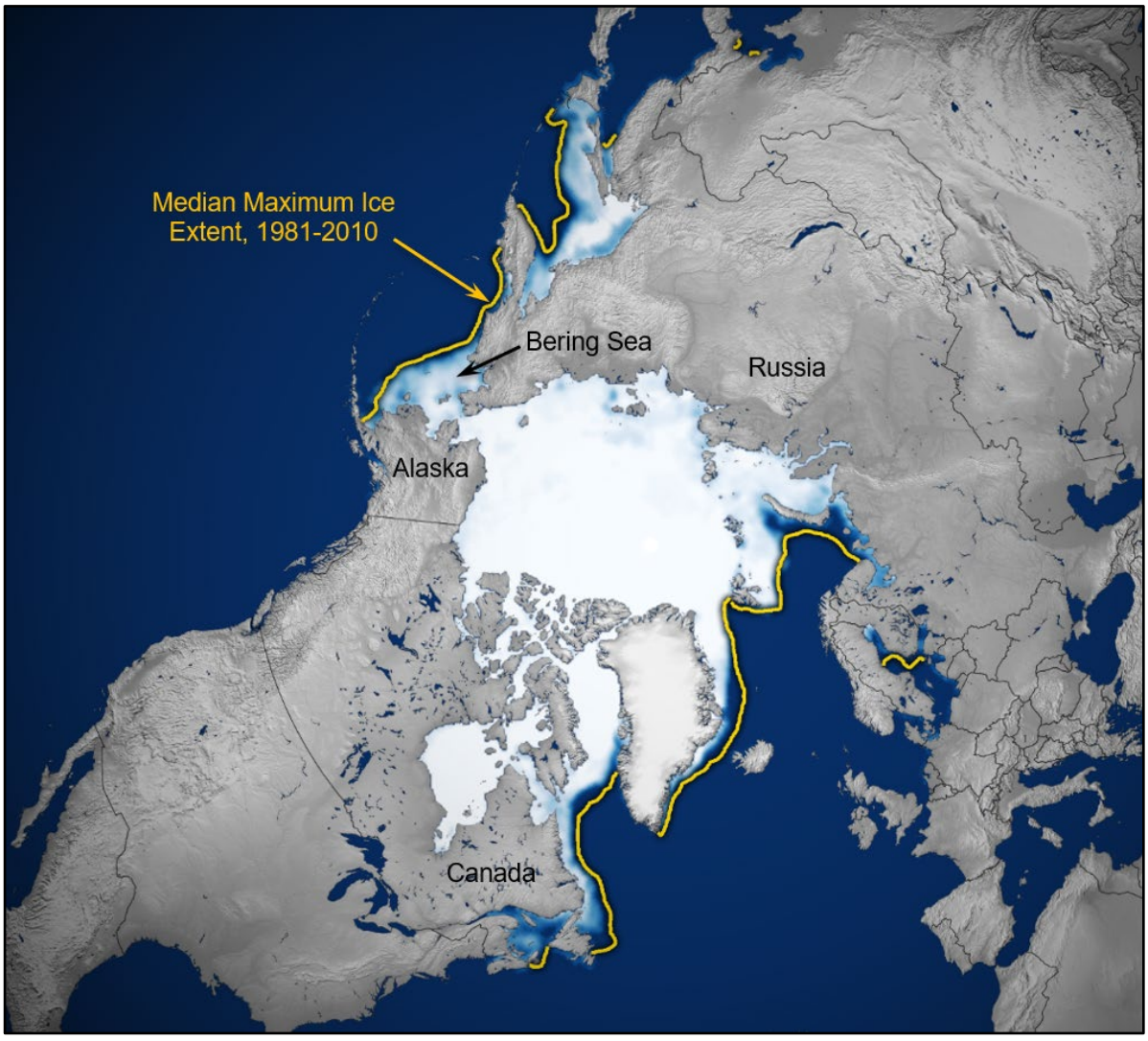

After: NASA, 2020b

Figure 5-1. Sea Ice Maximum Extent on March 5, 2020

"THIS INFORMATION IS DISTRIBUTED SOLELY FOR THE PURPOSE OF PRE-DISSEMINATION PEER REVIEW UNDER APPLICABLE INFORMATION QUALITY GUIDELINES. IT HAS NOT BEEN FORMALLY DISSEMINATED BY BSEE. IT DOES NOT REPRESENT AND SHOULD NOT BE CONSTRUED TO REPRESENT ANY BSEE DETERMINATION OR POLICY."

Notwithstanding the uptick that occurred in 2020, the average extent of the Arctic sea ice in March has declined at a rate of 2.6% per decade during the 42-year period of record (1979-2020; National Snow and Ice Data Center, 2020). As illustrated in Figure 5-2, substantial interannual variations have occurred around this long-term trend. It is noteworthy that the rate of decline in March represents only about 20% of that which has occurred in September (12.9% per decade), when the minimum ice extent occurs (National Snow and Ice Data Center, 2019).

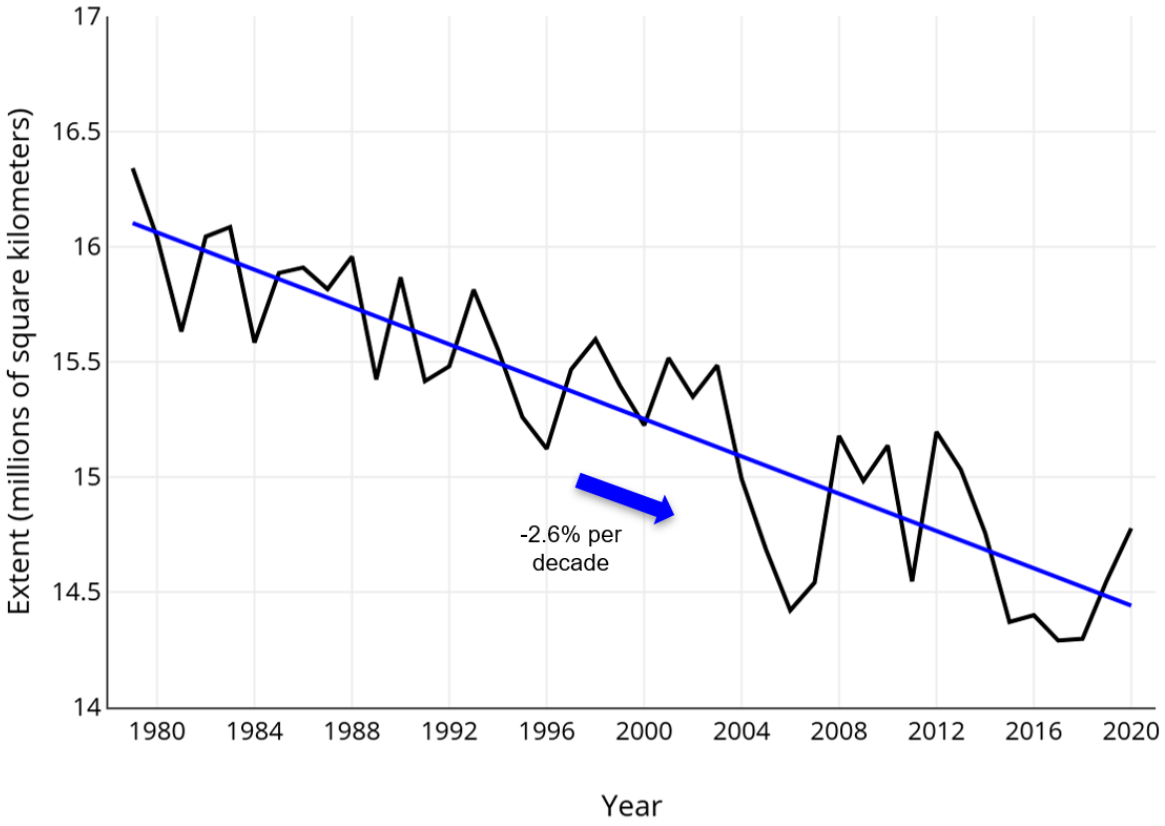

After: National Snow and Ice Data Center, 2020

Figure 5-2. Sea Ice Average Extent in March, 1979-2020

As reported in the 2019-20 Freeze-Up Study (Coastal Frontiers and Vaudrey, 2020), the air temperatures in the Alaskan Arctic cycled through a warm phase during the early portion of freeze-up (October through December) and cold phase during the later portion (January and February). Despite the occurrence of the cold phase, the winter of 2019-20 was the sixth warmest in the past 50 years based on temperature data recorded at Utqiagvik Airport.

The computed thickness of undeformed first-year ice at the end of the 2019-20 winter season was 148 cm in the Chukchi Sea and 162 cm in the Alaskan Beaufort Sea,

"THIS INFORMATION IS DISTRIBUTED SOLELY FOR THE PURPOSE OF PRE-DISSEMINATION PEER REVIEW UNDER APPLICABLE INFORMATION QUALITY GUIDELINES. IT HAS NOT BEEN FORMALLY DISSEMINATED BY BSEE. IT DOES NOT REPRESENT AND SHOULD NOT BE CONSTRUED TO REPRESENT ANY BSEE DETERMINATION OR POLICY."

corresponding to accumulations of 6,122 and 7,143 FDD at Utqiagvik and Deadhorse Airports, respectively (Coastal Frontiers and Vaudrey, 2020). The thickness in the Chukchi was 2 cm greater than the average value of 146 cm computed for the past 11 winters, while the thickness in the Beaufort was 8 cm thicker than the corresponding average of 154 cm. In both cases, the maximum thickness was attained on May 21st.

Figure 5-3 illustrates the condition of the ice canopy on April 30th, when a narrow flaw lead was present throughout most of the study area. The flaw lead in the Beaufort subsequently closed, but that in the Chukchi remained open and grew progressively wider over the course of break-up.

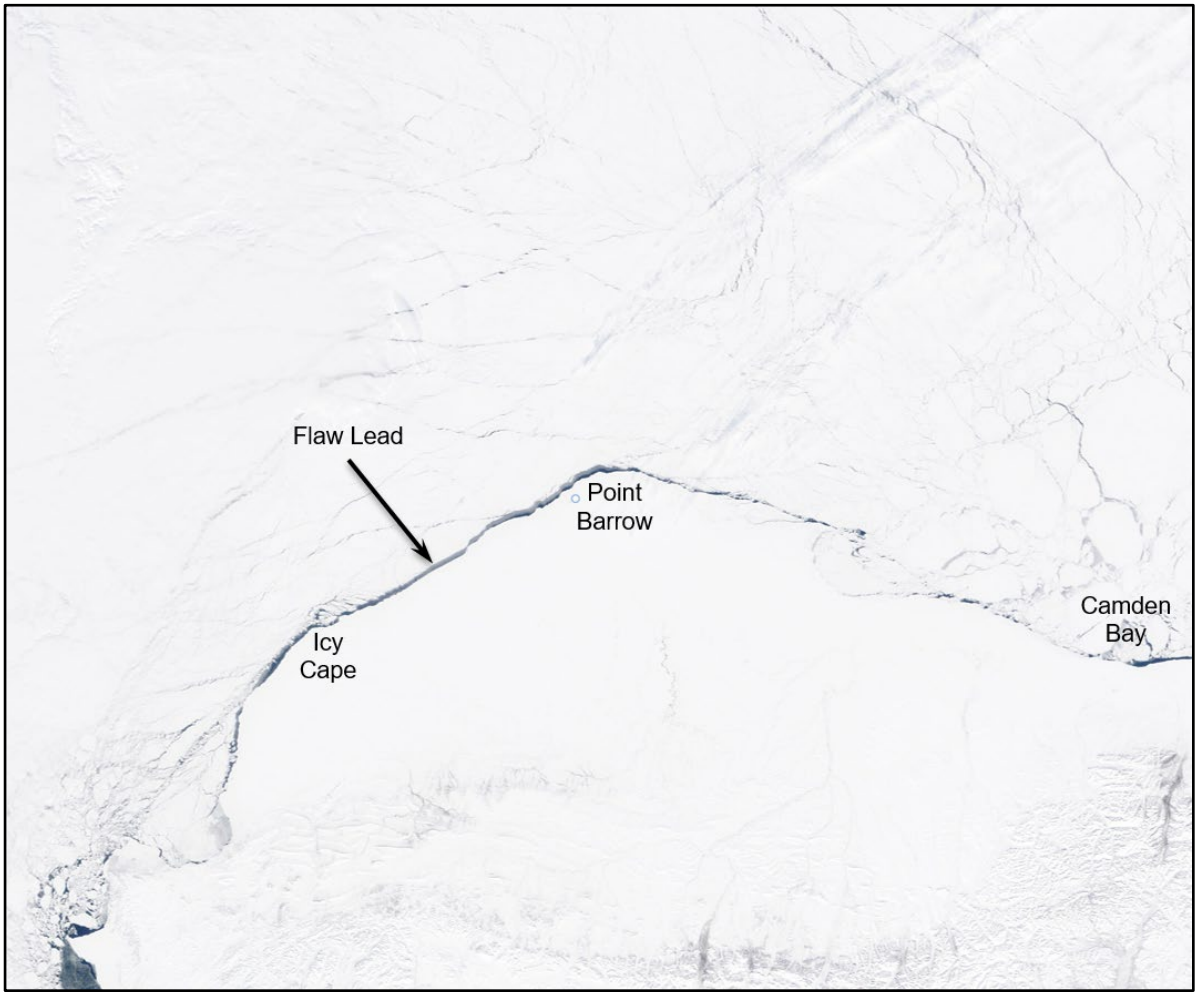

After: NASA, 2020a

Figure 5-3. MODIS Image Acquired on April 20, 2020

"THIS INFORMATION IS DISTRIBUTED SOLELY FOR THE PURPOSE OF PRE-DISSEMINATION PEER REVIEW UNDER APPLICABLE INFORMATION QUALITY GUIDELINES. IT HAS NOT BEEN FORMALLY DISSEMINATED BY BSEE. IT DOES NOT REPRESENT AND SHOULD NOT BE CONSTRUED TO REPRESENT ANY BSEE DETERMINATION OR POLICY."

6. CHUKCHI SEA BREAK-UP

Section 6.1 presents a concise overview of the 2020 break-up season in the northeast Chukchi Sea. Sections 6.2 through 6.5 present a month-by-month analysis of the conditions that prevailed during this period along with a summary of the observations made during the reconnaissance flights.

6.1. Overview

Air Temperatures: The daily average air temperatures at Utqiagvik Airport remained within or close to the normal range throughout the three-month study period encompassing May, June, and July. Over the entire 92-day span, the daily average values exceeded the normal range on 13 days (14% frequency) and fell below on six days (7% frequency). Thawing degree days (TDD) began to accumulate on May 29th, when the daily average air temperature reached 33°F (1°C).

Winds: Wind conditions during the 2020 break-up season are summarized in Table 6-1, which is based on the daily average speeds and directions recorded at Utqiagvik Airport. Easterlies outnumbered westerlies by wide margins in each of the three months. Over the entire period, easterlies occurred 77% of the time versus 23% for westerlies. The monthly average speeds were nearly constant, with values of 11 kt (6 m/s) in May, 10 kt (5 m/s) in June, and 11 kt (6 m/s) in July.

Table 6-1. Chukchi Sea Wind Characteristics, May–July 2020

Month	Easterly Wind Predominance (days)	Westerly Wind Predominance (days)	Average Speed (kt)
May	28	3	11
June	24	6	10
July	19	12	11
Total Days	**71**	**21**	n/a
Frequency (%)	**77**	**23**	n/a

Note: Table 6-1 is based on the daily average sustained wind speeds and directions recorded at Utqiagvik Airport.

Storms: The characteristics of all storm events with daily average sustained wind speeds that exceeded 15 kt (8 m/s) at Utqiagvik Airport are presented in Table 6-2. Only four storms occurred during the study period, consisting of three easterlies and one westerly. The most severe event in terms of peak wind speed (24 kt; 12 m/s) was a three-day easterly

"THIS INFORMATION IS DISTRIBUTED SOLELY FOR THE PURPOSE OF PRE-DISSEMINATION PEER REVIEW UNDER APPLICABLE INFORMATION QUALITY GUIDELINES. IT HAS NOT BEEN FORMALLY DISSEMINATED BY BSEE. IT DOES NOT REPRESENT AND SHOULD NOT BE CONSTRUED TO REPRESENT ANY BSEE DETERMINATION OR POLICY."

Table 6-2. Chukchi Sea Storm Characteristics, May–July 2020[1]

Month	Day	Duration (days)	Maximum Easterly Wind Speed[2] (kt)	Maximum Westerly Wind Speed[2] (kt)
May	11-13	3	24	-
June	May 31 - June 3	4	19	-
July	3	1	16	-
July	27-29	3	-	20
Total Duration	n/a	**11**	n/a	n/a
Total Number of Events	n/a	n/a	**3**	**1**

Notes:

[1] Table 6-2 includes all storm events with a daily average sustained wind speed exceeding 15 kt (8 m/s) at Utqiagvik Airport.

[2] "Maximum Wind Speed" refers to the highest daily average sustained wind speed that occurred during each storm event.

that began on May 11th. The longest duration was associated with a different easterly event that began on May 31st and continued for three additional days.

Ice Thickness: The thickness of the decaying, undeformed first-year ice sheet was estimated using the following relationship (Bilello, 1980) in concert with TDD accumulated at Utqiagvik Airport (Table 4-1):

$$t = t_{max} - \{0.508\ (\Sigma TDD)\} \qquad (1)$$

where:

t = ice thickness in cm;
t_{max} = maximum ice thickness in cm prior to decay;
ΣTDD = accumulated thawing degree days relative to 32°F.

The results are presented in Table 6-3, which indicates that the maximum computed thickness of 148 cm at the end of the winter season (Coastal Frontiers and Vaudrey, 2020) decreased to zero during the 59-day period that began on May 29th and ended on July 26th.

Coastal Flaw Lead: The narrow flaw lead that existed off the Chukchi Sea coast at the end of April (Figure 5-3) expanded throughout May, evolving into a large expanse of open water that was approximately 15 nm (37 km) wide off Point Barrow and 85 nm (158 km) wide off Point Lay at month-end. It continued to expand in June and July.

"THIS INFORMATION IS DISTRIBUTED SOLELY FOR THE PURPOSE OF PRE-DISSEMINATION PEER REVIEW UNDER APPLICABLE INFORMATION QUALITY GUIDELINES. IT HAS NOT BEEN FORMALLY DISSEMINATED BY BSEE. IT DOES NOT REPRESENT AND SHOULD NOT BE CONSTRUED TO REPRESENT ANY BSEE DETERMINATION OR POLICY."

Table 6-3. Chukchi Sea Computed Ice Thickness, 2020 Break-Up[1]

Date	TDD	Accumulated TDD	Ice Thickness (cm)
May 28	0	0	148[2]
May 30	2	2	147[3]
June 30	147	149	72
July 26	148	297	0

Notes:

[1] Table 6-3 is based on the daily average air temperatures recorded at Utqiagvik Airport.

[2] The ice thickness at end of 2019-20 the winter season was computed by Coastal Frontiers and Vaudrey (2020) from accumulated FDD using the method of Lebedev (Bilello, 1960).

[3] The ice thickness after May 28th was computed from accumulated TDD using the method of Bilello (1980).

River Overflood: Of the seven rivers that discharge in or adjacent to the Chukchi Sea study area, the Kukpowruk was the first to begin overflooding the sea ice, on May 12th, and the Kuk and Kugrua were the last, on June 1st. Most of the flood water was contained in the receiving lagoons with minimal penetration onto the landfast ice farther offshore. The date on which the discharge from each river first reached the sea ice, as estimated from MODIS imagery, is provided in Table 6-4.

Lagoon Ice: Break-up of the ice in South Kasegaluk Lagoon took place on May 24th, followed by that in North Kasegaluk Lagoon and the Kuk River Entrance on June 10th and Peard Bay on June 14th. Open water occurred in South Kasegaluk Lagoon on June 20th, North Kasegaluk Lagoon on June 27th or 28th, the Kuk River Entrance between June 25th and 30th, and Peard Bay on July 7th. This sequence of events, derived from a combination of MODIS and RADARSAT-2 imagery, is summarized in Table 6-5.

Landfast Ice: In early May, the landfast ice edge tended to follow the 18-m isobath between Point Lay and Point Franklin, and to describe a straight line in deeper water between Point Franklin and Point Barrow. The maximum width, 18 nm (33 km), was located off Skull Cliff; the minimum, 1.3 nm (2.4 km) was located between Point Belcher and the base of the Point Franklin Spit.

Break-up of the landfast ice occurred on May 13th when an easterly storm (Table 6-2) dislodged a large piece from the region between Wainwright and Icy Cape, and smaller pieces from the region between Icy Cape and Point Lay. Intermittent losses followed

"THIS INFORMATION IS DISTRIBUTED SOLELY FOR THE PURPOSE OF PRE-DISSEMINATION PEER REVIEW UNDER APPLICABLE INFORMATION QUALITY GUIDELINES. IT HAS NOT BEEN FORMALLY DISSEMINATED BY BSEE. IT DOES NOT REPRESENT AND SHOULD NOT BE CONSTRUED TO REPRESENT ANY BSEE DETERMINATION OR POLICY."

Table 6-4. Chukchi Sea River Overflood onto Sea Ice, 2020 Break-Up

River[1]	Receiving Body	Start of Overflood[2]
Kukpowruk[3]	South Kasegaluk Lagoon	May 12
Kokolik	South Kasegaluk Lagoon	May 13
Utukok	South Kasegaluk Lagoon	May 14
Avak	North Kasegaluk Lagoon	May 29
Nokotlek	North Kasegaluk Lagoon	May 28
Kuk	Kuk River Entrance	June 1
Kugrua	Peard Bay	June 1

Notes:
1. The rivers are listed from south to north, with their locations shown in Figure 1-4.
2. The date represents the first day on which overflood water was detected on the sea ice in MODIS imagery.
3. Although the Kukpowruk River discharges to the south of the study area, its overflood can reach the vicinity of Point Lay.

Table 6-5. Break-Up and Open Water in Chukchi Sea Lagoons, 2020

Lagoon	Break-Up[1]	Open Water[2]
South Kasegaluk Lagoon	May 24	June 20
North Kasegaluk Lagoon	June 10	June 27-28[3]
Kuk River Entrance	June 10	June 25-30[3]
Peard Bay	June 14	July 7

Notes:
1. The date of break-up represents the first occasion on which ice coverage below 10/10s was detected in MODIS and RADARSAT-2 imagery.
2. The date of open water represents the first occasion on which ice coverage below 1/10 was detected in MODIS and RADARSAT-2 imagery.
3. The exact date could not be determined due to a gap in useful satellite imagery.

during the remainder of May and first half of June, including a massive piece measuring 72 km long and 18 km wide that broke free from the region between Point Franklin and Utqiagvik on June 3rd.

"THIS INFORMATION IS DISTRIBUTED SOLELY FOR THE PURPOSE OF PRE-DISSEMINATION PEER REVIEW UNDER APPLICABLE INFORMATION QUALITY GUIDELINES. IT HAS NOT BEEN FORMALLY DISSEMINATED BY BSEE. IT DOES NOT REPRESENT AND SHOULD NOT BE CONSTRUED TO REPRESENT ANY BSEE DETERMINATION OR POLICY."

The rate of loss increased in mid-June in apparent response to a combination of moderate northeasterly winds and warm air temperatures. River overflood did not materially impact the degradation of the landfast ice due to its minimal penetration outside the lagoon areas.

At the beginning of July, the landfast ice that remained consisted of intermittent patches spanning the entire length of the study area. The largest accumulations were located in the vicinity of Icy Cape and Point Franklin. The last remnant, grounded off the base of the Point Franklin Spit, disappeared on July 16th or 17th.

Pack Ice: The pack ice retreated to the northwest in May, increasing the width of the flaw lead to approximately 15 nm (37 km) off Point Barrow and 85 nm (158 km) off Point Lay at month-end. Although the retreat continued in June, it proceeded at a slower pace that reflected occasional reversals. At the end of June, a large expanse of ice-free water existed to the west and south of the Kuk River Entrance as well as in a tongue that extended north through the Devil's Paw and Crackerjack Prospects.

The pack ice continued to dissipate in July, vacating the Siberian coast during the third week of the month. At the end of July, the southern edge trended northwest from the vicinity of Utqiagvik with the exception of a 50-nm (93-km) wide tongue that extended southwest as far as the Devil's Paw Prospects.

Ice Pile-Ups: Of the 57 ice pile-ups observed on the Chukchi Sea coast in late February (Coastal Frontiers and Vaudrey, 2020), 53 were evident at the time of the break-up flights in mid-June. The remaining four had decayed to the point that they were unrecognizable.

In addition to the relict pile-ups from freeze-up, five new pile-ups that had formed during break-up were identified. Two were located on the barrier islands between Point Lay and Icy Cape, while three were located on the mainland shore near the base of the Point Franklin Spit. As shown in Table 6-6, the heights ranged from 2 to 5 m, the encroachment distances from 3 to 5 m onto the subaerial beach, and the alongshore lengths from 600 to 2,800 m. All five appeared to have approached from the northwest quadrant.

The new pile-ups probably resulted from a wind shift that took place on June 8th. Strong easterly winds prevailed prior to this date, consisting of a four-day easterly storm from May 31st through June 3rd (Table 6-2) followed by one-hour sustained wind speeds greater than or equal to 15 kt (8 m/s) on portions of the 4th, 5th, and 6th. On the 8th, the wind backed abruptly from east through north to northwest and peaked at 11 kt (6 m/s).

"THIS INFORMATION IS DISTRIBUTED SOLELY FOR THE PURPOSE OF PRE-DISSEMINATION PEER REVIEW UNDER APPLICABLE INFORMATION QUALITY GUIDELINES. IT HAS NOT BEEN FORMALLY DISSEMINATED BY BSEE. IT DOES NOT REPRESENT AND SHOULD NOT BE CONSTRUED TO REPRESENT ANY BSEE DETERMINATION OR POLICY."

Table 6-6. Ice Pile-Ups on Chukchi Sea Coast during 2020 Break-Up Season

No.	Location	Formation Date	Arrived From	Length[1] (m)	Height[2] (m)	Encroachment[3] (m)
1	South of Icy Cape	Jun 8	W	600	3	5
2	South of Icy Cape	Jun 8	W	650	2	5
3	Pt. Belcher – Peard Bay	Jun 8	NW	2,750	5	5
4	Pt. Belcher – Peard Bay	Jun 8	NW	1,150	2	3
5	Pt. Belcher – Peard Bay	Jun 8	NW	2,800	5	3

Notes:
[1] "Length" indicates the alongshore extent of the pile-up.
[2] "Height" indicates the maximum height of the pile-up relative to MSL.
[3] "Encroachment" indicates the distance that the ice advanced onto the subaerial beach.

Multi-Year Ice: Multi-year ice was present in the Chukchi Sea study area throughout the break-up study period. As discussed in the 2019-20 Freeze-Up Study report (Coastal Frontiers and Vaudrey, 2020), relatively small multi-year floes with maximum horizontal dimensions typically less than 100 m were observed in the landfast ice zone in late February. The concentrations tended to range from negligible to 20%. The floes remained embedded in the landfast ice through early May, when they began to disperse. Their dispersal mirrored the break-up of the landfast ice, with the last vestige disappearing in mid-July.

Multi-year ice also was present in the pack ice. The concentrations ranged from negligible to 30%, while the maximum horizontal dimensions ranged from less than 10 m to more than 10 km. In mid-May, the southern edge was located approximately 4 nm (7 km) off Point Barrow and 40 nm (74 km) off Icy Cape. In mid-July, the distance off Point Barrow remained unchanged while that off Icy Cape had increased to 60 nm (111 km) due to the northward retreat of the pack.

Ice Drift: Ice drift was investigated using three telemetry buoys (Buoys A, B, and C) monitored through the International Arctic Buoy Programme (Section 4.4). Their trajectories are shown in Figure 6-1.

Buoy A, deployed in the landfast ice off Utqiagvik on May 29th, remained stationary until the surrounding ice broke up on June 11th. A MODIS image acquired on this date suggested that it was discharged into open water, and therefore was unsuitable for quantifying ice drift. Buoys B and C entered the Chukchi Sea study area in late June and moved to the northwest under the influence of easterly winds. Tracking was terminated on June 20th, when they appeared to be located in open water.

"THIS INFORMATION IS DISTRIBUTED SOLELY FOR THE PURPOSE OF PRE-DISSEMINATION PEER REVIEW UNDER APPLICABLE INFORMATION QUALITY GUIDELINES. IT HAS NOT BEEN FORMALLY DISSEMINATED BY BSEE. IT DOES NOT REPRESENT AND SHOULD NOT BE CONSTRUED TO REPRESENT ANY BSEE DETERMINATION OR POLICY."

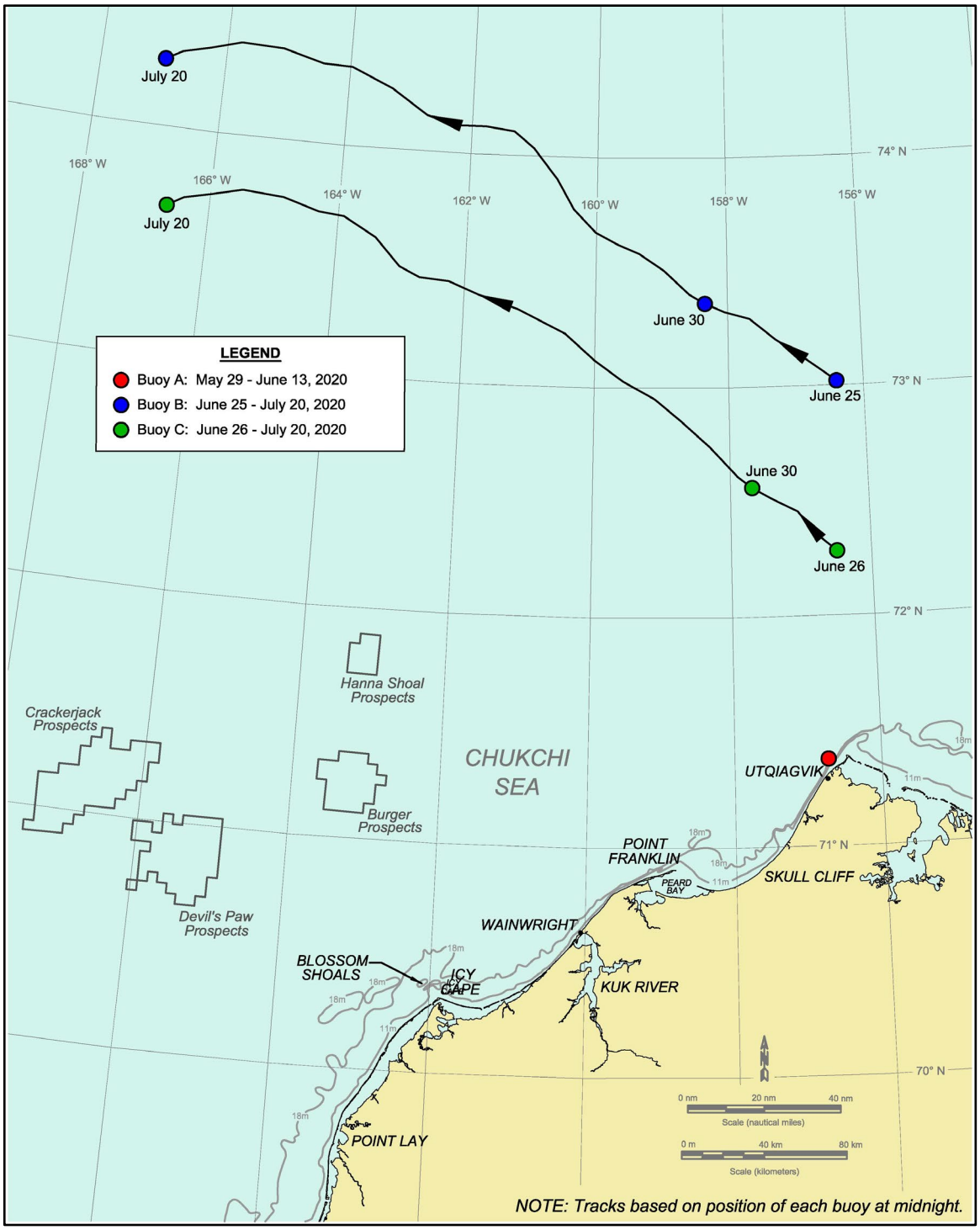

Figure 6-1. Chukchi Sea Drift Buoy Tracks, May-July 2020

In accordance with the convention adopted for previous freeze-up and break-up studies (*e.g.*, Coastal Frontiers and Vaudrey, 2020), monthly average speeds were computed for Buoys B and C using the net displacement of each floe between July 1st and July 20th. The

"THIS INFORMATION IS DISTRIBUTED SOLELY FOR THE PURPOSE OF PRE-DISSEMINATION PEER REVIEW UNDER APPLICABLE INFORMATION QUALITY GUIDELINES. IT HAS NOT BEEN FORMALLY DISSEMINATED BY BSEE. IT DOES NOT REPRESENT AND SHOULD NOT BE CONSTRUED TO REPRESENT ANY BSEE DETERMINATION OR POLICY."

speeds, 7.8 nm/day (14.5 km/day) for Buoy B and 8.5 nm/day (15.8 km/day) for Buoy C, averaged 8.2 nm/day (15.2 km/day), a relatively high value that reflects the amplifying effect of easterly winds on the Beaufort Gyre in concert with a low degree of confinement. Drift data that satisfied the minimum acceptable tracking period of 16 days for the derivation of a monthly average value were not available for May and June.

Table 6-7. Chukchi Sea Pack Ice Drift, May–July 2020

Month	No. of Buoys	Maximum Monthly Average Speed (nm/day)	Minimum Monthly Average Speed (nm/day)	Average Monthly Average Speed (nm/day)
May	0	-	-	-
June	0	-	-	-
July	2	8.5	7.8	8.1
Average	n/a	n/a	n/a	**8.1**

Note: Monthly average speeds were derived for a period of 20 days (July 1st–20th).

6.2. May 2020

Meteorological Conditions: The daily values of average sustained wind speed, maximum sustained wind speed, average wind direction, and average air temperature at Utqiagvik Airport are shown in Figure 6-2 along with the normal range of air temperatures derived by averaging the daily highs and lows over the 30-year period from 1981 through 2010. The significance of the red and blue color bands in this and all subsequent meteorological plots is illustrated in Table 6-8. Unless stated otherwise, the wind speeds cited in the text refer to the daily average values rather than the daily maximum values or hourly values.

The daily average air temperatures in May ranged from 6 to 33°F (-14 to 1°C). The average was 23°F (-5°C). The temperatures exceeded the normal range on seven days while falling below on four.

Easterly winds outnumbered westerlies by a wide margin, occurring on 28 of the 31 days (Table 6-1). The average speed was 11 kt (6 m/s), while the storm population consisted of a single easterly event (Table 6-2):

- May 11th-13th: three-day easterly with maximum speed of 24 kt (12 m/s).

"THIS INFORMATION IS DISTRIBUTED SOLELY FOR THE PURPOSE OF PRE-DISSEMINATION PEER REVIEW UNDER APPLICABLE INFORMATION QUALITY GUIDELINES. IT HAS NOT BEEN FORMALLY DISSEMINATED BY BSEE. IT DOES NOT REPRESENT AND SHOULD NOT BE CONSTRUED TO REPRESENT ANY BSEE DETERMINATION OR POLICY."

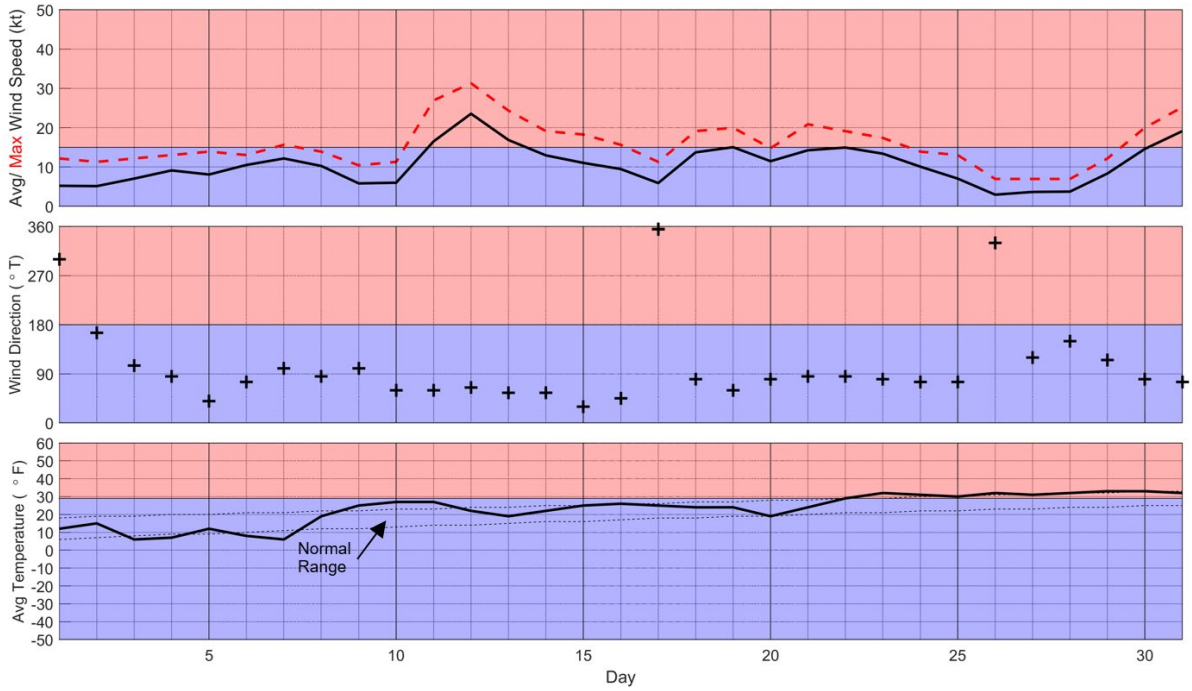

Figure 6-2 Meteorological Conditions at Utqiagvik Airport in May 2020

Table 6-8. Significance of Color Bands in Plots of Meteorological Conditions

Parameter	Blue Band	Red Band
Wind Speed	≤ 15 kt	> 15 kt (Storm)
Wind Direction	Easterly	Westerly
Air Temperature	≤ 32°F (Melting Point of Seawater)	>32°F

Ice Thickness: Using the method of Lebedev (Bilello, 1960) in concert with accumulated FDD at Utqiagvik Airport, the thickness of undisturbed first-year ice was computed to be 145 cm at the beginning of May (Coastal Frontiers and Vaudrey, 2020). The maximum thickness attained during the 2019-20 winter season, 148 cm, followed on May 21st (Section 5).

TDD began to accumulate on May 29th when the daily average air temperature reached 33°F (1°C). Two TDD had accumulated at month-end, reducing the computed thickness of undisturbed ice to 147 cm.

"THIS INFORMATION IS DISTRIBUTED SOLELY FOR THE PURPOSE OF PRE-DISSEMINATION PEER REVIEW UNDER APPLICABLE INFORMATION QUALITY GUIDELINES. IT HAS NOT BEEN FORMALLY DISSEMINATED BY BSEE. IT DOES NOT REPRESENT AND SHOULD NOT BE CONSTRUED TO REPRESENT ANY BSEE DETERMINATION OR POLICY."

Coastal Flaw Lead: The flaw lead that developed in early April (Section 5) continued to expand in May. As is evident from a comparison of Figures 5-3, 6-3 and 6-4, the feature evolved from a well-defined lead at the beginning of the month into a large expanse of open water at the end. It remained open and continued to expand throughout June and July.

River Overflood: The three major rivers that discharge into South Kasegaluk Lagoon began overflooding the sea ice in quick succession, beginning with the Kukpowruk on May 12th and followed by the Kokolik on the 13th and Utukok on the 14th. Discharge into North Kasegaluk Lagoon commenced several weeks later, with flood water from the Nokotlek and Avak Rivers reaching the lagoon ice on May 28th and 29th, respectively. At the end of the month, the overflood water covered about 90% of South Kasegaluk Lagoon and 70% of North Kasegaluk Lagoon (Figure 6-5). Nearly all of the water remained inside the lagoons, with minimal flooding of the landfast ice outside the barrier islands.

As discussed by Reimnitz, *et al*. (1974), and Leidersdorf, *et al. (*2007), through-ice drainage of the overflood water can create large depressions in the sea bottom known as "strudel scours". Although quantitative information on the severity of strudel scouring is lacking for the northeast Chukchi Sea, evidence of vigorous drainage observed during a reconnaissance flight conducted on June 1, 2011 suggests that substantial scour depressions can occur off the river mouths in Kasegaluk Lagoon (Plate 6-1; Coastal Frontiers, 2011).

Lagoon Ice: Break-up in South Kasegaluk Lagoon occurred on May 24th when the relatively warm discharge from the Kukpowruk began to melt through the lagoon ice in the immediate vicinity of the river mouth. Based on an analysis of MODIS and RADARSAT-2 imagery, the ice in North Kasegaluk Lagoon, the Kuk River Entrance, and Peard Bay remained intact throughout the month of May.

Landfast Ice: In early May, the seaward edge of the landfast ice tended to follow the 18-m isobath between Point Lay and Point Franklin, and to describe a straight line in deeper water between Point Franklin and Point Barrow. The maximum width, 18 nm (33 km), was located in the embayment off Skull Cliff; the minimum, 1.3 nm (2.4 km) was located between Point Belcher and the base of the Point Franklin Spit.

Break-up of the landfast ice occurred on May 13th when an easterly storm (Table 6-2) dislodged a large piece from the region between Wainwright and Icy Cape, and smaller pieces from the region between Icy Cape and Point Lay. Intermittent losses from these two regions followed during the remainder of the month. In contrast, the landfast ice between Utqiagvik and Wainwright remained intact throughout May. The locations of the ice edge on May 14th and 31st are shown in Figure 6-6.

“THIS INFORMATION IS DISTRIBUTED SOLELY FOR THE PURPOSE OF PRE-DISSEMINATION PEER REVIEW UNDER APPLICABLE INFORMATION QUALITY GUIDELINES. IT HAS NOT BEEN FORMALLY DISSEMINATED BY BSEE. IT DOES NOT REPRESENT AND SHOULD NOT BE CONSTRUED TO REPRESENT ANY BSEE DETERMINATION OR POLICY.”

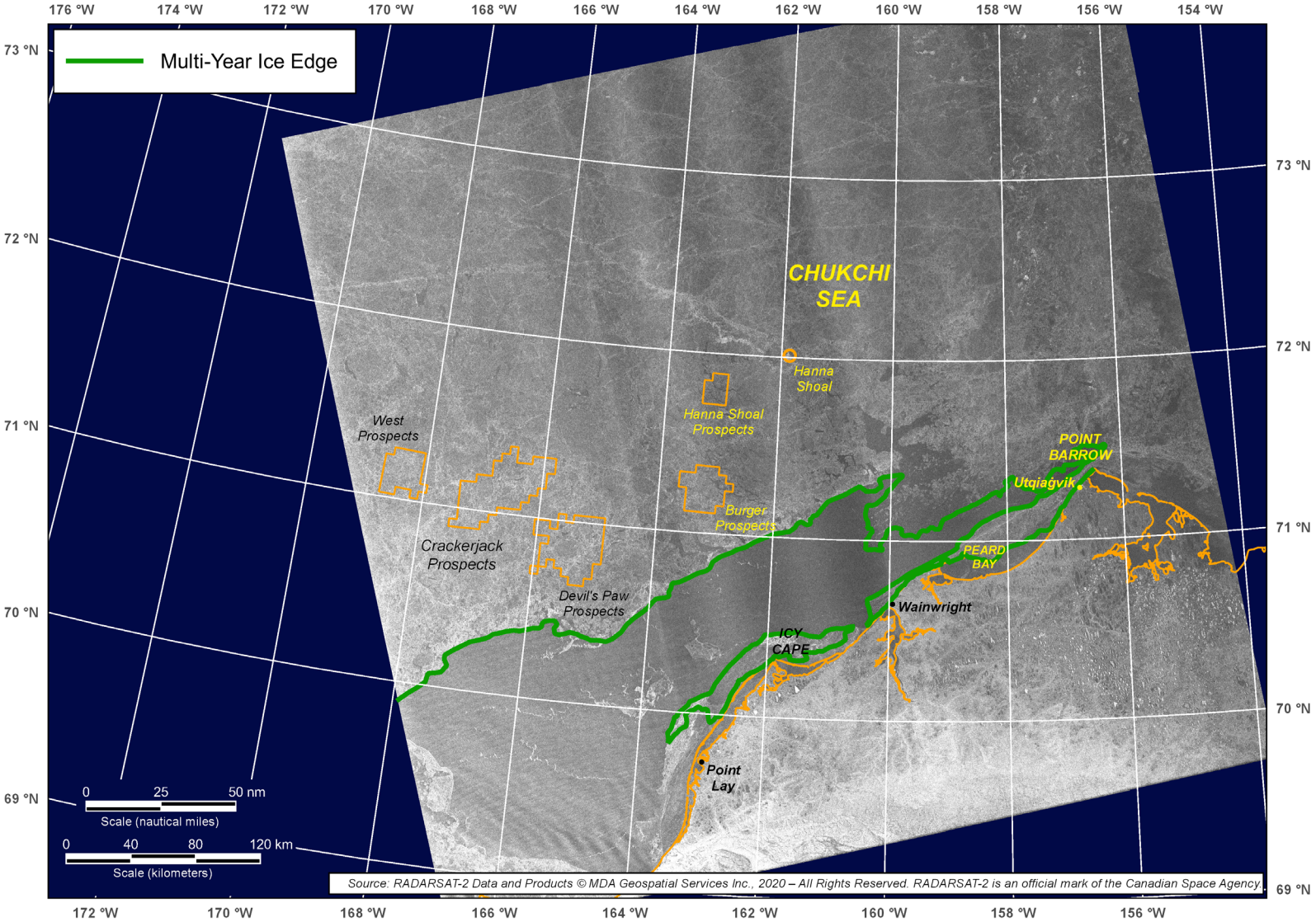

Figure 6-3. RADARSAT-2 Image of Chukchi Sea Acquired on May 14, 2020

"THIS INFORMATION IS DISTRIBUTED SOLELY FOR THE PURPOSE OF PRE-DISSEMINATION PEER REVIEW UNDER APPLICABLE INFORMATION QUALITY GUIDELINES. IT HAS NOT BEEN FORMALLY DISSEMINATED BY BSEE. IT DOES NOT REPRESENT AND SHOULD NOT BE CONSTRUED TO REPRESENT ANY BSEE DETERMINATION OR POLICY."

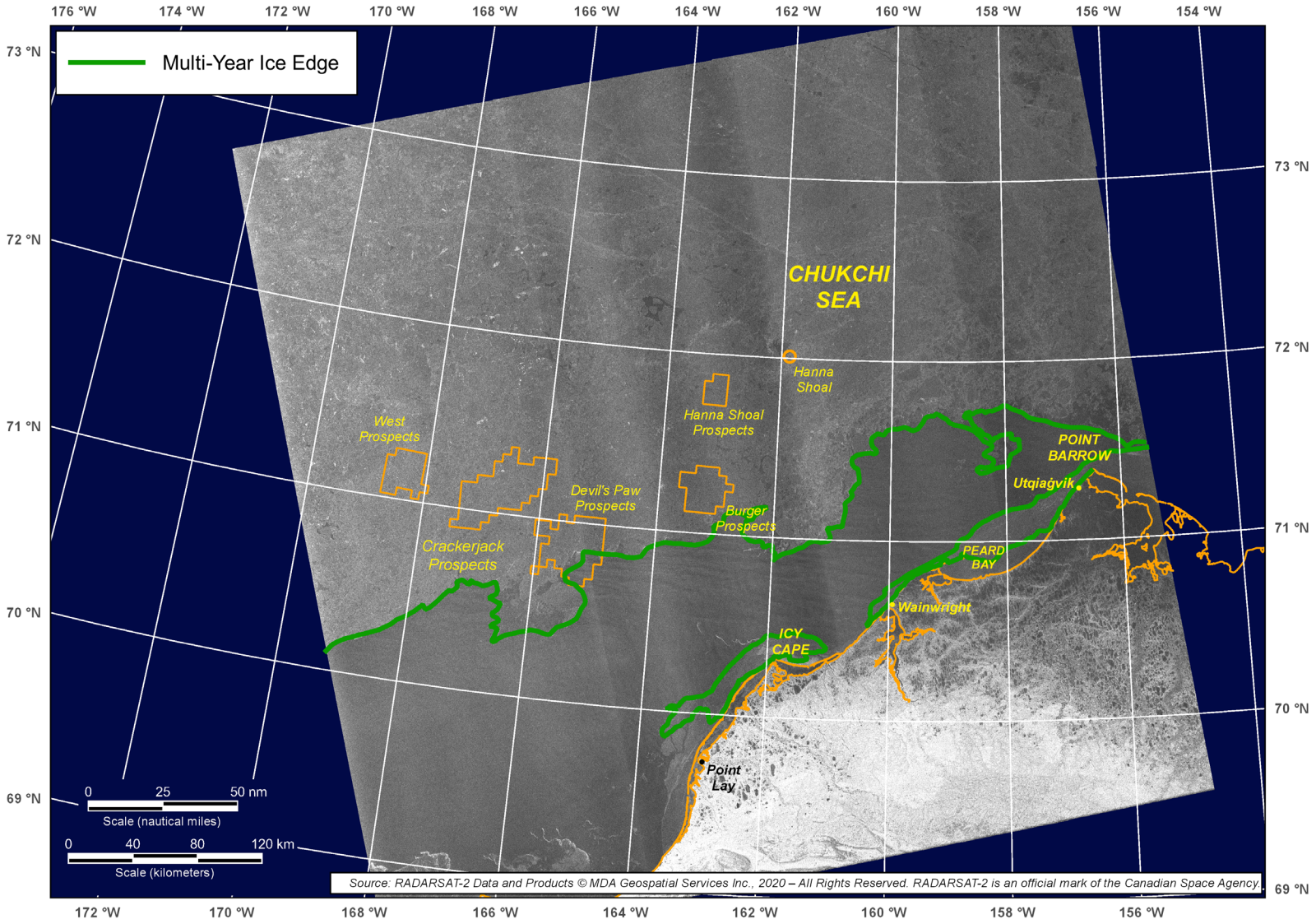

Figure 6-4. RADARSAT-2 Image of Chukchi Sea Acquired on May 31, 2020

"THIS INFORMATION IS DISTRIBUTED SOLELY FOR THE PURPOSE OF PRE-DISSEMINATION PEER REVIEW UNDER APPLICABLE INFORMATION QUALITY GUIDELINES. IT HAS NOT BEEN FORMALLY DISSEMINATED BY BSEE. IT DOES NOT REPRESENT AND SHOULD NOT BE CONSTRUED TO REPRESENT ANY BSEE DETERMINATION OR POLICY."

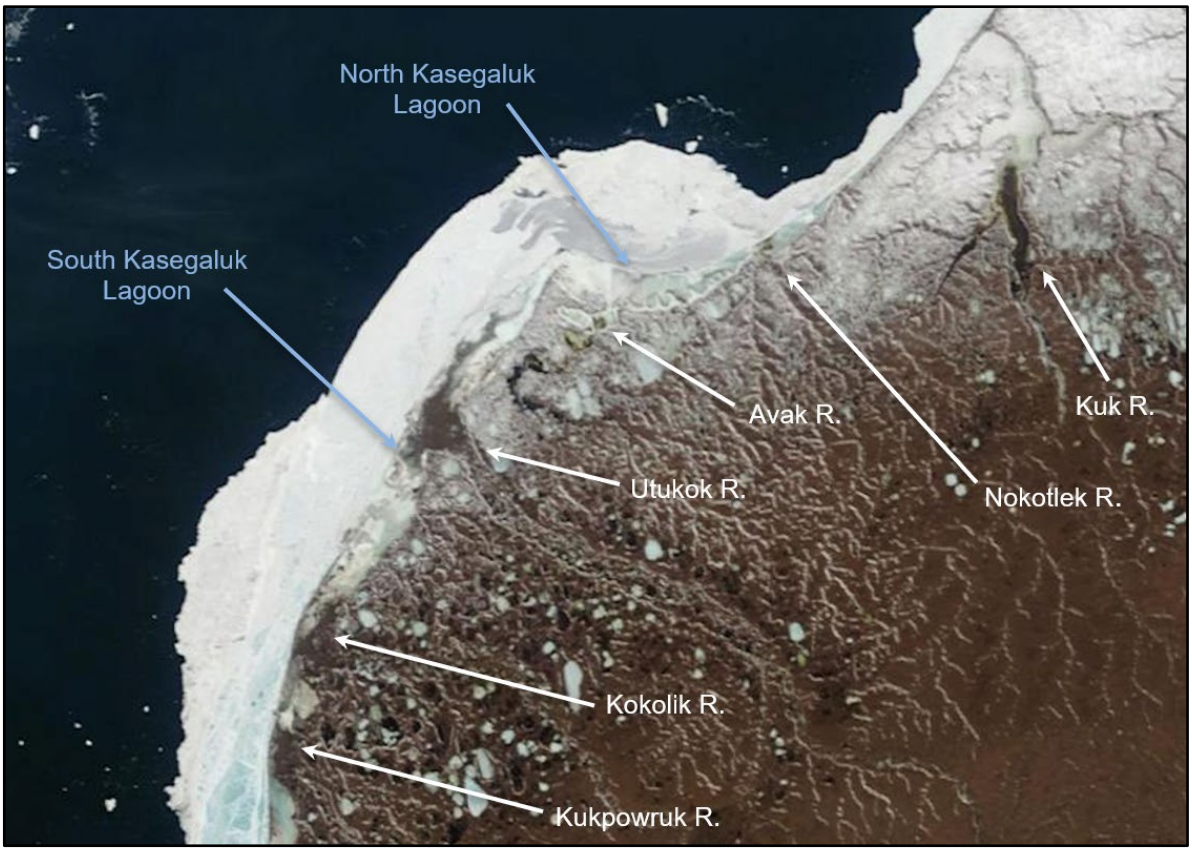

After: NASA, 2020a

Figure 6-5. MODIS Image of Chukchi Sea Acquired on May 30, 2020

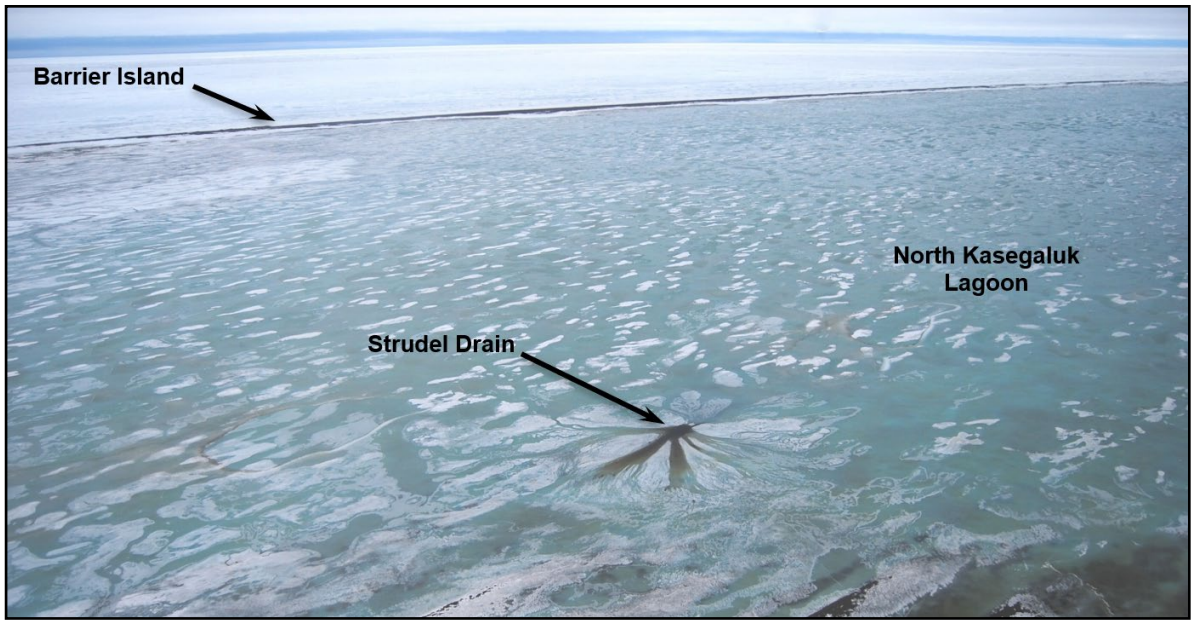

Source: Coastal Frontiers, 2011

Plate 6-1. Large Strudel Drain off Nokotlek River Mouth on June 1, 2011 (looking north)

"THIS INFORMATION IS DISTRIBUTED SOLELY FOR THE PURPOSE OF PRE-DISSEMINATION PEER REVIEW UNDER APPLICABLE INFORMATION QUALITY GUIDELINES. IT HAS NOT BEEN FORMALLY DISSEMINATED BY BSEE. IT DOES NOT REPRESENT AND SHOULD NOT BE CONSTRUED TO REPRESENT ANY BSEE DETERMINATION OR POLICY."

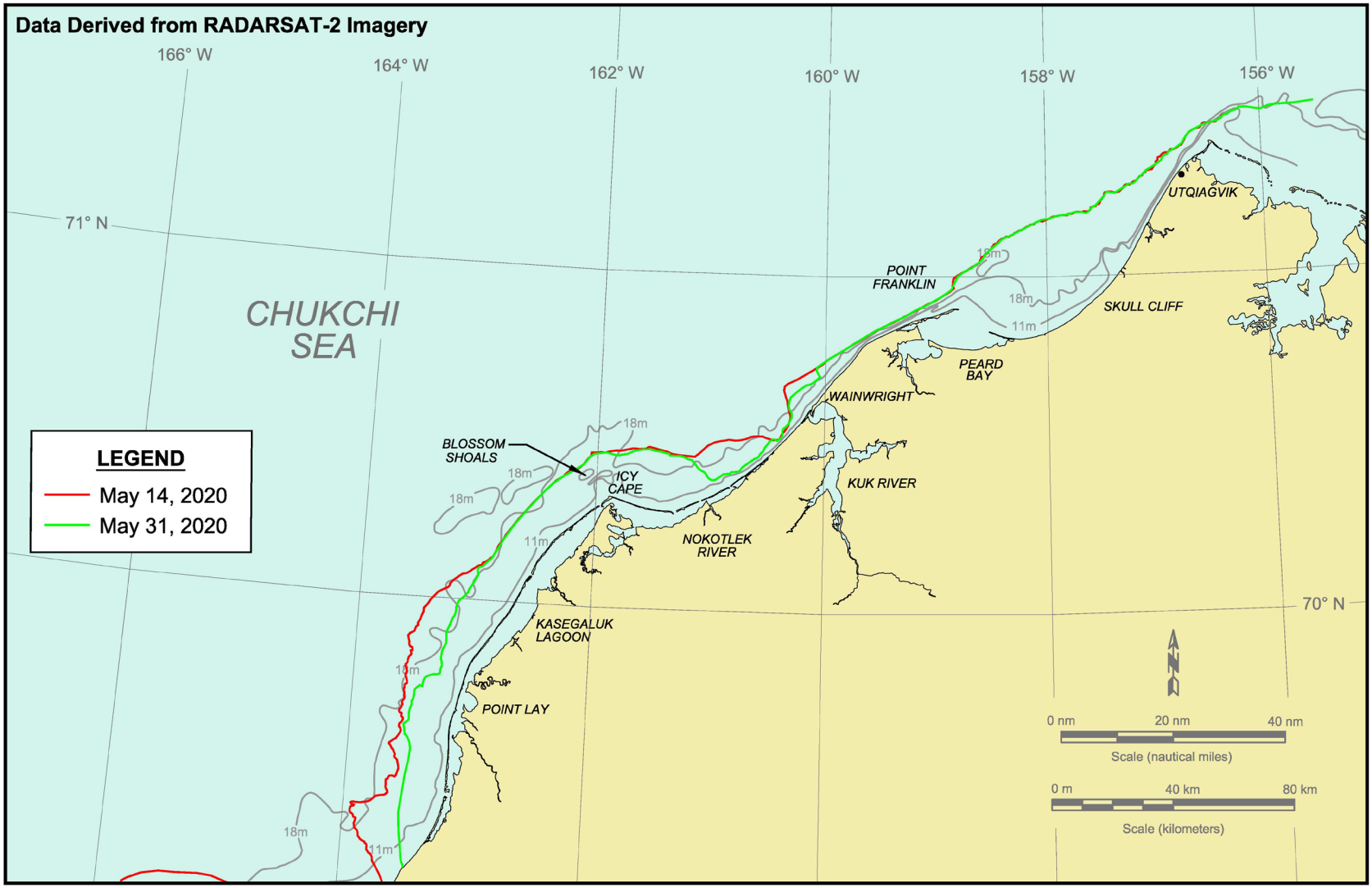

Figure 6-6. Chukchi Sea Landfast Ice Edge in May 2020

"THIS INFORMATION IS DISTRIBUTED SOLELY FOR THE PURPOSE OF PRE-DISSEMINATION PEER REVIEW UNDER APPLICABLE INFORMATION QUALITY GUIDELINES. IT HAS NOT BEEN FORMALLY DISSEMINATED BY BSEE. IT DOES NOT REPRESENT AND SHOULD NOT BE CONSTRUED TO REPRESENT ANY BSEE DETERMINATION OR POLICY."

Pack Ice: The pack ice retreated to the northwest at a relatively rapid rate in May, increasing the width of the flaw lead to approximately 15 nm (37 km) off Point Barrow and 85 nm (158 km) off Point Lay at month-end. This trend is evident from a comparison of Figures 6-3 and 6-4, which display the RADARSAT-2 images acquired on May 14th and 31st.

To provide a quantitative understanding of the progress of break-up in the Chukchi Sea lease areas, ice coverage was assessed in five representative prospects (Hanna Shoal, Burger, Devil's Paw, Crackerjack, and West) using MODIS images (NASA, 2020A), RADARSAT-2 images, and NIC ice charts (2020). The results are provided in Table 6-9. The values in maroon italics denote the transition period between break-up of the pack ice and the occurrence of ice-free conditions following the last seasonal ice invasion.

Break-up of the pack ice occurred on May 15th in the Burger Prospects, between May 21st and 24th in the Devil's Paw Prospects, on June 4th in the Crackerjack Prospects, on June 11th in the West Prospects, and between June 25th and July 1st in the Hanna Shoal Prospects.

Open water between June 1st and 3rd in the Devil's Paw Prospects, June 18th and 24th in the Crackerjack Prospects, July 6th and 11th in the Burger and West Prospects, and July 31st and August 8th in the Hanna Shoal Prospects. In the case of the Devil's Paw and Burger Prospects, the ice cover subsequently increased in response to a seasonal ice invasion in late July. Ice-free conditions occurred in the following date ranges:

- Crackerjack Prospects — July 6th – 11th
- West Prospects — July 12th – 21st
- Devil's Paw, Burger, and Hanna Shoal Prospects — July 31st – August 8th

Multi-Year Ice: Multi-year ice was present in the Chukchi Sea study area throughout the month of May. The locations of the multi-year ice edge on the 14th and 31st are shown in Figures 6-3 and 6-4, respectively.

As discussed in the 2019-20 Freeze-Up Study report (Coastal Frontiers and Vaudrey, 2020), relatively small multi-year floes with maximum horizontal dimensions typically less than 100 m were present in the landfast ice zone in late February at concentrations ranging from negligible to 20%. The floes remained embedded in the landfast ice through early May, after which they began to disperse in conjunction with the break-up of this ice.

"THIS INFORMATION IS DISTRIBUTED SOLELY FOR THE PURPOSE OF PRE-DISSEMINATION PEER REVIEW UNDER APPLICABLE INFORMATION QUALITY GUIDELINES. IT HAS NOT BEEN FORMALLY DISSEMINATED BY BSEE. IT DOES NOT REPRESENT AND SHOULD NOT BE CONSTRUED TO REPRESENT ANY BSEE DETERMINATION OR POLICY."

Table 6-9. Ice Cover in Chukchi Sea Prospects during 2020 Break-Up Season[1]

Date	Ice Cover at West	Ice Cover at Crackerjack	Ice Cover at Devil's Paw	Ice Cover at Burger	Ice Cover at Hanna Shoal
May 1[2]	100%	100%	100%	100%	100%
May 14[3]	100%	100%	100%	100%	100%
May 15[2]	100%	100%	100%	***90%***	100%
May 20[2]	100%	100%	100%	***90%***	100%
May 24[2]	100%	100%	***60%***	***80%***	100%
May 29[2]	100%	100%	***100%***	***100%***	100%
May 31[3]	100%	100%	***70%***	***100%***	100%
June 3[2]	100%	100%	***0%***	***100%***	100%
June 4[2]	100%	***90%***	***0%***	***90%***	100%
June 10[2]	100%	***70%***	***10%***	***90%***	100%
June 11[2]	100%	***50%***	***20%***	***90%***	100%
June 13[2]	***70%***	***20%***	***20%***	***90%***	100%
June 17[3]	***10%***	***10%***	***30%***	***100%***	90%
June 24[3]	***50%***	0%	***70%***	***100%***	100%
July 1[2]	***40%***	0%	***0%***	***100%***	100%
July 2[2]	***40%***	0%	***0%***	***90%***	***70%***
July 5[2]	***30%***	0%	***0%***	***20%***	***50%***
July 11[3]	0%	0%	***0%***	***0%***	***30%***
July 21[2]	0%	0%	***0%***	***0%***	***10%***
July 30[4]	0%	0%	***10%***	***10%***	***40%***
Aug 8[4]	0%	0%	0%	0%	0%

Notes:

1. Values in ***bold italics*** denote the period between break-up of the pack ice and the occurrence of ice-free conditions following the last seasonal ice invasion in the prospect.
2. Ice cover estimated using MODIS image (NASA, 2020A).
3. Ice cover estimated using RADARSAT-2 image.
4. Ice cover estimated using NIC Ice Chart (2020).

"THIS INFORMATION IS DISTRIBUTED SOLELY FOR THE PURPOSE OF PRE-DISSEMINATION PEER REVIEW UNDER APPLICABLE INFORMATION QUALITY GUIDELINES. IT HAS NOT BEEN FORMALLY DISSEMINATED BY BSEE. IT DOES NOT REPRESENT AND SHOULD NOT BE CONSTRUED TO REPRESENT ANY BSEE DETERMINATION OR POLICY."

Multi-year ice also was present in the pack ice. On May 14th, the southern edge was located approximately 4 nm (7 km) off Point Barrow and 40 nm (74 km) off Icy Cape. On the 31st, the distances had increased to 15 nm (28 km) and 45 nm (83 km) due to the northward retreat of the pack.

Ice Drift: Buoy A, the sole drift buoy located in the Chukchi Sea study area in May, was deployed in the landfast ice off Utqiagvik on the 29th. As shown in Figure 6-7, it remained stationary through month-end.

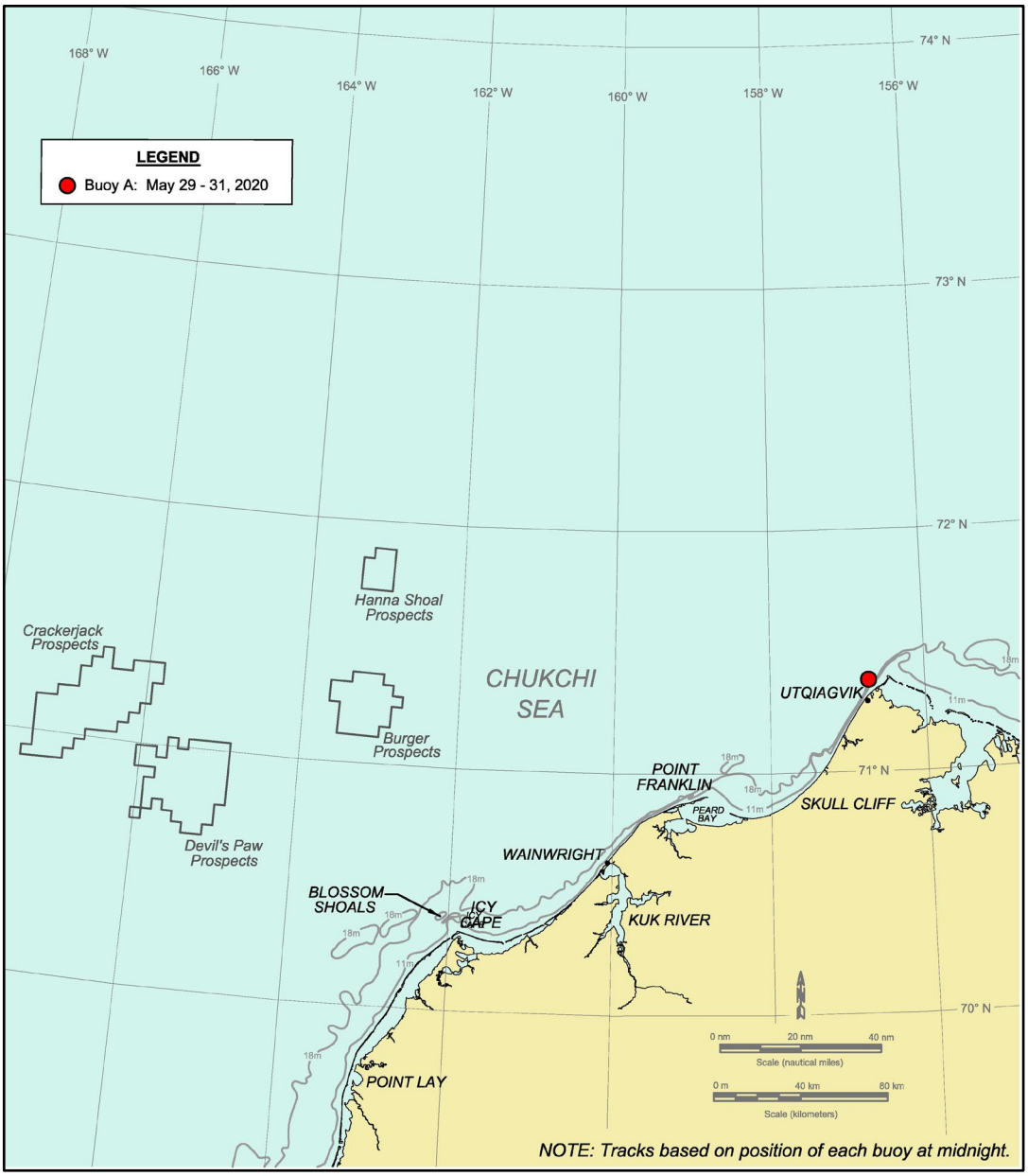

Figure 6-7. Chukchi Sea Drift Buoy Track, May 2020

"THIS INFORMATION IS DISTRIBUTED SOLELY FOR THE PURPOSE OF PRE-DISSEMINATION PEER REVIEW UNDER APPLICABLE INFORMATION QUALITY GUIDELINES. IT HAS NOT BEEN FORMALLY DISSEMINATED BY BSEE. IT DOES NOT REPRESENT AND SHOULD NOT BE CONSTRUED TO REPRESENT ANY BSEE DETERMINATION OR POLICY."

6.3. June 2020

Meteorological Conditions: The wind and temperature data acquired at Utqiagvik Airport in June are shown in Figure 6-8. The air temperatures ranged from normal to slightly above, resulting in an average temperature of 37°F (3°C). The daily average values exceeded the normal range on five occasions while never falling below.

As in May, easterlies outnumbered westerlies by a wide margin (24 of 30 days; Table 6-1). The average wind speed was slightly lower: 10 kt (5 m/s) in June versus 11 kt (6 m/s) in May. The only storm was an easterly that persisted for four days:

- May 31st - June 3rd: four-day easterly with maximum speed of 19 kt (10 m/s).

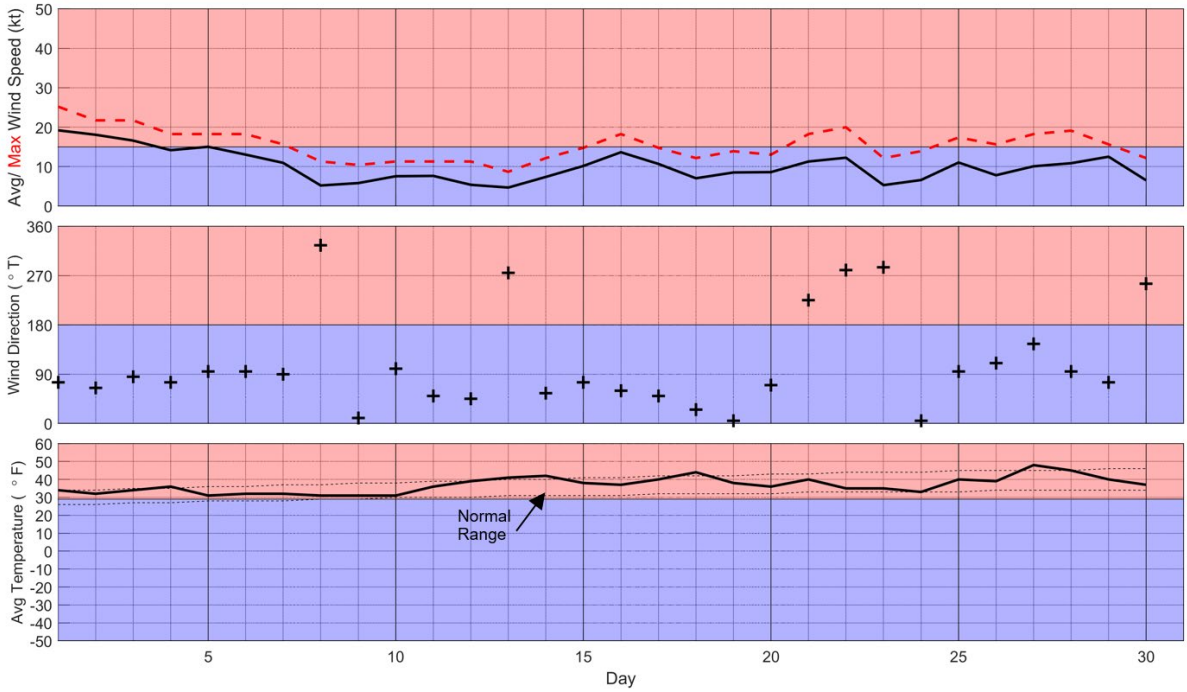

Figure 6-8. Meteorological Conditions at Utqiagvik Airport in June 2020

Ice Thickness: The number of accumulated TDD at Utqiagvik Airport increased from two to 149 over the course of June, decreasing the computed thickness of undeformed first-year ice from 147 to 72 cm (Table 6-3).

River Overflood: On June 1st, water from the Kuk River began to flood the landfast ice adjacent to the entrance. The aerial extent of the overflood increased gradually over the next two weeks but remained extremely small, peaking at less than 3 km^2.

"THIS INFORMATION IS DISTRIBUTED SOLELY FOR THE PURPOSE OF PRE-DISSEMINATION PEER REVIEW UNDER APPLICABLE INFORMATION QUALITY GUIDELINES. IT HAS NOT BEEN FORMALLY DISSEMINATED BY BSEE. IT DOES NOT REPRESENT AND SHOULD NOT BE CONSTRUED TO REPRESENT ANY BSEE DETERMINATION OR POLICY."

On the same date, June 1st, discharge from the Kugrua River (the northernmost river in the study area) entered Peard Bay. Although most of the water remained inside the Bay, a small amount began to flood the adjacent landfast ice two days later and expanded to an area of about 27 km^2 in the week that followed.

Lagoon Ice: Break-up in North Kasegaluk Lagoon and the Kuk River Entrance occurred on June 10th, followed by that in Peard Bay on the 13th. In each case, break-up resulted from relatively warm river discharge and surface meltwater melting through the underlying lagoon ice.

Open water occurred on June 20th in South Kasegaluk Lagoon, June 27th or 28th in North Kasegaluk Lagoon, and between June 25th and 30th in the Kuk River Entrance. Partial ice cover persisted in Peard Bay until July 7th.

Landfast Ice: As illustrated in Figure 6-9, most of the landfast ice that existed at the end of May was lost over the course of June. The degradation began with the four-day easterly storm that ended on June 3rd (Table 6-2), and that dislodged a massive piece of ice measuring 72 km long and 18 km wide from the region between Point Franklin and Utqiagvik and smaller pieces to the east of Icy Cape (Figure 6-10). Intermittent losses occurred in the weeks that followed, with the rate accelerating in mid-month in response to a combination of moderate northwesterly winds and warm air temperatures. River overflood did not materially impact the degradation of the landfast ice due to its minimal penetration outside the lagoons.

On June 24th, the last date in June on which a RADARSAT-2 image was acquired, regions bereft of landfast ice included a 14-nm (26-km) stretch south of Utqiagvik, an 18-nm (33-km) stretch off Skull Cliff, and a 22-nm (41-km) stretch off North Kasegaluk Lagoon. The largest remaining remnants extended 40 nm (74 km) along the coast between Wainwright and the east side of Peard Bay, and 32 nm (56 km) along the barrier islands between the central portion of South Kasegaluk Lagoon and Icy Cape.

Pack Ice: Continuing the trend that prevailed in May, the pack ice retreated to the north and west in June. The pace was slower, however, reflecting occasional reversals that produced temporary advances. At the end of June, a large expanse of ice-free water existed to the west and south of the Kuk River Entrance as well as in a tongue that extended north through the Devil's Paw and Crackerjack Prospects.

"THIS INFORMATION IS DISTRIBUTED SOLELY FOR THE PURPOSE OF PRE-DISSEMINATION PEER REVIEW UNDER APPLICABLE INFORMATION QUALITY GUIDELINES. IT HAS NOT BEEN FORMALLY DISSEMINATED BY BSEE. IT DOES NOT REPRESENT AND SHOULD NOT BE CONSTRUED TO REPRESENT ANY BSEE DETERMINATION OR POLICY."

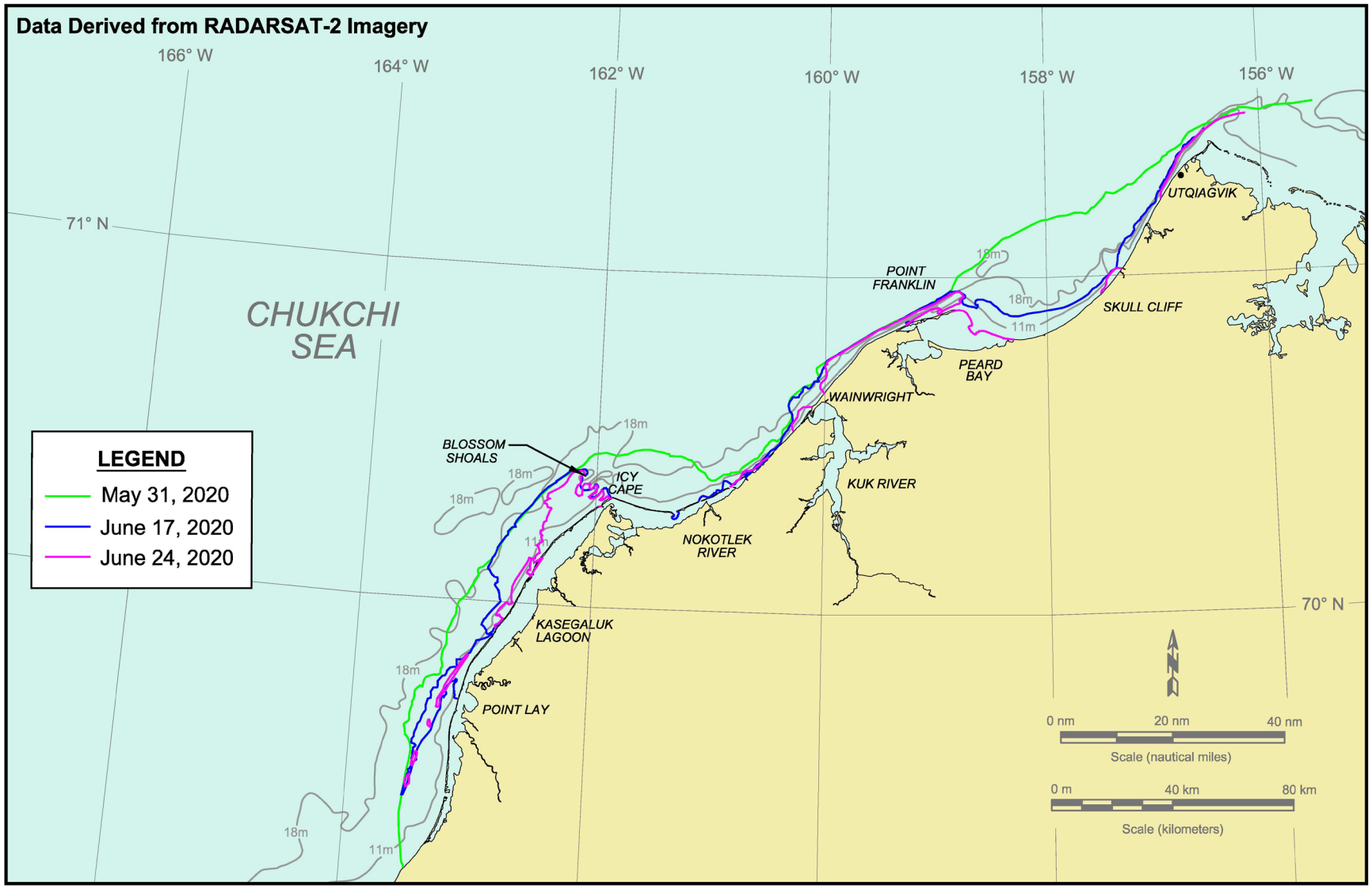

Figure 6-9. Chukchi Sea Landfast Ice Edge in June 2020

"THIS INFORMATION IS DISTRIBUTED SOLELY FOR THE PURPOSE OF PRE-DISSEMINATION PEER REVIEW UNDER APPLICABLE INFORMATION QUALITY GUIDELINES. IT HAS NOT BEEN FORMALLY DISSEMINATED BY BSEE. IT DOES NOT REPRESENT AND SHOULD NOT BE CONSTRUED TO REPRESENT ANY BSEE DETERMINATION OR POLICY."

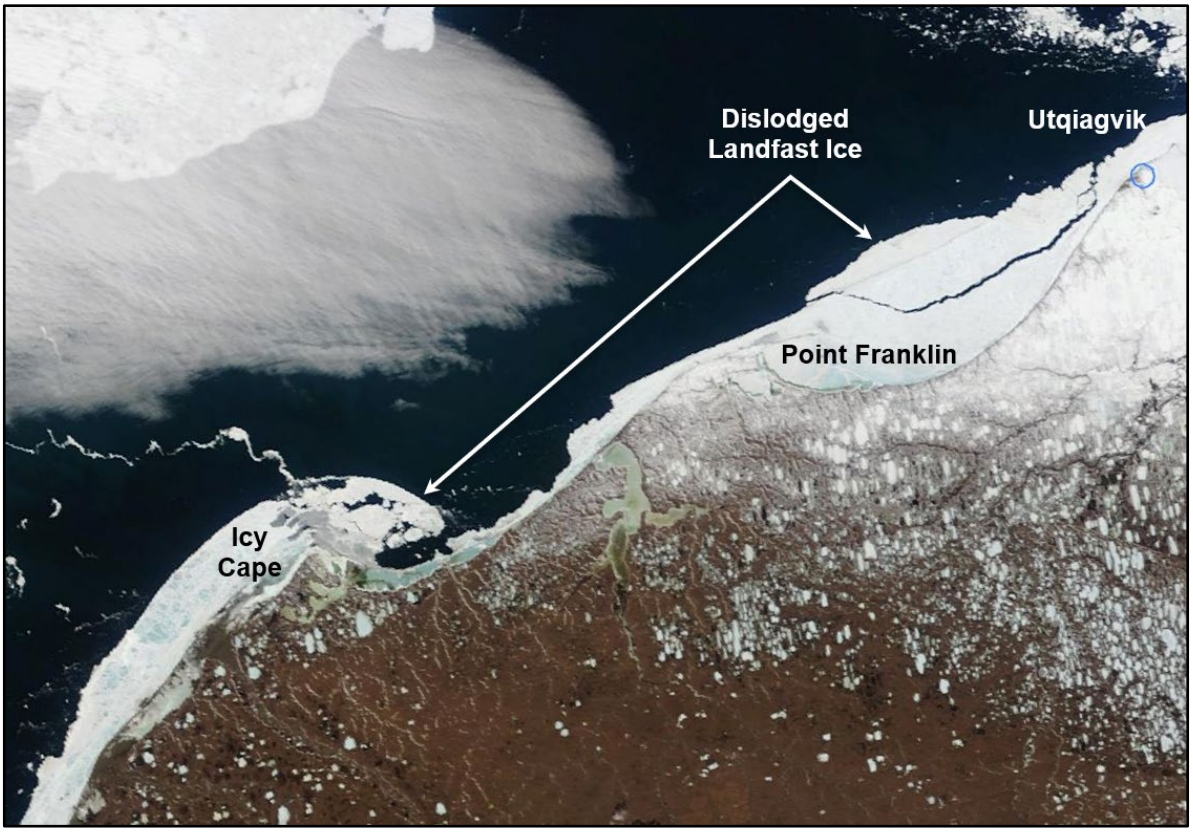

After: NASA, 2020a

Figure 6-10. MODIS Image of Chukchi Sea Acquired on June 3, 2020

Ice Pile-Ups: As discussed in Section 6.1, five pile-ups that had formed during break-up were discovered during a reconnaissance flight conducted on June 15th. They probably resulted from a wind shift that took place on June 8th. Strong easterly winds prevailed prior to this date, consisting of the four-day easterly storm from May 31st through June 3rd (Table 6-2) followed by one-hour sustained wind speeds greater than or equal to 15 kt (8 m/s) on portions of the 4th, 5th, and 6th. On the 8th, the wind backed abruptly to the northwest and peaked at 11 kt (6 m/s).

Multi-Year Ice: The loss of landfast ice that occurred in June produced a corresponding loss of the embedded multi-year ice. Farther offshore, the multi-year ice contained in the pack ice retreated to the north and west in the manner described above for the pack ice.

The locations of the multi-year ice edge on May 31st, June 17th, and June 24th are shown in Figures 6-4, 6-11, and 6-12, respectively. It should be noted that the ice edge retreated to the north between June 24th and the end of the month.

"THIS INFORMATION IS DISTRIBUTED SOLELY FOR THE PURPOSE OF PRE-DISSEMINATION PEER REVIEW UNDER APPLICABLE INFORMATION QUALITY GUIDELINES. IT HAS NOT BEEN FORMALLY DISSEMINATED BY BSEE. IT DOES NOT REPRESENT AND SHOULD NOT BE CONSTRUED TO REPRESENT ANY BSEE DETERMINATION OR POLICY."

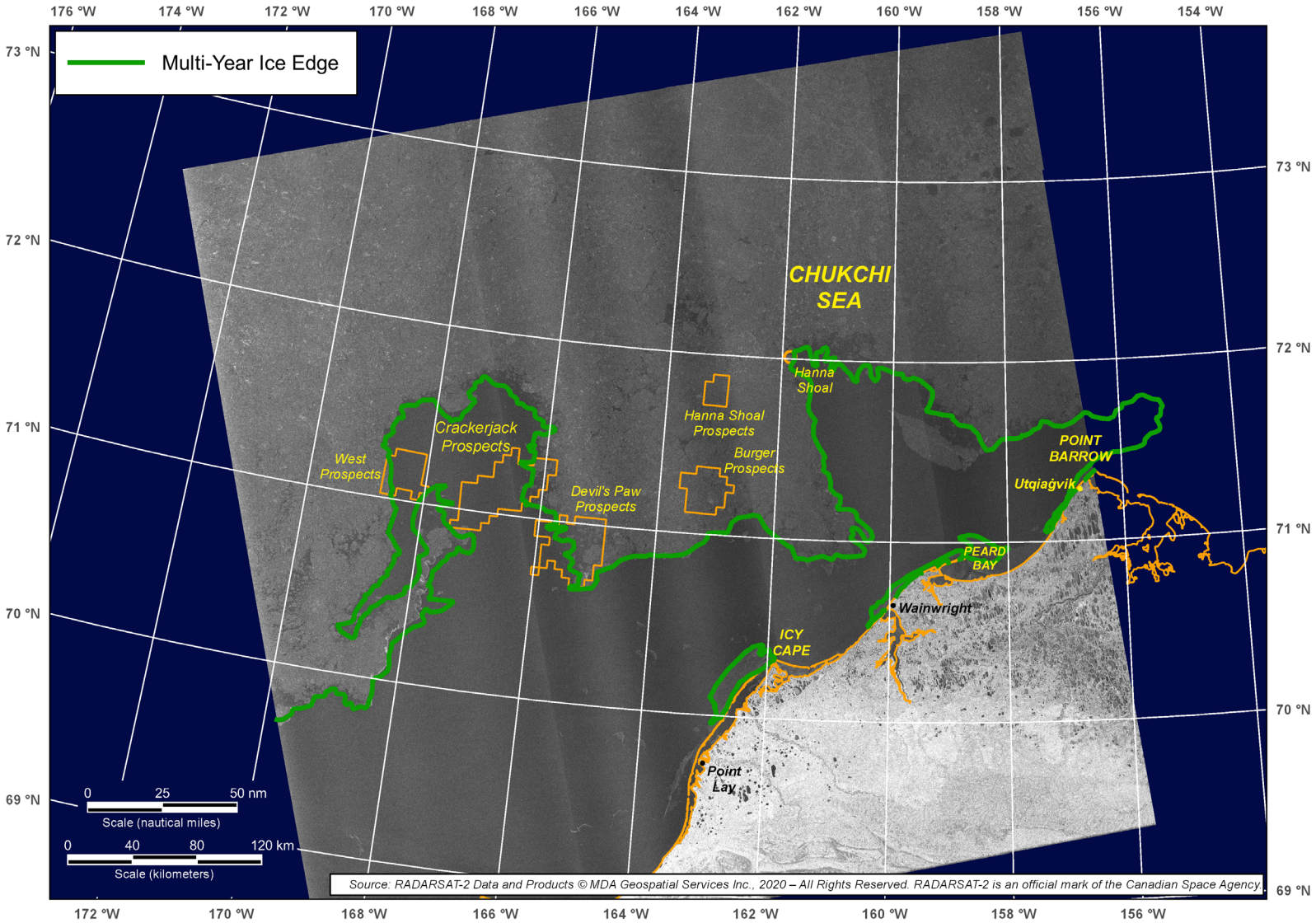

Figure 6-11. RADARSAT-2 Image of Chukchi Sea Acquired on June 17, 2020

"THIS INFORMATION IS DISTRIBUTED SOLELY FOR THE PURPOSE OF PRE-DISSEMINATION PEER REVIEW UNDER APPLICABLE INFORMATION QUALITY GUIDELINES. IT HAS NOT BEEN FORMALLY DISSEMINATED BY BSEE. IT DOES NOT REPRESENT AND SHOULD NOT BE CONSTRUED TO REPRESENT ANY BSEE DETERMINATION OR POLICY."

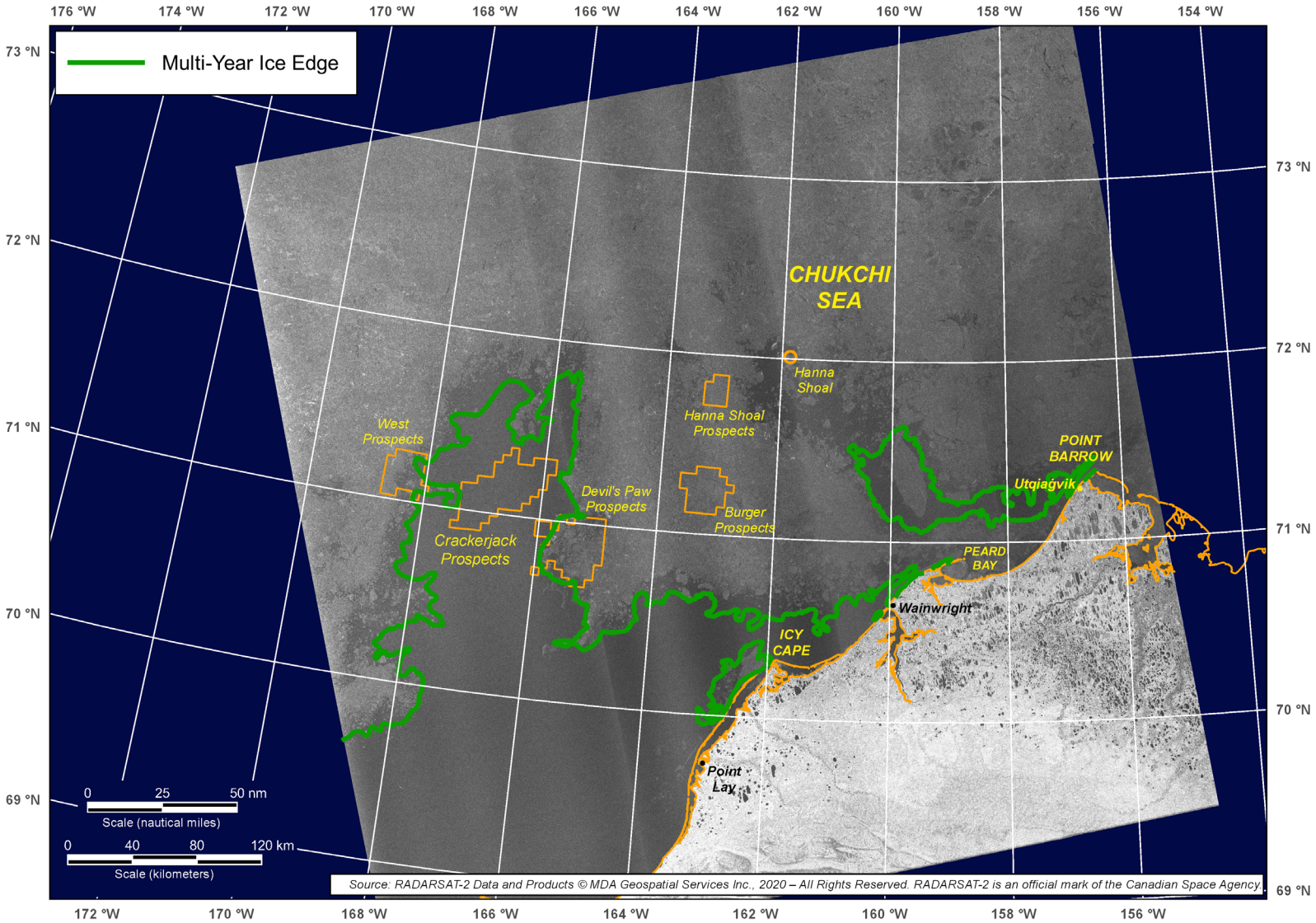

Figure 6-12. RADARSAT-2 Image of Chukchi Sea Acquired on June 24, 2020

"THIS INFORMATION IS DISTRIBUTED SOLELY FOR THE PURPOSE OF PRE-DISSEMINATION PEER REVIEW UNDER APPLICABLE INFORMATION QUALITY GUIDELINES. IT HAS NOT BEEN FORMALLY DISSEMINATED BY BSEE. IT DOES NOT REPRESENT AND SHOULD NOT BE CONSTRUED TO REPRESENT ANY BSEE DETERMINATION OR POLICY."

Ice Drift: All three ice drift buoys were present in the Chukchi Sea study area for limited periods in June. Their trajectories are illustrated in Figure 6-13, while their daily average speeds are plotted in concert with the corresponding daily average wind speeds and directions at Utqiagvik in Figure 6-14.

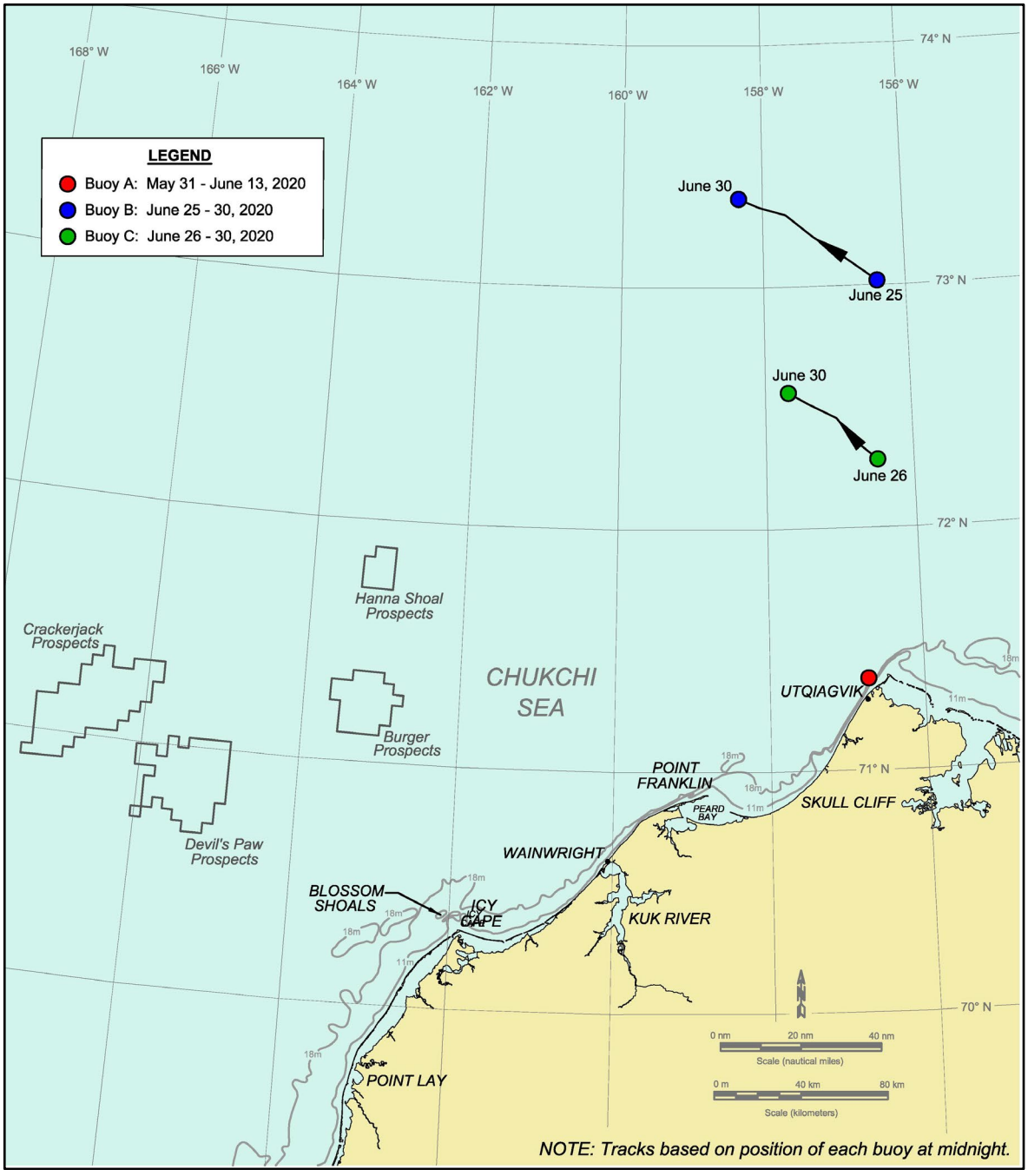

Figure 6-13. Chukchi Sea Drift Buoy Tracks, June 2020

"THIS INFORMATION IS DISTRIBUTED SOLELY FOR THE PURPOSE OF PRE-DISSEMINATION PEER REVIEW UNDER APPLICABLE INFORMATION QUALITY GUIDELINES. IT HAS NOT BEEN FORMALLY DISSEMINATED BY BSEE. IT DOES NOT REPRESENT AND SHOULD NOT BE CONSTRUED TO REPRESENT ANY BSEE DETERMINATION OR POLICY."

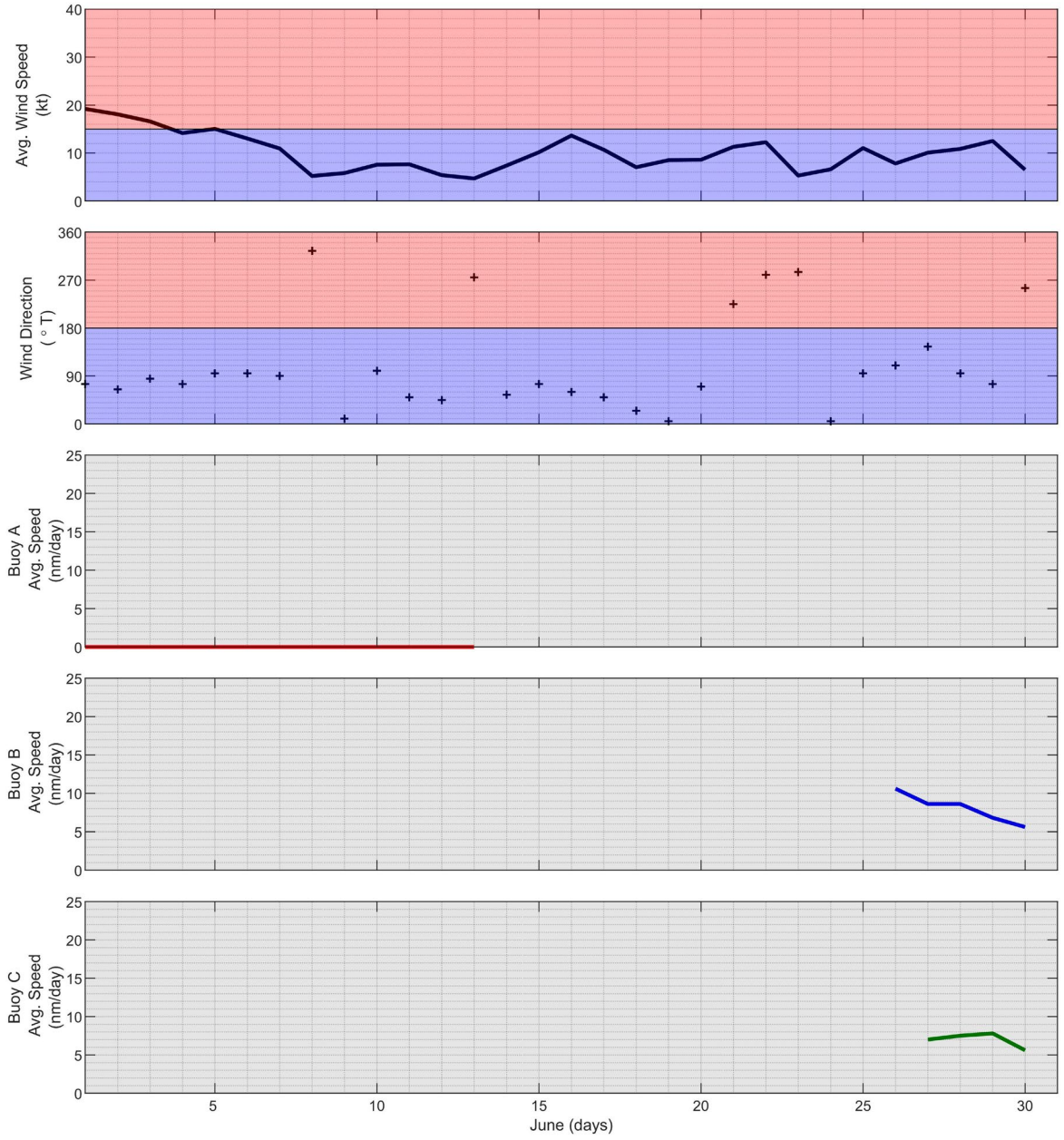

Figure 6-14. Chukchi Sea Drift Buoy Daily Average Speeds in June 2020

Buoy A, located in the landfast ice zone off Utqiagvik at the beginning of the month, remained stationary until it stopped transmitting on the 13th. Based on an analysis of MODIS images, its demise probably resulted from the break-up of landfast ice in the vicinity that occurred on or immediately preceding this date.

Buoys B and C moved from the Beaufort Sea into the Chukchi Sea study area on June 25th and 26th, respectively. Both drifted to the northwest for the remainder of the month,

"THIS INFORMATION IS DISTRIBUTED SOLELY FOR THE PURPOSE OF PRE-DISSEMINATION PEER REVIEW UNDER APPLICABLE INFORMATION QUALITY GUIDELINES. IT HAS NOT BEEN FORMALLY DISSEMINATED BY BSEE. IT DOES NOT REPRESENT AND SHOULD NOT BE CONSTRUED TO REPRESENT ANY BSEE DETERMINATION OR POLICY."

an outcome consistent with the predominance of moderate easterly winds and absence of westerly storms shown in Figure 6-14. The net displacement of Buoy B during its five-day period of record was 40 nm (74 km) while the average speed, computed on the basis of the net displacement, was 8.0 nm/day (14.8 km/day). The corresponding values for Buoy C during its four-day period of record were a net displacement of 28 nm (52 km/day) and an average speed of 7.0 nm/day (12.8 km/day).

The highest daily average speed, computed on the basis of each buoy's position at midnight each day, was 10.6 nm/day (19.6 km/day). It was recorded by Buoy B on June 26th, when the daily average wind speed at Utqiagvik Airport was 8 kt (4 m/s). The corresponding wind factor was 5.5%. Although this value is relatively high, the buoy was located 100 nm (185 km) north of Utqiagvik and therefore may have been subject to wind conditions that differed from those at the airport.

6.4. Reconnaissance Flights

As discussed in Section 4.5, aerial reconnaissance missions were undertaken in the Chukchi Sea on June 15th and 16th. Chukchi Sea Flight No. 1 (Flight "C1" on Drawing CFC-1070-02-001) focused on the offshore region to the northwest and west of Utqiagvik, including Hanna Shoal and the Hanna Shoal and Burger Prospects. It should be noted that the Hanna Shoal Prospects are centered approximately 25 nm (46 km) to the southwest of Hanna Shoal itself (Figure 1-4). Chukchi Sea Flight No. 2 (Flight "C2" on the same drawing) was used to observe the coastal and nearshore region between Utqiagvik and Point Lay. A MODIS image obtained on the 15th is provided in Figure 6-15, while the RADARSAT-2 image acquired on the 17th appears in Figure 6-11.

6.4.1. Lagoon Ice

The lagoon ice was observed to be in various stages of deterioration at the time of the nearshore flight on June 15th. The ice cover in the Kuk River Entrance was less than 10%, while that in the other lagoons ranged from an estimated 30% in South Kasegaluk to 80% in North Kasegaluk and greater than 90% in Peard Bay. As illustrated in Plate 6-1, the ice tended to be rotten with numerous melt ponds.

6.4.2. Landfast Ice

With the exception of the region to the east of Icy Cape, landfast ice was present along the entire stretch of coast between Point Lay and Point Barrow. The ice was anchored by grounded ridges and rubble that typically ranged from 2 to 5m high but peaked at 20 m off

"THIS INFORMATION IS DISTRIBUTED SOLELY FOR THE PURPOSE OF PRE-DISSEMINATION PEER REVIEW UNDER APPLICABLE INFORMATION QUALITY GUIDELINES. IT HAS NOT BEEN FORMALLY DISSEMINATED BY BSEE. IT DOES NOT REPRESENT AND SHOULD NOT BE CONSTRUED TO REPRESENT ANY BSEE DETERMINATION OR POLICY."

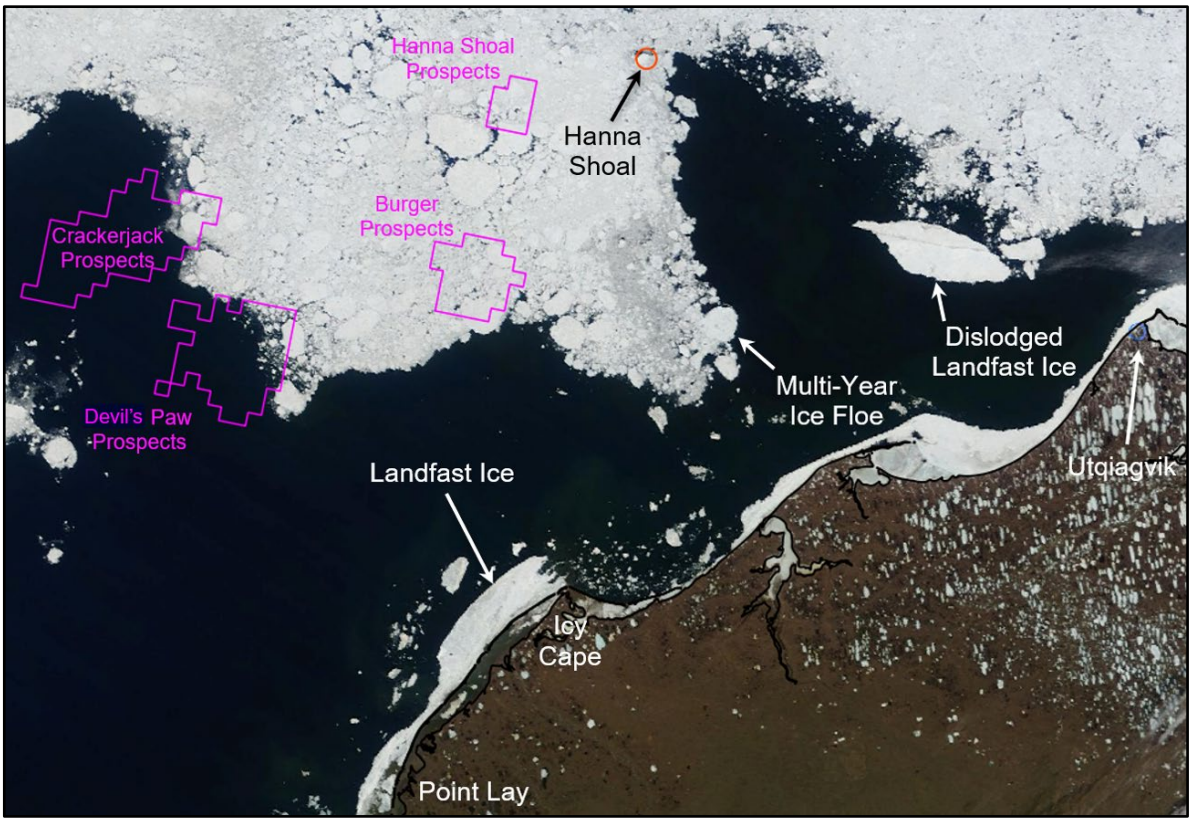

After: NASA, 2020a

Figure 6-15. MODIS Image of Chukchi Sea Acquired on June 15, 2020

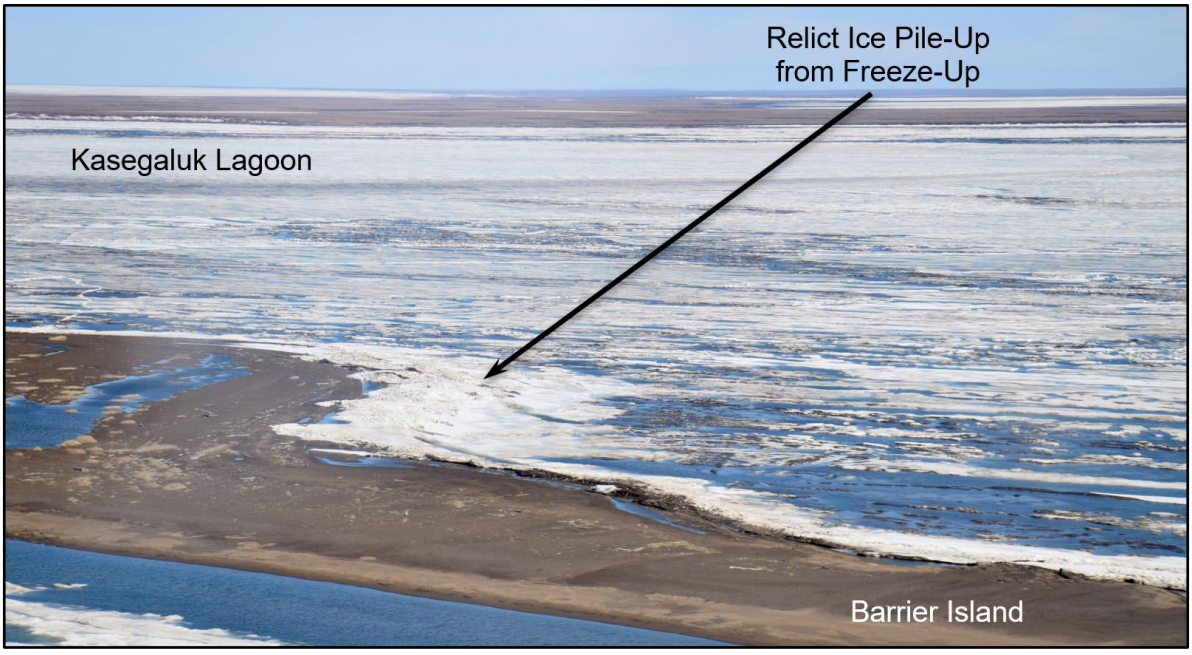

Plate 6-2. Rotten Ice in Northern Portion of South Kasegaluk Lagoon (looking east on June 15, 2020)

"THIS INFORMATION IS DISTRIBUTED SOLELY FOR THE PURPOSE OF PRE-DISSEMINATION PEER REVIEW UNDER APPLICABLE INFORMATION QUALITY GUIDELINES. IT HAS NOT BEEN FORMALLY DISSEMINATED BY BSEE. IT DOES NOT REPRESENT AND SHOULD NOT BE CONSTRUED TO REPRESENT ANY BSEE DETERMINATION OR POLICY."

Icy Cape; Plate 6-3). The maximum width, 10 nm, occurred off Peard Bay. As illustrated in Plate 6-4, multi-year ice was embedded in the landfast ice. The concentrations typically ranged from negligible to 20% but occasionally reached 30%.

6.4.3. Pack Ice

The pack ice, which extended as far south as the Burger and Devil's Paw Prospects at the time of the flight, contained a mixture of first-year and multi-year ice, with the concentration of the latter typically ranging from 10 to 30%. The ice displayed varying degrees of deterioration, with melt ponds omnipresent. A large multi-year floe with an approximate diameter of 12 km, located at the eastern edge of the pack ice 75 nm (139 km) west of Utqiagvik, is shown in Plate 6-5 and Figure 6-15.

6.4.4. Ice Edge

Reflecting the moderate easterly winds that prevailed during the offshore flight, the edge of the pack ice tended to be compact in those areas where it faced east (upwind) and semi-diffuse in those areas where it faced west (downwind). Plate 6-6 shows the diffuse ice edge that existed approximately 85 nm (158 km) northwest of Utqiagvik.

6.4.5. Ice Pile-Ups

As discussed in Section 6.1, 53 of the 57 ice pile-ups observed during the freeze-up reconnaissance flight in late February 2020 (Coastal Frontiers and Vaudrey, 2020) were evident at the time of the break-up flight in mid-June. Most of these features had experienced significant degradation, resulting in diminished heights and encroachment distances. A representative example is provided in Plate 6-7, which displays a relict pile-up that formerly extended 5 m above sea level and encroached 20 m onto a barrier island 0.5 nm (0.9 km) east of Icy Cape.

In addition to the 53 relict pile-ups, five new pile-ups that had formed during break-up were identified. Two were located on the barrier islands between Point Lay and Icy Cape, while three were located on the mainland shore near the base of the Point Franklin Spit. The characteristics of these features are summarized in Table 6-6. The largest of the five, which attained a height of 5 m and encroached 5 m onto the mainland shore 4 nm (7 km) northeast of Point Belcher, is shown in Plate 6-8. The new pile-ups probably resulted from a wind shift from east to northwest that took place on June 8th.

"THIS INFORMATION IS DISTRIBUTED SOLELY FOR THE PURPOSE OF PRE-DISSEMINATION PEER REVIEW UNDER APPLICABLE INFORMATION QUALITY GUIDELINES. IT HAS NOT BEEN FORMALLY DISSEMINATED BY BSEE. IT DOES NOT REPRESENT AND SHOULD NOT BE CONSTRUED TO REPRESENT ANY BSEE DETERMINATION OR POLICY."

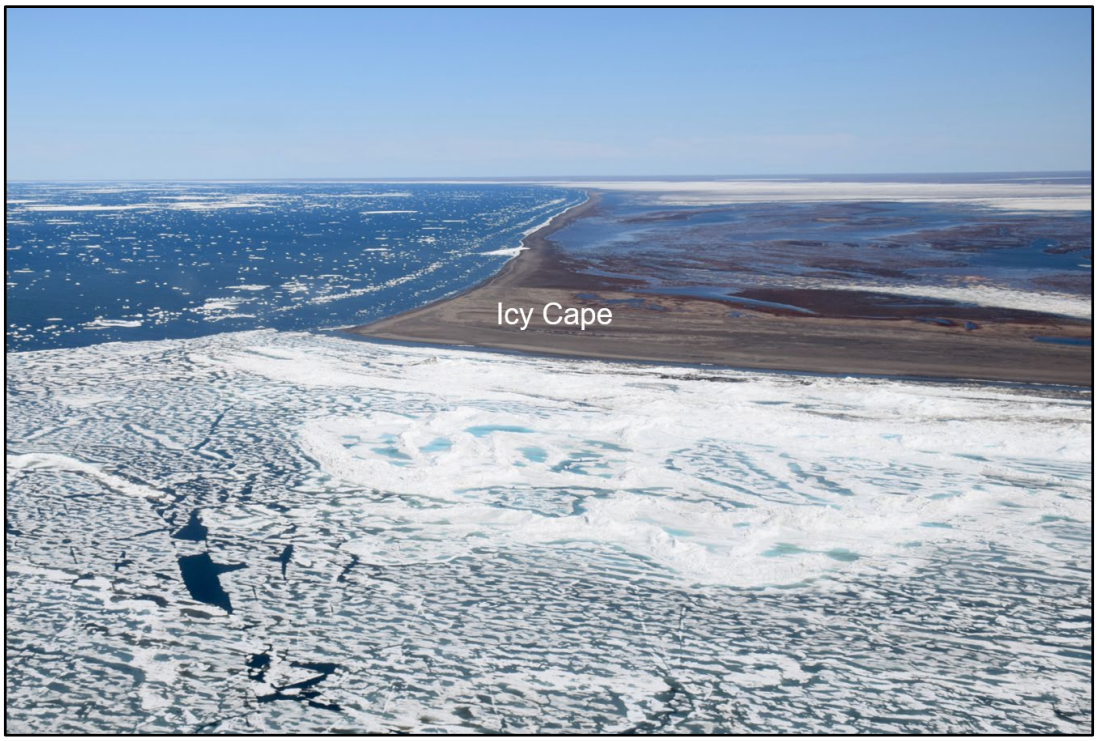

Plate 6-3. Relict 20-m Pile-Up Anchoring Landfast Ice off Icy Cape (looking east on June 15, 2020)

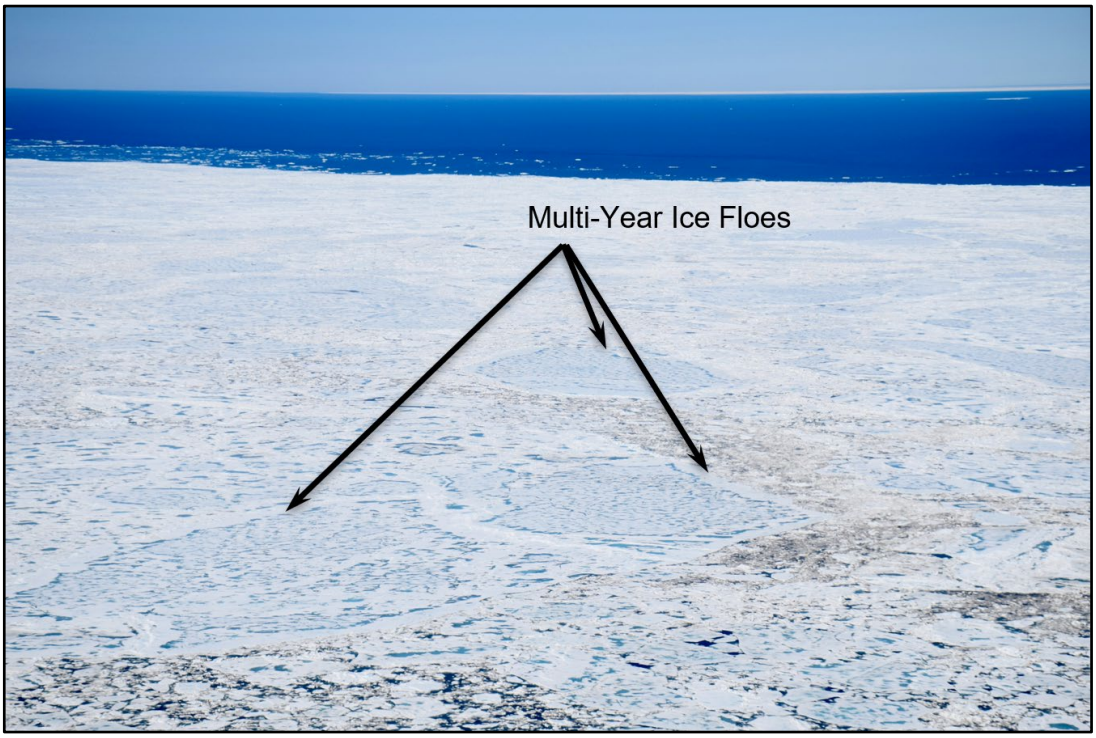

Plate 6-4. Landfast Ice with Embedded Multi-Year Floes off Icy Cape (looking north on June 15, 2020)

"THIS INFORMATION IS DISTRIBUTED SOLELY FOR THE PURPOSE OF PRE-DISSEMINATION PEER REVIEW UNDER APPLICABLE INFORMATION QUALITY GUIDELINES. IT HAS NOT BEEN FORMALLY DISSEMINATED BY BSEE. IT DOES NOT REPRESENT AND SHOULD NOT BE CONSTRUED TO REPRESENT ANY BSEE DETERMINATION OR POLICY."

Plate 6-5. Large Multi-Year Ice Floe 75 nm West of Utqiagvik (looking north on June 16, 2020)

Plate 6-6. Diffuse Ice Edge 85 nm Northwest of Utqiagvik (looking southwest on June 16, 2020)

"THIS INFORMATION IS DISTRIBUTED SOLELY FOR THE PURPOSE OF PRE-DISSEMINATION PEER REVIEW UNDER APPLICABLE INFORMATION QUALITY GUIDELINES. IT HAS NOT BEEN FORMALLY DISSEMINATED BY BSEE. IT DOES NOT REPRESENT AND SHOULD NOT BE CONSTRUED TO REPRESENT ANY BSEE DETERMINATION OR POLICY."

Plate 6-7. Relict Ice Pile-Up on Barrier Island 0.5 nm East of Icy Cape (looking southeast on June 15, 2020)

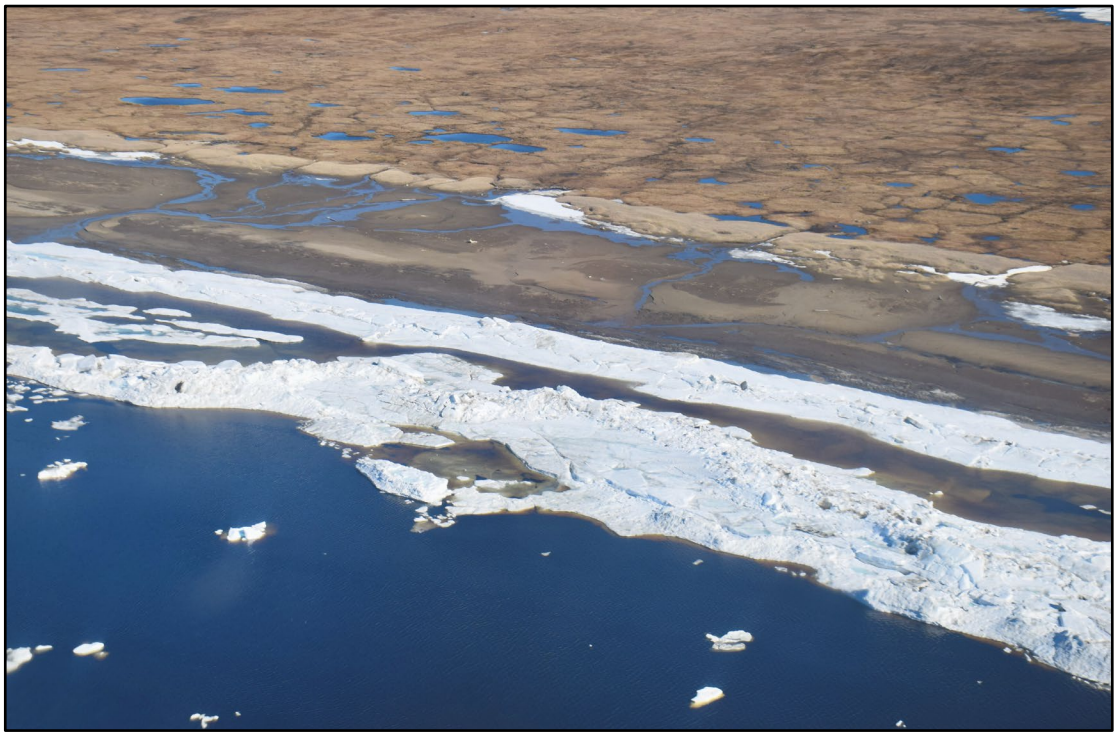

Plate 6-8. 5-m High Pile-Up that Encroached 20 m onto Mainland Shore 4 nm Northeast of Point Belcher (looking east on June 16, 2020)

"THIS INFORMATION IS DISTRIBUTED SOLELY FOR THE PURPOSE OF PRE-DISSEMINATION PEER REVIEW UNDER APPLICABLE INFORMATION QUALITY GUIDELINES. IT HAS NOT BEEN FORMALLY DISSEMINATED BY BSEE. IT DOES NOT REPRESENT AND SHOULD NOT BE CONSTRUED TO REPRESENT ANY BSEE DETERMINATION OR POLICY."

6.4.6. Multi-Year Ice

As discussed in Sections 6.4.2 and 6.4.3, multi-year ice floes were embedded in both the landfast ice and the pack ice at concentrations ranging from negligible to 30%. The floes in the landfast ice zone were relatively small, with maximum horizontal dimensions typically less than 100 m. The horizontal dimensions in the pack ice varied across a wide spectrum, from less than 10 m to more than 10 km.

6.4.7. Ice Conditions in Chukchi Sea Prospects

In the Hanna Shoal Prospects, the ice cover diminished from 80% in the northern and central portions (Plate 6-9) to 70% in the southern portion. The concentration of multi-year ice was estimated at 20% throughout the Prospects. The floe sizes ranged from brash ice to more than 1 km in diameter. Ridge and rubble heights of 2 to 3 m were typical, but heights to 4 m were observed.

The Burger Prospects were located just inside the southern edge of the pack ice (Figure 6-15). The ice cover varied between 70 and 80% and included multi-year floes at concentrations of 10 to 20% (Plate 6-10). Although the floe sizes ranged from brash ice to more than 1 km in diameter, values near the lower end of this range predominated. Ridge and rubble heights to 2 m were observed.

6.4.8. Katie's Floeberg

Katie's Floeberg forms each winter when ice floes become grounded on Hanna Shoal, which lies 110 nm (204 km) northwest of Utqiagvik at 72°N, 162°W (Drawing CFC-1070-02-001). The shallowest water depth over the shoal is about 12 m, while the surrounding depths exceed 30 m.

The floeberg, which can consist of multi-year as well as first-year ice rubble, typically resembles an oval in plan form with the major axis oriented northeast-southwest, and the minor axis northwest-southeast. Its formation and growth have been described by a number of prior investigators, including Stringer and Barrett (1975), Kovacs, *et al*. (1976), Toimil and Grantz (1976), Barrett and Stringer (1978), and Vaudrey and Thomas (1981). Although Hanna Shoal is located well north of the Chukchi Sea prospects, the floeberg can impact these areas if the ice remains grounded during break-up, and then floats free and drifts south during the ensuing open-water season – a sequence of events that resulted in the temporary suspension of exploratory drilling in the Burger Prospects during the 2012 open-water season (Bailey, 2012).

"THIS INFORMATION IS DISTRIBUTED SOLELY FOR THE PURPOSE OF PRE-DISSEMINATION PEER REVIEW UNDER APPLICABLE INFORMATION QUALITY GUIDELINES. IT HAS NOT BEEN FORMALLY DISSEMINATED BY BSEE. IT DOES NOT REPRESENT AND SHOULD NOT BE CONSTRUED TO REPRESENT ANY BSEE DETERMINATION OR POLICY."

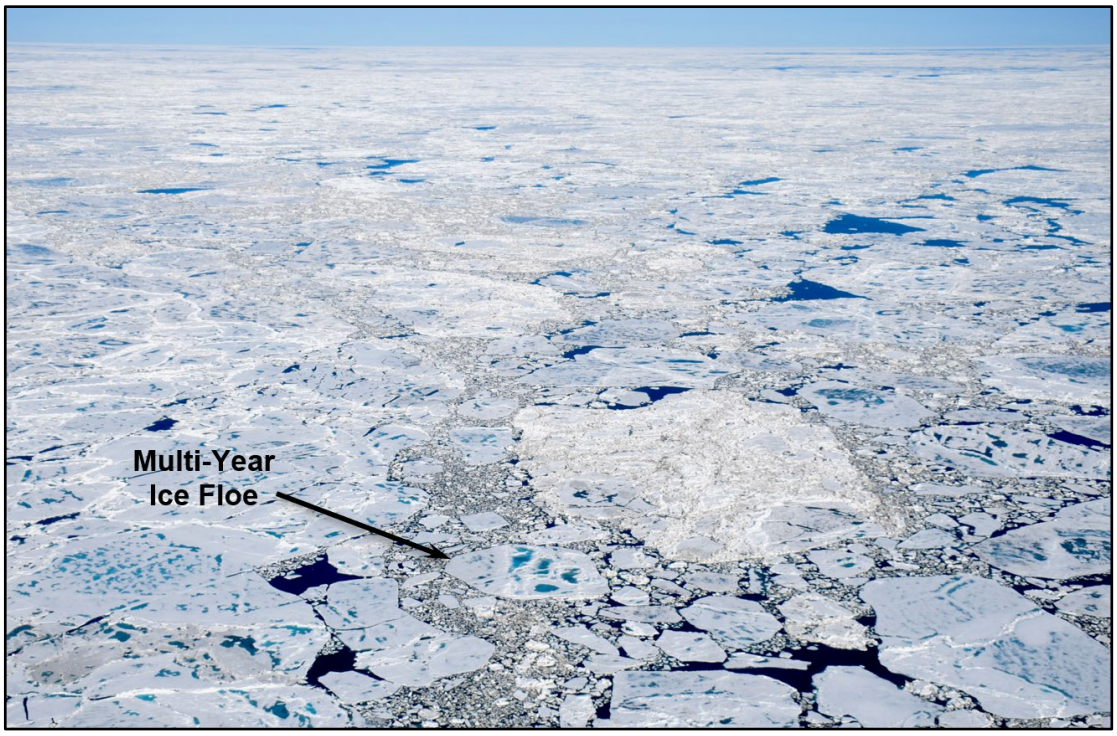

Plate 6-9. 80% Ice Concentration in Northern Portion of Hanna Shoal Prospects (looking northwest on June 16, 2020)

Plate 6-10. 70% Ice Concentration in Central Portion of Burger Prospects (looking southwest on June 16, 2020)

"THIS INFORMATION IS DISTRIBUTED SOLELY FOR THE PURPOSE OF PRE-DISSEMINATION PEER REVIEW UNDER APPLICABLE INFORMATION QUALITY GUIDELINES. IT HAS NOT BEEN FORMALLY DISSEMINATED BY BSEE. IT DOES NOT REPRESENT AND SHOULD NOT BE CONSTRUED TO REPRESENT ANY BSEE DETERMINATION OR POLICY."

During the nine freeze-up studies conducted between 2009-10 and 2019-20, the floeberg was observed during mid-winter reconnaissance flights on five occasions: February 2011, February 2012, March 2014, February 2015, and February 2016 (Coastal Frontiers and Vaudrey, 2011; 2012; 2014; 2015; 2016). The dimensions varied substantially with lengths ranging from 2.8 to 10.0 km, widths from 1.2 to 5.0 km, and maximum rubble heights from 8 to 12 m above sea level. The feature had not developed yet when the mid-winter flights were conducted in 2010, 2013, 2017, and 2020 (Coastal Frontiers and Vaudrey, 2010; 2013; 2017; 2020). In each case, however, it appeared in satellite imagery acquired subsequent to the flight.

Katie's Floeberg was clearly evident at the time of the 2020 break-up reconnaissance flight (Plate 6-11). Composed of an estimated 80% first-year ice and 20% multi-year ice, it measured 5.5 km long and 2.5 km wide. The major axis was oriented northeast-southwest. The maximum rubble height, 20 m, was located on the southwest side of a multi-year floe near the center of the floeberg. An open-water wake was present on the downwind (west) side, indicating that the feature was well-grounded at the time of the flight.

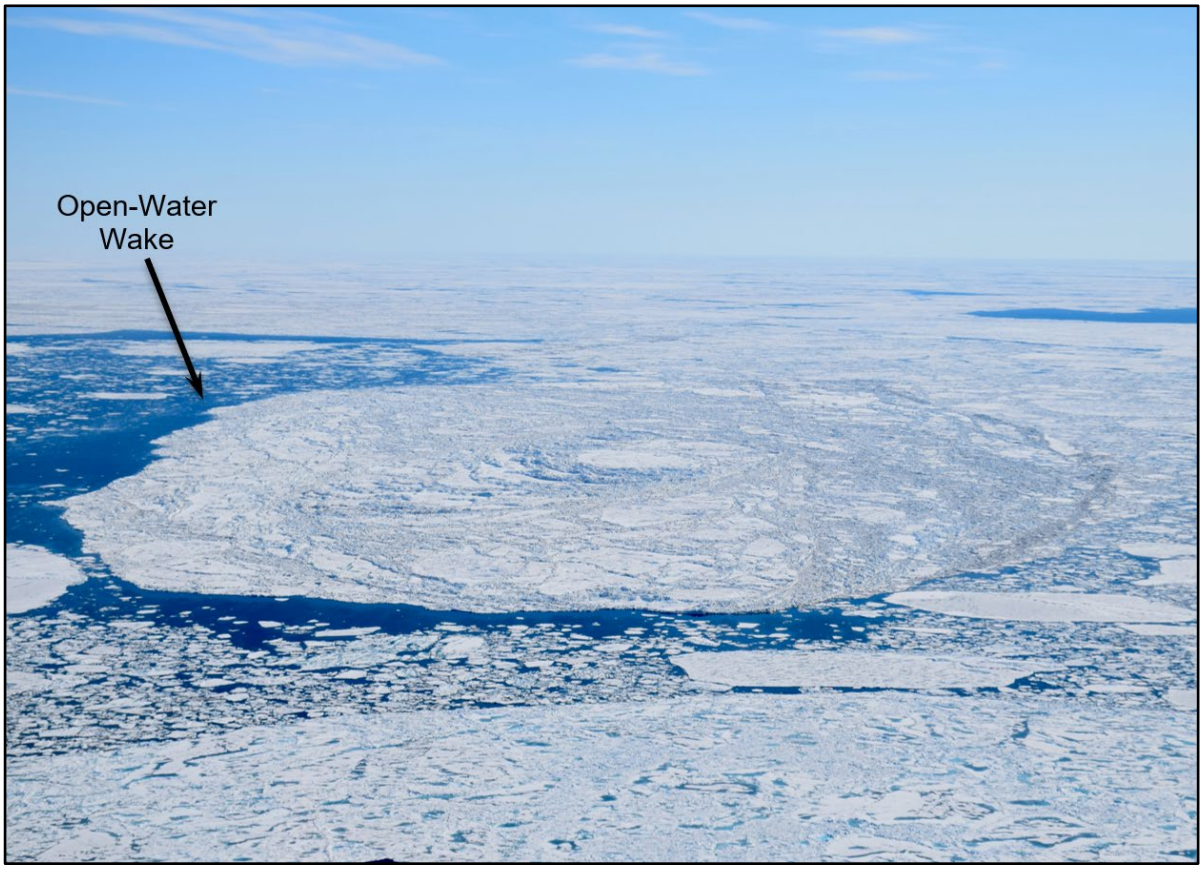

Plate 6-11. Katie's Floeberg
(looking northeast on June 16, 2020)

"THIS INFORMATION IS DISTRIBUTED SOLELY FOR THE PURPOSE OF PRE-DISSEMINATION PEER REVIEW UNDER APPLICABLE INFORMATION QUALITY GUIDELINES. IT HAS NOT BEEN FORMALLY DISSEMINATED BY BSEE. IT DOES NOT REPRESENT AND SHOULD NOT BE CONSTRUED TO REPRESENT ANY BSEE DETERMINATION OR POLICY."

6.5. July 2020

Meteorological Conditions: The wind and temperature data recorded at Utqiagvik Airport in July 2020 are provided in Figure 6-16. The air temperatures tended to remain within the normal range, rising above by 1°F (1°C) on only one day while falling below by 1°F (1°C) on two days. The temperatures were above freezing throughout the month, producing an average monthly value of 38°F (3°C).

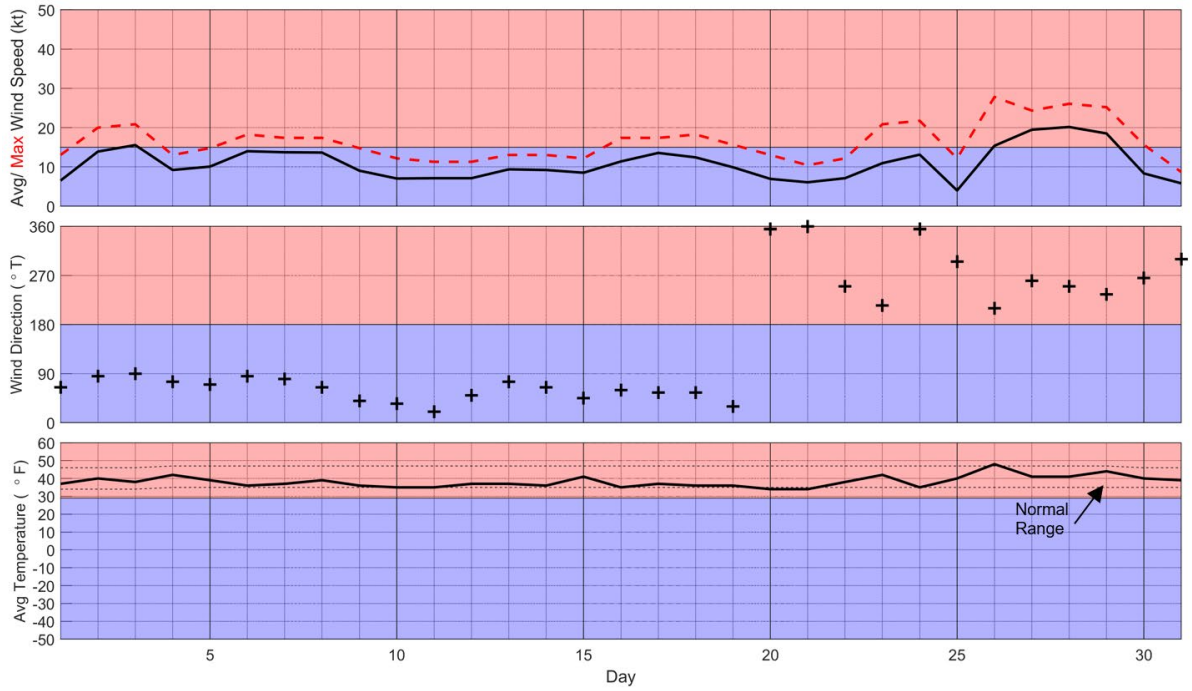

Figure 6-16. Meteorological Conditions at Utqiagvik Airport in July 2020

As in May and June, easterly winds predominated in July. The degree of predominance decreased, however, with easterlies prevailing during the first 19 days of the month and westerlies during the last 12. The average speed, 11 kt (6 m/s), was identical to that in May and slightly higher than that in June (10 kt; 5 m/s). With respect to storm activity, a one-day easterly at the beginning of the month was followed by a three-day westerly at the end:

- July 3rd: one-day easterly with maximum speed of 16 kt (8 m/s);
- July 27th-29th: three-day westerly with maximum speed of 20 kt (10 m/s).

Ice Thickness: The computed thickness of undeformed first-year ice, 72 cm at the beginning of the month, decreased to zero on July 26th based on the accumulation of 297 TDD at Utqiagvik Airport since May 29th (Table 6-3).

"THIS INFORMATION IS DISTRIBUTED SOLELY FOR THE PURPOSE OF PRE-DISSEMINATION PEER REVIEW UNDER APPLICABLE INFORMATION QUALITY GUIDELINES. IT HAS NOT BEEN FORMALLY DISSEMINATED BY BSEE. IT DOES NOT REPRESENT AND SHOULD NOT BE CONSTRUED TO REPRESENT ANY BSEE DETERMINATION OR POLICY."

Lagoon Ice: As illustrated in Figure 6-17, the only lagoon ice that remained at the beginning of July was located in Peard Bay. North Kasegaluk Lagoon, South Kasegaluk Lagoon, and the Kuk River Entrance were ice-free. Based on an analysis of MODIS images, Peard Bay became ice-free on July 7th.

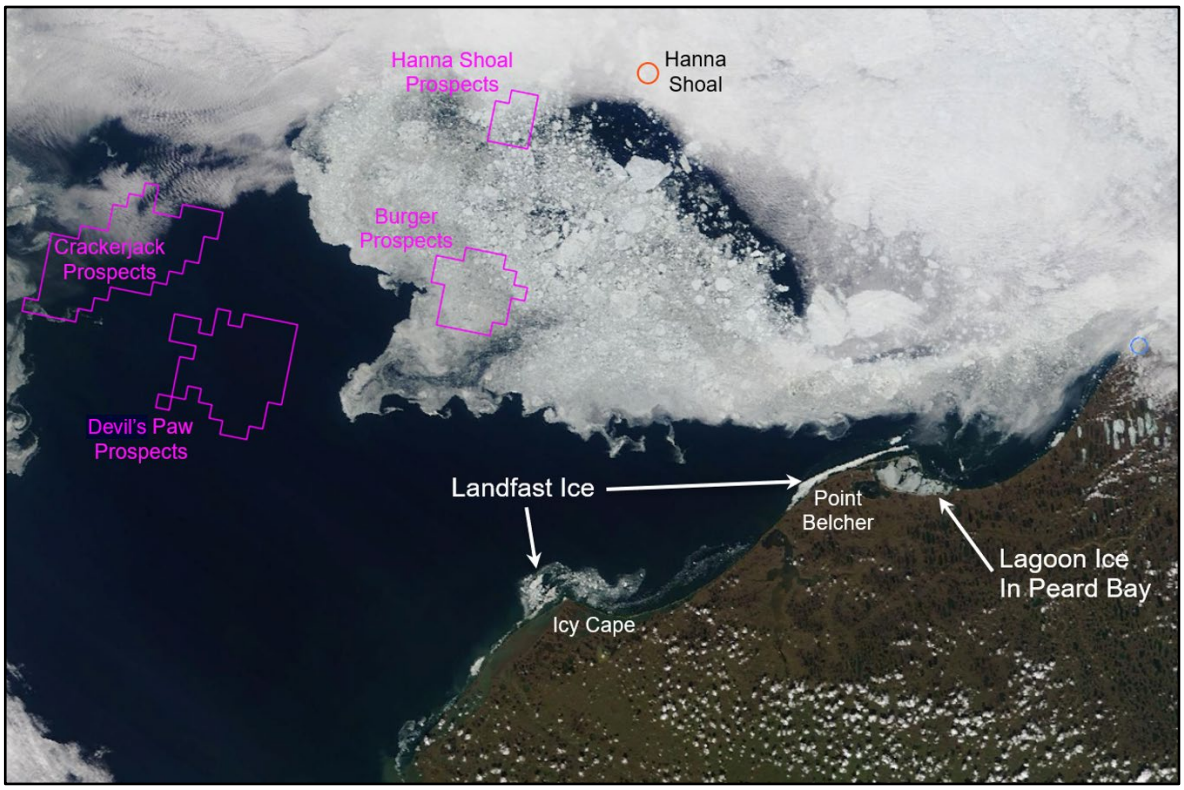

After: NASA, 2020a

Figure 6-17. MODIS Image of Chukchi Sea Acquired on July 1, 2020

Landfast Ice: The locations of the landfast ice edge on June 24th and July 11th are shown in Figure 6-18, while the intermittent patches that existed at the beginning of July are displayed in Figure 6-17. The patches diminished rapidly during the first half of the month, causing the last remnant, grounded off the base of the Point Franklin Spit, to disappear on the 16th or 17th.

Pack Ice: The pack ice continued to dissipate in July, vacating the Siberian coast during the third week of the month as it retreated to the north. Its extent on July 11th is shown in Figure 6-19.

At the end of July, the southern edge trended northwest from the vicinity of Utqiagvik with the exception of a 50-nm (93-km) wide tongue that extended southwest as far as the Devil's Paw Prospects (Figures 4-2 and 6-20).

"THIS INFORMATION IS DISTRIBUTED SOLELY FOR THE PURPOSE OF PRE-DISSEMINATION PEER REVIEW UNDER APPLICABLE INFORMATION QUALITY GUIDELINES. IT HAS NOT BEEN FORMALLY DISSEMINATED BY BSEE. IT DOES NOT REPRESENT AND SHOULD NOT BE CONSTRUED TO REPRESENT ANY BSEE DETERMINATION OR POLICY."

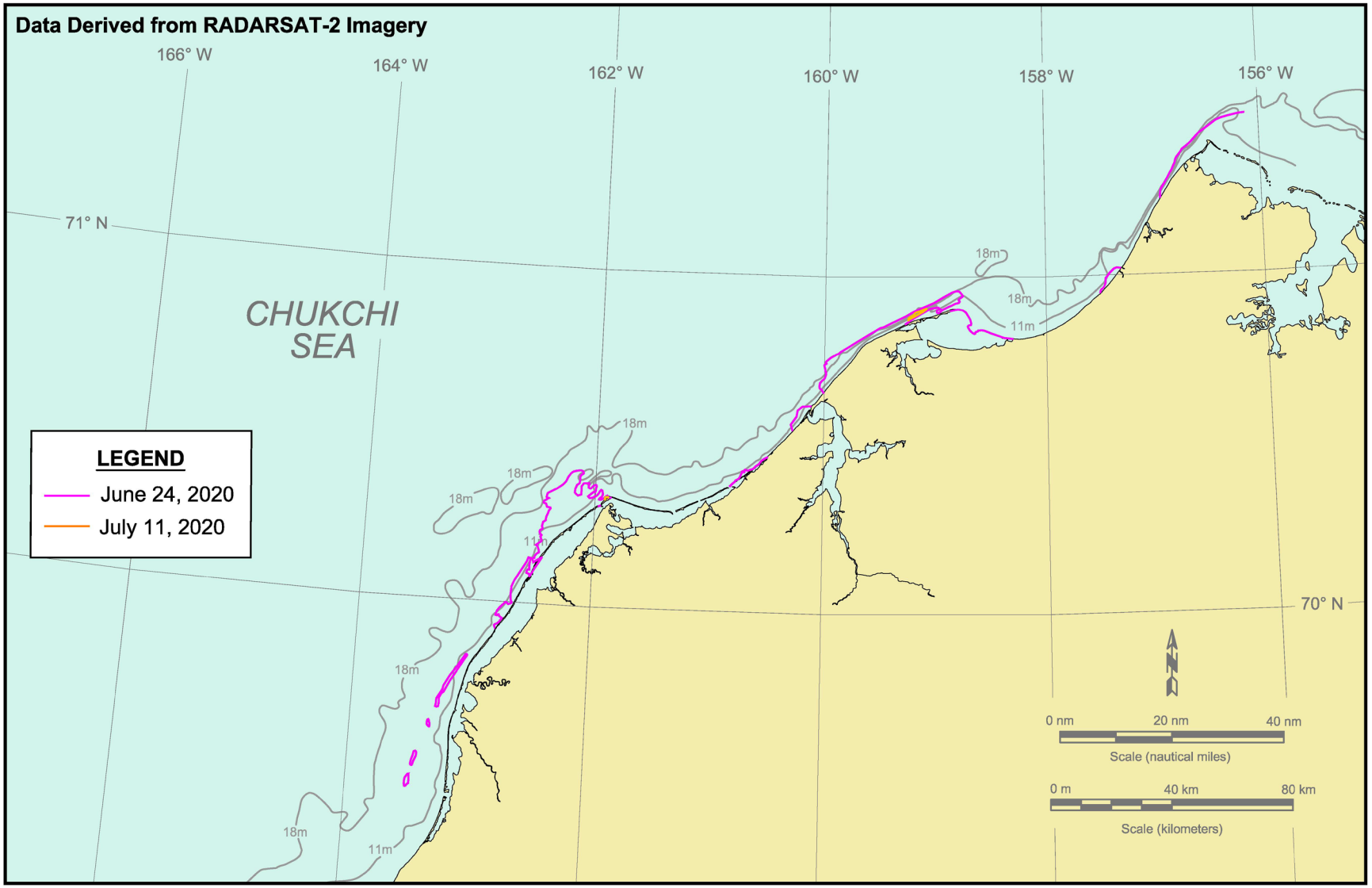

Figure 6-18. Chukchi Sea Landfast Ice Edge in July 2020

“THIS INFORMATION IS DISTRIBUTED SOLELY FOR THE PURPOSE OF PRE-DISSEMINATION PEER REVIEW UNDER APPLICABLE INFORMATION QUALITY GUIDELINES. IT HAS NOT BEEN FORMALLY DISSEMINATED BY BSEE. IT DOES NOT REPRESENT AND SHOULD NOT BE CONSTRUED TO REPRESENT ANY BSEE DETERMINATION OR POLICY.”

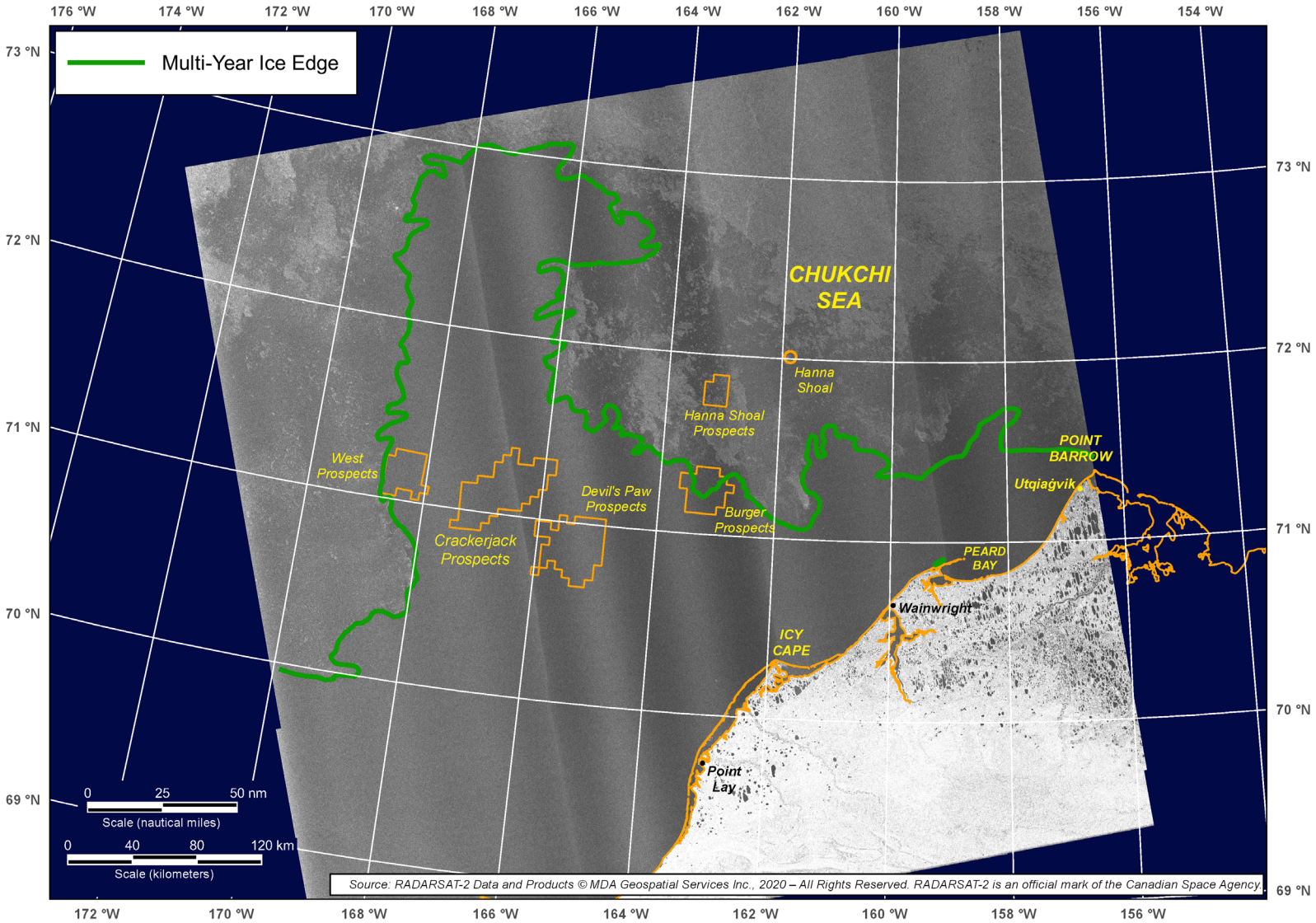

Figure 6-19. RADARSAT-2 Image of Chukchi Sea Acquired on July 11, 2020

"THIS INFORMATION IS DISTRIBUTED SOLELY FOR THE PURPOSE OF PRE-DISSEMINATION PEER REVIEW UNDER APPLICABLE INFORMATION QUALITY GUIDELINES. IT HAS NOT BEEN FORMALLY DISSEMINATED BY BSEE. IT DOES NOT REPRESENT AND SHOULD NOT BE CONSTRUED TO REPRESENT ANY BSEE DETERMINATION OR POLICY."

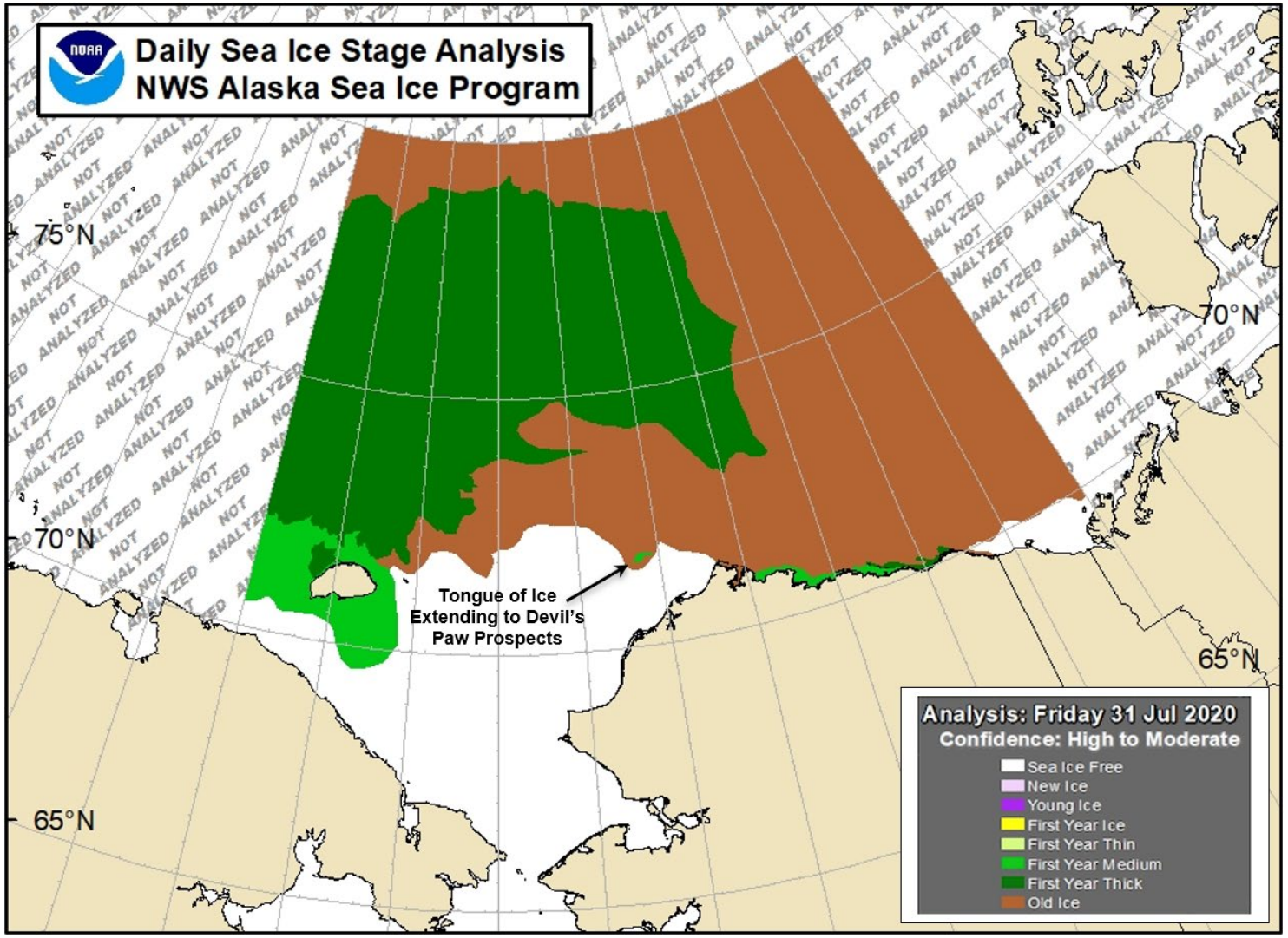

After: NWS, 2020

Figure 6-20. NWS Stage of Development Ice Chart for July 31, 2020

"THIS INFORMATION IS DISTRIBUTED SOLELY FOR THE PURPOSE OF PRE-DISSEMINATION PEER REVIEW UNDER APPLICABLE INFORMATION QUALITY GUIDELINES. IT HAS NOT BEEN FORMALLY DISSEMINATED BY BSEE. IT DOES NOT REPRESENT AND SHOULD NOT BE CONSTRUED TO REPRESENT ANY BSEE DETERMINATION OR POLICY."

Multi-Year Ice: The location of the multi-year ice edge on July 11th is shown in Figure 6-19. As in June, the loss of landfast ice that occurred in July produced a corresponding loss of the embedded multi-year ice. The last vestige, located at the base of the Point Franklin Spit, vanished on the 16th or 17th. Farther offshore, the multi-year floes in the pack ice retreated in concert with the first-year floes, leaving the region to the west and south of Point Barrow nearly devoid of multi-year ice at month-end (Figure 6-20).

Ice Drift: Ice drift was investigated using Buoys B and C, both of which were located in the pack ice in Chukchi Sea study area from July 1st through 20th. Their tracks are shown in Figure 6-21; their daily average speeds are plotted in concert with the corresponding wind data from Utqiagvik in Figure 6-22.

In keeping with the easterly winds that prevailed on all but the last day of the 20-day period of record, both buoys moved steadily to the northwest. Buoy B experienced a net displacement of 155 nm (287 km), while that of Buoy C was 170 nm (315 km). The corresponding monthly average speeds, computed on the basis of the net displacements, were 7.8 and 8.5 nm/day (14.5 and 15.8 km/day).

As in June, a daily average speed was computed for each buoy using its position at midnight on each day in the period of record. The peak value, 13.8 nm/day (25.6 km/day) was attained by Buoy C on July 8th. The daily average wind speed at Utqiagvik was 14 kt (7 m/s) on this date, producing a wind factor of 4.1%. It should be noted, however, that the buoy was located more than 125 nm (232 km) to the northwest of Utqiagvik and therefore may have experienced different wind conditions.

"THIS INFORMATION IS DISTRIBUTED SOLELY FOR THE PURPOSE OF PRE-DISSEMINATION PEER REVIEW UNDER APPLICABLE INFORMATION QUALITY GUIDELINES. IT HAS NOT BEEN FORMALLY DISSEMINATED BY BSEE. IT DOES NOT REPRESENT AND SHOULD NOT BE CONSTRUED TO REPRESENT ANY BSEE DETERMINATION OR POLICY."

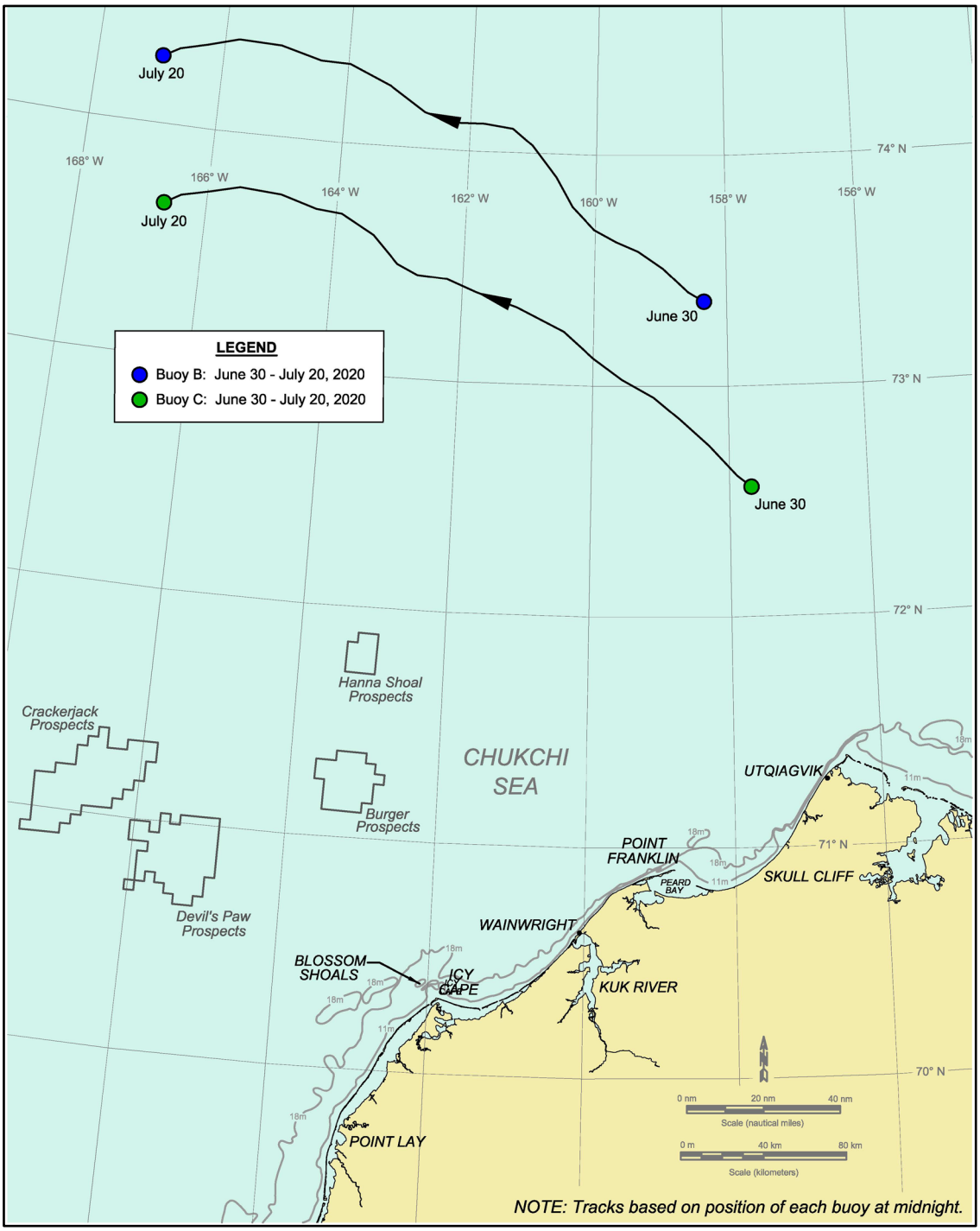

Figure 6-21. Chukchi Sea Drift Buoy Tracks, July 2020

“THIS INFORMATION IS DISTRIBUTED SOLELY FOR THE PURPOSE OF PRE-DISSEMINATION PEER REVIEW UNDER APPLICABLE INFORMATION QUALITY GUIDELINES. IT HAS NOT BEEN FORMALLY DISSEMINATED BY BSEE. IT DOES NOT REPRESENT AND SHOULD NOT BE CONSTRUED TO REPRESENT ANY BSEE DETERMINATION OR POLICY.”

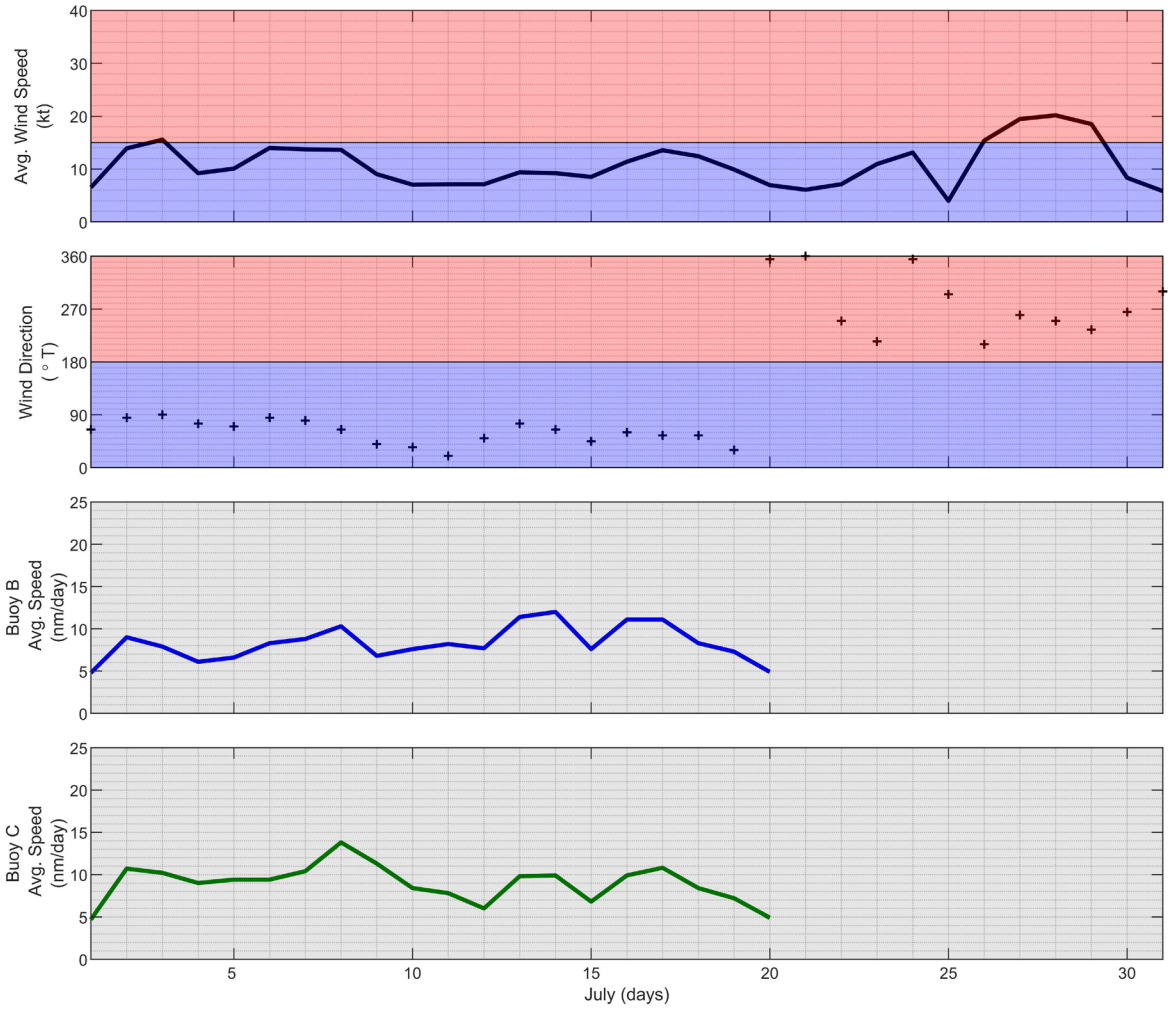

Figure 6-22. Chukchi Sea Drift Buoy Daily Average Speeds in July 2020

"THIS INFORMATION IS DISTRIBUTED SOLELY FOR THE PURPOSE OF PRE-DISSEMINATION PEER REVIEW UNDER APPLICABLE INFORMATION QUALITY GUIDELINES. IT HAS NOT BEEN FORMALLY DISSEMINATED BY BSEE. IT DOES NOT REPRESENT AND SHOULD NOT BE CONSTRUED TO REPRESENT ANY BSEE DETERMINATION OR POLICY."

7. BEAUFORT SEA BREAK-UP

Section 7.1 provides an overview of the 2020 break-up season in the Alaskan Beaufort Sea, while Sections 7.2 through 7.5 present a more in-depth look at the conditions that prevailed during this period as well as a summary of the observations made during the reconnaissance flights.

7.1. Overview

Air Temperatures: The daily average air temperatures at Deadhorse Airport tended to fall with the normal range in May, June, and July. When excursions outside the range did occur, they were of limited extent and duration. Over the course of the 92-day study period, the daily average values exceeded the normal range on ten occasions (11% frequency) and fell below on four (4% frequency). Thawing degree days (TDD) began to accumulate on May 23rd, when the daily average temperature reached 33°F (1°C).

Winds: Table 7-1 presents the daily average wind speeds and directions recorded at Deadhorse Airport during the 2020 break-up season. Easterlies predominated in each of the three months, with frequencies of 77% in May, 93% in June, and 68% in July. Over the entire three-month period, easterlies outnumbered westerlies by a margin of 79% to 21%. The average monthly speeds decreased from 13 kt (7 m/s) in May to 12 kt (6 m/s) in June and 9 kt (5 m/s) in July.

Table 7-1. Beaufort Sea Wind Characteristics, May–July 2020

Month	Easterly Wind Predominance (days)	Westerly Wind Predominance (days)	Average Speed (kt)
May	24	7	13
June	28	2	12
July	21	10	9
Total Days	**73**	**19**	n/a
Frequency (%)	**79**	**21**	n/a

Note: Table 7-1 is based on the daily average values recorded at Deadhorse Airport.

Storms: The characteristics of all storms with a daily average sustained wind speed exceeding 15 kt (8 m/s) at Deadhorse Airport are presented in Table 7-2. Only four such events took place during the study period, all of which were easterlies. The most severe, with a maximum daily average wind speed of 32 kt (16 m/s), began on May 11th and

"THIS INFORMATION IS DISTRIBUTED SOLELY FOR THE PURPOSE OF PRE-DISSEMINATION PEER REVIEW UNDER APPLICABLE INFORMATION QUALITY GUIDELINES. IT HAS NOT BEEN FORMALLY DISSEMINATED BY BSEE. IT DOES NOT REPRESENT AND SHOULD NOT BE CONSTRUED TO REPRESENT ANY BSEE DETERMINATION OR POLICY."

Table 7-2. Beaufort Sea Storm Characteristics, May–July 2020[1]

Month[2]	Day	Duration (days)	Maximum Easterly Wind Speed (kt)[3]	Maximum Westerly Wind Speed (kt)[3]
May	7	1	16	-
May	11-13	3	32	-
May	18-23[4]	6	21	-
June	May 30 – Jun 6	8	26	-
Total Duration	n/a	**18**	n/a	n/a
Total Number of Events	n/a	n/a	**4**	**0**

Notes:

[1] Table 7-2 includes all storm events with a daily average sustained wind speed exceeding 15 kt (8 m/s) at Deadhorse Airport.

[2] No storms occurred in July 2020.

[3] "Maximum Wind Speed" refers to the highest daily average sustained wind speed that occurred during each storm event.

[4] Daily average sustained wind speed decreased to 13 kt on May 20th but freshened to 17 kt on May 21st.

continued for three additional days. The most persistent, with a maximum daily average wind speed of 26 kt (13 m/s), began on May 30th and continued for seven additional days. This storm proved to be the last to occur within the study period.

Ice Thickness: The thickness of decaying, undeformed first-year ice was estimated using the relationship of Bilello (1980) in concert with TDD accumulated at Deadhorse Airport (Table 4-1). The method of calculation is identical to that presented for the Chukchi Sea in Section 6.1. The results, which appear in Table 7-3, indicate that the computed thickness of first-year ice at the end of the winter season, 162 cm (Coastal Frontiers and Vaudrey, 2020), decreased to zero during the 47-day period that began on May 23rd and ended on July 8th.

River Overflood: Of the many rivers and streams that discharge into the Beaufort Sea study area, five of the largest were selected for the analysis of overflood onto the sea ice: the Canning, Sagavanirktok, Kuparuk, Colville, and Ikpikpuk (Figures 1-2 and 1-3; Table 7-4). Water from the Canning began to flood the ice east of Brownlow Point on May 19th, and that in the eastern portion of Stefansson Sound (Leffingwell Lagoon) on May 26th. Discharge from the Sagavanirktok first appeared in Stefansson Sound on May 19th, while that from the

"THIS INFORMATION IS DISTRIBUTED SOLELY FOR THE PURPOSE OF PRE-DISSEMINATION PEER REVIEW UNDER APPLICABLE INFORMATION QUALITY GUIDELINES. IT HAS NOT BEEN FORMALLY DISSEMINATED BY BSEE. IT DOES NOT REPRESENT AND SHOULD NOT BE CONSTRUED TO REPRESENT ANY BSEE DETERMINATION OR POLICY."

Table 7-3. Beaufort Sea Computed Ice Thickness, 2020 Break-Up[1]

Date	TDD	Accumulated TDD	Ice Thickness (cm)
May 22	0	0	162[2]
May 31	12	12	155
Jun 30	221	233	43[3]
Jul 8	86	319	0[3]

Notes:
1 Table 7-3 is based on the daily average air temperatures recorded at Deadhorse Airport.
2 The ice thickness at end of 2019-20 the winter season was computed by Coastal Frontiers and Vaudrey (2020) from accumulated FDD using the method of Lebedev (Bilello, 1960).
3 The ice thickness after May 22nd was computed from accumulated TDD using the method of Bilello (1980).

Table 7-4. Beaufort Sea River Overflood onto Sea Ice, 2020 Break-Up

River[1]	Receiving Body	Beginning of Overflood[2]
Canning	Beaufort Sea/Leffingwell Lagoon[3]	May 19/May 26
Sagavanirktok	Stefansson Sound	May 19
Kuparuk	Gwydyr Bay	May 27
Colville	Harrison Bay	May 22
Ikpikpuk	Smith Bay	May 29

Notes:
1 The rivers are listed from east to west, with their locations shown in Figures 1-2 and 1-3.
2 The date represents the first day on which overflood water was detected on the sea ice based on an analysis of MODIS imagery.
3 Leffingwell Lagoon constitutes the eastern portion of Stefansson Sound.

Colville reached Harrison Bay on the 22nd. The Kuparuk began flooding Gwydyr Bay on May 27th, followed by the Ikpikpuk flooding Smith Bay on the 29th. Most of the flood water remained in the receiving bays and lagoons. The sole exceptions consisted of the aforementioned discharge of the Canning River directly onto the sea ice east of Brownlow Point, and small tongues of water from the Kuparuk that pushed past the barrier islands off Gwydyr Bay.

Lagoon Ice: Break-up of the lagoon ice began on or about June 4th when flood water from the Sagavanirktok River melted through the ice in Prudhoe Bay (Table 7-5). Through-

"THIS INFORMATION IS DISTRIBUTED SOLELY FOR THE PURPOSE OF PRE-DISSEMINATION PEER REVIEW UNDER APPLICABLE INFORMATION QUALITY GUIDELINES. IT HAS NOT BEEN FORMALLY DISSEMINATED BY BSEE. IT DOES NOT REPRESENT AND SHOULD NOT BE CONSTRUED TO REPRESENT ANY BSEE DETERMINATION OR POLICY."

Table 7-5. Break-Up and Open Water in Beaufort Sea Lagoons, 2020

Lagoon	Break-Up[1]	Open Water[2]
South Camden Bay	Jun 9	Jun 30 - Jul 1[3]
Stefansson Sound	Jun 8	Jul 10
Prudhoe Bay	Jun 4	Jun 30 – Jul 2[3]
Gwydyr Bay	Jun 9	Jun 20 - 26[3]
Simpson Lagoon	Jun 26	Jun 29 – Jul 2[3]
South Harrison Bay	Jun 8	Jun 28 – Jul 2[3]
Smith Bay	Jun 11	Jul 5-7[3]

Notes:

[1] The date of break-up represents the first occasion on which ice coverage below 10/10s was detected in MODIS imagery.

[2] The date of open water represents the first occasion on which ice coverage below 1/10 was detected in MODIS imagery.

[3] The exact date could not be determined due to a gap in useful satellite imagery.

ice melting followed in the eastern portion of Stefansson Sound (Leffingwell Lagoon; Canning River overflood) and South Harrison Bay (Colville River overflood) on the 8th, South Camden Bay (Canning River overflood), and Gwydyr Bay (Kuparuk River overflood) on the 9th, and Smith Bay (Ikpikpuk River overflood) on the 11th. In Simpson Lagoon, break-up took place on or about June 26th in response to the heat emanating from the mainland coast east of Oliktok Point.

Open water in the lagoon areas occurred over a period of several weeks that began with Gwydyr Bay between June 20th and 26th and ended with Stefansson Sound on July 10th. All of the sites shown in Table 7-5 became ice-free by the end of July.

Landfast Ice: In mid-May, the seaward edge of the landfast ice was located offshore of the 18-m isobath from Point Barrow to Cape Halkett, between the 18- and 11-m isobaths from Cape Halkett to western Camden Bay, and offshore of the 18-m isobath in eastern Camden Bay. Of particular note was the absence of landfast ice on Weller Bank and Stamukhi Shoal, which typically serve as anchor points for such ice in the vicinity of Harrison Bay.

Break-up of the landfast ice between Point Barrow and Cross Island occurred on May 23rd, when a small loss occurred off Cape Halkett at the end of a six-day easterly storm (Table 6-2). Three days later, a one-day wind shift from easterly to southwesterly produced substantial losses between Smith Bay and Cape Halkett. Farther east, between Cross Island

"THIS INFORMATION IS DISTRIBUTED SOLELY FOR THE PURPOSE OF PRE-DISSEMINATION PEER REVIEW UNDER APPLICABLE INFORMATION QUALITY GUIDELINES. IT HAS NOT BEEN FORMALLY DISSEMINATED BY BSEE. IT DOES NOT REPRESENT AND SHOULD NOT BE CONSTRUED TO REPRESENT ANY BSEE DETERMINATION OR POLICY."

and Barter Island, break-up of the landfast ice began with modest losses off Stefansson Sound and Camden Bay on May 27th.

In early June, the landfast ice edge tended to lie between the 18- and 11-m isobaths from Point Barrow to Flaxman Island, and to protrude seaward of the 18-m isobath in Camden Bay. In the absence of westerly storms, losses were minimal until the last week in June. At that time, a combination of warm air temperatures, increased wind speeds, and warm sea surface temperatures resulting both from river overflood and from the arrival of warm-water plumes from the Alaska Coastal Current to the west and Mackenzie River to the east, caused substantial losses off Smith Bay and in Harrison and Camden Bays. At the end of June, the ice edge paralleled the 18-m isobath off Admiralty Bay before dipping inside the 11-m isobath off Smith Bay and in Harrison Bay. East of Harrison Bay, it tended to trend between the two isobaths.

The accelerated rate of landfast ice deterioration that began in late June continued during the first half of July. As in June, in the absence of storm activity, the driving forces appear to have been the warming air and sea surface temperatures in concert with moderate wind speeds. By mid-July, the ice was confined to a patch in Elson Lagoon, narrow strips on both sides of Smith Bay, small patches on the west side of Harrison Bay, and a narrow, discontinuous strip fronting the barrier islands from Cross to Flaxman. At the end of the month, small patches of landfast ice persisted between Pole and Flaxman Islands.

Pack Ice: The pack ice remained compact until late May. Although narrow flaw leads developed on several occasions, they proved to be ephemeral. During the last ten days of the month, however, warm water from the Alaska Coastal Current (Figure 1-1) moved around Point Barrow and produced patches of open water adjacent to the landfast ice as far east as Harrison Bay. On May 31st, warm water moving west from the Mackenzie River created a patch of open water adjacent to the landfast ice in Camden Bay.

In June, unrelenting easterly winds propelled the Mackenzie plume to the west while impeding the easterly progress of the plume from the Alaska Coastal Current. At mid-month, the former had advanced to the region off Prudhoe Bay, while the latter was stalled in the region off Admiralty Bay. Farther offshore, the pack ice remained compact.

During the final week of June, the pack ice concentrations in the nearshore region declined markedly in response to the westward progression of the Mackenzie plume to Harrison Bay and the eastern progression of the Alaska Coastal Current plume to Smith Bay. At month-end, the only two areas in which dense pack ice extended as far south as the landfast

"THIS INFORMATION IS DISTRIBUTED SOLELY FOR THE PURPOSE OF PRE-DISSEMINATION PEER REVIEW UNDER APPLICABLE INFORMATION QUALITY GUIDELINES. IT HAS NOT BEEN FORMALLY DISSEMINATED BY BSEE. IT DOES NOT REPRESENT AND SHOULD NOT BE CONSTRUED TO REPRESENT ANY BSEE DETERMINATION OR POLICY."

ice were located off western Harrison Bay and Admiralty Bay. Offshore, small patches of open water had begun to develop between the larger ice floes.

The deterioration of the pack ice continued in July, with the dense tongues that approached western Harrison Bay and Admiralty Bay dispersing by mid-month. At that time, the ice concentrations off the coast ranged from less than 10% to 50% in a band that narrowed from more than 50 nm (93 km) wide off Camden Bay to about 20 nm wide (37 km) off Smith Bay. At month-end, the southern boundary was separated from the coast by distances that ranged from only 1 nm (2 km) off Thetis Island to more than 40 nm (74 km) off Flaxman Island.

Ice Pile-Ups: When reconnaissance flights were undertaken in late February, 32 ice pile-ups were discovered in the central portion of the Alaskan Beaufort Sea (Coastal Frontiers and Vaudrey, 2020). Six were located on manmade islands and 26 on natural barrier islands and shoals bounded by Duchess Island on the east and Thetis Island on the west. Half of these remained when the break-up flights were conducted in early July, including three on manmade islands and 13 on barrier islands and shoals. In all cases, the dimensions of the relict pile-ups had been diminished by melting. No new pile-ups or ride-ups that had formed during break-up were discovered during the July reconnaissance flights.

Multi-Year Ice: At the end of February, multi-year ice was embedded in the landfast ice at concentrations typically less than 10% and in the pack ice at concentrations ranging from less than 10% to 50% (Coastal Frontiers and Vaudrey, 2020). The only region lacking such ice was a tongue of first-year ice that extended from the U.S.-Canadian border to the eastern edge of Harrison Bay just offshore of the landfast ice.

At the beginning of May, the locations and concentrations of multi-year ice bore a close resemblance to those at the end of February, with concentrations typically less than 10% in the landfast ice and from less than 10% to 50% in the pack ice. In addition, the aforementioned nearshore tongue of first-year ice remained devoid of multi-year ice.

The multi-year ice embedded in the landfast ice remained in place until late May, when losses began to occur in conjunction with the disintegration of the latter. The dispersal of the multi-year ice continued through the end of the study period, mirroring that of the landfast ice.

With the exception of the nearshore tongue of first-year ice, which closed during the first week in June, multi-year ice remained omnipresent in the pack ice through the end of July. The concentrations ranged from less than 10% to a maximum of 70%, with the latter

"THIS INFORMATION IS DISTRIBUTED SOLELY FOR THE PURPOSE OF PRE-DISSEMINATION PEER REVIEW UNDER APPLICABLE INFORMATION QUALITY GUIDELINES. IT HAS NOT BEEN FORMALLY DISSEMINATED BY BSEE. IT DOES NOT REPRESENT AND SHOULD NOT BE CONSTRUED TO REPRESENT ANY BSEE DETERMINATION OR POLICY."

confined to a small region just west of the U.S.-Canadian border in late May and early June. Thereafter, the maximum concentration remained constant at 40% (CIS, 2020). The floe sizes varied over a wide range, from brash ice to maximum horizontal dimensions exceeding 25 km.

Ice Drift: Figure 7-1 illustrates the tracks of five drift buoys (Buoys B, C, D, E, and F) that were embedded in the pack ice within the study area during various portions of the study period. They had been deployed for a variety of purposes prior to the start of the study and were monitored through the International Arctic Buoy Program (Section 4.4).

In May, June, and the first 20 days of July, the Beaufort Gyre was reinforced by an overwhelming predominance of easterly winds (Table 7-1). All of the buoys tracked during this period experienced substantial displacements to the northwest. Subsequently, during the last 11 days of July, the winds shifted to westerly and the sole buoy that remained in the study area, Buoy F, reversed course and moved to the northeast.

A monthly average drift rate was computed for each buoy for each month in which the tracking period exceeded 15 days based on its net displacement during this period. The results are presented in Table 7-6. The speeds of the individual buoys ranged from a maximum of 6.3 nm/day (11.7 km/day) in May to a minimum of 1.1 nm/day (2.0 km/day) in July. The values averaged over all buoys decreased from 5.4 nm/day (10.0 km day) in May to 4.3 nm/day (8.0 km/day) in June and 2.9 nm/day (5.4 km/day) in July.

Table 7-6. Beaufort Sea Pack Ice Drift, May–July 2020

Month	No. of Buoys	Maximum Monthly Average Speed (nm/day)	Minimum Monthly Average Speed (nm/day)	Average Monthly Average Speed (nm/day)
May	3	6.3	4.3	5.4
June	5	5.9	2.2	4.3
July	2	4.6	1.1	2.9
Average	n/a	n/a	n/a	**4.2**

Note: Monthly average speeds were derived for periods that ranged from 16 to 31 days.

"THIS INFORMATION IS DISTRIBUTED SOLELY FOR THE PURPOSE OF PRE-DISSEMINATION PEER REVIEW UNDER APPLICABLE INFORMATION QUALITY GUIDELINES. IT HAS NOT BEEN FORMALLY DISSEMINATED BY BSEE. IT DOES NOT REPRESENT AND SHOULD NOT BE CONSTRUED TO REPRESENT ANY BSEE DETERMINATION OR POLICY."

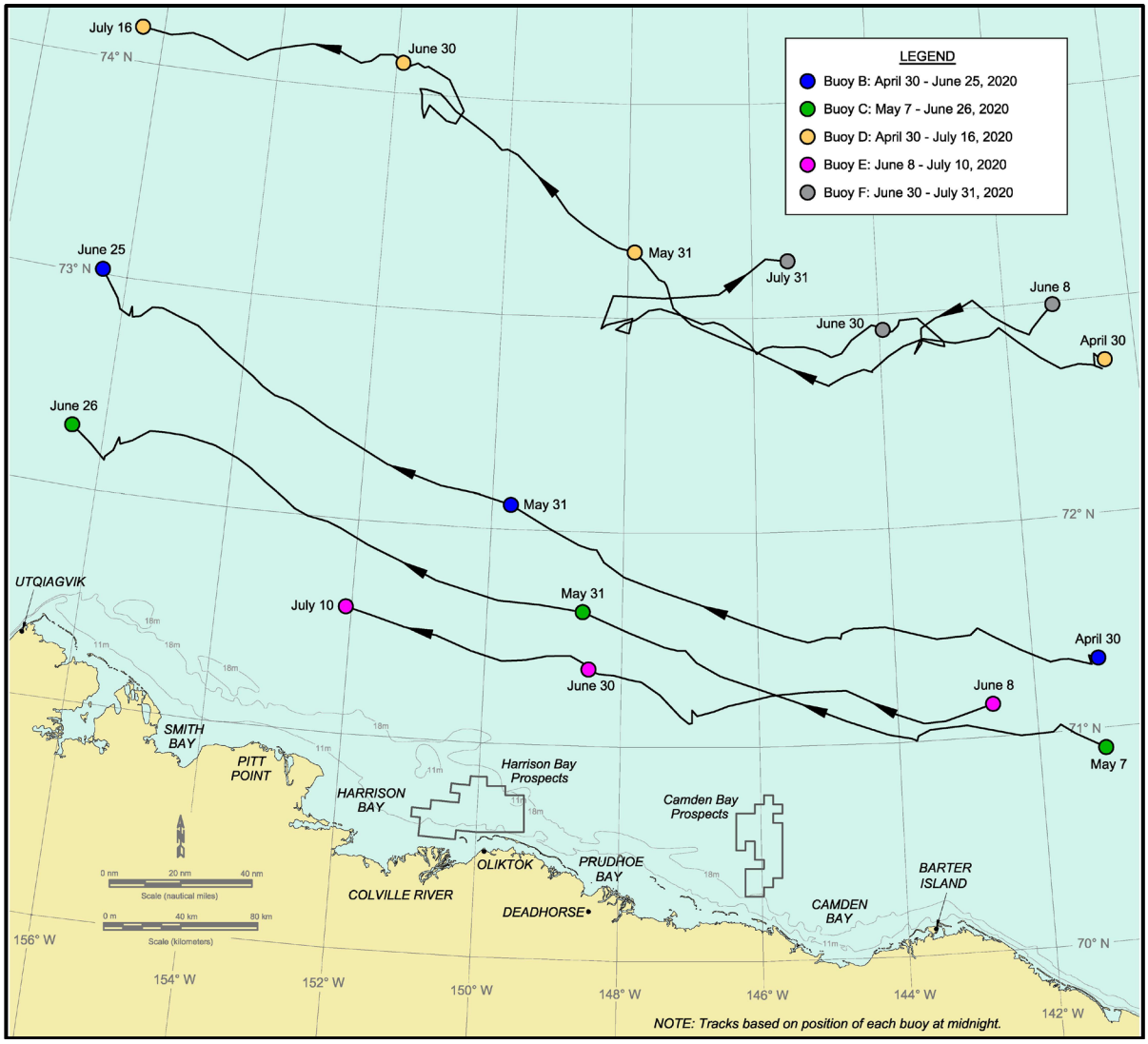

Figure 7-1. Beaufort Sea Drift Buoy Tracks, May–July 2020

7.2. May 2020

Meteorological Conditions: The daily values of average and maximum sustained wind speed, average wind direction, and average air temperature at Deadhorse Airport are shown in Figure 7-2. As in Section 6, the red and blue color bands in this and all subsequent meteorological plots denote the ranges of parameters defined in Table 6–8. Unless indicated otherwise, the wind speeds discussed in the text refer to the daily average values of the sustained speed rather than the daily maximum values or hourly values.

The air temperatures tended to follow the lower bound of the normal range during the first half of the month, and the upper bound during the second. The daily average values,

"THIS INFORMATION IS DISTRIBUTED SOLELY FOR THE PURPOSE OF PRE-DISSEMINATION PEER REVIEW UNDER APPLICABLE INFORMATION QUALITY GUIDELINES. IT HAS NOT BEEN FORMALLY DISSEMINATED BY BSEE. IT DOES NOT REPRESENT AND SHOULD NOT BE CONSTRUED TO REPRESENT ANY BSEE DETERMINATION OR POLICY."

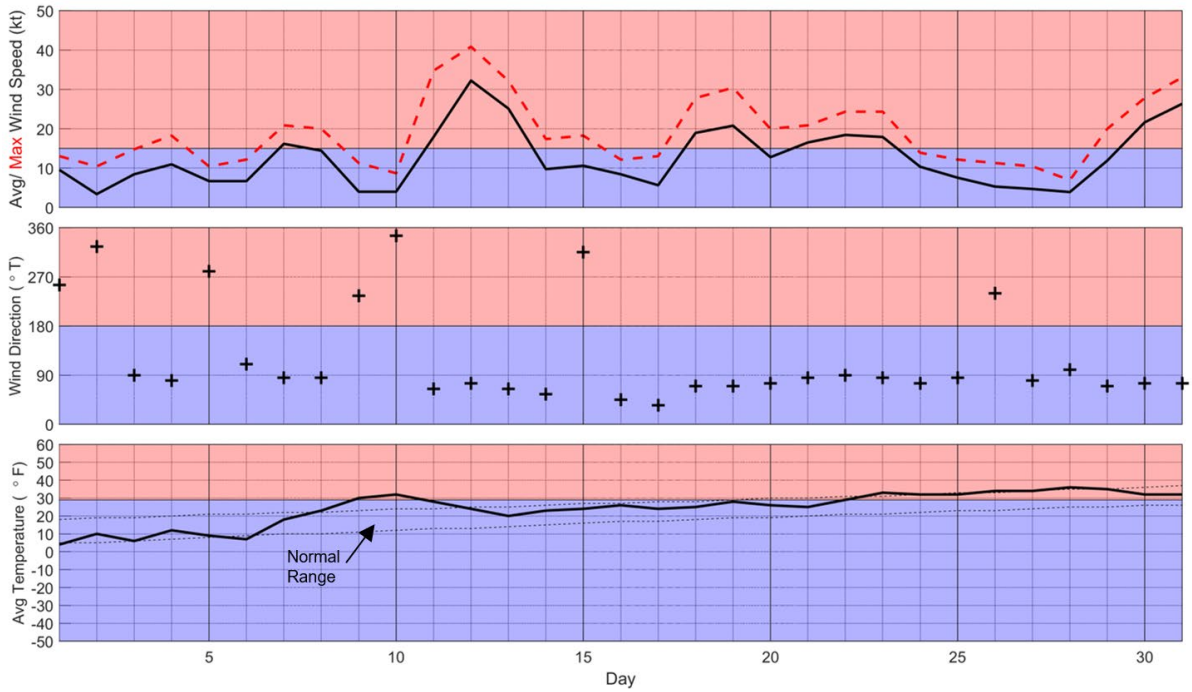

Figure 7-2 Meteorological Conditions at Deadhorse Airport in May 2020

which varied between 4 and 36°F (-16 and 2°C), exceeded the normal range on seven occasions and fell below on two. The average temperature for the month was 24°F (-4°C).

Easterly winds outnumbered westerlies by a wide margin, occurring on 24 of the 31 days (Table 7-1). The average speed was 13 kt (7 m/s). Three storms, all of which were easterlies, occurred over the course of the month (Table 7-2):

- May 7th: one-day easterly with maximum speed of 16 kt (8 m/s);
- May 11th-13th: three-day easterly with maximum speed of 32 kt (16 m/s);
- May 18th-23rd: six-day easterly with maximum speed of 21 kt (11 m/s).

A fourth storm, also an easterly, began on May 30th but is attributed to June because it continued through June 4th.

Ice Thickness: Based on accumulated FDD at Deadhorse Airport, the computed thickness of undeformed first-year ice increased from 159 cm at the beginning of May to 162 cm on the 21st (Coastal Frontiers and Vaudrey, 2020). TDD began to accumulate two days later, reducing the computed thickness to 155 cm at month-end (Table 7-3).

River Overflood: The Canning River began overflooding the sea ice east of Brownlow Point on May 19th, and that in the eastern portion of Stefansson Sound (Leffingwell Lagoon) on the 26th. Discharge from the Sagavanirktok first appeared in Stefansson Sound on the 19th,

"THIS INFORMATION IS DISTRIBUTED SOLELY FOR THE PURPOSE OF PRE-DISSEMINATION PEER REVIEW UNDER APPLICABLE INFORMATION QUALITY GUIDELINES. IT HAS NOT BEEN FORMALLY DISSEMINATED BY BSEE. IT DOES NOT REPRESENT AND SHOULD NOT BE CONSTRUED TO REPRESENT ANY BSEE DETERMINATION OR POLICY."

while that from the Colville reached Harrison Bay on the 22nd. The Kuparuk began flooding Gwydyr Bay on May 27th. Flood water from the Ikpikpuk entered Smith Bay on the 29th, the same day on which the modest overflood from the Canning attained its maximum areal extent (Figure 7-3). Most of the flood water remained in the receiving bays and lagoons. The sole exceptions consisted of the aforementioned discharge of the Canning River directly onto the sea ice east of Brownlow Point, and small tongues of water from the Kuparuk that pushed past the barrier islands off Gwydyr Bay.

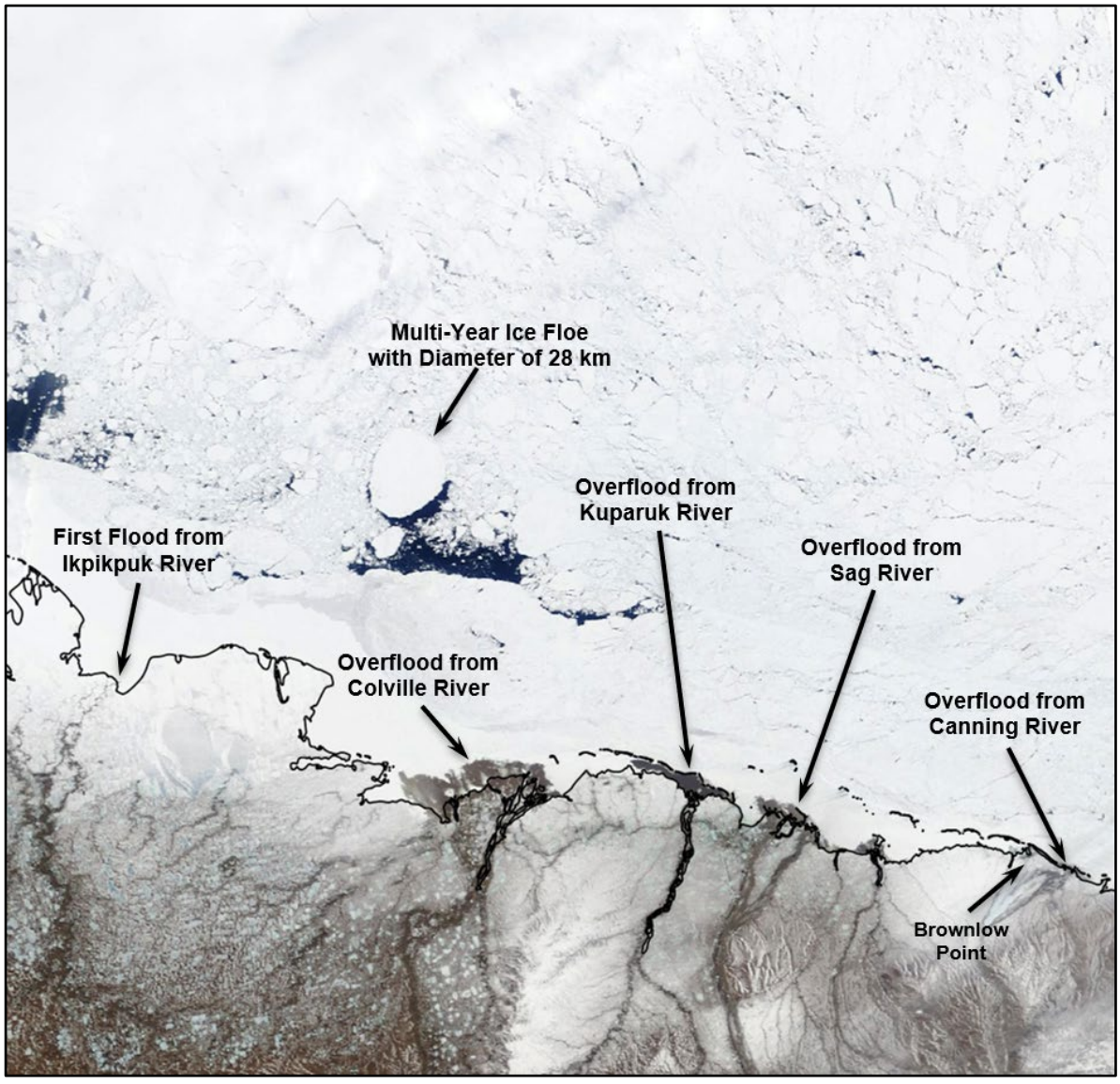

After: NASA, 2020a

Figure 7-3. MODIS Image of Beaufort Sea Acquired on May 29, 2020

"THIS INFORMATION IS DISTRIBUTED SOLELY FOR THE PURPOSE OF PRE-DISSEMINATION PEER REVIEW UNDER APPLICABLE INFORMATION QUALITY GUIDELINES. IT HAS NOT BEEN FORMALLY DISSEMINATED BY BSEE. IT DOES NOT REPRESENT AND SHOULD NOT BE CONSTRUED TO REPRESENT ANY BSEE DETERMINATION OR POLICY."

Lagoon Ice: The ice in the semi-protected nearshore areas that included Smith Bay, the southern portion of Harrison Bay, Simpson Lagoon, Gwydyr Bay, Prudhoe Bay, Stefansson Sound, and the southern portion of Camden Bay remained intact throughout May despite overflooding in the vicinity of the river mouths (Figure 7-3). As defined in Section 2.2, "South Harrison Bay" denotes the region to the south of a line between Atigaru Point and Spy Island (Figure 1-3), while "South Camden Bay" denotes the region to the south of a line between the mouth of the Canning River and Anderson Point (Figure 1-2).

Landfast Ice: Figure 7-4 illustrates the locations of the landfast ice edge derived from RADARSAT-2 images obtained on May 17th and June 3rd. In mid-May, the edge was located offshore of the 18-m isobath from Point Barrow to Cape Halkett, between the 18- and 11-m isobaths from Cape Halkett to western Camden Bay, and offshore of the 18-m isobath in eastern Camden Bay. Of particular note was the absence of landfast ice on Weller Bank and Stamukhi Shoal, which typically serve as anchor points for such ice in the vicinity of Harrison Bay.

Break-up of the landfast ice between Point Barrow and Cross Island occurred on May 23rd, when a small loss occurred off Cape Halkett at the end of a six-day easterly storm (Table 6-2). Three days later, a one-day wind shift from easterly to southwesterly produced substantial losses between Smith Bay and Cape Halkett. Farther east, between Cross Island and Barter Island, break-up of the landfast ice began with modest losses off Stefansson Sound and Camden Bay on May 27th. At the end of the month, the ice edge followed the 18-m isobath from Point Barrow to Cape Halkett, retreated to the region between the 11- and 18-m isobaths between Cape Halkett and Brownlow Point, and returned to the vicinity of the 18-m isobath in Camden Bay (Figure 7-4).

Pack Ice: The pack ice remained compact until late May, with a paucity of large leads (Figure 7-5). Although narrow flaw leads developed on several occasions, they proved to be ephemeral. During the last ten days of the month, however, warm water from the Alaska Coastal Current (Figure 1-1) moved around Point Barrow and produced patches of open water adjacent to the landfast ice as far east as Harrison Bay. On May 31st, warm water moving west from the Mackenzie River created a tongue of open water adjacent to the landfast ice in Camden Bay. Both plumes are evident in Figure 7-6, which displays a MODIS image acquired on the 31st.

Multi-Year Ice: At the beginning of May, the locations and concentrations of multi-year ice bore a close resemblance to those at the end of February (Coastal Frontiers and Vaudrey, 2020). Concentrations less than 10% were typical in the landfast ice zone and varied from less than 10% to 50% in the pack ice. The only region that lacked multi-year

"THIS INFORMATION IS DISTRIBUTED SOLELY FOR THE PURPOSE OF PRE-DISSEMINATION PEER REVIEW UNDER APPLICABLE INFORMATION QUALITY GUIDELINES. IT HAS NOT BEEN FORMALLY DISSEMINATED BY BSEE. IT DOES NOT REPRESENT AND SHOULD NOT BE CONSTRUED TO REPRESENT ANY BSEE DETERMINATION OR POLICY."

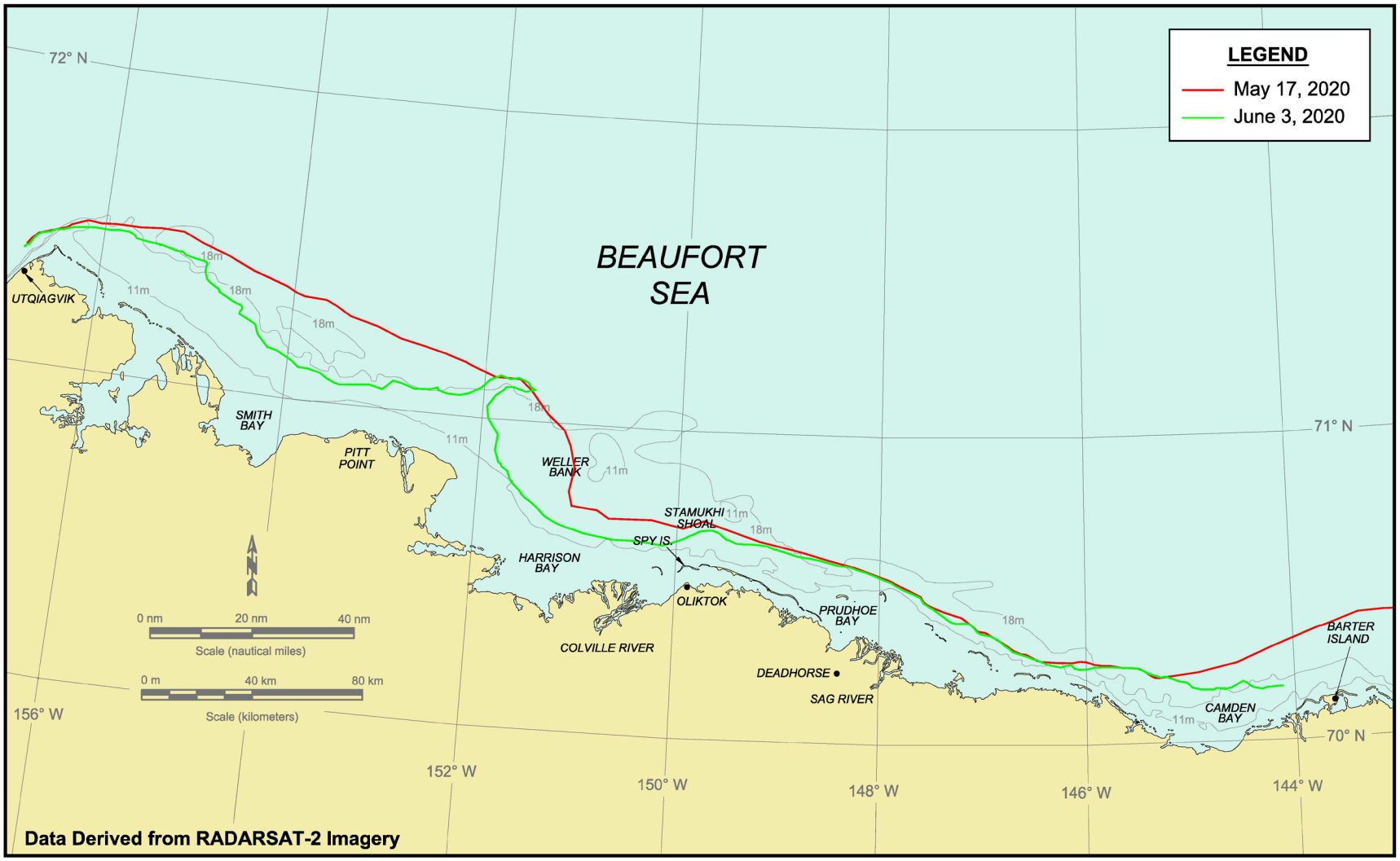

Figure 7-4. Beaufort Sea Landfast Ice Edge in May 2020

"THIS INFORMATION IS DISTRIBUTED SOLELY FOR THE PURPOSE OF PRE-DISSEMINATION PEER REVIEW UNDER APPLICABLE INFORMATION QUALITY GUIDELINES. IT HAS NOT BEEN FORMALLY DISSEMINATED BY BSEE. IT DOES NOT REPRESENT AND SHOULD NOT BE CONSTRUED TO REPRESENT ANY BSEE DETERMINATION OR POLICY."

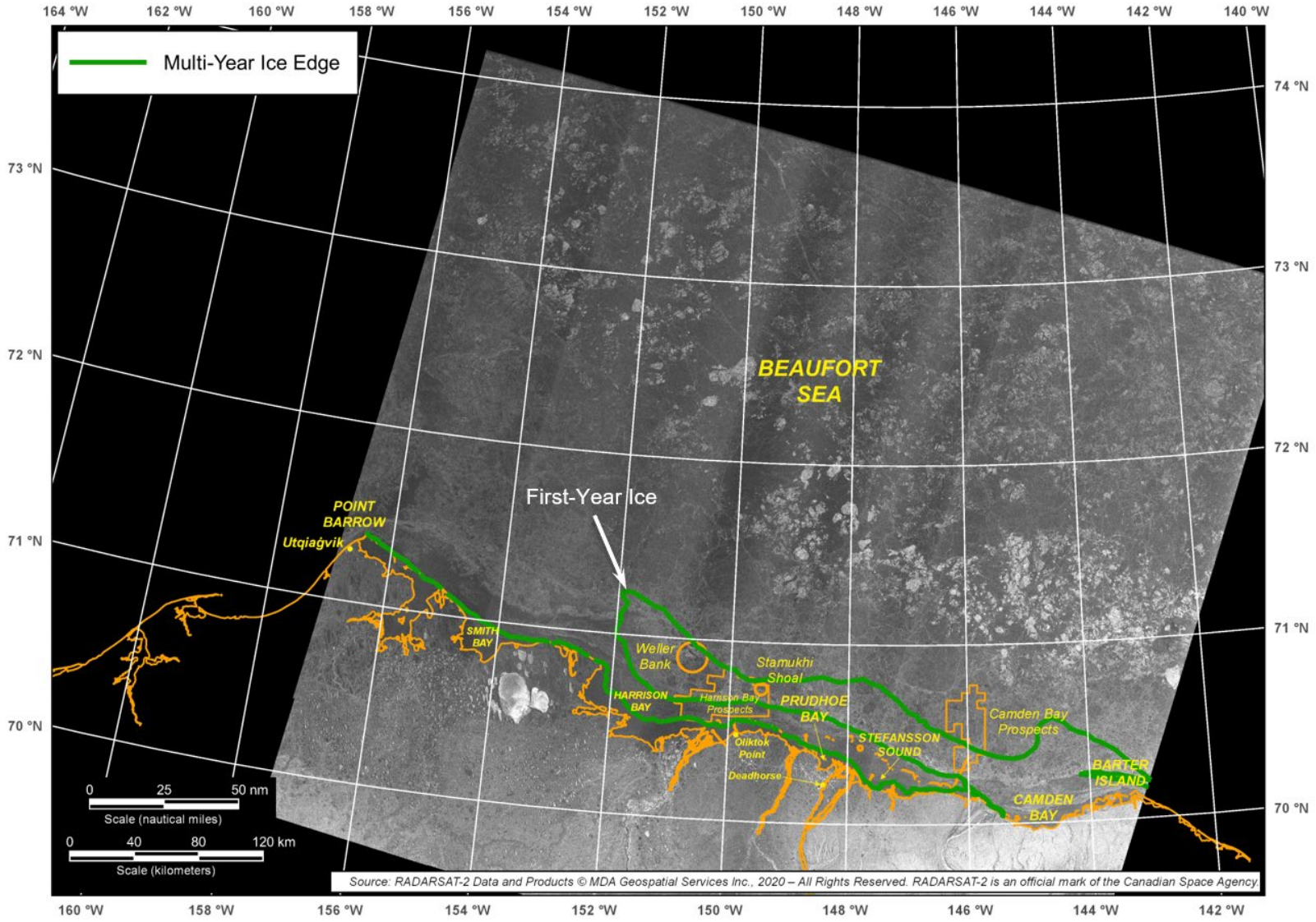

Figure 7-5. RADARSAT-2 Image of Beaufort Sea Acquired on May 17, 2020

"THIS INFORMATION IS DISTRIBUTED SOLELY FOR THE PURPOSE OF PRE-DISSEMINATION PEER REVIEW UNDER APPLICABLE INFORMATION QUALITY GUIDELINES. IT HAS NOT BEEN FORMALLY DISSEMINATED BY BSEE. IT DOES NOT REPRESENT AND SHOULD NOT BE CONSTRUED TO REPRESENT ANY BSEE DETERMINATION OR POLICY."

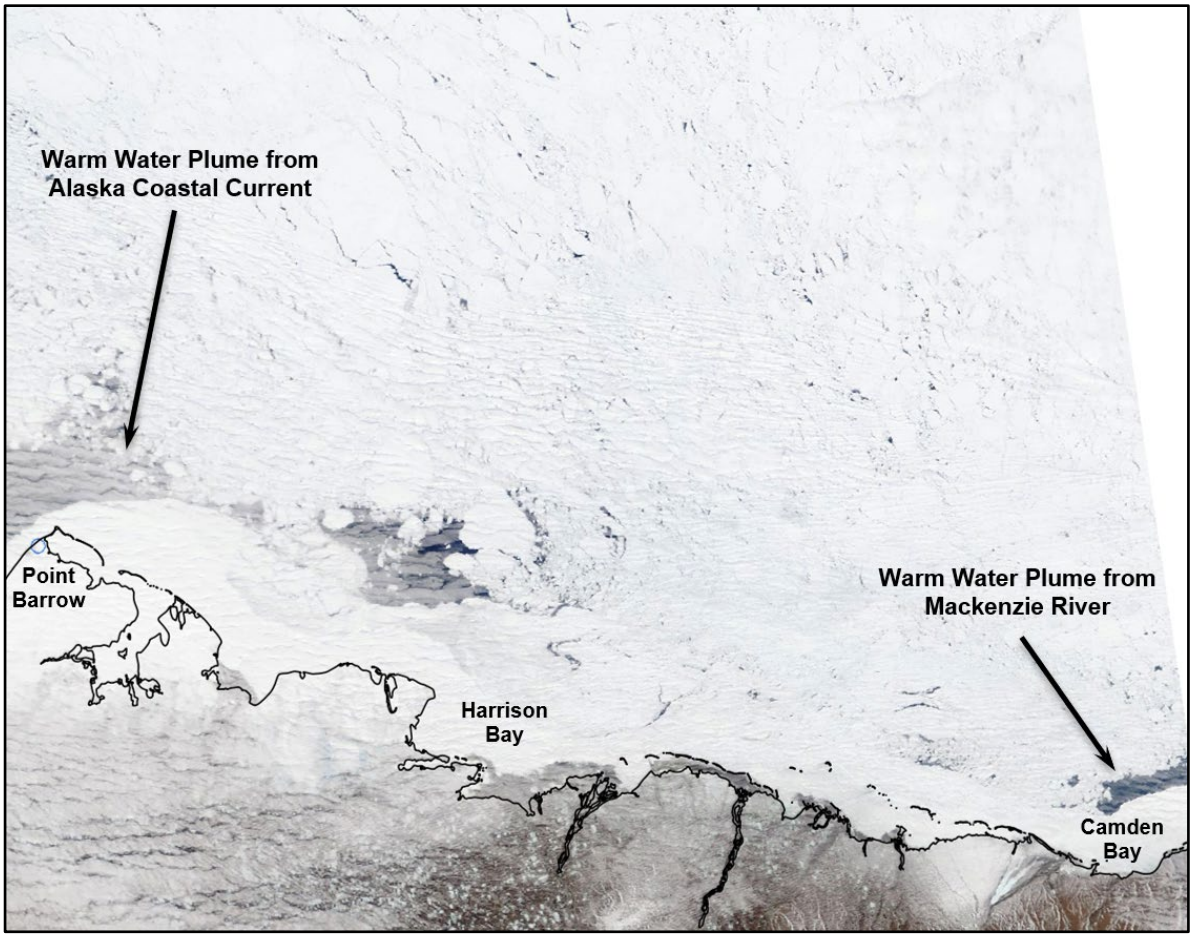

After: NASA, 2020a

Figure 7-6. MODIS Image of Beaufort Sea Acquired on May 31, 2020

ice was a tongue of first-year ice extending from the U.S.-Canadian border to the eastern edge of Harrison Bay just offshore of the landfast ice zone (Figure 7-5).

The multi-year ice embedded in the landfast ice remained in place until May 23rd, when losses began to occur in conjunction with the break-up of the latter. The dispersal of the multi-year ice mirrored that of the landfast ice, continuing through the end of the study period.

With the exception of the nearshore tongue of first-year ice, which persisted until early June, multi-year ice remained omnipresent in the pack ice throughout May. The concentrations ranged from less than 10% to a maximum of 70%, with the latter confined to a small region just west of the U.S.-Canadian border in late May and early June. As illustrated in Figure 7-3, the diameters of the largest multi-year floes exceeded 20 km.

"THIS INFORMATION IS DISTRIBUTED SOLELY FOR THE PURPOSE OF PRE-DISSEMINATION PEER REVIEW UNDER APPLICABLE INFORMATION QUALITY GUIDELINES. IT HAS NOT BEEN FORMALLY DISSEMINATED BY BSEE. IT DOES NOT REPRESENT AND SHOULD NOT BE CONSTRUED TO REPRESENT ANY BSEE DETERMINATION OR POLICY."

Ice Drift: Ice drift was investigated using Buoys B, C, and D. Buoys B and D were located in the Beaufort Sea study area throughout the month of May, while Buoy C entered on the 7th and remained in the study area thereafter. Their tracks are shown in Figure 7-7.

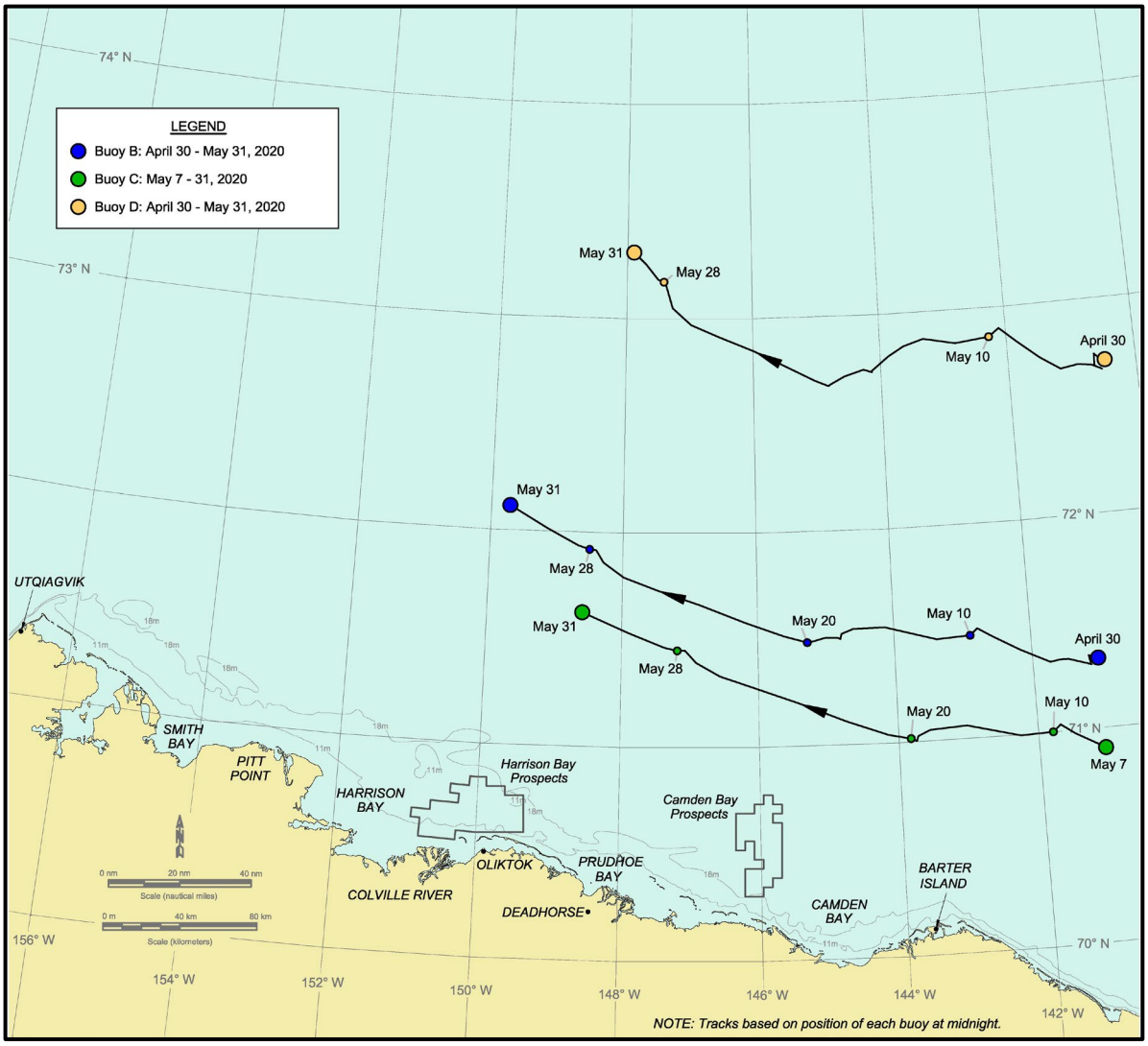

Figure 7-7. Beaufort Sea Drift Buoy Tracks in May 2020

All three buoys moved steadily to the northwest, an outcome consistent with the predominance of easterly winds and absence of westerly storms shown in Figure 7-2. Their monthly average speeds, computed on the basis of each buoy's first and last positions, decreased with distance offshore: 6.3 nm/day (11.7 km/day) for Buoy C, 5.5 nm/day (10.2 km/day) for Buoy B, and 4.3 nm/day (8.0 km day) for Buoy D. The average value was 5.4 nm/day (10.0 km/day).

"THIS INFORMATION IS DISTRIBUTED SOLELY FOR THE PURPOSE OF PRE-DISSEMINATION PEER REVIEW UNDER APPLICABLE INFORMATION QUALITY GUIDELINES. IT HAS NOT BEEN FORMALLY DISSEMINATED BY BSEE. IT DOES NOT REPRESENT AND SHOULD NOT BE CONSTRUED TO REPRESENT ANY BSEE DETERMINATION OR POLICY."

The daily average speeds, computed on the basis of each buoy's position at midnight each day, are plotted in concert with the corresponding daily average wind conditions at Deadhorse Airport in Figure 7-8. The highest value, 15.4 nm/day (28.5 km/day), was recorded by Buoy C on May 12th. The daily average wind speed was 32 kt (16 m/s), producing a wind factor of 2.0%. During the next easterly storm, on May 23rd, Buoy C attained a speed of 14.5 nm/day (26.9 km/day) when the wind speed was 18 kt (9 m/s). The corresponding wind factor was 3.4%. These values, while substantially lower than those recorded on some occasions in the past (*e.g.*, Coastal Frontiers and Vaudrey, 2020), are consistent with fact that the ice bearing the buoy was deeply embedded in the pack ice and therefore subject to a high degree of confinement.

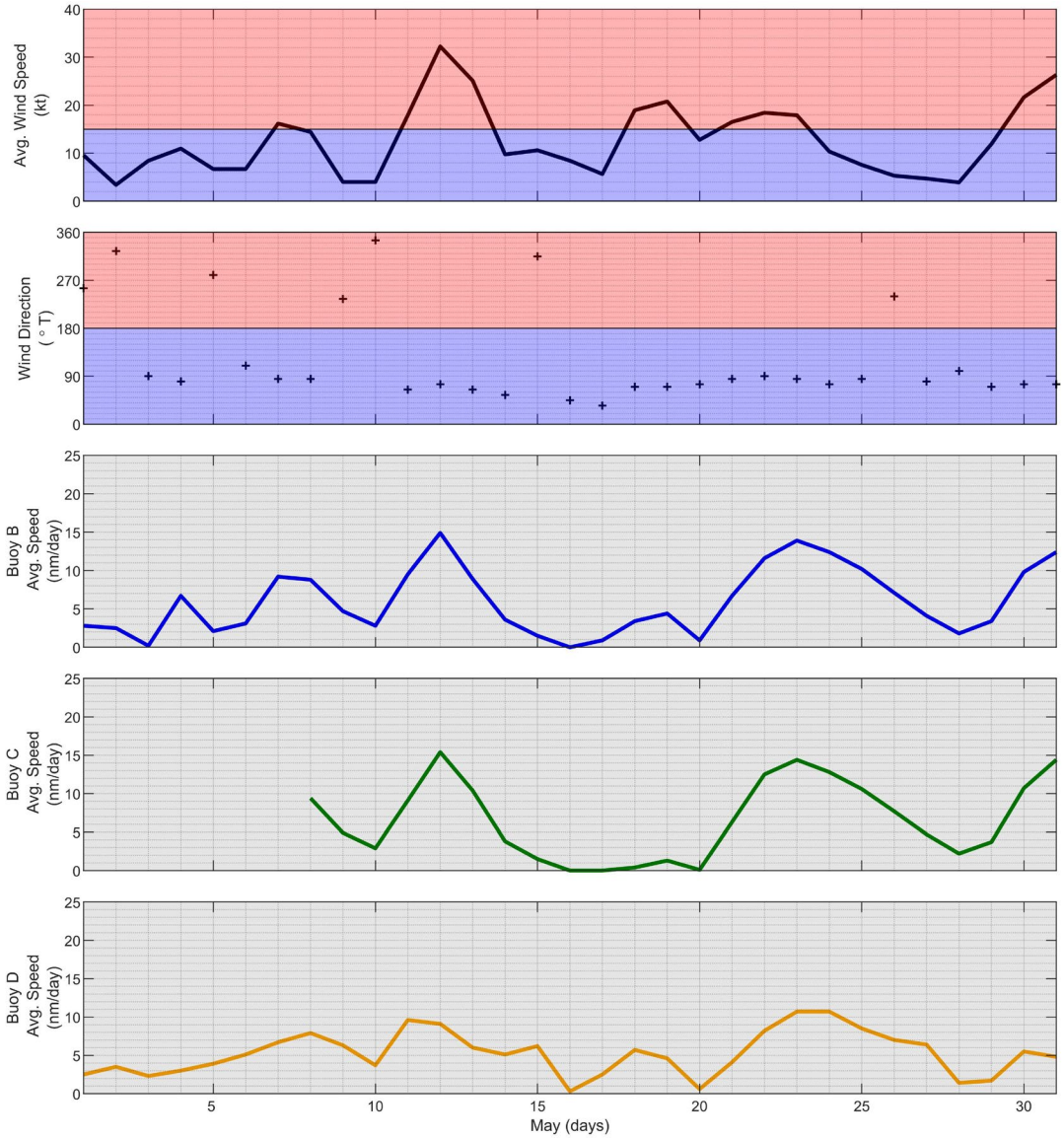

Figure 7-8. Beaufort Sea Drift Buoy Daily Average Speeds in May 2020

"THIS INFORMATION IS DISTRIBUTED SOLELY FOR THE PURPOSE OF PRE-DISSEMINATION PEER REVIEW UNDER APPLICABLE INFORMATION QUALITY GUIDELINES. IT HAS NOT BEEN FORMALLY DISSEMINATED BY BSEE. IT DOES NOT REPRESENT AND SHOULD NOT BE CONSTRUED TO REPRESENT ANY BSEE DETERMINATION OR POLICY."

7.3. June 2020

Meteorological Conditions: The meteorological conditions at Deadhorse Airport in June are summarized in Figure 7-9. The daily average air temperatures remained within the normal range throughout the month with the exception of two days on which they rose above by modest amounts. The temperatures ranged from 29°F (-2°C) to 52°F (11°C); the average was 39°F (4°C).

The predominance of easterly winds in May became more pronounced in June, with easterlies prevailing on 28 of the 30 days. The average speed was 12 kt (6 m/s). Although the storm population consisted of only one easterly event (Table 7-2), it proved to be the longest of the three-month study period:

- May 30th – June 6th: eight-day easterly with maximum speed of 26 kt (13 m/s).

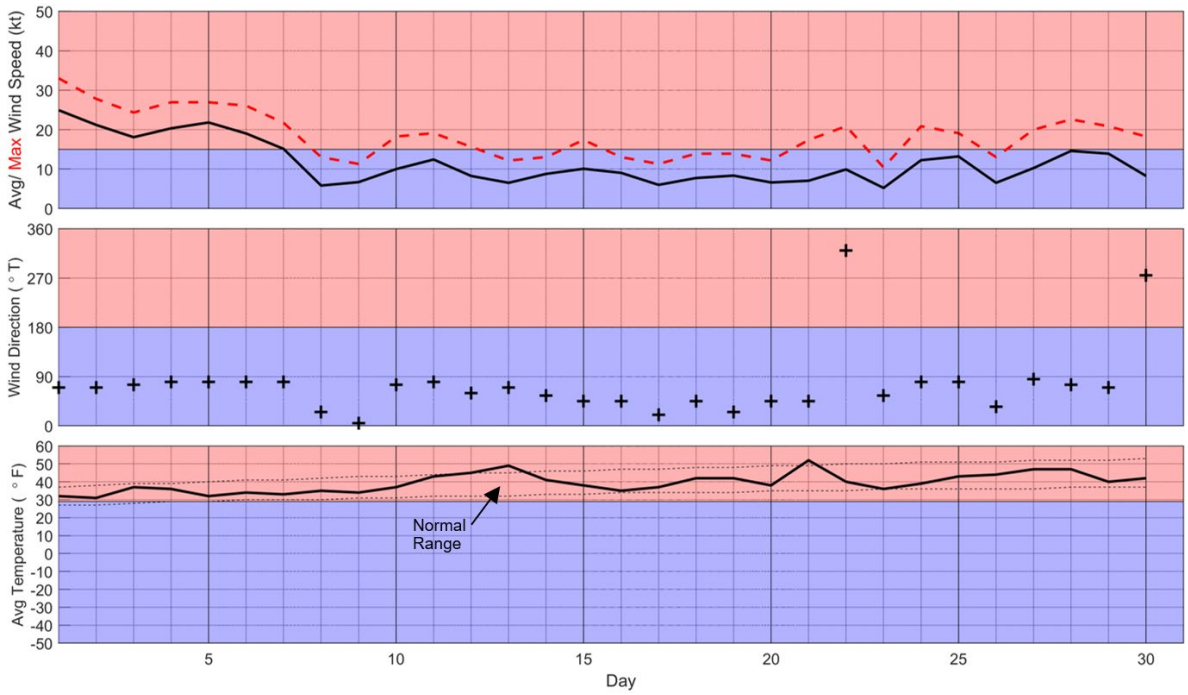

Figure 7-9. Meteorological Conditions at Deadhorse Airport in June 2020

Ice Thickness: The computed thickness of first-year ice decreased from 155 cm at the beginning of the month to 43 cm at the end, a loss of 112 cm (Table 7-3).

River Overflood: The flood waters from the Sagavanirktok and Ikpikpuk Rivers attained their maximum areal extents on the sea ice on June 3rd, while those from the Kuparuk and Colville peaked on the following day. The extent of the flooding on June 3rd is shown in Figure 7-10.

"THIS INFORMATION IS DISTRIBUTED SOLELY FOR THE PURPOSE OF PRE-DISSEMINATION PEER REVIEW UNDER APPLICABLE INFORMATION QUALITY GUIDELINES. IT HAS NOT BEEN FORMALLY DISSEMINATED BY BSEE. IT DOES NOT REPRESENT AND SHOULD NOT BE CONSTRUED TO REPRESENT ANY BSEE DETERMINATION OR POLICY."

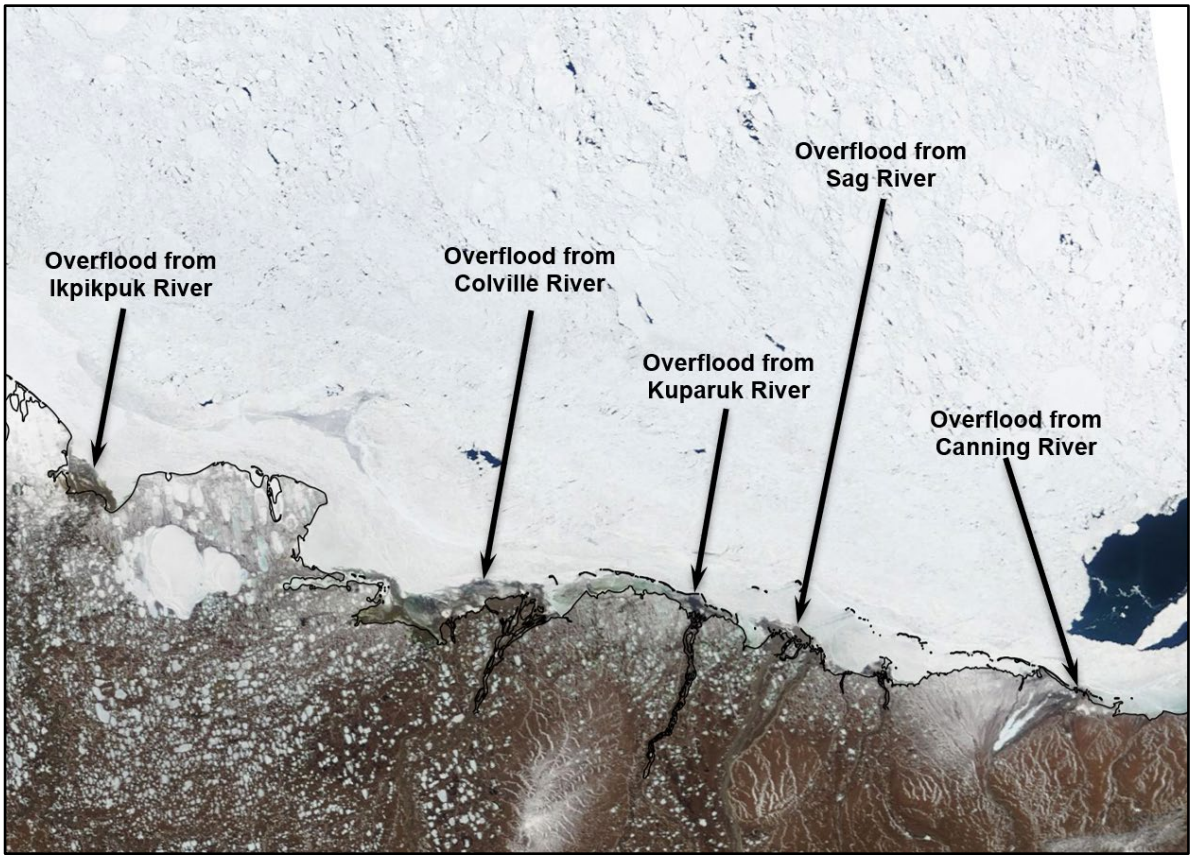

After: NASA, 2020a

Figure 7-10. MODIS Image of Beaufort Sea Acquired on June 3, 2020

Lagoon Ice: Break-up of the lagoon ice began on or about June 4th when flood water from the Sagavanirktok River melted through the ice in Prudhoe Bay (Table 7-5). Through-ice melting followed in the Leffingwell Lagoon (Canning River overflood) and South Harrison Bay (Colville River overflood) on the 8th, South Camden Bay (Canning River overflood) and Gwydyr Bay (Kuparuk River overflood) on the 9th, and Smith Bay (Ikpikpuk River overflood) on the 11th. In Simpson Lagoon, where the discharge from the Kuparuk was insufficient to melt through the ice, break-up took place on or about June 26th in response to the heat emanating from the shoreline east of Oliktok Point.

Open water occurred in Gwydyr Bay between June 20th and 26th, followed by South Harrison Bay between June 28th and July 2nd, Simpson Lagoon between June 29th and July 2nd, South Camden Bay between June 30th and July 1st, and Prudhoe Bay between June 30th and July 2nd. The exact dates could not be determined due to gaps in useful (*i.e.*, cloud-free) satellite imagery. The extent of the open water on July 3rd is displayed in Figure 7-11.

"THIS INFORMATION IS DISTRIBUTED SOLELY FOR THE PURPOSE OF PRE-DISSEMINATION PEER REVIEW UNDER APPLICABLE INFORMATION QUALITY GUIDELINES. IT HAS NOT BEEN FORMALLY DISSEMINATED BY BSEE. IT DOES NOT REPRESENT AND SHOULD NOT BE CONSTRUED TO REPRESENT ANY BSEE DETERMINATION OR POLICY."

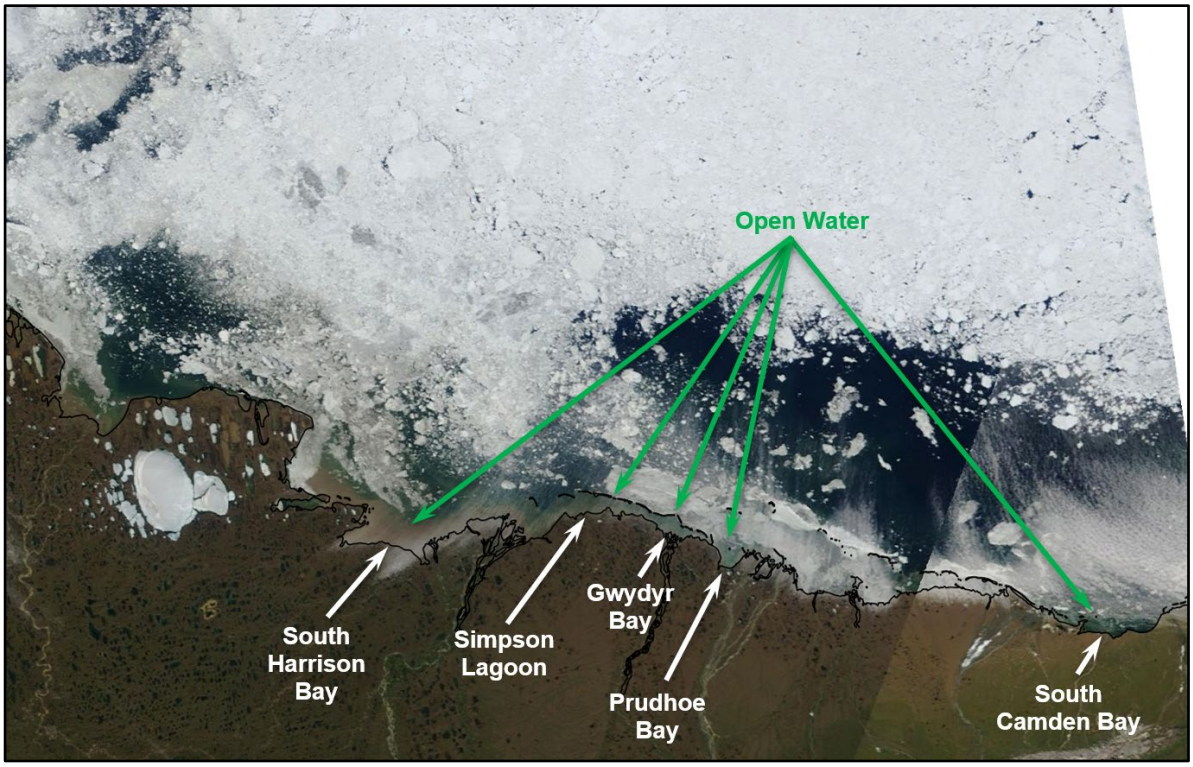

After: NASA, 2020a

Figure 7-11. MODIS Image of Beaufort Sea Acquired on July 3, 2020

Landfast Ice: The locations of the landfast ice edge on June 3rd, 20th, and 27th are shown in Figure 7-12. During the first three weeks of the month, a period of uninterrupted easterly winds with an onshore component (Figure 7-9), changes in the landfast ice edge were modest: (1) losses averaging about 2 nm (3.7 km) between Smith Bay and Harrison Bay, and also between Simpson Lagoon and Camden Bay, and (2) the dispersal of a narrow promontory of landfast ice that formerly extended to the 18-m isobath off Cape Halkett. In all other areas, the landfast ice remained substantially intact.

During the last week in June, a combination of warm air temperatures, increased wind speeds, and warm sea surface temperatures resulting both from river overflood and from the arrival of warm-water plumes from the Alaska Coastal Current to the west and Mackenzie River to the east, caused substantial losses off Smith Bay and in Harrison and Camden Bays. The maximum retreat, approximately 8 nm (15 km), occurred in Harrison and Camden Bays. At the end of June, the ice edge paralleled the 18-m isobath off Admiralty Bay before dipping inside the 11-m isobath off Smith Bay and in Harrison Bay. East of Harrison Bay, it tended to trend between the two isobaths.

"THIS INFORMATION IS DISTRIBUTED SOLELY FOR THE PURPOSE OF PRE-DISSEMINATION PEER REVIEW UNDER APPLICABLE INFORMATION QUALITY GUIDELINES. IT HAS NOT BEEN FORMALLY DISSEMINATED BY BSEE. IT DOES NOT REPRESENT AND SHOULD NOT BE CONSTRUED TO REPRESENT ANY BSEE DETERMINATION OR POLICY."

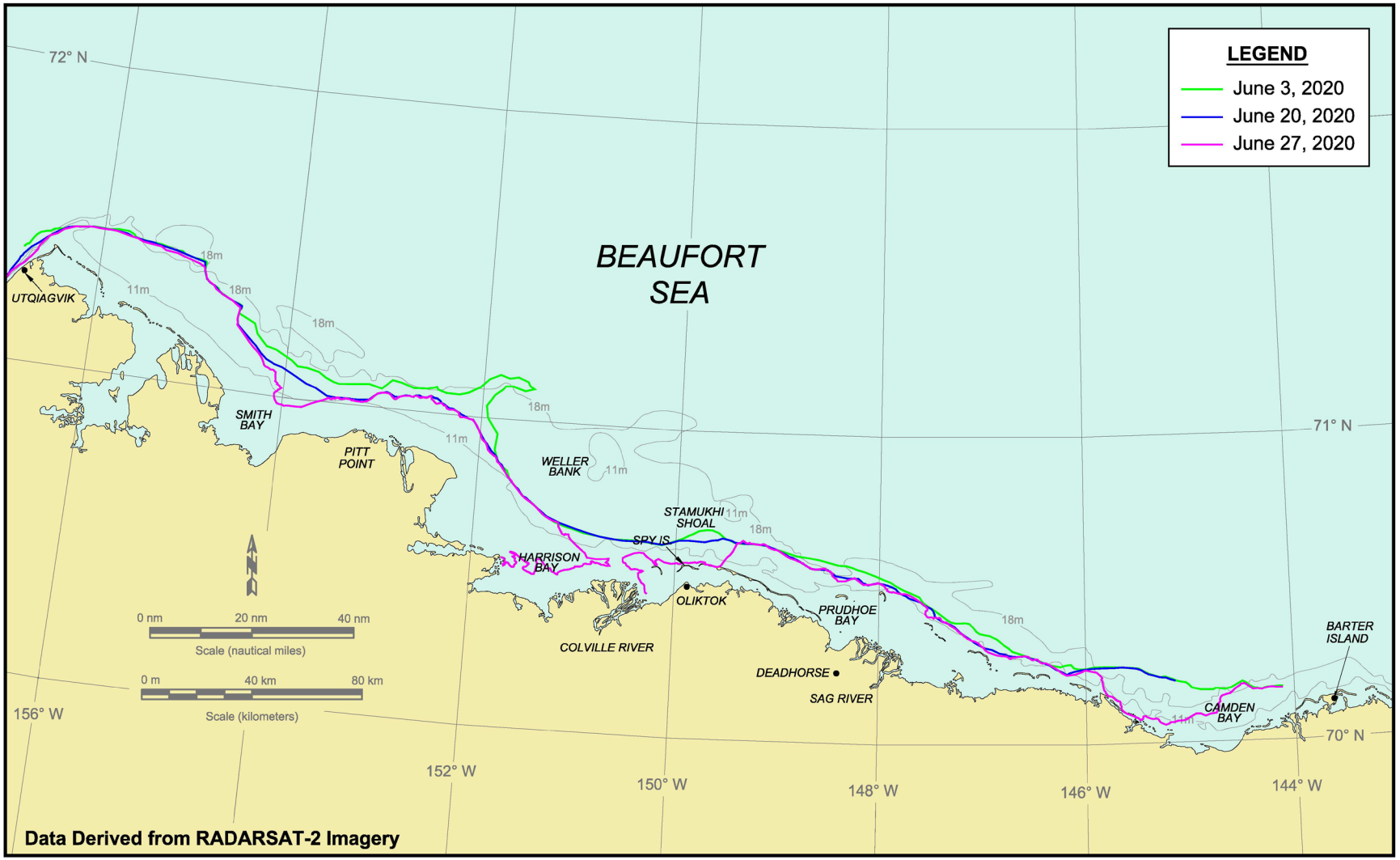

Figure 7-12. Beaufort Sea Landfast Ice Edge in June 2020

"THIS INFORMATION IS DISTRIBUTED SOLELY FOR THE PURPOSE OF PRE-DISSEMINATION PEER REVIEW UNDER APPLICABLE INFORMATION QUALITY GUIDELINES. IT HAS NOT BEEN FORMALLY DISSEMINATED BY BSEE. IT DOES NOT REPRESENT AND SHOULD NOT BE CONSTRUED TO REPRESENT ANY BSEE DETERMINATION OR POLICY."

Pack Ice: The persistent easterly winds in June propelled the warm-water plume from the Mackenzie River to the west while halting the easterly progress of the plume from the Alaska Coastal Current. At mid-month, the former had advanced to the region offshore of Prudhoe Bay while the latter remained stalled in the region offshore of Admiralty Bay (Figure 7-13). Farther offshore, the pack ice remained compact despite the appearance of small patches of open water between the larger ice floes.

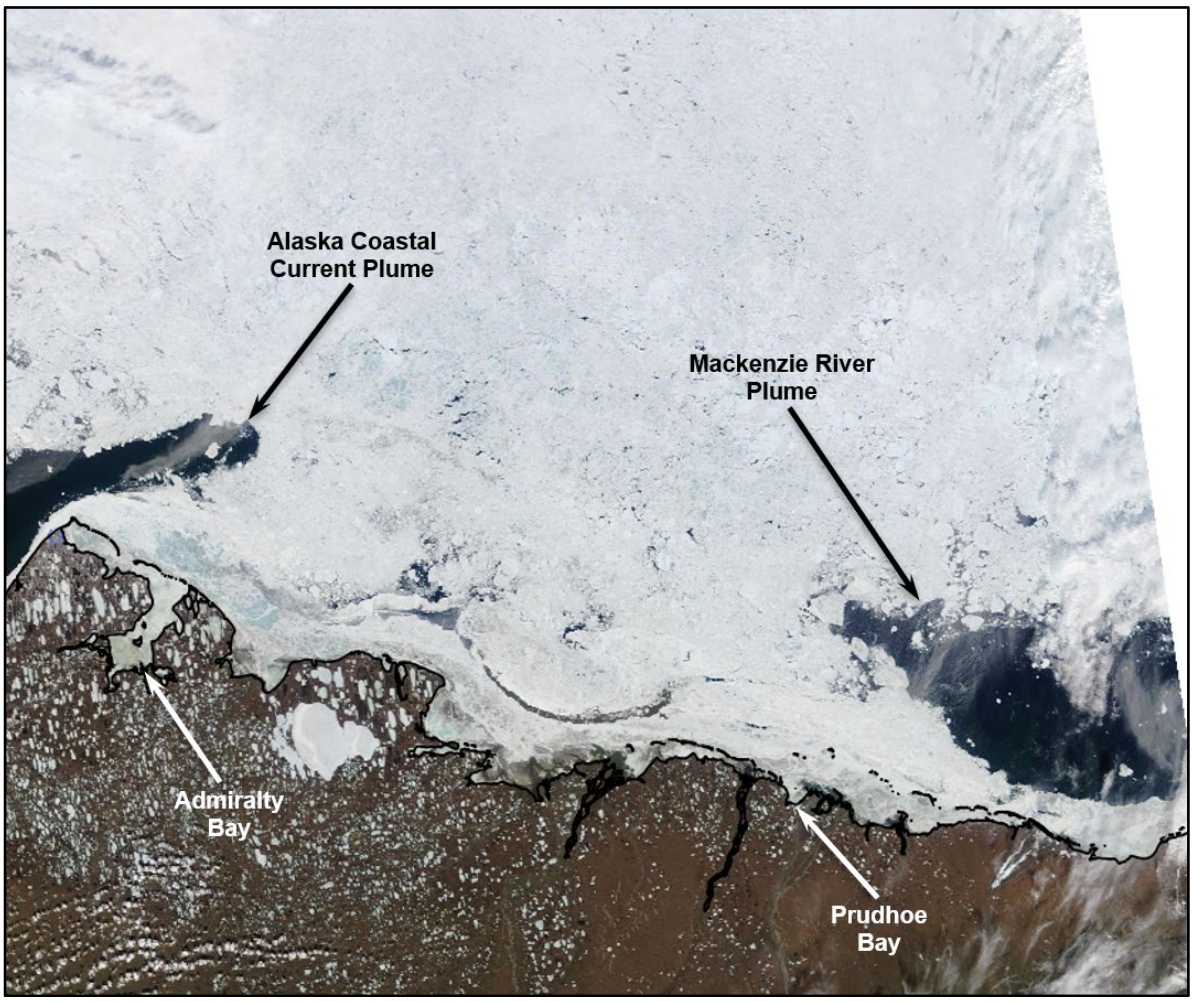

After: NASA, 2020a

Figure 7-13. MODIS Image of Beaufort Sea Acquired on June 14, 2020

During the final week of June, the rate of deterioration increased. In the nearshore region, the pack ice concentration declined over the entire length of the study area in response to the westward progression of the Mackenzie plume to Harrison Bay and the eastern progression of the Alaska Coastal Current plume to Smith Bay. At month-end, the only two areas in which dense pack ice extended as far south as the landfast ice were located off western Harrison Bay and Admiralty Bay (Figure 7-14).

"THIS INFORMATION IS DISTRIBUTED SOLELY FOR THE PURPOSE OF PRE-DISSEMINATION PEER REVIEW UNDER APPLICABLE INFORMATION QUALITY GUIDELINES. IT HAS NOT BEEN FORMALLY DISSEMINATED BY BSEE. IT DOES NOT REPRESENT AND SHOULD NOT BE CONSTRUED TO REPRESENT ANY BSEE DETERMINATION OR POLICY."

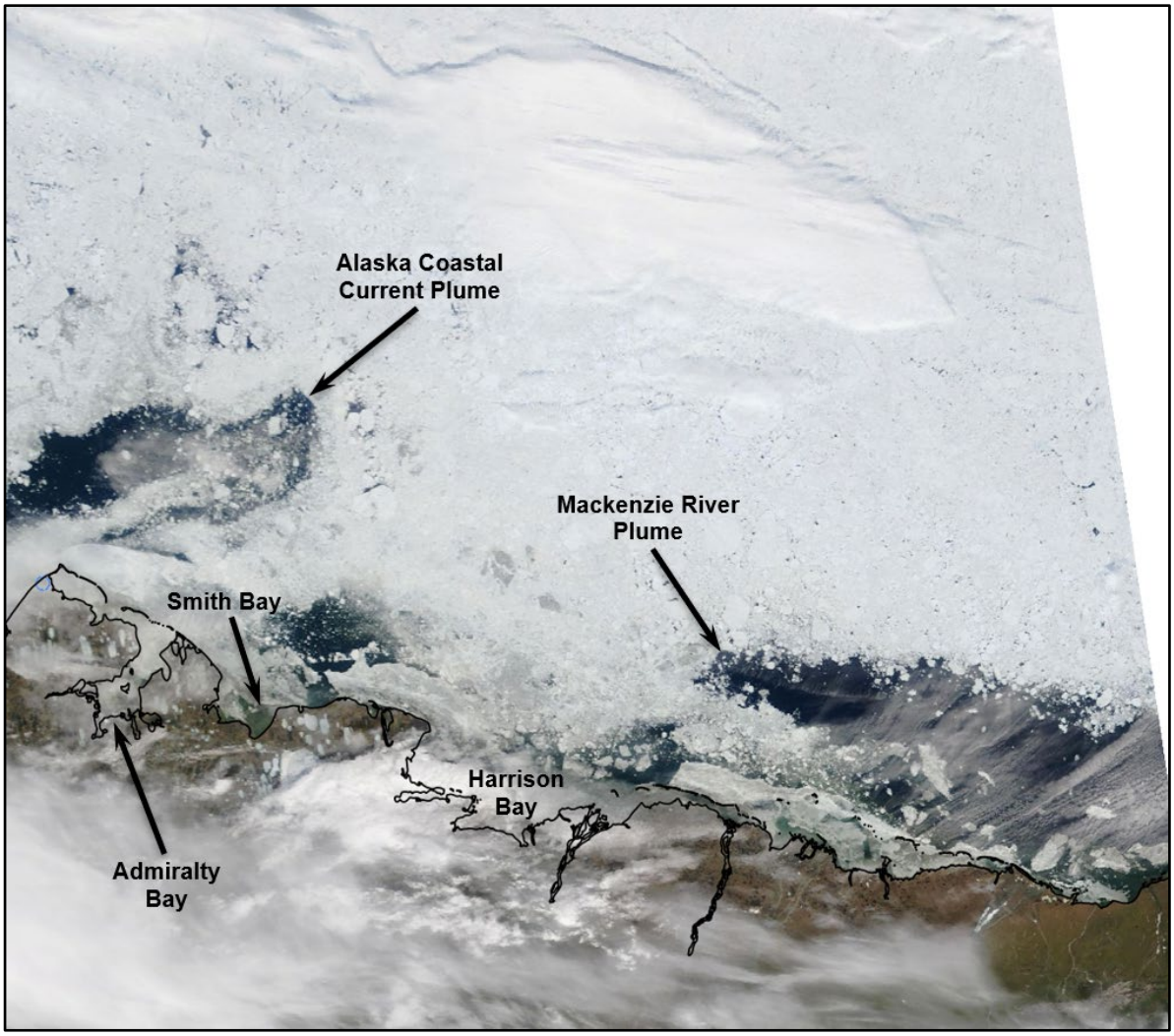

After: NASA, 2020a

Figure 7-14. MODIS Image of Beaufort Sea Acquired on June 29, 2020

Multi-Year Ice: The locations of the multi-year ice edge on June 3rd, 20th, and 27th are displayed in Figures 7-15, 7-16, and 7-17, respectively. In the case of the multi-ice embedded in the landfast ice, the dispersal that began in late May continued throughout June with the rate of loss increasing during the last week of the month. In the case of the multi-year ice embedded in the pack ice, the concentrations varied from less than 10% to 70% at the beginning of the month. The maximum concentration decreased to 40% during the first week, however, and remained at this level for the remainder of the month. The nearshore tongue of first-year ice that had persisted since the end of the 2019-20 Freeze-Up Study in February (Coastal Frontiers and Vaudrey, 2020) also disappeared during the first week of June.

“THIS INFORMATION IS DISTRIBUTED SOLELY FOR THE PURPOSE OF PRE-DISSEMINATION PEER REVIEW UNDER APPLICABLE INFORMATION QUALITY GUIDELINES. IT HAS NOT BEEN FORMALLY DISSEMINATED BY BSEE. IT DOES NOT REPRESENT AND SHOULD NOT BE CONSTRUED TO REPRESENT ANY BSEE DETERMINATION OR POLICY.”

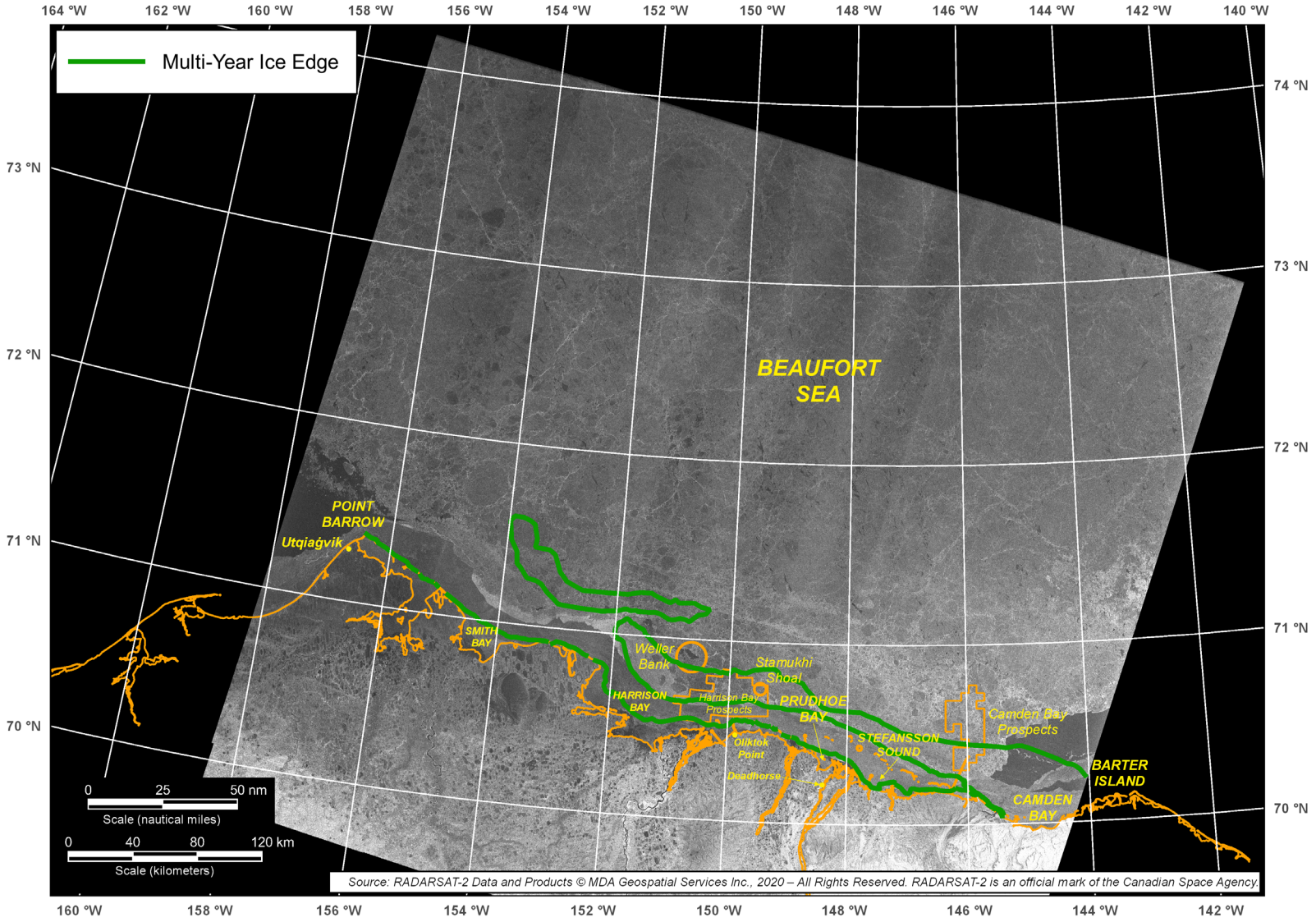

Figure 7-15. RADARSAT-2 Image of Beaufort Sea Acquired on June 3, 2020

“THIS INFORMATION IS DISTRIBUTED SOLELY FOR THE PURPOSE OF PRE-DISSEMINATION PEER REVIEW UNDER APPLICABLE INFORMATION QUALITY GUIDELINES. IT HAS NOT BEEN FORMALLY DISSEMINATED BY BSEE. IT DOES NOT REPRESENT AND SHOULD NOT BE CONSTRUED TO REPRESENT ANY BSEE DETERMINATION OR POLICY.”

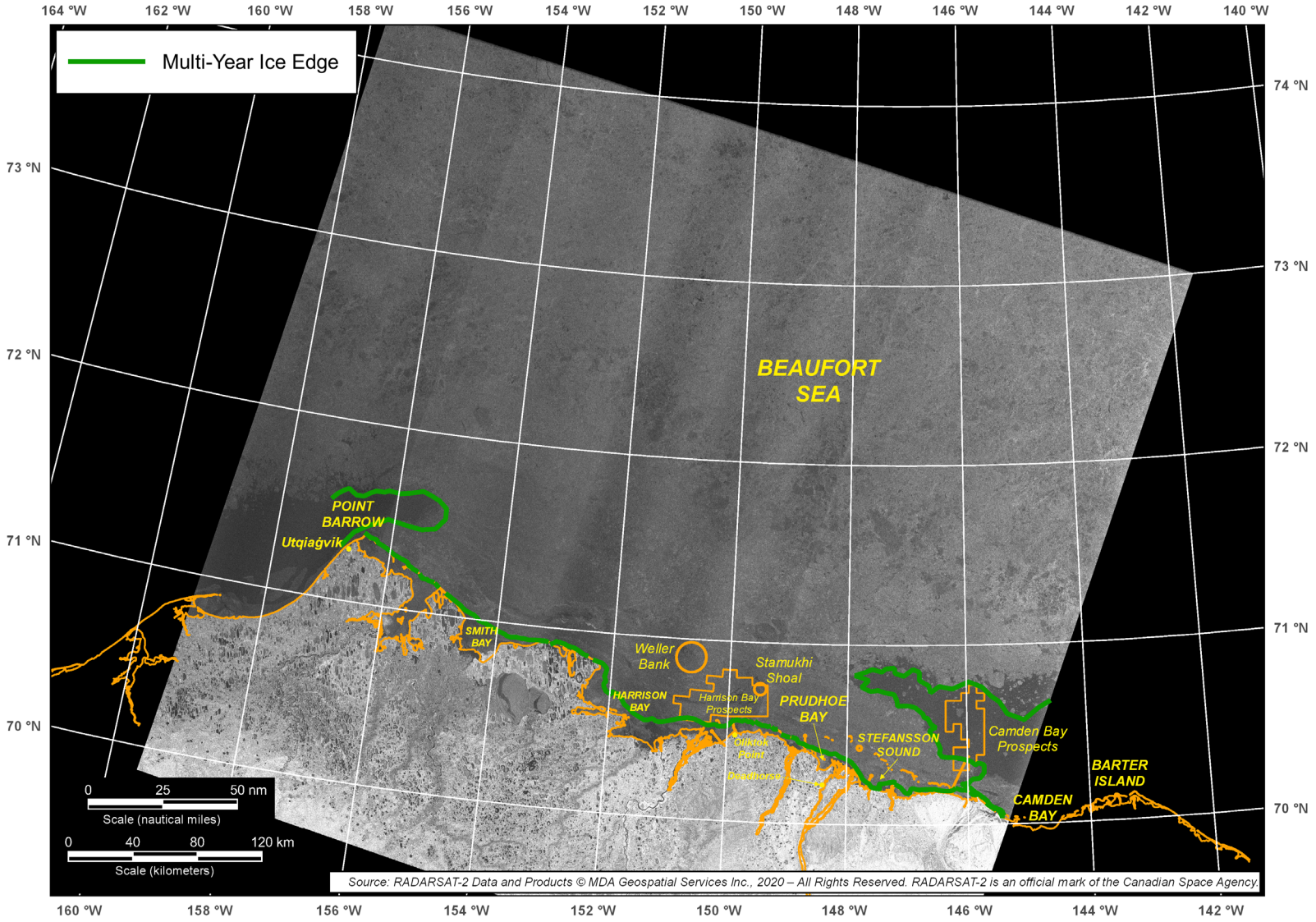

Figure 7-16. RADARSAT-2 Image of Beaufort Sea Acquired on June 20, 2020

“THIS INFORMATION IS DISTRIBUTED SOLELY FOR THE PURPOSE OF PRE-DISSEMINATION PEER REVIEW UNDER APPLICABLE INFORMATION QUALITY GUIDELINES. IT HAS NOT BEEN FORMALLY DISSEMINATED BY BSEE. IT DOES NOT REPRESENT AND SHOULD NOT BE CONSTRUED TO REPRESENT ANY BSEE DETERMINATION OR POLICY.”

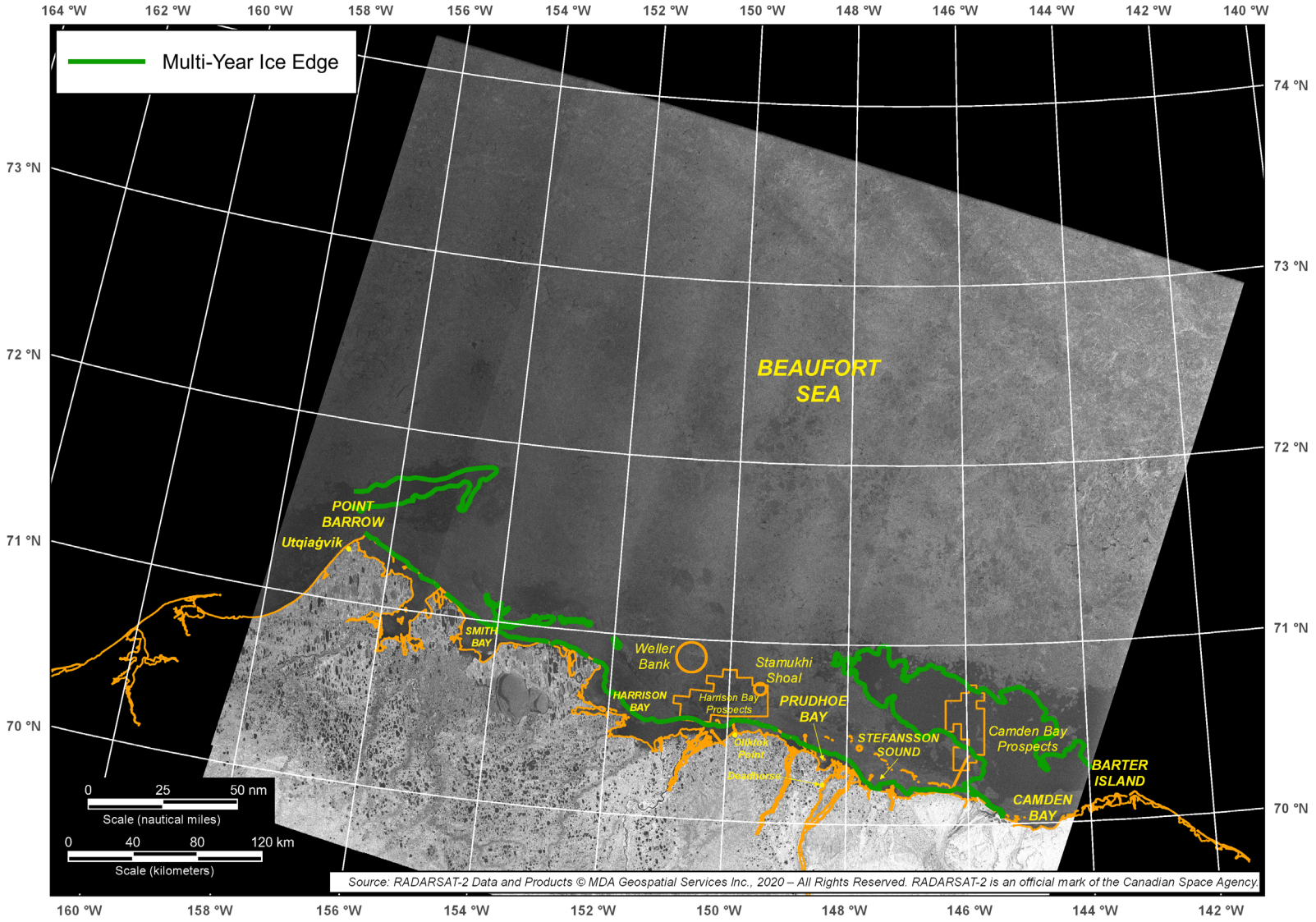

Figure 7-17. RADARSAT-2 Image of Beaufort Sea Acquired on June 27, 2020

"THIS INFORMATION IS DISTRIBUTED SOLELY FOR THE PURPOSE OF PRE-DISSEMINATION PEER REVIEW UNDER APPLICABLE INFORMATION QUALITY GUIDELINES. IT HAS NOT BEEN FORMALLY DISSEMINATED BY BSEE. IT DOES NOT REPRESENT AND SHOULD NOT BE CONSTRUED TO REPRESENT ANY BSEE DETERMINATION OR POLICY."

Ice Drift: Buoys B, C, and D, which were used to monitor ice drift in May, continued to move through the Beaufort Sea study area in June. Buoys B and C exited the study area during the last week, while Buoy D remained in the Beaufort for the entire month. Two additional buoys, E and F, entered the study area on June 8th and provided useful drift data through month-end. As shown in Figure 7-18, all five buoys experienced net displacements to the west. Their daily average speeds and the corresponding wind conditions at Deadhorse Airport are plotted in Figure 7-19.

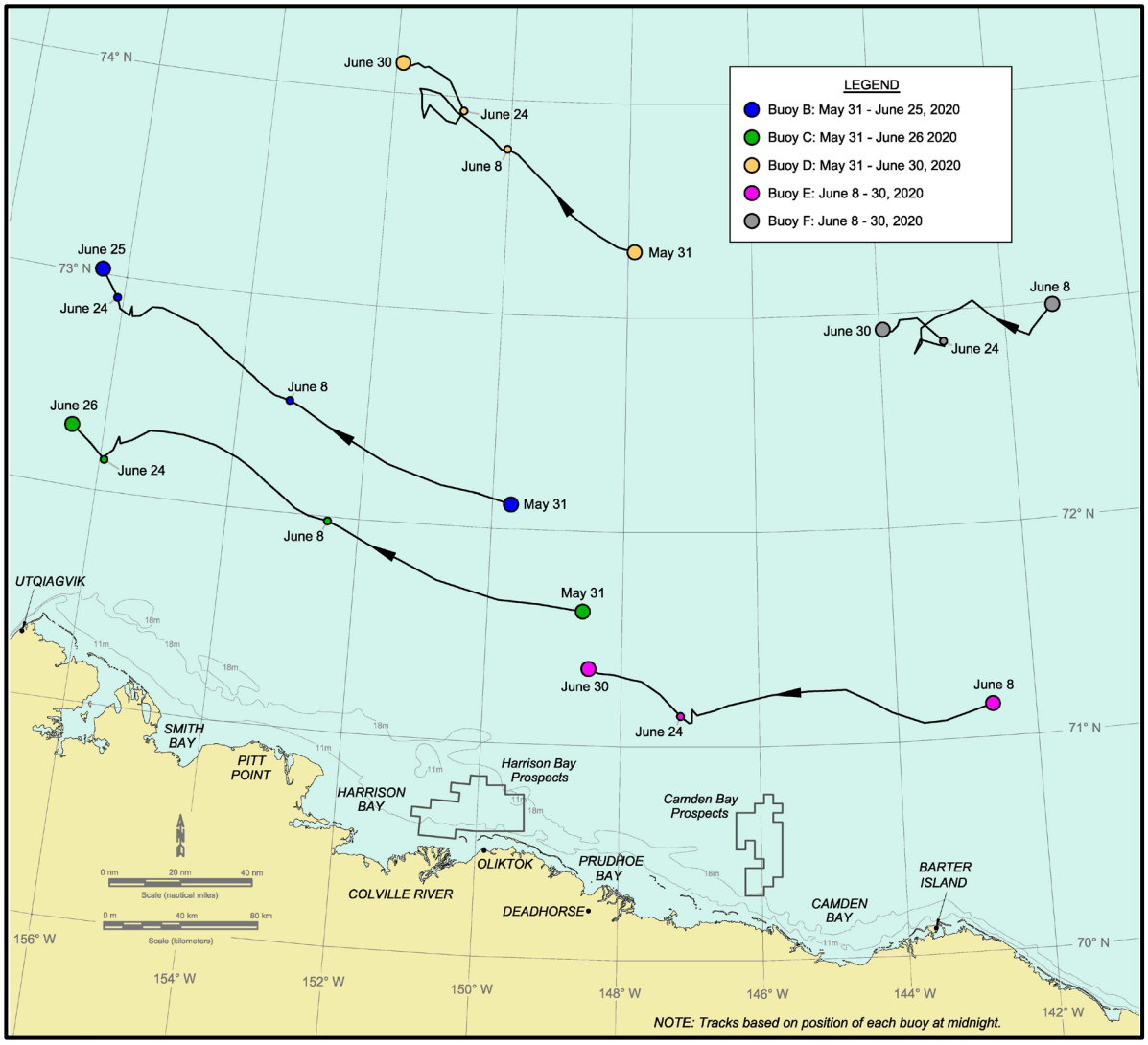

Figure 7-3. Beaufort Sea Drift Buoy Tracks in June 2020

As in May, the monthly average speeds (computed on the basis of each buoy's first and last positions) trended lower with distance offshore in apparent response to the increasing degree of confinement afforded by the surrounding pack ice. The drift rates ranged

“THIS INFORMATION IS DISTRIBUTED SOLELY FOR THE PURPOSE OF PRE-DISSEMINATION PEER REVIEW UNDER APPLICABLE INFORMATION QUALITY GUIDELINES. IT HAS NOT BEEN FORMALLY DISSEMINATED BY BSEE. IT DOES NOT REPRESENT AND SHOULD NOT BE CONSTRUED TO REPRESENT ANY BSEE DETERMINATION OR POLICY.”

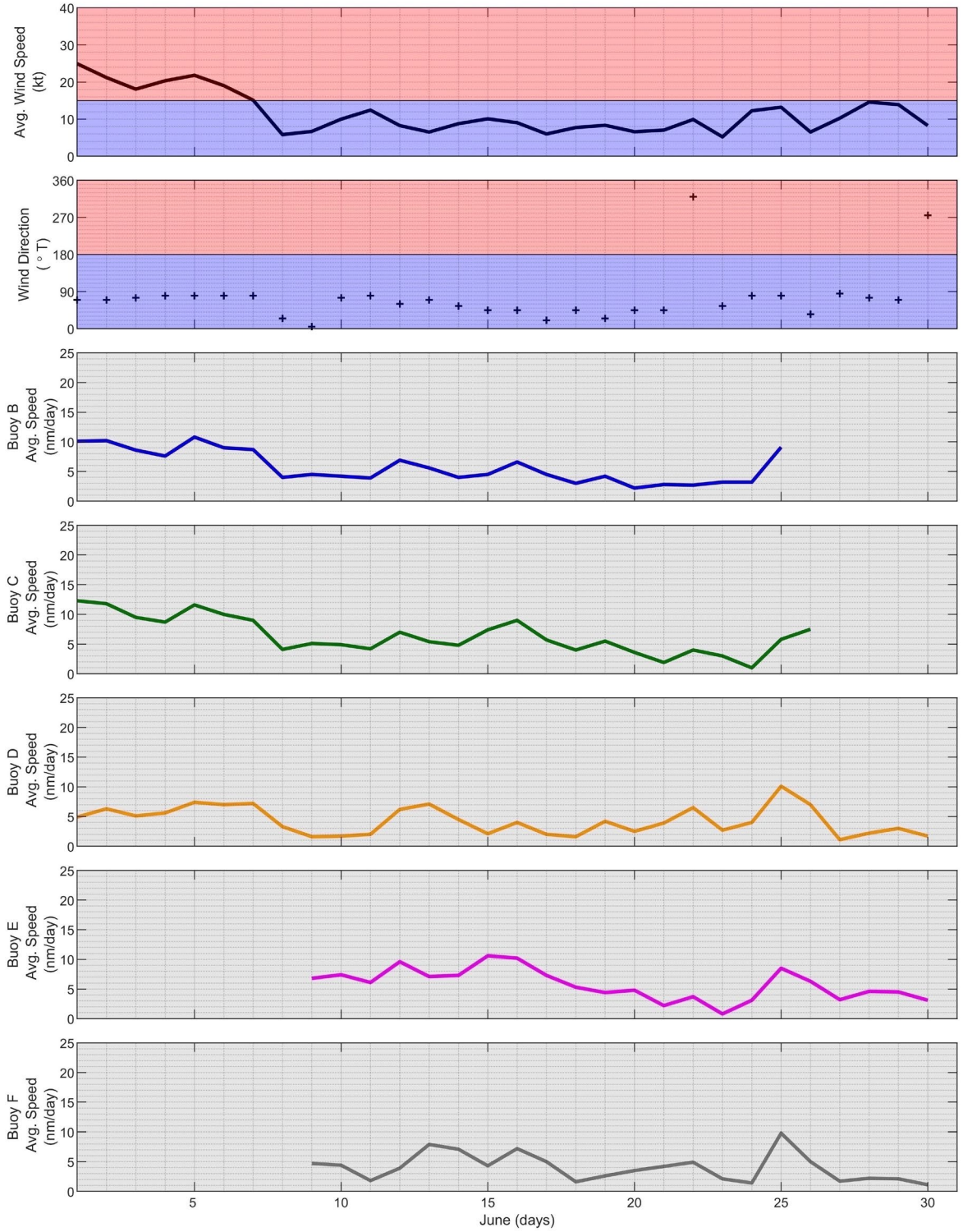

Figure 7-4 Beaufort Sea Drift Buoy Daily Average Speeds in June 2020

"THIS INFORMATION IS DISTRIBUTED SOLELY FOR THE PURPOSE OF PRE-DISSEMINATION PEER REVIEW UNDER APPLICABLE INFORMATION QUALITY GUIDELINES. IT HAS NOT BEEN FORMALLY DISSEMINATED BY BSEE. IT DOES NOT REPRESENT AND SHOULD NOT BE CONSTRUED TO REPRESENT ANY BSEE DETERMINATION OR POLICY."

from 5.9, 5.3, and 5.2 nm/day (10.9, 9.8, and 9.6 km/day) for the three southernmost buoys (C, B, and E) to 2.8 and 2.2 nm/day (5.2 and 4.1 km/day) for the two northernmost buoys (D and F). The average for all five buoys was 4.3 nm/day (8.0 km/day).

The highest daily average speed (computed on the basis of the buoy's position at midnight on each day) occurred on June 1st during the aforementioned eight-day easterly storm. As shown in Figure 7-19, Buoy C attained a speed of 12.3 nm/day (22.8 km/day) when the daily average wind speed at Deadhorse Airport was 25 kt (13 m/s). The corresponding wind factor, a modest 2.1%, was commensurate with the high degree of confinement that prevailed in the vicinity of the buoy.

The tracks of the two offshore buoys, D and F, included a counterclockwise loop that occurred between June 18th and 24th (Figure 7-18). As this week-long period contained only one day of westerly winds at Deadhorse Airport (Figure 7-19), it is likely that the conditions experienced by the buoys differed substantially from those at the airport (which was located approximately 200 nm or 371 km to the south).

7.4. July 2020

Meteorological Conditions: Figure 7-20 presents the wind and temperature data recorded at Deadhorse Airport in July. As in June, the daily average air temperatures tended to lie within the normal range, rising above on only one day and falling below on only two. The average for the month was 43°F (6°C).

The daily average wind speed, 9 kt (5 m/s), was substantially lower that that recorded in May (13 kt; 7 m/sº) and June (12 kt; 6 m/s), but the predominance of easterly winds that occurred in each of these two prior months continued in July. Easterlies prevailed on 21 of the 31 days, with the westerlies concentrated at month-end. There were no storms.

Ice Thickness: The computed thickness of undeformed first-year ice decreased from 43 cm at the beginning of July to zero on the 8th, based on the accumulation of 319 TDD at Deadhorse Airport since May 23rd (Table 7-3).

Lagoon Ice: As discussed in Section 7.3, open water occurred in South Harrison Bay, Simpson Lagoon, South Camden Bay, and Prudhoe Bay between June 28th and July 2nd (Figure 7-11). This milestone followed in Smith Bay between July 5th and 7th, and in Stefansson Sound on July 10th. All of these lagoons as well as Gwydyr Bay became ice-free by the end of the month.

"THIS INFORMATION IS DISTRIBUTED SOLELY FOR THE PURPOSE OF PRE-DISSEMINATION PEER REVIEW UNDER APPLICABLE INFORMATION QUALITY GUIDELINES. IT HAS NOT BEEN FORMALLY DISSEMINATED BY BSEE. IT DOES NOT REPRESENT AND SHOULD NOT BE CONSTRUED TO REPRESENT ANY BSEE DETERMINATION OR POLICY."

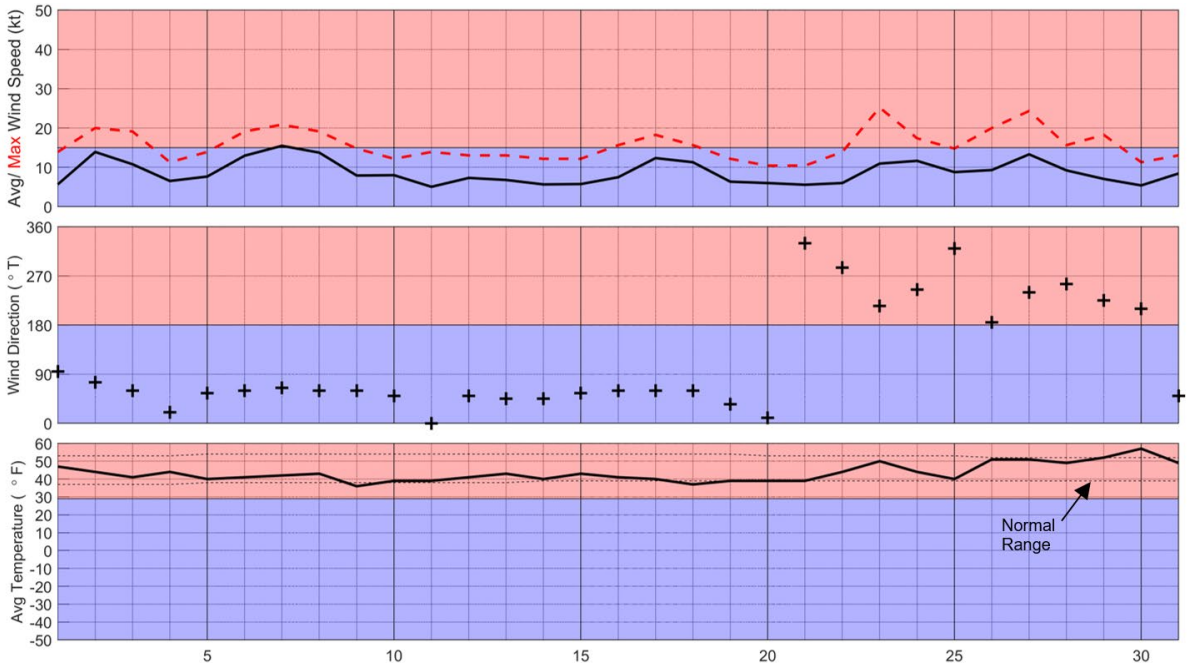

Figure 7-20. Meteorological Conditions at Deadhorse Airport in July 2020

Landfast Ice: The locations of the landfast ice edge on June 27th and July 14th are shown in Figure 7-21. The rapid deterioration of the landfast ice that began in late June continued during the first half of July. The primary driving forces appear to have been the warming air and sea surface temperatures in concert with moderate wind speeds, which produced waves in areas of reduced ice cover.

By mid-July, the ice was confined to a patch in Elson Lagoon, narrow strips on both sides of Smith Bay, small patches on the west side of Harrison Bay, and a narrow, discontinuous strip adjacent to the barrier islands from Cross to Flaxman (Figure 7-22). On July 28th, the last day of the study period for which a useful MODIS image is available, small patches of landfast ice remained between Pole and Flaxman Islands.

Pack Ice: The pack ice in the nearshore region continued to deteriorate in July, with the dense tongues that approached western Harrison Bay and Admiralty Bay in late June dispersing by mid-month. At that time, the ice concentrations off the coast ranged from less than 10% to 50% in a band that narrowed from more than 50 nm (93 km) wide off Camden Bay to about 20 nm (37 km) wide off Smith Bay (Figure 7-22). With the exception of a diffuse ice edge, the pack ice to the north of the band remained relatively compact.

The configuration of the pack ice on July 27th is shown in Figure 7-23. The southern boundary was separated from the coast by distances that varied widely, from only 1 nm (2 km) off Thetis Island to more than 40 nm (74 km) off Flaxman Island.

"THIS INFORMATION IS DISTRIBUTED SOLELY FOR THE PURPOSE OF PRE-DISSEMINATION PEER REVIEW UNDER APPLICABLE INFORMATION QUALITY GUIDELINES. IT HAS NOT BEEN FORMALLY DISSEMINATED BY BSEE. IT DOES NOT REPRESENT AND SHOULD NOT BE CONSTRUED TO REPRESENT ANY BSEE DETERMINATION OR POLICY."

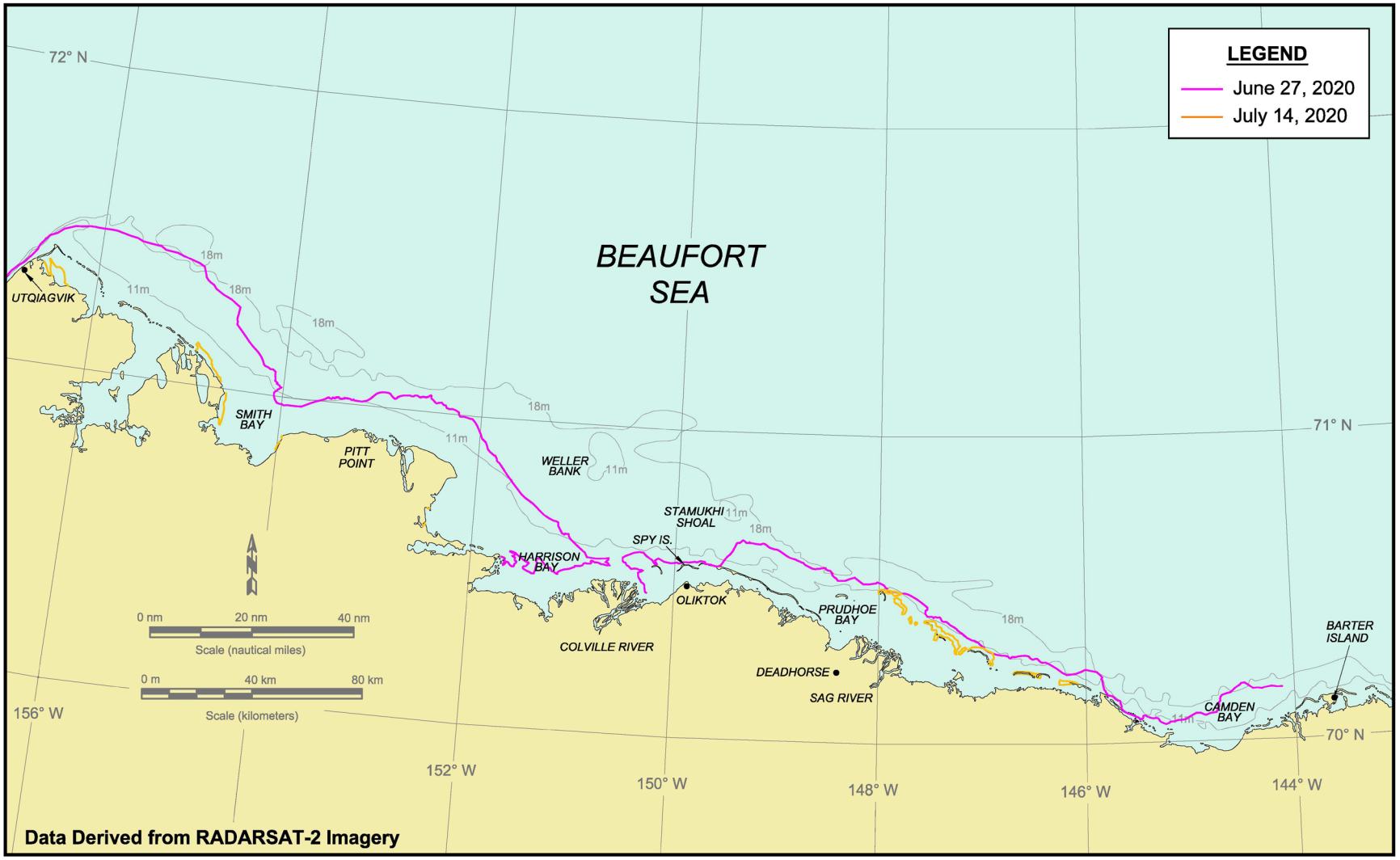

Figure 7-21. Beaufort Sea Landfast Ice Edge in July 2020

"THIS INFORMATION IS DISTRIBUTED SOLELY FOR THE PURPOSE OF PRE-DISSEMINATION PEER REVIEW UNDER APPLICABLE INFORMATION QUALITY GUIDELINES. IT HAS NOT BEEN FORMALLY DISSEMINATED BY BSEE. IT DOES NOT REPRESENT AND SHOULD NOT BE CONSTRUED TO REPRESENT ANY BSEE DETERMINATION OR POLICY."

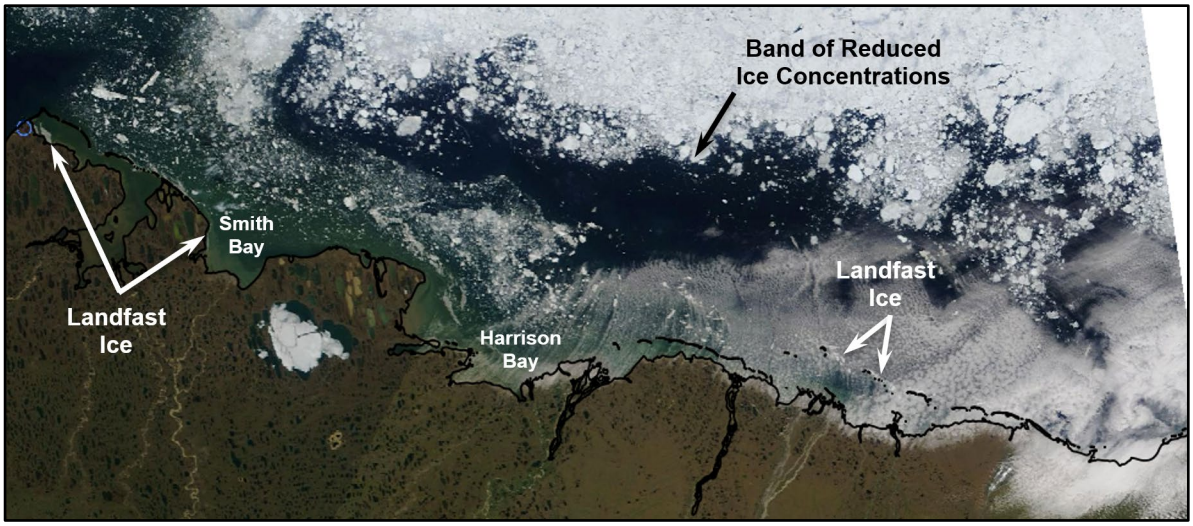

After: NASA, 2020a

Figure 7-22. MODIS Image of Beaufort Sea Acquired on July 15, 2020

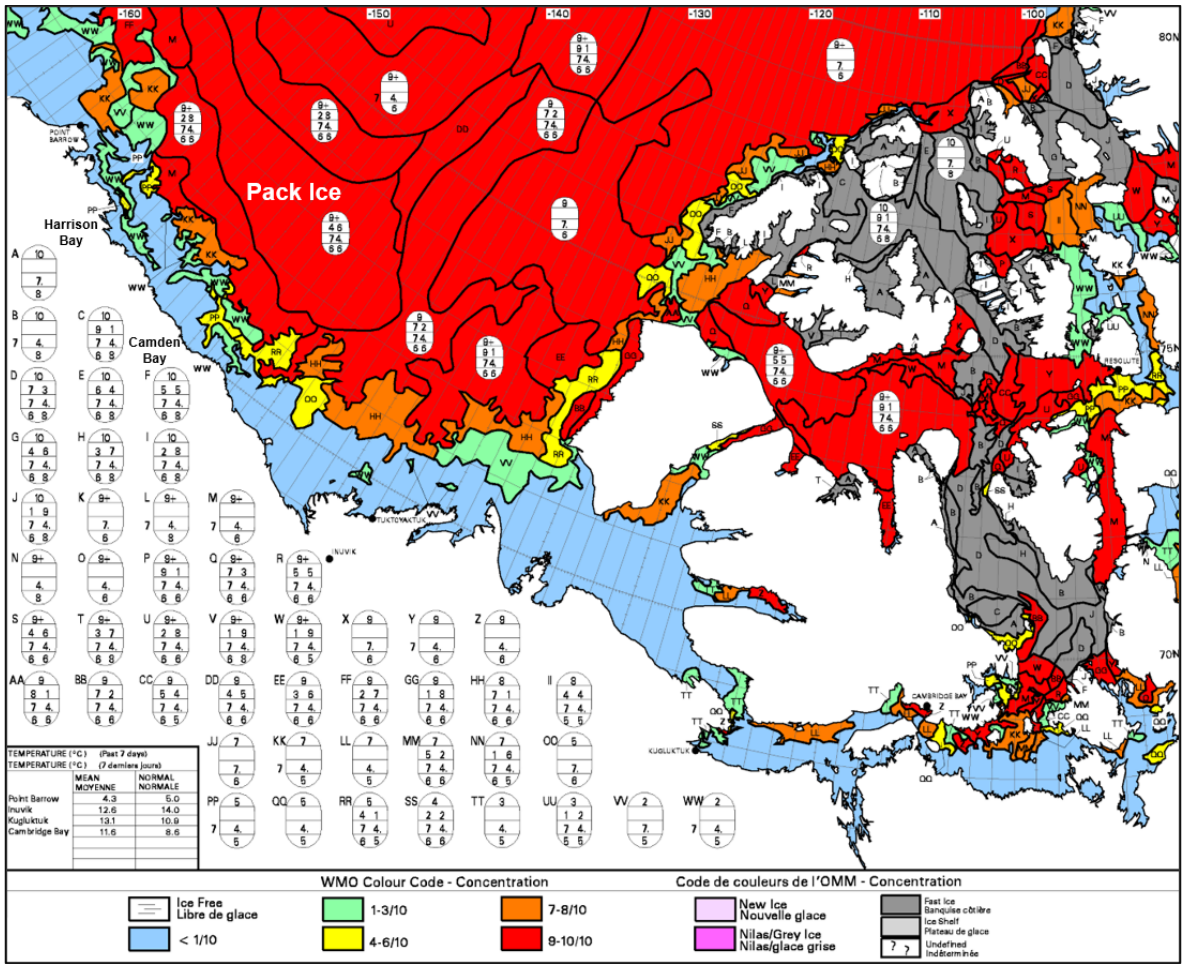

After: Canadian Ice Service, 2020

Figure 7-23. CIS Ice Concentration Chart of Beaufort Sea for July 27, 2020

"THIS INFORMATION IS DISTRIBUTED SOLELY FOR THE PURPOSE OF PRE-DISSEMINATION PEER REVIEW UNDER APPLICABLE INFORMATION QUALITY GUIDELINES. IT HAS NOT BEEN FORMALLY DISSEMINATED BY BSEE. IT DOES NOT REPRESENT AND SHOULD NOT BE CONSTRUED TO REPRESENT ANY BSEE DETERMINATION OR POLICY."

Multi-Year Ice: The location of the multi-year edge on July 11th is shown in Figure 7-24. The rapid loss of landfast ice that occurred during the first half of July resulted in a corresponding loss of the multi-year ice embedded therein. When the RADARSAT-2 image was acquired on the 11th, the only embedded ice that remained was located in the strip of landfast ice on the west side of Smith Bay and the strip of landfast ice adjacent to the barrier islands east of Prudhoe Bay. On July 28th, the last vestige of this ice was confined to the small patches of landfast ice between Pole and Flaxman Islands.

Multi-year ice remained omnipresent in the pack ice through the month of July. The concentrations were commensurate with those that had prevailed since early June, ranging from less than 10% to a maximum of 40%, (CIS, 2020).

Ice Drift: Buoys D, E, and F were located in the Beaufort Sea study area at the beginning of July, but Buoy D moved into the Chukchi in mid-month. A comparison of the track of Buoy E with the available satellite imagery indicated that the buoy may have exited the region of dense ice coverage as early as July 11th. As a result, its tracking period was terminated at midnight on the 10th. Buoy F remained in the study area for the entire month. The buoy tracks are provided in Figure 7-25.

Although all three buoys experienced net displacements to the northwest during their respective tracking periods, Buoy F reversed course and headed northeast from July 25th through 31st. Easterly winds prevailed through the 20th, followed by an uninterrupted string of westerlies from the 21st through the 30th. The four-day lag between the wind shift at Deadhorse Airport and the buoy's course change probably resulted from one or more of the following factors:

- The buoy was constrained by the surrounding pack ice;
- An extended period was required to reverse the westerly set of the Beaufort Gyre due to the relatively low westerly wind speeds that prevailed on and after the 21st;
- The wind conditions at the buoy differed from those at the airport (which was located approximately 180 nm or 334 km to the south).

The tracks of Buoys D and E do not exhibit similar changes in direction because the tracking periods ended before the onset of westerly winds.

The monthly average speed of Buoy D (computed on the basis of the buoy's first and last positions) was 4.6 nm/day (8.5 km/day). The corresponding value for Buoy F, a miniscule 1.1 nm/day (2.0 km/day) reflected the aforementioned displacement to the

"THIS INFORMATION IS DISTRIBUTED SOLELY FOR THE PURPOSE OF PRE-DISSEMINATION PEER REVIEW UNDER APPLICABLE INFORMATION QUALITY GUIDELINES. IT HAS NOT BEEN FORMALLY DISSEMINATED BY BSEE. IT DOES NOT REPRESENT AND SHOULD NOT BE CONSTRUED TO REPRESENT ANY BSEE DETERMINATION OR POLICY."

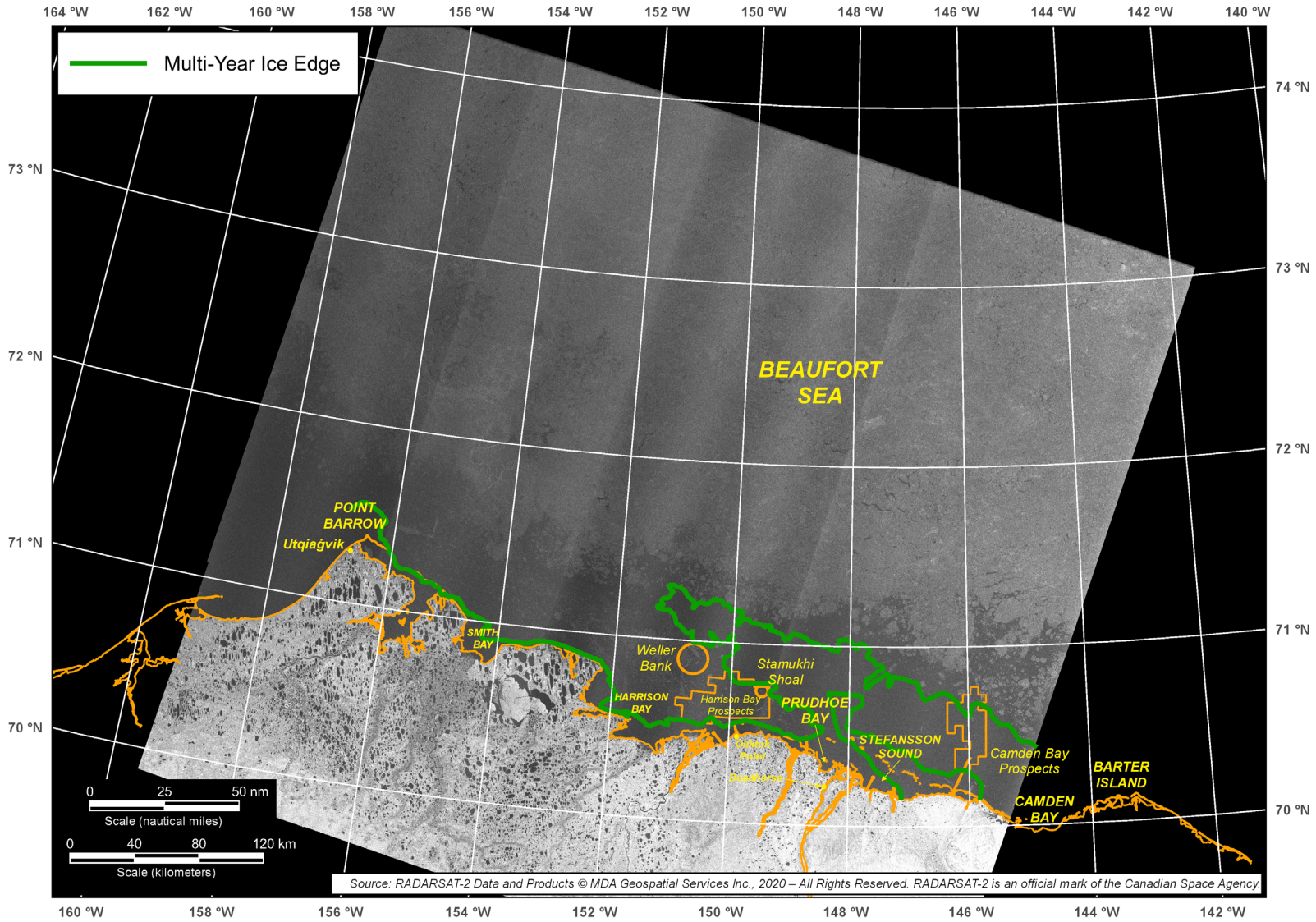

Figure 7-24. RADARSAT-2 Image of Beaufort Sea Acquired on July 14, 2020

"THIS INFORMATION IS DISTRIBUTED SOLELY FOR THE PURPOSE OF PRE-DISSEMINATION PEER REVIEW UNDER APPLICABLE INFORMATION QUALITY GUIDELINES. IT HAS NOT BEEN FORMALLY DISSEMINATED BY BSEE. IT DOES NOT REPRESENT AND SHOULD NOT BE CONSTRUED TO REPRESENT ANY BSEE DETERMINATION OR POLICY."

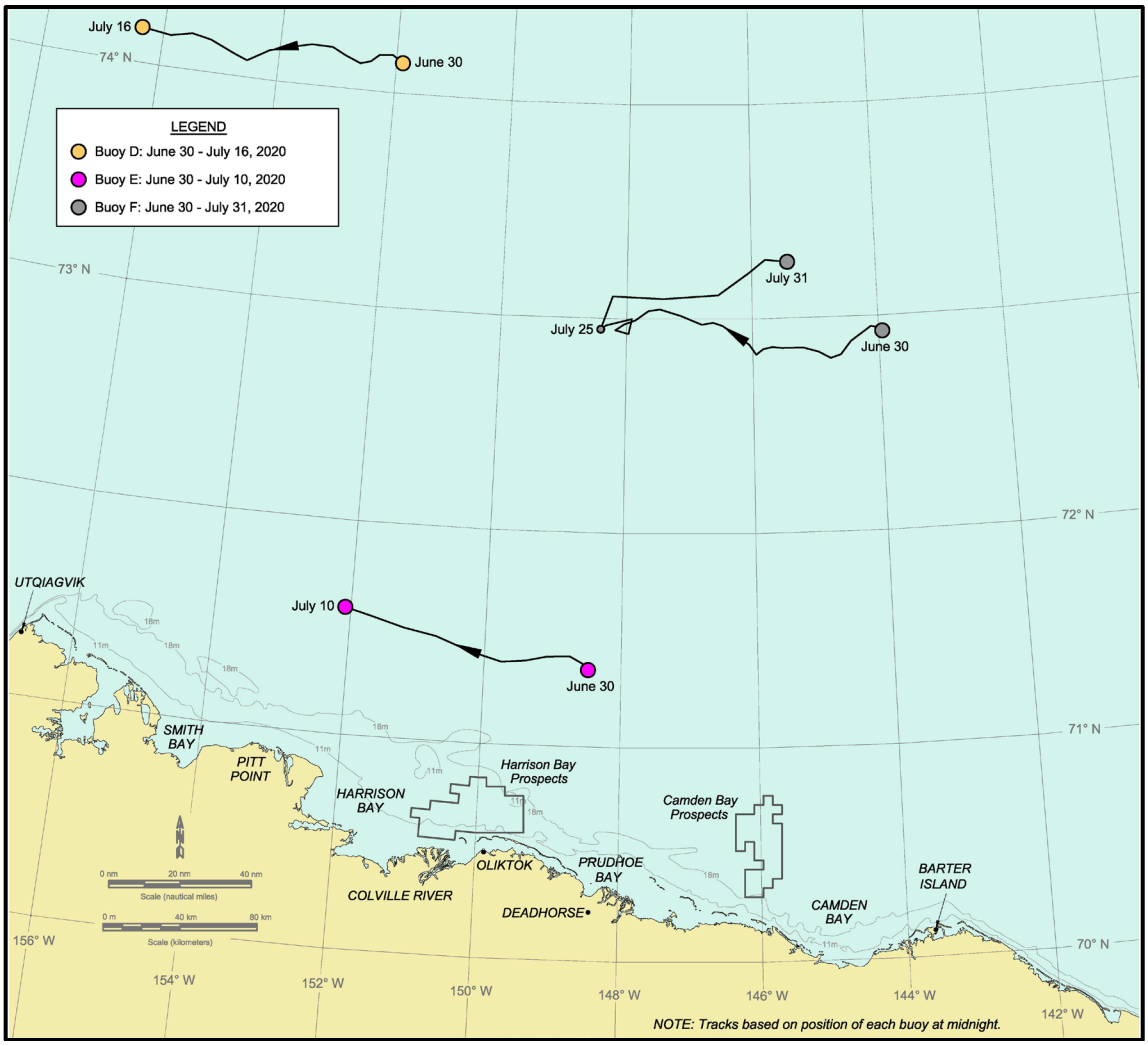

Figure 7-5 Beaufort Sea Drift Buoy Track in July 2020

northeast that occurred after the tracking period for Buoy D had ended. A monthly average speed was not computed for Buoy E because its tracking period in July did not attain the minimum acceptable duration of 16 days.

The daily average buoy speeds and corresponding daily average wind conditions at Deadhorse Airport are plotted in Figure 7-26. The highest daily average speed, 15.4 nm/day (28.5 km/day), was attained by Buoy F on July 28th. The daily average wind speed on this date was only 9 kt (5 m/s), producing a wind factor of 7.1%. This value is substantially higher than would be expected for an ice floe that is confined by the surrounding pack ice and located far offshore, where it is not subject to the influence of the coastal jet (Tekmarine, *et al*., 1985). As in the case of the four-day time lag between the onset of westerly winds at Deadhorse and the course change exhibited by the buoy, it is likely that the wind conditions at the buoy differed from those at the coast.

"THIS INFORMATION IS DISTRIBUTED SOLELY FOR THE PURPOSE OF PRE-DISSEMINATION PEER REVIEW UNDER APPLICABLE INFORMATION QUALITY GUIDELINES. IT HAS NOT BEEN FORMALLY DISSEMINATED BY BSEE. IT DOES NOT REPRESENT AND SHOULD NOT BE CONSTRUED TO REPRESENT ANY BSEE DETERMINATION OR POLICY."

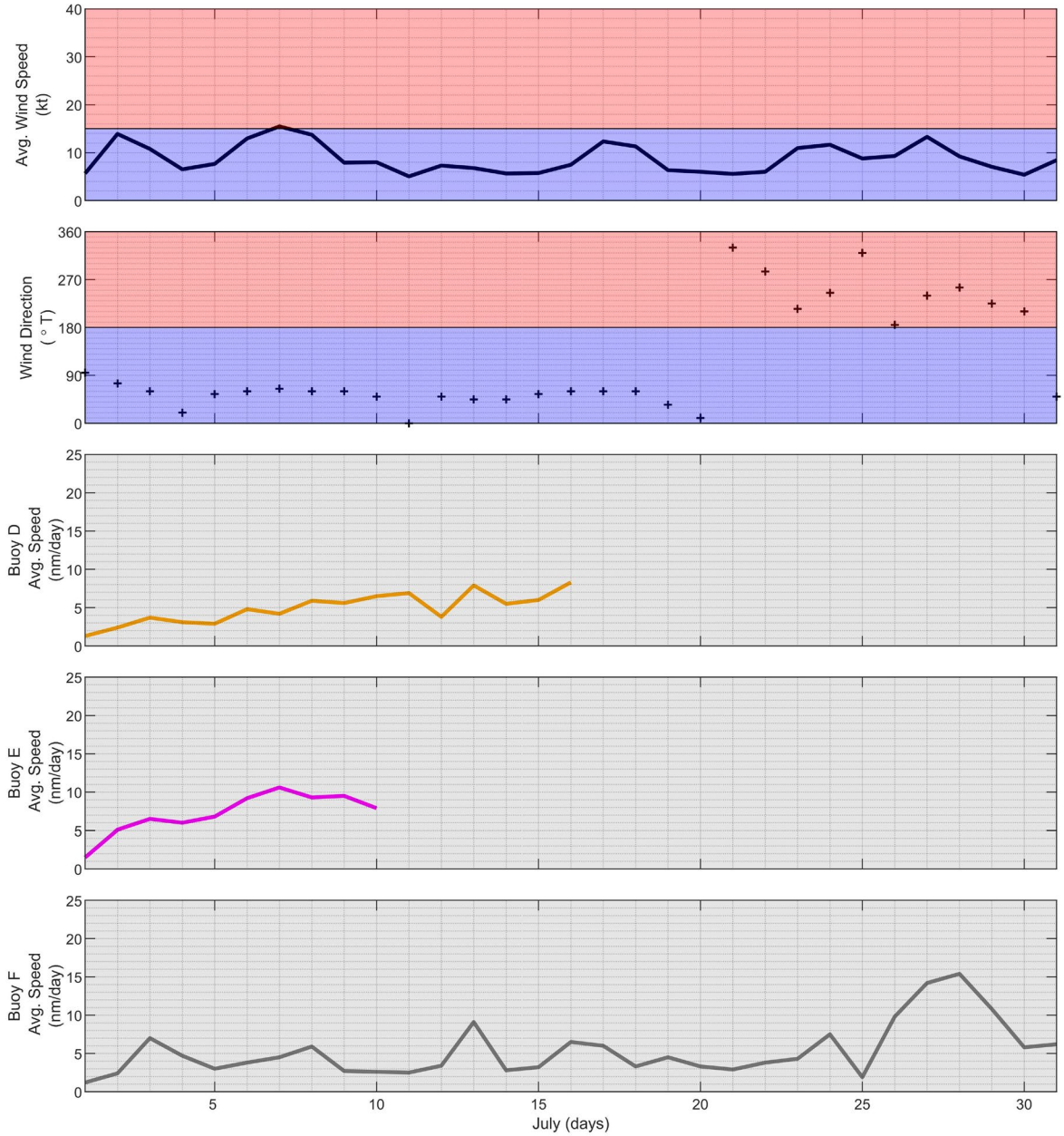

Figure 7-26. Beaufort Sea Drift Buoy Daily Average Speeds in July 2020

7.5. Reconnaissance Flights

As discussed in Section 4.5, two aerial reconnaissance missions were undertaken to document the ice conditions that prevailed in the Alaskan Beaufort Sea near the end of the break-up study period. Beaufort Sea Flight No. 1 (Flight "B1" on Drawing CFC-1070-02-002) was conducted on July 9th in the western Beaufort Sea, followed by Beaufort Sea Flight No. 2 (Flight "B2" on Drawing CFC-1070-02-003) on July 10th in the central Beaufort. A

"THIS INFORMATION IS DISTRIBUTED SOLELY FOR THE PURPOSE OF PRE-DISSEMINATION PEER REVIEW UNDER APPLICABLE INFORMATION QUALITY GUIDELINES. IT HAS NOT BEEN FORMALLY DISSEMINATED BY BSEE. IT DOES NOT REPRESENT AND SHOULD NOT BE CONSTRUED TO REPRESENT ANY BSEE DETERMINATION OR POLICY."

MODIS image depicting the ice conditions on the 10th is provided in Figure 7-27, while the RADARSAT-2 image acquired on the 14th is provided in Figure 7-24.

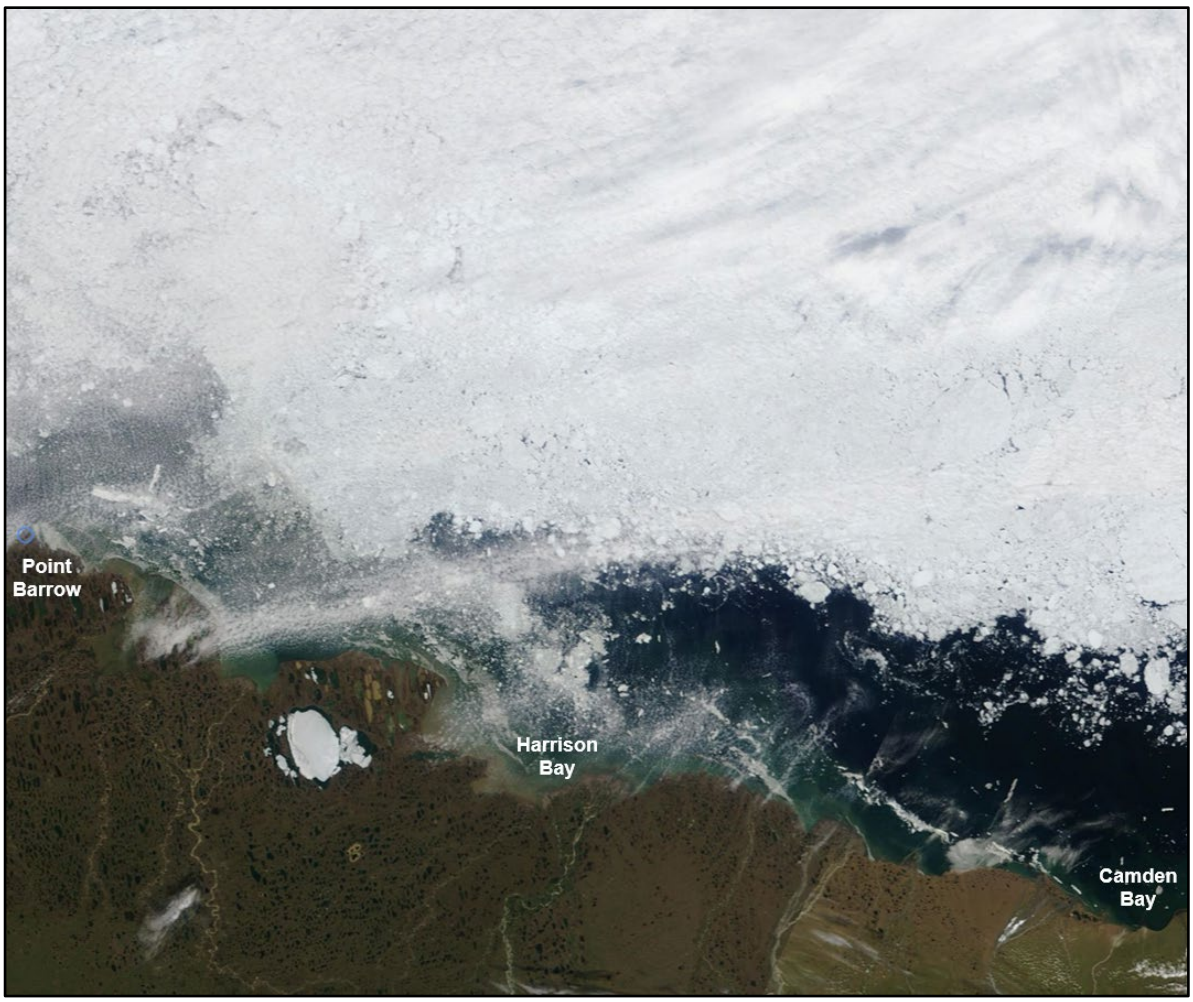

After: NASA, 2020a

Figure 7-27. MODIS Image of Beaufort Sea Acquired on July 10, 2020

7.5.1. Lagoon Ice

Many of the lagoon areas were found to be ice-free at the time of the flight, including Smith Bay, Simpson Lagoon, Gwydyr Bay, Prudhoe Bay, and South Camden Bay. Widely-scattered ice cakes and small floes at concentrations less than 10% were present in South Harrison Bay and Stefansson Sound (Plate 7-1). In addition, a relatively dense accumulation of cakes and small floes was noted at the shoreline on the west side of Foggy Island Bay and along the east-facing portions of the Endicott Project (Plate 7-2), reflecting the easterly winds that prevailed prior to and during the flights. In all instances where ice was present, it was badly deteriorated as evidenced by numerous melt ponds and through-ice holes.

“THIS INFORMATION IS DISTRIBUTED SOLELY FOR THE PURPOSE OF PRE-DISSEMINATION PEER REVIEW UNDER APPLICABLE INFORMATION QUALITY GUIDELINES. IT HAS NOT BEEN FORMALLY DISSEMINATED BY BSEE. IT DOES NOT REPRESENT AND SHOULD NOT BE CONSTRUED TO REPRESENT ANY BSEE DETERMINATION OR POLICY.”

Plate 7-1. Open Water with Widely Scattered Ice Cakes and Floes in Stefansson Sound (looking west on July 10, 2020)

Plate 7-2. Ice Cakes and Small Floes on East Side of Endicott Main Production Island and Causeway (looking west on July 10, 2020)

"THIS INFORMATION IS DISTRIBUTED SOLELY FOR THE PURPOSE OF PRE-DISSEMINATION PEER REVIEW UNDER APPLICABLE INFORMATION QUALITY GUIDELINES. IT HAS NOT BEEN FORMALLY DISSEMINATED BY BSEE. IT DOES NOT REPRESENT AND SHOULD NOT BE CONSTRUED TO REPRESENT ANY BSEE DETERMINATION OR POLICY."

7.5.2. Landfast Ice

As discussed in Section 7-4, the vast majority of the landfast ice had dispersed prior to the reconnaissance flights. The only ice of this nature observed during the flights was the narrow, discontinuous strip that stretched from Cross Island to Flaxman Island (Plate 7-3).

7.5.3. Nearshore Ice

Numerous ice cakes and small floes that appeared to be floating rather than grounded were present on the seaward side of many of the barrier islands (Plate 7-4). The ice was rotten, with numerous melt ponds and through-ice holes.

Although substantial accumulations of ice were noted on Weller Bank and Stamukhi Shoal during the flight on July 9th, a subsequent analysis of MODIS satellite images revealed that most of this ice was mobile and therefore not firmly grounded. The patches that were grounded contained ridges and rubble to heights of 7 m on Weller Bank (Plate 7-5) and 4 m on Stamukhi Shoal. In the case of the former, the concentration of first-year ice was estimated to range from 40 to 50%, while that of multi-year ice was estimated to range from 10 to 20%. In the case of the latter, the corresponding values were 50% for first-year ice and 20% for multi-year ice. Patches of grounded ice that had become surrounded by floating ice also were observed immediately east of Point Barrow (Plate 7-6), between Smith and Harrison Bays, and off Barter Island.

7.5.4. Pack Ice

Both flights were conducted within 30 nm (56 km) of the coast, limiting the opportunities to observe the relatively dense canopy of pack ice that existed farther offshore (Figure 7-27). A high concentration of pack ice was observed to the west of Weller Bank, however, when the flight path in the western Beaufort crossed the dense tongue of ice that extended toward Harrison Bay. The total ice concentrations in this region ranged from 20% to 90%, including multi-year ice concentrations from negligible to 30%. All of the ice, both first- and multi-year, was rotten with numerous through-ice holes (Plate 7-7).

7.5.5. Ice Edge

As is evident in Figure 7-27, the southern edge of the pack ice was diffuse throughout the Beaufort Sea study area. A representative view from the northern portion of the Camden Bay Prospects, where the ice concentration was estimated to average 10%, is provided in Plate 7-8.

“THIS INFORMATION IS DISTRIBUTED SOLELY FOR THE PURPOSE OF PRE-DISSEMINATION PEER REVIEW UNDER APPLICABLE INFORMATION QUALITY GUIDELINES. IT HAS NOT BEEN FORMALLY DISSEMINATED BY BSEE. IT DOES NOT REPRESENT AND SHOULD NOT BE CONSTRUED TO REPRESENT ANY BSEE DETERMINATION OR POLICY.”

Plate 7-3. Strip of Landfast Ice on North Side of Cross Island (looking northeast on July 10, 2020)

Plate 7-4. Ice Cakes and Small Floes Floating on North Side of Bodfish Island (looking southeast on July 9, 2020)

"THIS INFORMATION IS DISTRIBUTED SOLELY FOR THE PURPOSE OF PRE-DISSEMINATION PEER REVIEW UNDER APPLICABLE INFORMATION QUALITY GUIDELINES. IT HAS NOT BEEN FORMALLY DISSEMINATED BY BSEE. IT DOES NOT REPRESENT AND SHOULD NOT BE CONSTRUED TO REPRESENT ANY BSEE DETERMINATION OR POLICY."

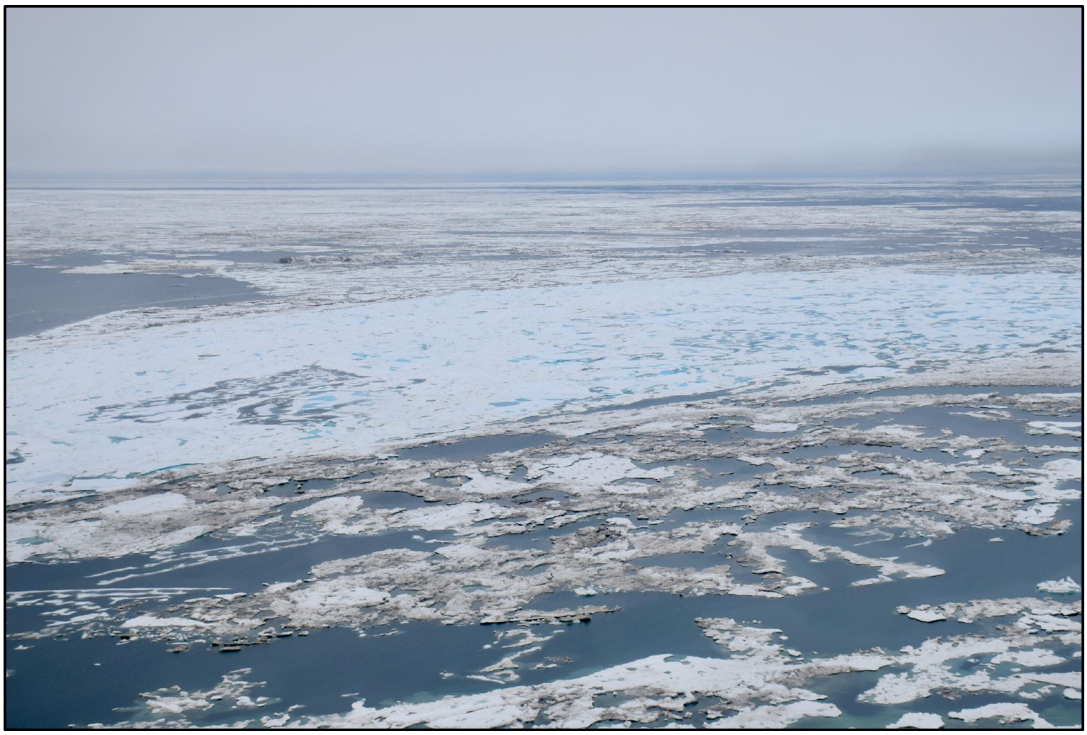

Plate 7-5. Patch of 7-m Ridges and Rubble Grounded on Weller Bank (looking northeast on July 9, 2020)

Plate 7-6. 6-m Ridges and Rubble Grounded 16 nm Northeast of Point Barrow (looking southeast on July 9, 2020)

"THIS INFORMATION IS DISTRIBUTED SOLELY FOR THE PURPOSE OF PRE-DISSEMINATION PEER REVIEW UNDER APPLICABLE INFORMATION QUALITY GUIDELINES. IT HAS NOT BEEN FORMALLY DISSEMINATED BY BSEE. IT DOES NOT REPRESENT AND SHOULD NOT BE CONSTRUED TO REPRESENT ANY BSEE DETERMINATION OR POLICY."

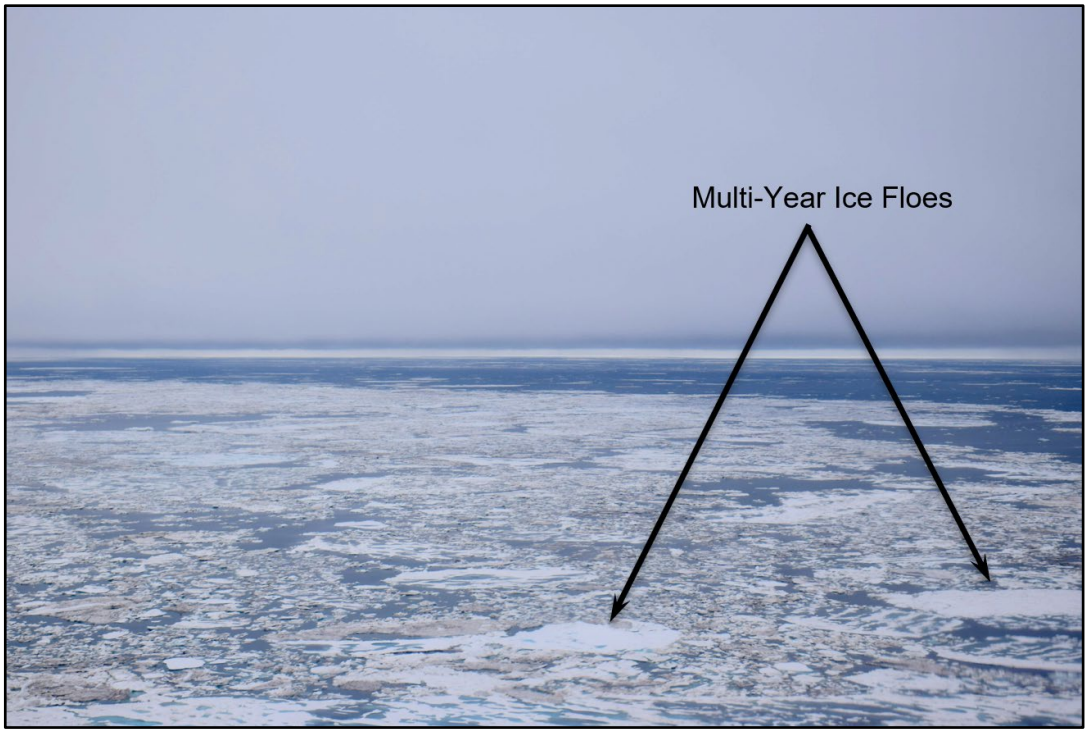

Plate 7-7. Dense Pack Ice 22 nm Northeast of Cape Halkett (looking northeast on July 9, 2020)

Plate 7-8. Diffuse Ice Edge in Northern Portion of Camden Bay Prospects (looking north on July 10, 2020)

"THIS INFORMATION IS DISTRIBUTED SOLELY FOR THE PURPOSE OF PRE-DISSEMINATION PEER REVIEW UNDER APPLICABLE INFORMATION QUALITY GUIDELINES. IT HAS NOT BEEN FORMALLY DISSEMINATED BY BSEE. IT DOES NOT REPRESENT AND SHOULD NOT BE CONSTRUED TO REPRESENT ANY BSEE DETERMINATION OR POLICY."

7.5.6. Ice Pile-Ups

As indicated in Section 7.1, 16 of the 32 ice pile-ups observed in the central Beaufort Sea in late February (Coastal Frontiers and Vaudrey, 2020) were present when the break-up flights were conducted in July. The other 16 pile-ups were no longer discernible, and new pile-ups or ride-ups that formed during break-up were conspicuously absent. As illustrated in Plate 7-9, which displays a pile-up that formerly extended 7 m above sea level and encroached 5 m onto the subaerial beach of Thetis Island, the dimensions of the remaining pile-ups had been substantially reduced by melting.

7.5.7. Multi-Year Ice

Multi-year ice floes at concentrations as high as 30% were observed in the dense tongue of pack ice to the west of Weller Bank (Section 7.5.4; Plate 7-7). Widely-scattered clusters of multi-year floes also were noted in Camden Bay, in the vicinity of Northstar Production Island, seaward of the barrier islands east of Oliktok Point, off Harrison Bay (including Weller Bank and Stamukhi Shoal) and off Smith Bay (Plate 7-10). At each of these sites, the concentrations ranged from 10 to 20%.

7.5.8. Ice Conditions in Camden Bay Prospects

Open water predominated in the southern portion of the Camden Bay Prospects, while ice concentrations as high as 50% were observed in the northern portion. All of the ice was rotten, with substantial melt ponds and through-ice holes. The floe diameters ranged from several meters to several kilometers. Of particular note were two patches of grounded ice on or adjacent to the prospective Sivulliq pipeline route. The first, consisting of multiple ridges and rubble with heights to 5 m, was located at the southern boundary of the Prospects (Plate 7-11). The second, a 5-m ridge, was located south of the Prospects, 1.5 nm (2.8 km) north of Mary Sachs Entrance (Plate 7-12).

7.5.9. Ice Conditions in Harrison Bay Prospects

The ice concentrations in the Harrison Bay Prospects tended to be higher than those in the Camden Bay Prospects, with values ranging from 20 to 60%. As indicated in Section 7.5.3, ridges and rubble with heights to 4 m were grounded on Stamukhi Shoal, in the northeast corner of the Prospects. Elsewhere, ridge and rubble heights of 1 to 2 m were typical but peaked at 5 m near the northern boundary. Multi-year ice was confined to the northern portion of the Prospects, where concentrations of 20% were noted in some areas. Floe sizes varied over a wide range, from cakes to more than 3 km in diameter (Plate 7-13). In all cases, the ice was rotten.

"THIS INFORMATION IS DISTRIBUTED SOLELY FOR THE PURPOSE OF PRE-DISSEMINATION PEER REVIEW UNDER APPLICABLE INFORMATION QUALITY GUIDELINES. IT HAS NOT BEEN FORMALLY DISSEMINATED BY BSEE. IT DOES NOT REPRESENT AND SHOULD NOT BE CONSTRUED TO REPRESENT ANY BSEE DETERMINATION OR POLICY."

Plate 7-9. Relict Pile-Up on West End of Thetis Island (looking southeast on July 9, 2020)

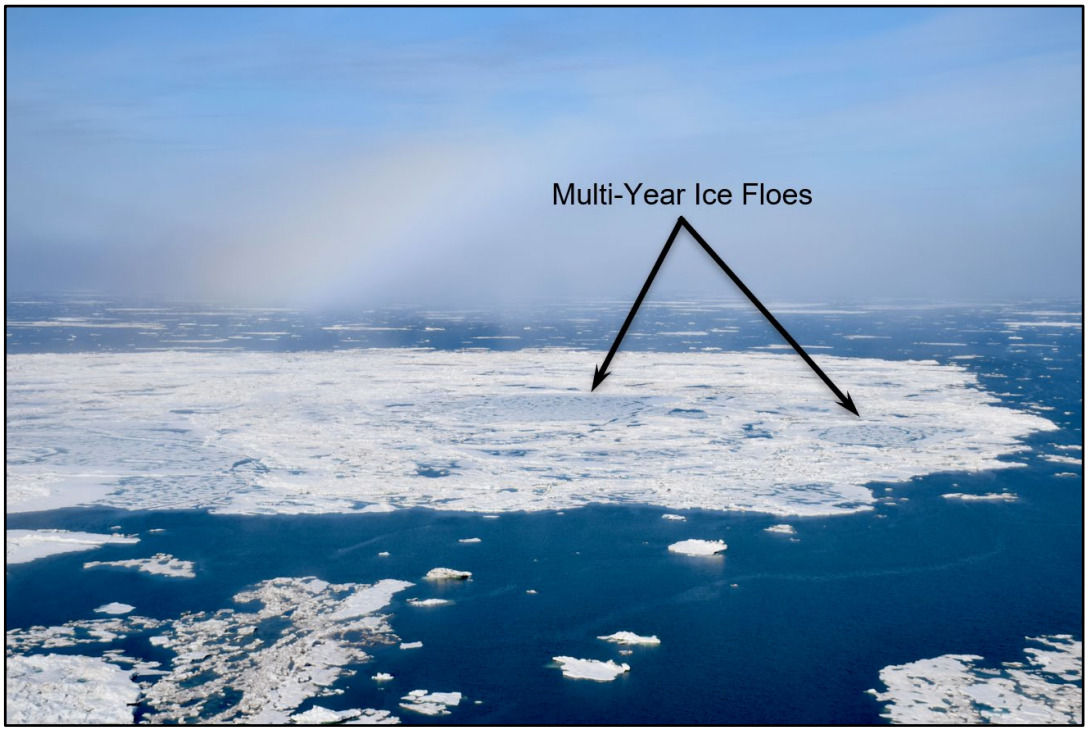

Plate 7-10. Agglomeration of First- and Multi-Year Ice Floes 15 nm North of Smith Bay (looking northeast on July 9, 2020)

“THIS INFORMATION IS DISTRIBUTED SOLELY FOR THE PURPOSE OF PRE-DISSEMINATION PEER REVIEW UNDER APPLICABLE INFORMATION QUALITY GUIDELINES. IT HAS NOT BEEN FORMALLY DISSEMINATED BY BSEE. IT DOES NOT REPRESENT AND SHOULD NOT BE CONSTRUED TO REPRESENT ANY BSEE DETERMINATION OR POLICY.”

Plate 7-11. 5-m Grounded Ridges and Rubble at Southern Edge of Camden Bay Prospects (looking northeast on July 10, 2020)

Plate 7-12. 5-m Grounded Ridge 1.5 nm North of Mary Sachs Entrance (looking southeast on July 10, 2020)

“THIS INFORMATION IS DISTRIBUTED SOLELY FOR THE PURPOSE OF PRE-DISSEMINATION PEER REVIEW UNDER APPLICABLE INFORMATION QUALITY GUIDELINES. IT HAS NOT BEEN FORMALLY DISSEMINATED BY BSEE. IT DOES NOT REPRESENT AND SHOULD NOT BE CONSTRUED TO REPRESENT ANY BSEE DETERMINATION OR POLICY.”

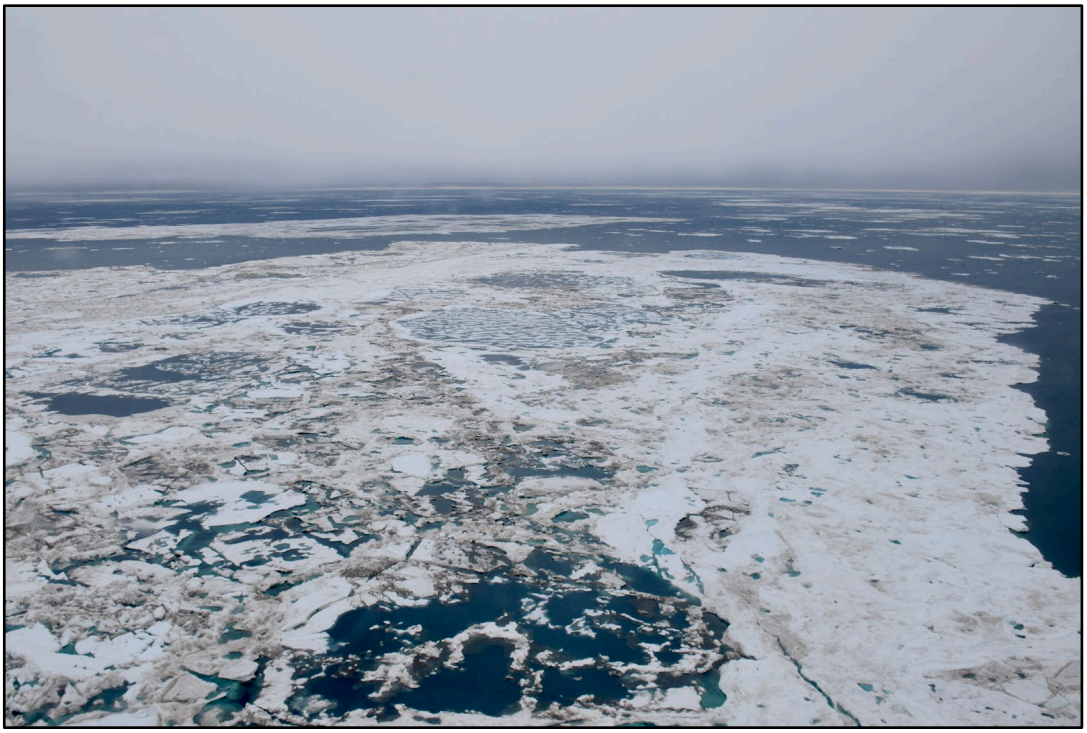

Plate 7-13. Large, Rotten Ice Floe in Northwest Portion of Harrison Bay Prospects (looking North on July 10, 2020)

7.5.10. Ice Conditions in Liberty Prospect

With the exception of ice cakes and small floes at the shoreline analogous to those on the east side of the Endicott Project (Plate 7-2), the prospective Liberty pipeline route and site of the Liberty Drilling and Production Island were ice-free.

"THIS INFORMATION IS DISTRIBUTED SOLELY FOR THE PURPOSE OF PRE-DISSEMINATION PEER REVIEW UNDER APPLICABLE INFORMATION QUALITY GUIDELINES. IT HAS NOT BEEN FORMALLY DISSEMINATED BY BSEE. IT DOES NOT REPRESENT AND SHOULD NOT BE CONSTRUED TO REPRESENT ANY BSEE DETERMINATION OR POLICY."

8. TRENDS

The primary objectives of this section are to summarize the break-up processes that occurred in 2020, and to develop a preliminary assessment of long-term changes by comparing those observed in 2017 (Coastal Frontiers and Vaudrey, 2018) and 2020 with those observed in the past.

Factors that exert a significant influence on break-up include air temperatures, storms, and river overflood onto the sea ice. Accordingly, the temperature and wind data from Utqiagvik Airport are analyzed to investigate perceived trends toward warmer conditions and higher storm frequencies, and river overflood is analyzed to determine whether this phenomenon occurs earlier than in the past. Utqiagvik was selected over Deadhorse as the source of wind and temperature data due to its longer period of record.

Following an analysis of the aforementioned causative factors, trends in the timing of break-up, the length of the open-water season, and the absence or presence of multi-year ice are investigated. It should be recognized that two years (2017 and 2020) represent an extremely small sample that may not be representative of present-day break-up conditions. As a result, the assessments presented below should be regarded as preliminary, and subject to verification and substantial refinement as more data become available.

8.1. Air Temperatures

As discussed in Section 4.1, thawing-degree days (TDD) were computed as the difference between the melting point of freshwater ice (32°F; 0°C) and the daily average air temperature, and then accumulated by month. Negative TDD (<32°F) that occurred after break-up had begun were subtracted from the total.

Table 8-1 presents the accumulated TDD at Utqiagvik Airport at the end of May, June, and July for each year from 1970 through 2020. The value shown for each month represents the total number of TDD that accumulated from May 1st through the end of the month. The table is divided into two halves, with the top portion showing the 26-year period from 1970 through 1995 and the bottom portion the subsequent 25-year period from 1996 through 2020. The column on the right side displays the rank of each break-up season over the 51-year period-of-record, with the highest ranking (No. 1) assigned to the warmest break-up (largest number of TDD at the end of July) and the lowest ranking (No. 51) assigned to the coldest (smallest number of TDD at the end of July). The ten warmest break-up seasons (Nos. 1 through 10) are shown in red type.

"THIS INFORMATION IS DISTRIBUTED SOLELY FOR THE PURPOSE OF PRE-DISSEMINATION PEER REVIEW UNDER APPLICABLE INFORMATION QUALITY GUIDELINES. IT HAS NOT BEEN FORMALLY DISSEMINATED BY BSEE. IT DOES NOT REPRESENT AND SHOULD NOT BE CONSTRUED TO REPRESENT ANY BSEE DETERMINATION OR POLICY."

Table 8-1. Accumulated Thawing-Degree Days (>32°F) at Utqiagvik Airport from May through July, 1970-2020

Year	May	June	July	51-yr Rank
1970	0	90	280	46
1971	0	105	373	29
1972	0	51	393	23
1973	0	51	296	42
1974	0	19	247	51
1975	0	77	250	50
1976	0	59	266	47
1977	0	71	292	43
1978	0	52	303	41
1979	5	34	381	28
1980	0	169	290	44
1981	0	107	353	32
1982	0	75	265	48
1983	6	90	283	45
1984	0	184	469	15
1985	1	121	344	34
1986	0	114	430	19
1987	0	84	306	40
1988	0	91	311	38
1989	11	150	578	4
1990	19	193	520	13
1991	7	163	349	33
1992	15	139	384	25
1993	11	151	565	7
1994	0	52	354	31
1995	0	155	418	22
Average	**3**	**102**	**358**	
Std. Dev.	**5**	**49**	**93**	
Year	**May**	**June**	**July**	**51-yr Rank**
1996	22	204	529	11
1997	0	100	382	26
1998	28	208	605	3
1999	0	122	464	16
2000	0	179	382	26
2001	0	110	322	36
2002	0	78	309	39
2003	0	82	367	30
2004	0	219	554	9
2005	0	92	316	37
2006	0	208	436	18
2007	0	135	521	12
2008	0	167	420	20
2009	0	102	473	14
2010	0	74	388	24
2011	0	119	437	17
2012	0	165	543	10
2013	13	225	616	2
2014	0	69	264	49
2015	35	283	556	8
2016	19	199	569	6
2017	0	131	572	5
2018	0	64	420	20
2019	0	162	676	1
2020	2	149	342	35
Average	**5**	**146**	**459**	
Std. Dev.	**10**	**59**	**111**	

Note: TDD were calculated using daily average air temperatures from NOAA (2020).

"THIS INFORMATION IS DISTRIBUTED SOLELY FOR THE PURPOSE OF PRE-DISSEMINATION PEER REVIEW UNDER APPLICABLE INFORMATION QUALITY GUIDELINES. IT HAS NOT BEEN FORMALLY DISSEMINATED BY BSEE. IT DOES NOT REPRESENT AND SHOULD NOT BE CONSTRUED TO REPRESENT ANY BSEE DETERMINATION OR POLICY."

Although six of the ten warmest break-up seasons occurred during the past decade, 2020 was relatively cold, ranking 35th out of the 51 years. The accumulated TDD, 342, barely exceeded half of those recorded in 2019, which was the warmest break-up on record with 676 TDD.

The accumulated TDD at the end of each break-up season are plotted as a time series in Figure 8-1. The long-term warming trend implied by the large values in recent years is readily apparent, with the number of TDD increasing at an average rate of 4.2 per year since 1970. The rate of warming has varied substantially from decade to decade, however. Based on the data presented in Table 8-1, the average annual accumulated TDD increased by 17.8% from the 1970s to the 1980s and 25.9% from the 1980s to the 1990s but then declined by 10.3% from the 1990s to the 2000s. The upward trend resumed during the past 11 years (2010-2020), with an increase of 20.3% relative to the 2000s (equivalent to decadal increase of 18.5%). When compared to the 1970's, when the accumulated TDD averaged 308 per year, the average of 489 over the past 11 years represents an increase of nearly 60%.

Short-term deviations from the warming trend, with durations of one to several years, are clearly evident in Figure 8-1. The magnitude of these deviations has increased; as shown in Table 8-1, the standard deviation in accumulated TDD at the end of July increased from 93 during the first half of the period-of-record (1970 through 1995) to 111 during the second (1996 through 2020).

Figure 8-2 compares the monthly average air temperatures at Utqiagvik in May, June, and July of 2020 with the long-term average values derived for the 30-year period from 1971 through 2000. The monthly average temperatures averaged over 2017 and 2020 also are compared with the long-term averages. The temperatures in May and June of 2020 exceeded the corresponding long-term averages by 2.4 and 1.9°F (1.3 and 1.1°C, respectively), but the temperature in July was 2.2°F (1.2°C) lower. Over the entire three-month period, the average temperature in 2020 exceeded the long-term average by a modest 0.7°F (0.4°C). In the case of the monthly values averaged over 2017 and 2020, the resulting average temperature over the three-month period exceeds the long-term average by 2.0°F (1.1°C). The implied rate of warming (about 0.6°F or 0.3°C per decade) is less than that reported by Serreze, *et al*. (2000), who found that between 1966 and 1995, temperatures in the vicinity of Utqiagvik increased at approximate rates of 1.4°F (0.8°C) per decade in spring and 1.1°F (0.6°C) per decade in summer. Although the small sample size for recent temperatures argues against definitive conclusions, a possible explanation for the slower rate of increase relative to 1971-2000 may be the aforementioned cooling trend that occurred in the 2000s relative to the 1990s.

"THIS INFORMATION IS DISTRIBUTED SOLELY FOR THE PURPOSE OF PRE-DISSEMINATION PEER REVIEW UNDER APPLICABLE INFORMATION QUALITY GUIDELINES. IT HAS NOT BEEN FORMALLY DISSEMINATED BY BSEE. IT DOES NOT REPRESENT AND SHOULD NOT BE CONSTRUED TO REPRESENT ANY BSEE DETERMINATION OR POLICY."

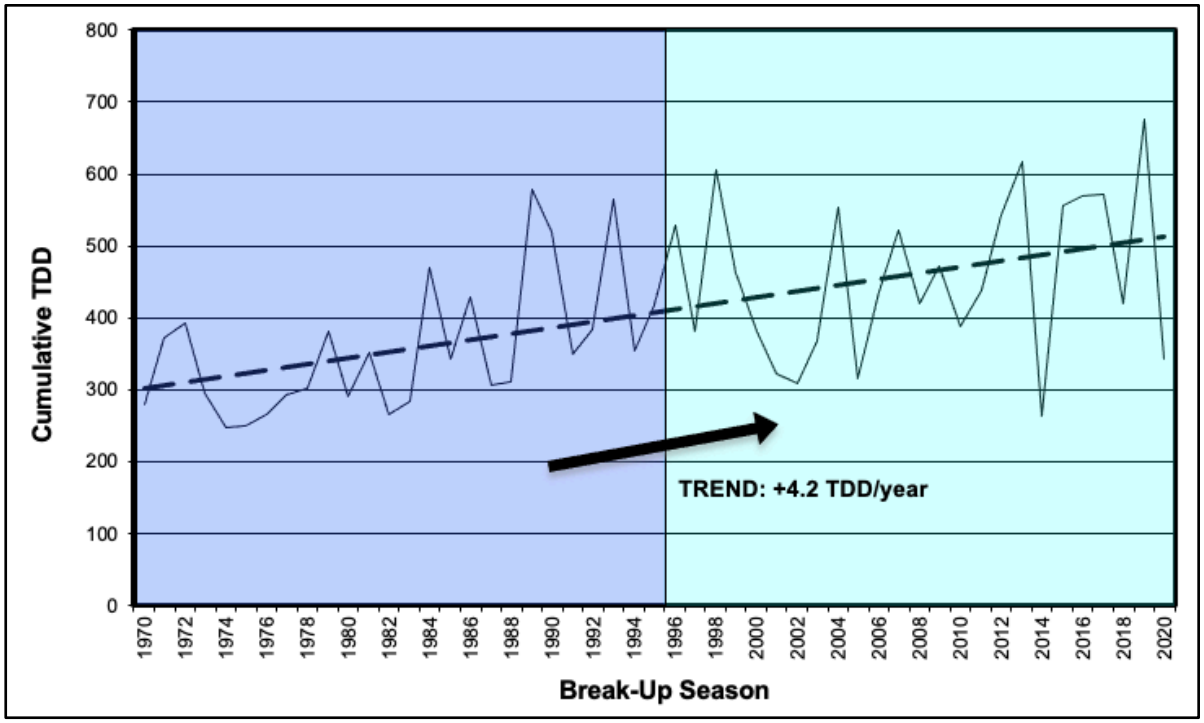

Figure 8-1. Accumulated Thawing-Degree Days (>32°F) at Utqiagvik Airport from May through July, 1970-2020

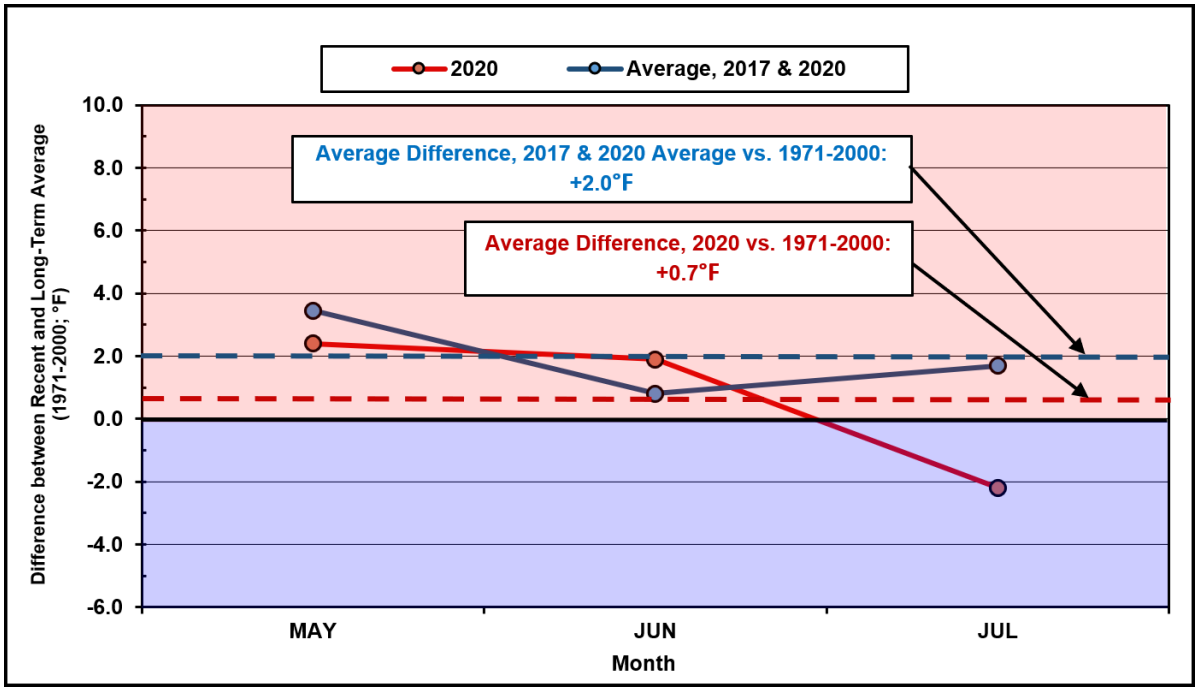

Figure 8-2. Differences between Recent Monthly Average Air Temperatures and Long-Term Average Values from May through July at Utqiagvik Airport

"THIS INFORMATION IS DISTRIBUTED SOLELY FOR THE PURPOSE OF PRE-DISSEMINATION PEER REVIEW UNDER APPLICABLE INFORMATION QUALITY GUIDELINES. IT HAS NOT BEEN FORMALLY DISSEMINATED BY BSEE. IT DOES NOT REPRESENT AND SHOULD NOT BE CONSTRUED TO REPRESENT ANY BSEE DETERMINATION OR POLICY."

Trends: Since the 1970s, progressively warmer break-up seasons have caused the number of accumulated thawing-degree days at Utqiagvik to increase at an average rate of 4.2 per year. The rate of warming has varied widely, however, on time scales ranging from interannual to interdecadal.

8.2. Storms

The storms that occurred at Utqiagvik and Deadhorse Airports during the 2017 and 2020 break-up seasons are summarized in Tables 8-2 and 8-3. Both the number of discrete storm events and the total number of days with storm conditions ("storm-days") are shown. As in the case of Sections 6 and 7, a storm is defined as an event during which the daily average sustained wind speed exceeds 15 kt (8 m/s).

Table 8-2. Chukchi Sea Storms during 2017 and 2020 Break-Up Seasons[1,2]

Basin	Easterly Storm Events	Westerly Storm Events	Total Storm Events	Easterly Storm-Days	Westerly Storm-Days	Total Storm-Days
2017	4	3	7	11	3	14
2020	3	1	4	8	3	11
Average	3.5	2.0	5.5	9.5	3.0	12.5

Notes:
1. Table 8-2 includes all storm events with a daily average sustained wind speed exceeding 15 kt (8 m/s) at Utqiagvik Airport.
2. The period of record extends from May 1st through July 31st.

Table 8-3. Beaufort Sea Storms during 2017 and 2020 Break-Up Seasons[1,2]

Basin	Easterly Storm Events	Westerly Storm Events	Total Storm Events	Easterly Storm-Days	Westerly Storm-Days	Total Storm-Days
2017	8	1	9	23	1	24
2020	4	0	4	18	0	18
Average	6.0	0.5	6.5	20.5	0.5	21.0

Notes:
1. Table 8-3 includes all storm events with a daily average sustained wind speed exceeding 15 kt (8 m/s) at Deadhorse Airport.
2. The period of record extends from May 1st through July 31st.

"THIS INFORMATION IS DISTRIBUTED SOLELY FOR THE PURPOSE OF PRE-DISSEMINATION PEER REVIEW UNDER APPLICABLE INFORMATION QUALITY GUIDELINES. IT HAS NOT BEEN FORMALLY DISSEMINATED BY BSEE. IT DOES NOT REPRESENT AND SHOULD NOT BE CONSTRUED TO REPRESENT ANY BSEE DETERMINATION OR POLICY."

In the Chukchi, 3.5 easterly and 2.5 westerly storms occurred on average during each break-up season (Table 8-2). In addition to being more numerous, the easterlies tended to be of longer duration, persisting for an average of 2.7 days/event versus 1.5 days/event for the westerlies. The numbers of easterly storms, westerly storms, easterly storm days, and total storm days all were lower in 2020 than 2017 while the number of westerly storm days was identical.

In the Beaufort, which tended to experience more storms and more storm days than the Chukchi, easterly events predominated by a wide margin. The annual averages consisted of 6.0 easterly events producing 20.5 storm-days (3.4 days/event) and only 0.5 westerly events producing 0.5 storm-days (1.0 days/event). All measures of storm activity, consisting of easterly storms, westerly storms, easterly storm days, and westerly storm days, were lower in 2020 than 2017.

To provide a first indication of whether the frequency of storm events has changed, the daily average sustained wind speeds at Utqiagvik Airport (Weather Underground, 2017; NOAA, 2020a) were used to identify all storms that occurred during the five break-up seasons from 1981 through 1985 and five recent break-up seasons consisting of 2014 through 2017 and 2020. The early 1980s was selected as the basis for comparison because it represents the period in which break-up studies were conducted by Vaudrey (Section 3.2). The results, which are compiled in Tables 8-4 and 8-5, indicate that the storm frequency increased from 3.2 events per break-up season in the early 1980s to 5.8 events per season in recent years. The magnitude of the change is displayed graphically in Figure 8-3.

Table 8-4. Chukchi Sea Storms during Break-Up Season, 1981-1985[1,2]

Month	1981	1982	1983	1984	1985	Average (1981-1985)
May	0	1	2	1	0	-
June	2	2	2	0	1	-
July	1	1	0	2	1	-
Total	**3**	**4**	**4**	**3**	**2**	**3.2 Storms/Year**

Notes:

[1] Table 8-4 includes all storm events with a daily average sustained wind speed exceeding 15 kt (8 m/s) from May 1st through July 31st at Utqiagvik Airport.

[2] Storm count was developed using wind data from Weather Underground (2017).

"THIS INFORMATION IS DISTRIBUTED SOLELY FOR THE PURPOSE OF PRE-DISSEMINATION PEER REVIEW UNDER APPLICABLE INFORMATION QUALITY GUIDELINES. IT HAS NOT BEEN FORMALLY DISSEMINATED BY BSEE. IT DOES NOT REPRESENT AND SHOULD NOT BE CONSTRUED TO REPRESENT ANY BSEE DETERMINATION OR POLICY."

Table 8-5. Chukchi Sea Storms during Break-Up Season, 2014-2017 and 2020[1,2]

Month	2014	2015	2016	2017	2020	Average (2014-17 & 2020)
May	3	2	2	1	1	-
June	1	1	2	3	1	-
July	3	3	1	3	2	-
Total	**7**	**6**	**5**	**7**	**4**	**5.8 Storms/Year**

Notes:

[1] Table 8-5 includes all storm events with a daily average sustained wind speed exceeding 15 kt (8 m/s) from May 1st through July 31st at Utqiagvik Airport.

[2] Storm count was developed using wind data from Weather Underground (2017) and NOAA (2020a).

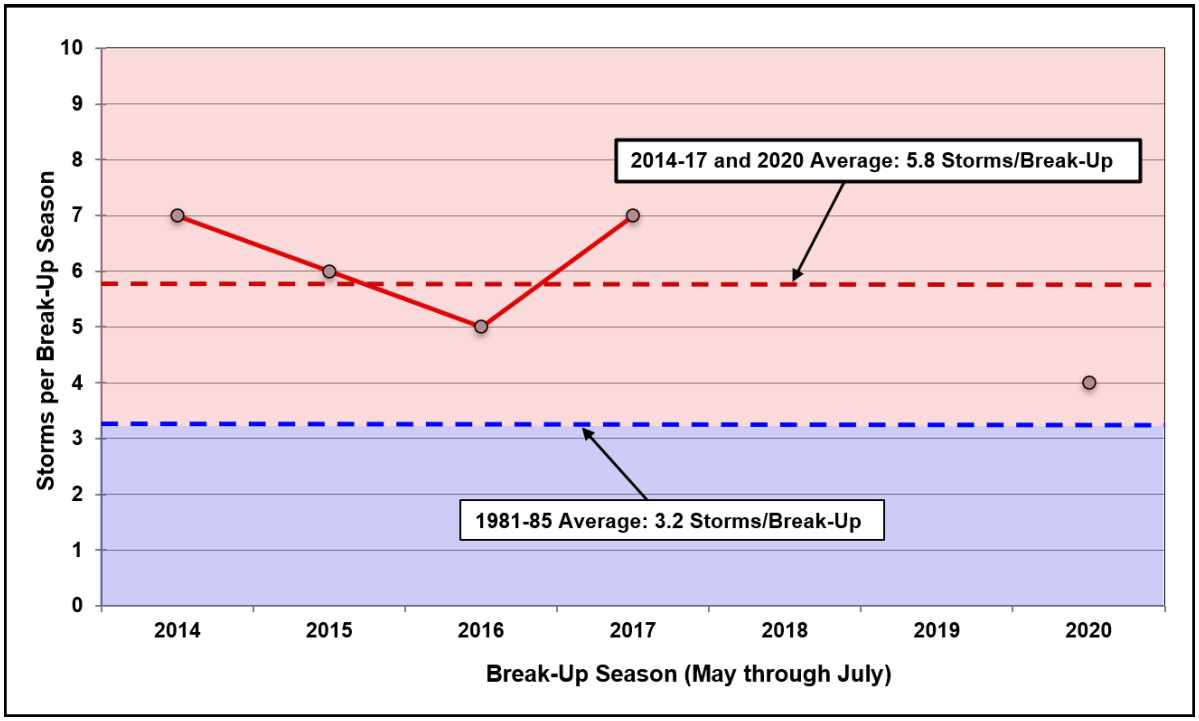

Figure 8-3. Storms during Break-Up Season at Utqiagvik Airport, 2014-20

Trend: Since the early 1980s, the frequency of storm events during break-up has nearly doubled, from 3.2 to 5.8 storms per year.

"THIS INFORMATION IS DISTRIBUTED SOLELY FOR THE PURPOSE OF PRE-DISSEMINATION PEER REVIEW UNDER APPLICABLE INFORMATION QUALITY GUIDELINES. IT HAS NOT BEEN FORMALLY DISSEMINATED BY BSEE. IT DOES NOT REPRESENT AND SHOULD NOT BE CONSTRUED TO REPRESENT ANY BSEE DETERMINATION OR POLICY."

8.3. River Overflood

A key finding of the break-up studies conducted in the 1980s was the limited influence of river overflood on break-up of the landfast ice in the northeast Chukchi Sea (Section 3.1). Nevertheless, as observed in both 2017 and 2020, overflood can initiate break-up in the protected lagoon areas by melting through the sea ice adjacent to the river mouths (Sections 6.2 and 6.3).

The only historical data on the timing of river overflood in the Chukchi Sea identified for this study was compiled by Coastal Frontiers in 2014. Using MODIS and RADARSAT-2 imagery, the date on which river discharge began to flood the sea ice was estimated for six rivers in or adjacent to the current study area for each break-up season from 2004 through 2014. These dates, along with the corresponding dates from 2017 and 2020, are plotted in Figure 8-4 and summarized in Table 8-6. The figure and table also include the linear trend for each river derived from the combined data set (2004-14, 2017, and 2020). The start of the overflood has been trending earlier for all six rivers, with values ranging from -0.1 to -0.8 days per year (with negative values indicating earlier occurrence). The average is -0.4 days per year.

In the Beaufort, which receives the discharge of rivers that are both larger and more numerous than those in the Chukchi, overflood can exert a substantial influence on break-up through *in-situ* melting of large expanses of lagoon ice (Sections 3.1 and 7.3). Although data are sparse, useful information on the timing of overflood can be inferred from the annual monitoring of break-up in the Sagavanirktok and Kuparuk Rivers conducted in support of oil field operations (Burris, 2020; Visser, 2020).

In the case of the Sagavanirktok, the date on which the river ice breaks up at the Sag River Bridge has been logged since 1980, with the results plotted in Figure 8-5. Because the bridge lies only about 6 nm (11 km) south of the river mouth, break-up at this site provides a first-order approximation of the date on which overflooding of the sea ice begins. The plot indicates that the date has been trending earlier at an average rate of -0.2 days per year.

In the case of the Kuparuk, the date on which the road crossing is closed by flooding has been recorded since 1980. As in the case of break-up at the Sag River Bridge, this milestone serves as an imperfect but reasonable proxy for the initiation of river overflood onto the sea ice by virtue of the crossing's proximity to the coast (6 nm; 11 km). The data, which appear in Figure 8-6, indicate that the timing of overflood has remained essentially unchanged during the past four decades.

"THIS INFORMATION IS DISTRIBUTED SOLELY FOR THE PURPOSE OF PRE-DISSEMINATION PEER REVIEW UNDER APPLICABLE INFORMATION QUALITY GUIDELINES. IT HAS NOT BEEN FORMALLY DISSEMINATED BY BSEE. IT DOES NOT REPRESENT AND SHOULD NOT BE CONSTRUED TO REPRESENT ANY BSEE DETERMINATION OR POLICY."

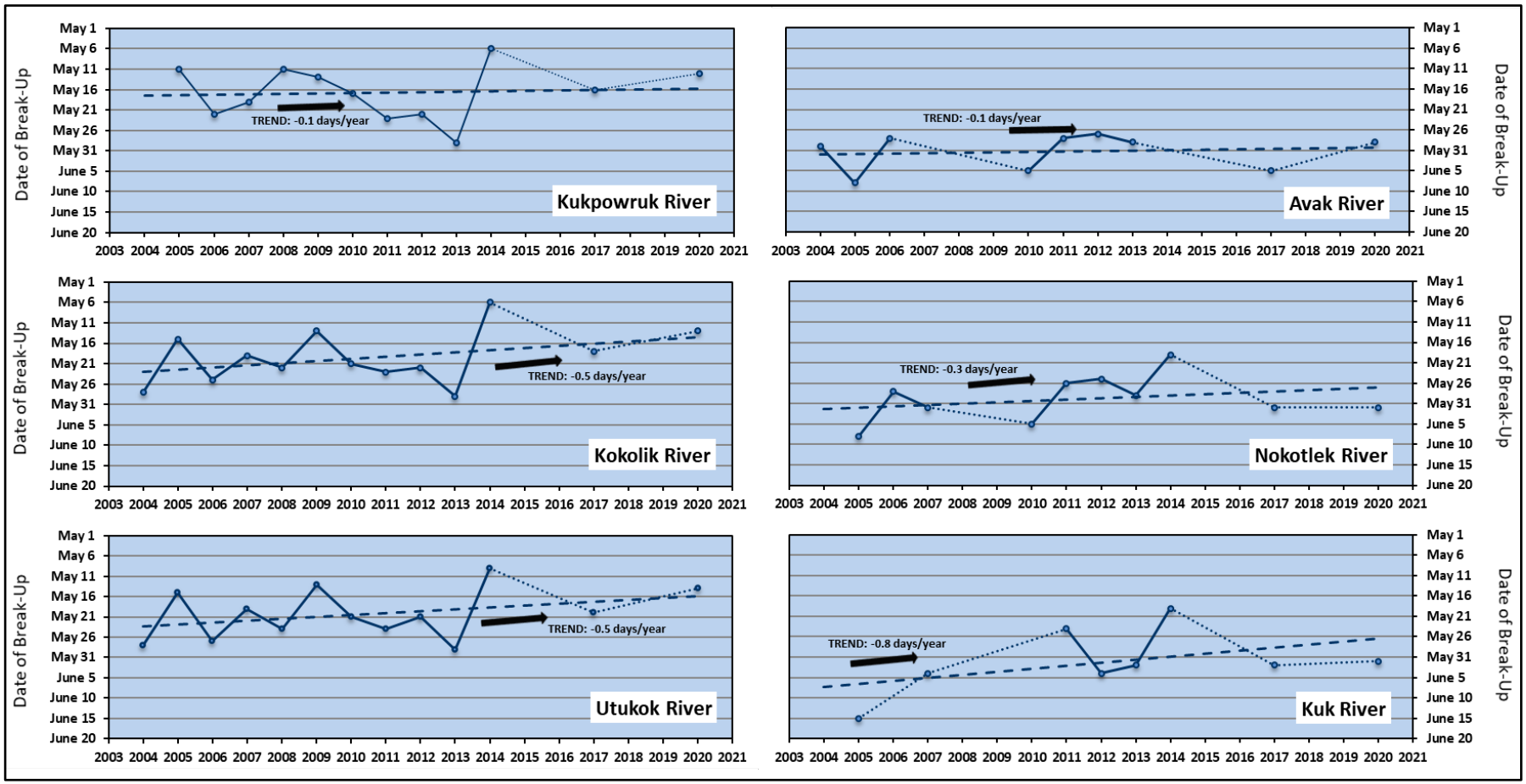

Note: Dotted lines are used to bridge data gaps

Data Source: Coastal Frontiers, 2014

Figure 8-4. Timing of River Overflood in Chukchi Sea, 2004-14, 2017 and 2020

"THIS INFORMATION IS DISTRIBUTED SOLELY FOR THE PURPOSE OF PRE-DISSEMINATION PEER REVIEW UNDER APPLICABLE INFORMATION QUALITY GUIDELINES. IT HAS NOT BEEN FORMALLY DISSEMINATED BY BSEE. IT DOES NOT REPRESENT AND SHOULD NOT BE CONSTRUED TO REPRESENT ANY BSEE DETERMINATION OR POLICY."

Table 8-6. Timing of River Overflood in Chukchi Sea, 2004-14, 2017 and 2020[1]

River[2]	Overflood Start, 2004-14[3]	Overflood Start in 2017	Overflood Start in 2020	Trend[4] (days per year)
Kukpowruk	May 6 - May 29	May 16	May 12	-0.1
Kokolik	May 6 – May 29	May 18	May 13	-0.5
Utukok	May 9 – May 29	May 20	May 14	-0.5
Avak	May 27 - Jun 8	June 5	May 29	-0.1
Nokotlek	May 19 – Jun 8	June 1	June 1	-0.3
Kuk	May 19 – Jun 15	June 2	June 1	-0.8
Average	n/a	n/a	n/a	**-0.4**

Notes:

1 The date represents the first day on which overflood water was detected on the sea ice in MODIS and/or RADARSAT-2 imagery.

2 The rivers are listed from south to north, with their locations shown in Figure 1-4.

3 Data from Coastal Frontiers (2014).

4 A negative value indicates that the date is trending earlier.

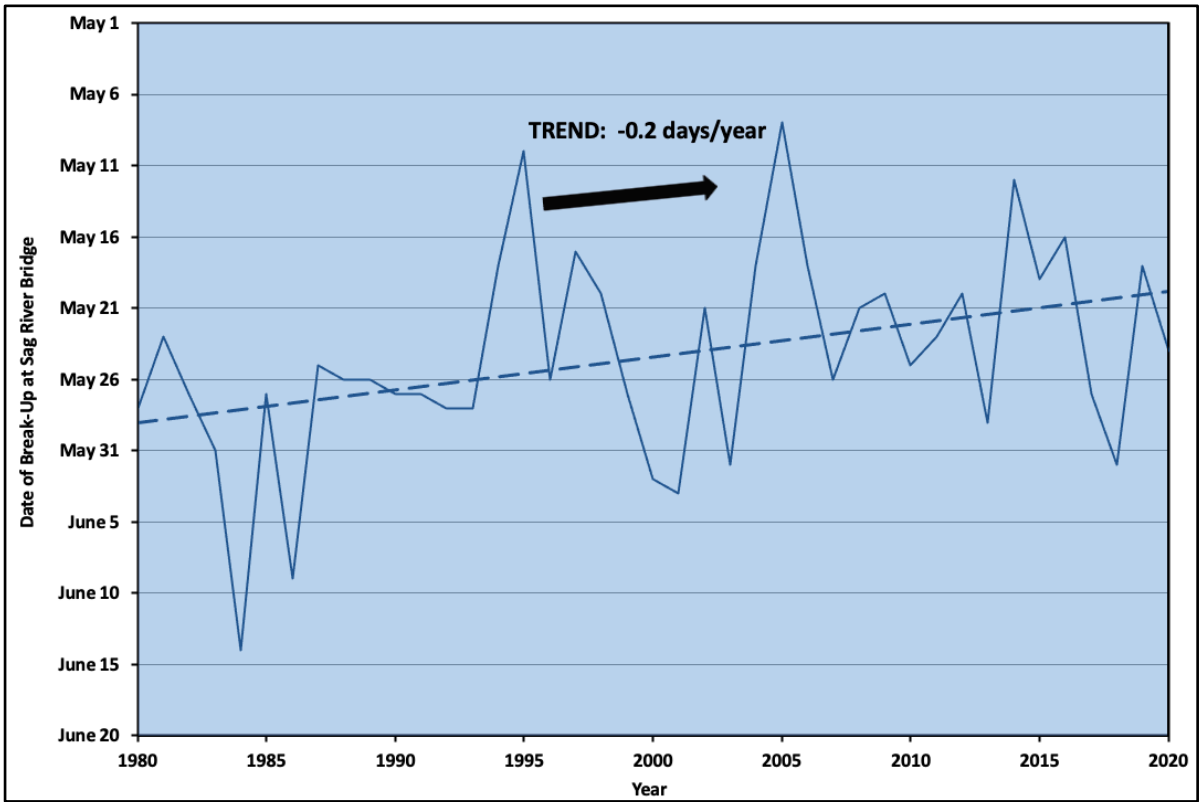

Data Source: Burris, 2020

Figure 8-5. River Ice Break-Up at Sagavanirktok River Bridge, 1980-2020

"THIS INFORMATION IS DISTRIBUTED SOLELY FOR THE PURPOSE OF PRE-DISSEMINATION PEER REVIEW UNDER APPLICABLE INFORMATION QUALITY GUIDELINES. IT HAS NOT BEEN FORMALLY DISSEMINATED BY BSEE. IT DOES NOT REPRESENT AND SHOULD NOT BE CONSTRUED TO REPRESENT ANY BSEE DETERMINATION OR POLICY."

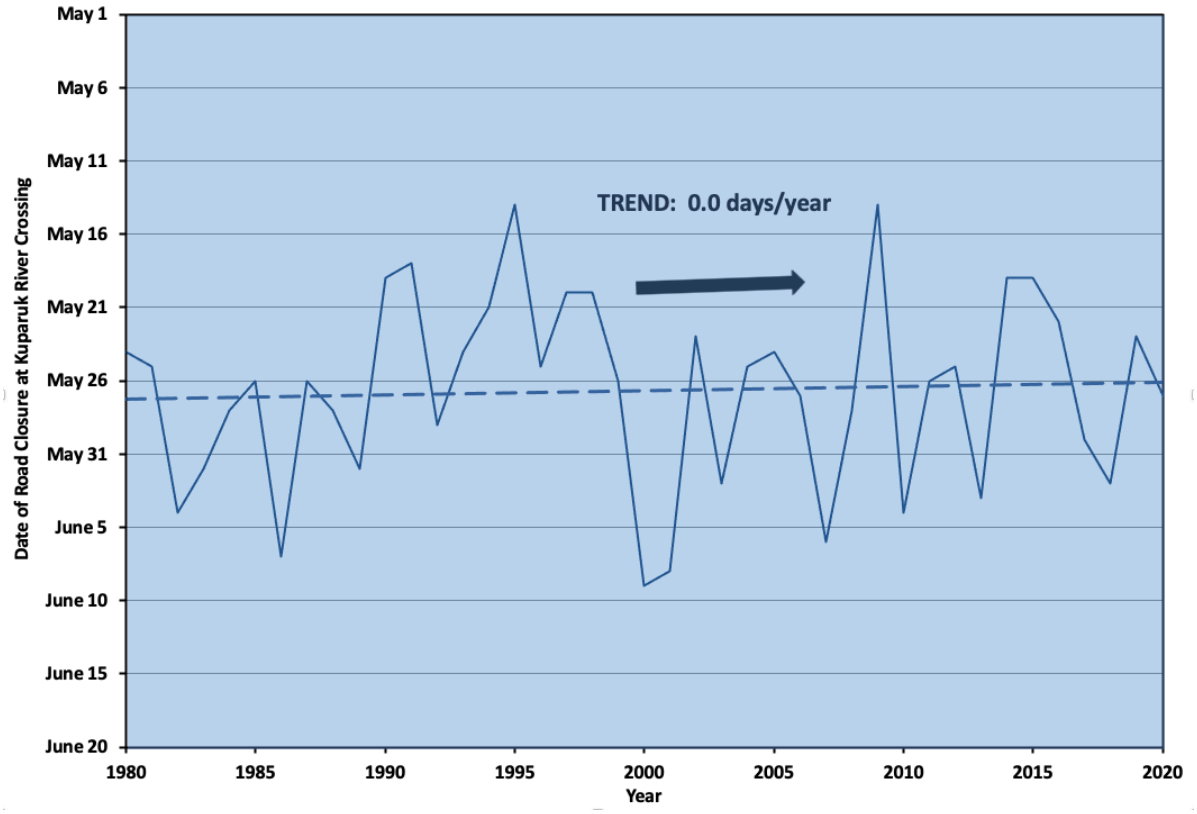

Data Source: Visser, 2020

Figure 8-6. Road Closure at Kuparuk River Crossing, 1980-2020

Trend: The limited data available suggest that the initiation of river overflood onto the sea ice in the Chukchi and Beaufort Seas has been trending earlier at rates ranging from negligible to about one day per year.

8.4. Timing of Break-Up

The three studies conducted in the northeast Chukchi Sea by Vaudrey (1984a; 1984b; 1985a; 1985b; 1986; see also Section 3.1) documented wide variations in the timing of break-up of the landfast ice: prior to June 25th in 1983, between July 1st and 3rd in 1984, and between July 6th and 25th in 1985. The dates in 2017 and 2020 also varied widely – June 3rd in 2017 and May 13th in 2020 – but in both cases were substantially earlier than any of those reported by Vaudrey.

In the Beaufort, the five studies conducted by Vaudrey from through 1985 (1982; 1983; 1984a; 1984b; 1985a; 1985b; 1986; see also Section 3.1) documented break-up dates ranging from June 27th through July 9th for lagoon ice and July 4th through July 28th for landfast ice. The average values were July 3rd and July 11th, respectively. Unfortunately, these dates are not suitable for direct comparison with those recorded in 2017 or 2020 (Section 7) due to the

"THIS INFORMATION IS DISTRIBUTED SOLELY FOR THE PURPOSE OF PRE-DISSEMINATION PEER REVIEW UNDER APPLICABLE INFORMATION QUALITY GUIDELINES. IT HAS NOT BEEN FORMALLY DISSEMINATED BY BSEE. IT DOES NOT REPRESENT AND SHOULD NOT BE CONSTRUED TO REPRESENT ANY BSEE DETERMINATION OR POLICY."

use of definitions that differ from those adopted in Section 2.2. Specific differences in the earlier studies consist of excluding through-ice melting off river mouths in determining the date of lagoon ice break-up (resulting in a later date), and the use of a smaller offshore extent for landfast ice (again, resulting in a later date for break-up).

Based on an analysis of satellite imagery, Eicken, *et al.* (2006) concluded that trends in the timing of break-up were absent in both the northeastern Chukchi and Alaskan Beaufort Seas during the period that began in 1994 and ended in 2004. However, when they compared their findings with those of Barry, *et al.* (1979), for the period from 1973 through 1977, they found that break-up was occurring between six days and one month earlier in the Chukchi, and between three weeks and six weeks earlier in the Beaufort. These wide ranges were caused by uncertainty in the interpretation of the earlier study, but it also should be noted that the break-up seasons from 1973 through 1977 were particularly cold (Table 8-1). A follow-up study conducted by Mahoney, *et al*. (2012), arrived at a similar conclusion regarding the recent past: pronounced changes in the timing of break-up were absent from both basins during the period from 1997 through 2007. These findings suggest that the timing of break-up in each basin is changing at a rate too low to be detected over the course of a single decade.

To provide additional insight into long-term changes, the dates on which break-up and open water occurred at each of 20 sites in the central Beaufort Sea in 2017 and 2020 were averaged and then compared with the average values at those sites reported by Cox and Dehn (1981) for the period from 1953 through 1975. Their study, which used a combination of ice observer flight logs, annual ice reconnaissance reports, ship reports, and low-resolution satellite imagery, derived the 10%, 50%, and 90% probabilities of occurrence of break-up and open water in terms of six-day windows. To facilitate comparisons with the dates in recent years, each six-day window was approximated by its mid-point, and the date corresponding to the 50% probability of occurrence was selected as the date on which the phenomenon of interest occurred. The dates of break-up and open water in 2017 and 2020 were derived from NIC ice charts rather than satellite imagery in the interest of replicating the coarse spatial and temporal resolution available for the earlier study. Finally, the 20 sites (Figure 8-7) were divided by location in accordance with the categories defined in Section 2.2, and the results were averaged by category to aid in the identification of trends. The breakdown is as follows:

- Beaufort Sea Lagoon Ice: Sites 2, 5, 7, 8, 12, 13, and 16;
- Beaufort Sea Landfast Ice: Sites 1, 3, 4, 6, 9, 10, 14, 17, 18, and 20;
- Beaufort Sea Pack Ice: Sites 11, 15, and 19.

The dates on which break-up and open water occurred at each site in 2017 and 2020 are displayed in accordance with these categories in Tables 8-7, 8-8, and 8-9. The tables also include the average dates at each site.

"THIS INFORMATION IS DISTRIBUTED SOLELY FOR THE PURPOSE OF PRE-DISSEMINATION PEER REVIEW UNDER APPLICABLE INFORMATION QUALITY GUIDELINES. IT HAS NOT BEEN FORMALLY DISSEMINATED BY BSEE. IT DOES NOT REPRESENT AND SHOULD NOT BE CONSTRUED TO REPRESENT ANY BSEE DETERMINATION OR POLICY."

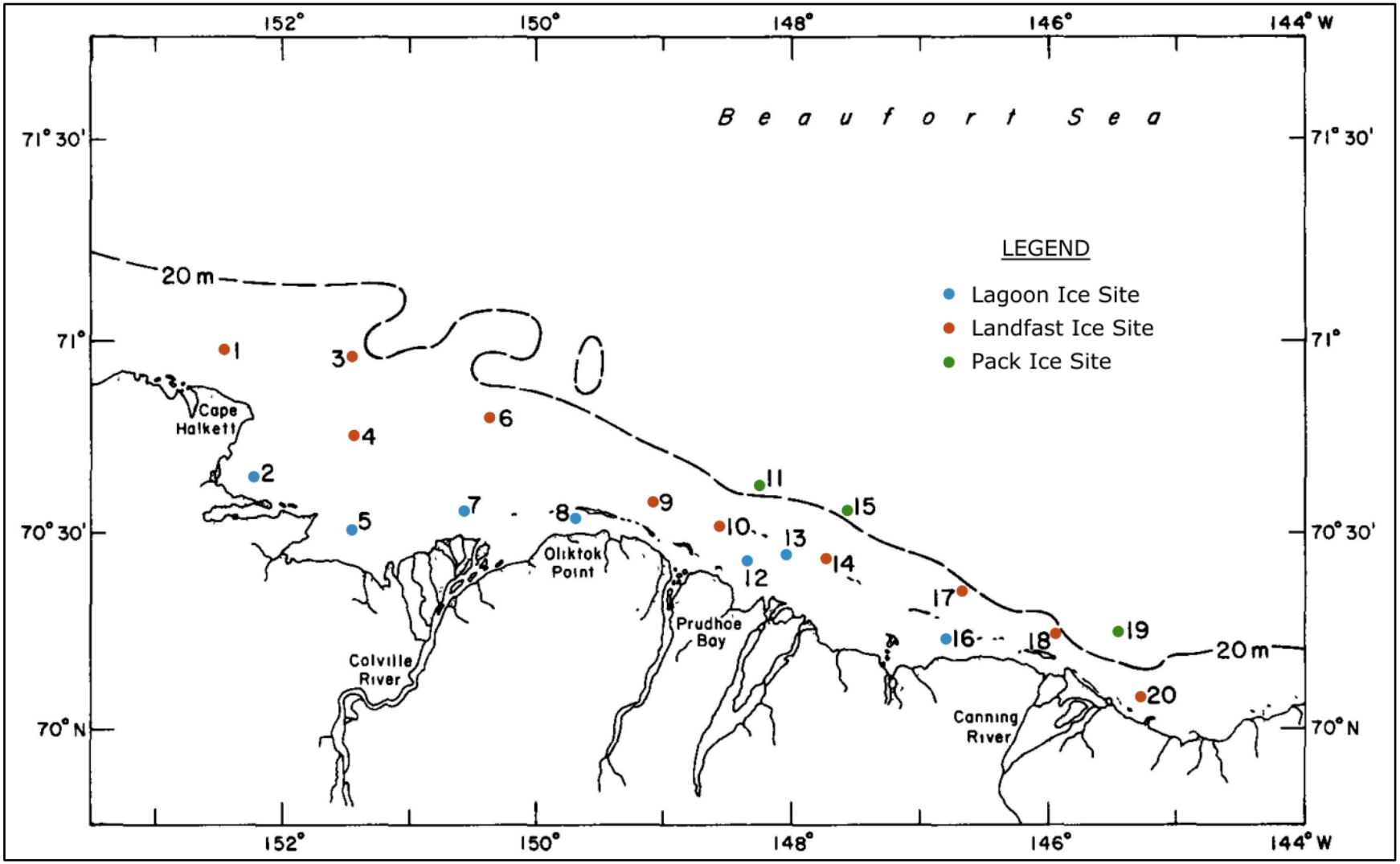

After: Cox and Dehn, 1981

Figure 8-7. Ice Analysis Sites Adopted by Cox and Dehn

"THIS INFORMATION IS DISTRIBUTED SOLELY FOR THE PURPOSE OF PRE-DISSEMINATION PEER REVIEW UNDER APPLICABLE INFORMATION QUALITY GUIDELINES. IT HAS NOT BEEN FORMALLY DISSEMINATED BY BSEE. IT DOES NOT REPRESENT AND SHOULD NOT BE CONSTRUED TO REPRESENT ANY BSEE DETERMINATION OR POLICY."

Table 8-7. Dates of Break-Up and Open Water for Beaufort Sea Lagoon Ice, 2017 and 2020

Site[1]	Break-Up, 2017[2]	Break-Up, 2020[2]	Break-Up, Average	Open Water, 2017[2]	Open Water, 2020[2]	Open Water, Average
2	Jul 6	Jun 18	Jun 27	Jul 13	Jul 16	Jul 15
5	Jul 6	Jun 18	Jun 27	Jul 6	Jul 16	Jul 11
7	Jul 6	Jul 2	Jul 4	Jul 13	Jul 2	Jul 8
8	Jul 4	Jun 18	Jun 26	Jul 6	Jul 16	Jul 11
12	Jul 3	Jul 9	Jul 6	Jul 13	Jul 16	Jul 15
13	Jul 3	Jul 9	Jul 6	Jul 13	Jul 16	Jul 15
16	Jun 30	Jul 9	Jul 5	Jul 13	Jul 23	Jul 18
Average	**Jul 4**	**Jun 29**	**Jul 2**	**Jul 11**	**Jul 15**	**Jul 13**

Notes:
[1] The site locations are shown in Figure 8-7.
[2] Data derived from NIC ice charts (2020).

Table 8-8. Dates of Break-Up and Open Water for Beaufort Sea Landfast Ice, 2017 and 2020

Site[1]	Break-Up, 2017[2]	Break-Up, 2020[2]	Break-Up, Average	Open Water, 2017[2]	Open Water, 2020[2]	Open Water, Average
1	Jul 6	Jul 9	Jul 8	Aug 3	Aug 6	Aug 5
3	Jul 6	Jun 11	Jun 24	Aug 3	Jul 30	Aug 1
4	Jul 6	Jun 11	Jun 24	Jul 27	Aug 6	Aug 1
6	Jul 6	Jun 11	Jun 24	Aug 3	Jul 16	Jul 25
9	Jul 6	Jul 9	Jul 8	Aug 3	Jul 30	Aug 1
10	Jul 6	Jul 9	Jul 8	Aug 3	Jul 16	Jul 25
14	Jun 30	Jul 9	Jul 5	Aug 3	Jul 23	Jul 29
17	Jun 1	Jun 11	Jun 6	Jul 20	Jul 16	Jul 18
18	Jun 1	Jul 2	Jun 17	Jul 20	Jul 23	Jul 22
20	Jul 6	Jul 2	Jul 4	Jul 13	Jul 16	Jul 15
Average	**Jun 28**	**Jun 26**	**Jun 27**	**Jul 28**	**Jul 24**	**Jul 26**

Notes:
[1] The site locations are shown in Figure 8-7.
[2] Data derived from NIC ice charts (2020).

"THIS INFORMATION IS DISTRIBUTED SOLELY FOR THE PURPOSE OF PRE-DISSEMINATION PEER REVIEW UNDER APPLICABLE INFORMATION QUALITY GUIDELINES. IT HAS NOT BEEN FORMALLY DISSEMINATED BY BSEE. IT DOES NOT REPRESENT AND SHOULD NOT BE CONSTRUED TO REPRESENT ANY BSEE DETERMINATION OR POLICY."

Table 8-9. Dates of Break-Up and Open Water for Beaufort Sea Pack Ice, 2017 and 2020

Site[1]	Break-Up, 2017[2]	Break-Up, 2020[2]	Break-Up, Average	Open Water, 2017[2]	Open Water, 2020[2]	Open Water, Average
11	Jun 29	Jun 11	Jun 20	Aug 3	Jul 16	Jul 25
15	Jun 1	Jun 11	Jun 6	Jul 20	Jul 16	Jul 18
19	Jun 1	Jun 11	Jun 6	Jul 20	Jun 25	Jul 8
Average	**Jun 10**	**Jun 11**	**Jun 11**	**Jul 25**	**Jul 9**	**Jul 17**

Notes:
[1] The site locations are shown in Figure 8-7.
[2] Data derived from NIC ice charts (2020).

The recent average dates for break-up and open water are compared with those for the period from 1953 through 1975 in Tables 8-10, 8-11, and 8-12. As indicated earlier, the average dates for 1953-75 correspond to the 50% probability of occurrence reported by Cox and Dean. Key findings are as follows:

Table 8-10. Average Dates of Break-Up and Open Water for Beaufort Sea Lagoon Ice, 1953-75 vs. 2017 and 2020

Site[1]	Break-Up, 1953-75[2]	Break-Up, 2017 & 2020[3]	Open-Water, 1953-75[2]	Open Water 2017 & 2020[3]
2	Jul 10	Jun 27	Jul 16	Jul 15
5	Jul 4	Jun 27	Jul 10	Jul 11
7	Jul 10	Jul 4	Jul 16	Jul 8
8	Jul 4	Jun 26	Jul 10	Jul 11
12	Jul 10	Jul 6	Jul 22	Jul 15
13	Jul 10	Jul 6	Jul 28	Jul 15
16	Jul 10	Jul 5	Jul 16	Jul 18
Average	**Jul 8**	**Jul 2**	**Jul 17**	**Jul 13**
Difference Relative to 1953-75[4]	**-**	**-6 days**	**-**	**-4 days**

Notes:
[1] The site locations are shown in Figure 8-7.
[2] Data from Cox and Dehn (1981).
[3] Data derived from NIC ice charts (2020).
[4] A negative value indicates that the date is trending earlier.

"THIS INFORMATION IS DISTRIBUTED SOLELY FOR THE PURPOSE OF PRE-DISSEMINATION PEER REVIEW UNDER APPLICABLE INFORMATION QUALITY GUIDELINES. IT HAS NOT BEEN FORMALLY DISSEMINATED BY BSEE. IT DOES NOT REPRESENT AND SHOULD NOT BE CONSTRUED TO REPRESENT ANY BSEE DETERMINATION OR POLICY."

Table 8-11. Average Dates of Break-Up and Open Water for Beaufort Sea Landfast Ice, 1953-75 vs. 2017 and 2020

Site[1]	Break-Up, 1953-75[2]	Break-Up, 2017 & 2020[3]	Open-Water, 1953-75[2]	Open Water 2017 & 2020[3]
1	Jul 4	Jul 8	Aug 15	Aug 5
3	Jul 4	Jun 24	Sep 2	Aug 1
4	Jul 10	Jun 24	Aug 15	Aug 1
6	Jul 4	Jun 24	Aug 21	Jul 25
9	Jul 10	Jul 8	Aug 9	Aug 1
10	Jul 10	Jul 8	Aug 3	Jul 25
14	Jul 10	Jul 5	Aug 3	Jul 29
17	Jul 10	Jun 6	Aug 9	Jul 18
18	Jul 4	Jun 17	Aug 15	Jul 22
20	Jul 10	Jul 4	Jul 28	Jul 15
Average	**Jul 8**	**Jun 27**	**Aug 12**	**Jul 26**
Difference Relative to 1953-75[4]	**-**	**-11 days**	**-**	**-17 days**

Notes:
1 The site locations are shown in Figure 8-7.
2 Data from Cox and Dehn (1981).
3 Data derived from NIC ice charts (2020).
4 A negative value indicates that the date is trending earlier.

Table 8-12. Average Dates of Break-Up and Open Water for Beaufort Sea Pack Ice, 1953-75 vs. 2017 and 2020

Site[1]	Break-Up, 1953-75[2]	Break-Up, 2017 & 2020[3]	Open-Water, 1953-75[2]	Open Water 2017 & 2020[3]
11	Jul 4	Jun 20	Aug 27	Jul 25
15	Jul 4	Jun 6	Aug 27	Jul 18
19	Jul 4	Jun 6	Aug 21	Jul 8
Average	**Jul 4**	**Jun 11**	**Aug 25**	**Jul 17**
Difference Relative to 1953-75[4]	**-**	**-23 days**	**-**	**-39 days**

Notes:
1 The site locations are shown in Figure 8-7.
2 Data from Cox and Dehn (1981).
3 Data derived from NIC ice charts (2020).
4 A negative value indicates that the date is trending earlier.

"THIS INFORMATION IS DISTRIBUTED SOLELY FOR THE PURPOSE OF PRE-DISSEMINATION PEER REVIEW UNDER APPLICABLE INFORMATION QUALITY GUIDELINES. IT HAS NOT BEEN FORMALLY DISSEMINATED BY BSEE. IT DOES NOT REPRESENT AND SHOULD NOT BE CONSTRUED TO REPRESENT ANY BSEE DETERMINATION OR POLICY."

- Beaufort Sea Break-Up: Break-up occurred, on average, six days earlier for the lagoon ice, 11 days earlier for the landfast ice, and 23 days earlier for the pack ice;
- Beaufort Sea Open-Water: Open water occurred, on average, four days earlier for the lagoon ice, 17 days earlier for the landfast ice, and 39 days earlier for the pack ice.

In the case of the lagoon ice, the results for both break-up and open water should be regarded with caution in that the apparent change is less than or equal to the length of the six-day reporting period adopted by Cox and Dehn. As a result, these relatively small changes may not be statistically significant.

In the case of both the landfast ice and the pack ice, the advance in the timing of open water relative to 1953-75 was greater than the advance in the timing of break-up. As a result, the average duration of the two recent break-up seasons (break-up to open water) was shorter than that which prevailed during the period studied by Cox and Dehn. This outcome contrasts with the trend toward longer freeze-up seasons documented in recent years in both the Beaufort and Chukchi Seas. As discussed by Coastal Frontiers and Vaudrey (2020), the duration of freeze-up (first ice to nearshore freeze-up) is increasing at an average rate of 1.0 days per year in the Beaufort and 1.9 days per year in the Chukchi.

Also noteworthy is an apparent correlation between the ice type and the magnitude of the changes in the timing of break-up and open water. The greatest changes were associated with the pack ice (-23 days for break-up and -39 days for open water; Table 8-12), lesser changes with the landfast ice (-11 and -17 days; Table 8-11), and insignificant changes with the lagoon ice (-6 and -4 days; Table 8-10). This trend, if substantiated in future years, implies that factors like increased storminess (Section 8.2) and reduced multi-year ice concentrations (Section 8.6), the impact of which increases with distance offshore, are altering the nature of break-up more than the timing of river overflood, the impact of which decreases with distance offshore.

Trend: In the northeast Chukchi Sea, the occurrence of break-up appears to be trending earlier. The rate of change cannot be quantified, however, due to the variability inherent in the timing coupled with a paucity of both historical and recent data. In the Alaskan Beaufort Sea, a comparison of the data acquired in 2017 and 2020 with those from 1953 through 1975 suggest that both break-up and open water are trending earlier, with the occurrence of open water advancing more rapidly than that of break-up. As a result, the duration of the break-up season appears to be decreasing. In addition, the rates of change in the timing of both break-up and open water appear to be highest for pack ice, intermediate for landfast ice, and

"THIS INFORMATION IS DISTRIBUTED SOLELY FOR THE PURPOSE OF PRE-DISSEMINATION PEER REVIEW UNDER APPLICABLE INFORMATION QUALITY GUIDELINES. IT HAS NOT BEEN FORMALLY DISSEMINATED BY BSEE. IT DOES NOT REPRESENT AND SHOULD NOT BE CONSTRUED TO REPRESENT ANY BSEE DETERMINATION OR POLICY."

insignificant for lagoon ice. It is cautioned, however, that additional data will be required to substantiate and refine these preliminary results.

8.5. Length of Open-Water Season

Since 2009-10, the timing of nearshore freeze-up has trended later at a rate of +4.6 days per year in the Chukchi and +2.3 days per year in the Alaskan Beaufort (Figure 8-8; Coastal Frontiers and Vaudrey, 2020). These changes, when coupled with the earlier occurrence of break-up described in Section 8.4, suggest that the length of the open-water season is increasing at a rapid rate -- a conclusion supported by the research of Rodrigues (2009), who found that the length of the ice-free season between Point Barrow and Point Lay increased from approximately 30 days in the 1970s to 125 days in the early 2000s.

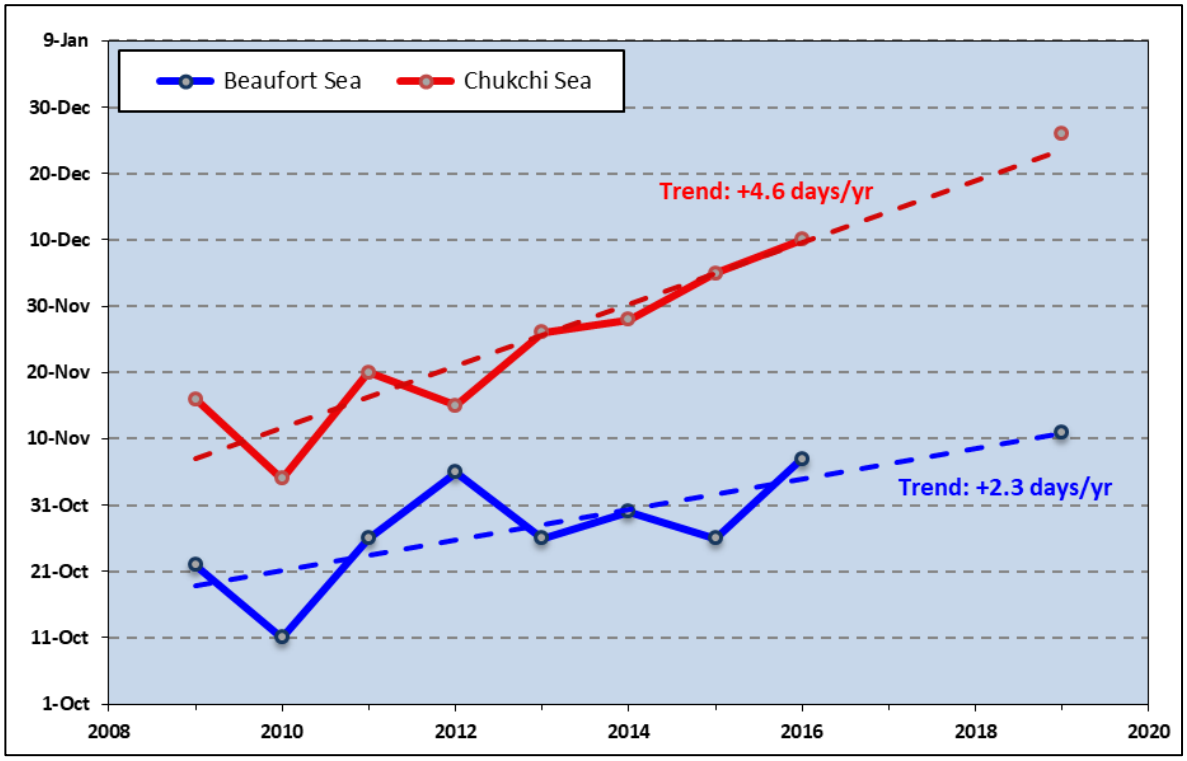

Source: Coastal Frontiers and Vaudrey, 2020

Figure 8-8 Timing of Nearshore Freeze-Up in Alaskan Beaufort and Chukchi Seas, 2009-2019

Trend: Trends toward an earlier occurrence of break-up and a later occurrence of freeze-up are causing the length of the open-water season to increase at rapid rates in both the Chukchi and Beaufort Seas.

"THIS INFORMATION IS DISTRIBUTED SOLELY FOR THE PURPOSE OF PRE-DISSEMINATION PEER REVIEW UNDER APPLICABLE INFORMATION QUALITY GUIDELINES. IT HAS NOT BEEN FORMALLY DISSEMINATED BY BSEE. IT DOES NOT REPRESENT AND SHOULD NOT BE CONSTRUED TO REPRESENT ANY BSEE DETERMINATION OR POLICY."
"THIS INFORMATION IS DISTRIBUTED SOLELY FOR THE PURPOSE OF PRE-DISSEMINATION PEER REVIEW UNDER APPLICABLE INFORMATION QUALITY GUIDELINES. IT HAS NOT BEEN FORMALLY DISSEMINATED BY BSEE. IT DOES NOT REPRESENT AND SHOULD NOT BE CONSTRUED TO REPRESENT ANY BSEE DETERMINATION OR POLICY.""THIS INFORMATION IS DISTRIBUTED SOLELY FOR THE PURPOSE OF PRE-DISSEMINATION PEER REVIEW UNDER APPLICABLE INFORMATION QUALITY GUIDELINES. IT HAS NOT BEEN FORMALLY DISSEMINATED BY BSEE. IT DOES NOT REPRESENT AND SHOULD NOT BE CONSTRUED TO REPRESENT ANY BSEE DETERMINATION OR POLICY."EER REVIEW UNDER APPLICABLE FORMALLY DISSEMINATED BY BSEE. IT DOES NOT REPRESENT AND SHOULD NOT BE CONSTRUED TO REPRESENT ANY BSEE DETERMINATION OR POLICY."

8.6 Multi-Year Ice

Two types of multi-year ice can occur in the Beaufort and Chukchi Seas: (1) true multi-year floes from the permanent polar pack ("pack floes"), and (2) second-year floes that develop when grounded fragments of thick first-year features survive the summer months due to factors that may include cold air temperatures and mild winds. As indicated in Section 2.2, the term "multi-year ice" is used to refer to both pack floes and second-year floes in this study.

Multi-year ice floes were present in the northeast Chukchi Sea during each of the three break-up seasons from 1983 through 1985 (Vaudrey, 1984a; 1984b; 1985a; 1985b; 1986; see also Section 3.1). Some were grounded or trapped in the landfast ice zone, while others remained adrift. The concentrations typically ranged from less than 10% to 50%, but grounded fragments attained local concentrations as high as 80%.

Multi-year ice remained absent from the Chukchi Sea during the 2017 break-up season (Coastal Frontiers and Vaudrey, 2018) but was present throughout the 2020 break-up season (Section 6). Although these findings are inconclusive, the reduced frequency of multi-year ice invasions during freeze-up and mid-winter noted in recent years (Ward, *et al*., 2015; Coastal Frontiers and Vaudrey, 2020) suggests that the probability of multi-year ice residing in the Chukchi Sea during break-up is lower than in the 1980s. Factors contributing to the decline are likely to include a reduction in the amount of multi-year ice comprising the permanent polar pack (Perovich, *et al*., 2013) and an increase in the northerly retreat of the ice edge during the summer months, both of which have reduced the opportunities for pack floes to enter the Chukchi. In addition, warmer air temperatures, longer open-water seasons, and increased storminess have decreased the likelihood that first-year ridges and rubble will survive the summer melt season to become second-year floes of any consequence. Nevertheless, as demonstrated in 2020, the possibility of encountering multi-year floes in the Chukchi during break-up cannot be dismissed.

A similar situation prevailed in the nearshore region of the Beaufort, where multi-year ice was present during each of the five break-up seasons from 1981 through 1985 (Vaudrey, 1984a; 1984b; 1985a; 1985b; 1986; see also Section 3.1), absent in 2017 (Section 7), and present in 2020. The frequency of multi-year ice invasions during freeze-up and mid-winter has declined to an even greater degree than in the Chukchi (Coastal Frontiers and Vaudrey, 2020), suggesting that the probability of multi-year ice residing in the nearshore portion of the Beaufort during break-up is substantially lower than in the 1980s.

"THIS INFORMATION IS DISTRIBUTED SOLELY FOR THE PURPOSE OF PRE-DISSEMINATION PEER REVIEW UNDER APPLICABLE INFORMATION QUALITY GUIDELINES. IT HAS NOT BEEN FORMALLY DISSEMINATED BY BSEE. IT DOES NOT REPRESENT AND SHOULD NOT BE CONSTRUED TO REPRESENT ANY BSEE DETERMINATION OR POLICY."

Trend: The probability of multi-year ice residing in the Chukchi Sea and nearshore portion of the Beaufort Sea during break-up appears to have decreased since the 1980s. Nevertheless, as demonstrated in 2020, the possibility of encountering such ice cannot be dismissed.

"THIS INFORMATION IS DISTRIBUTED SOLELY FOR THE PURPOSE OF PRE-DISSEMINATION P"THIS INFORMATION IS DISTRIBUTED SOLELY FOR THE PURPOSE OF PRE-DISSEMINATION PEER REVIEW UNDER APPLICABLE INFORMATION QUALITY GUIDELINES. IT HAS NOT BEEN FORMALLY DISSEMINATED BY BSEE. IT DOES NOT REPRESENT AND SHOULD NOT BE CONSTRUED TO REPRESENT ANY BSEE DETERMINATION OR POLICY." PEER REVIEW UNDER APPLICABLE
FORMALLY DISSEMINATED BY BSEE. IT DOES NOT REPRESENT AND SHOULD NOT BE
CONSTRUED TO REPRESENT ANY BSEE DETERMINATION OR POLICY."

9. SUMMARY AND CONCLUSIONS

Methods

1. ***Reconnaissance Flights:*** Reconnaissance flights provide invaluable opportunities to confirm and refine the data derived from remote sensing, and to identify small-scale features and processes that otherwise would escape detection. Conducting the flights in the Chukchi several weeks before those in the Beaufort, with the timing dictated by the progress of break-up in each basin, represented a substantial improvement in 2020 over 2017, when all of the break-up flights were undertaken in rapid succession (Coastal Frontiers and Vaudrey, 2018).

Chukchi Sea

1. ***Air Temperatures:*** The daily average air temperatures at Utqiagvik Airport remained within or close to the normal range throughout May, June, and July. Over the entire three-month period, the daily average values exceeded the normal range on 13 days (14% frequency) and fell below on six days (7% frequency). Although six of the ten warmest break-up seasons occurred during the past decade, 2020 was relatively cold, ranking 35th out of the past 51 years in terms of the number of TDD.

2. ***Wind Regime:*** Easterlies outnumbered westerlies by substantial margins in each of the three months from May through July. Over the entire period, easterlies occurred 77% of the time versus 23% for westerlies. The monthly average speeds were nearly constant, with values of 11 kt (6 m/s) in May and July, and 10 kt (5 m/s) in June.

3. ***Storm Events:*** The 2020 break-up season was relatively storm-free, in that storm events with daily average wind speeds exceeding 15 kt (8 m/s) occurred on only four occasions encompassing 11 days. Three of the storms were easterlies, with an average duration of 2.7 days/event, while one was a westerly with a duration of three days.

4. ***Ice Thickness:*** TDD began to accumulate on May 29th, when the daily average air temperature at Utqiagvik Airport reached 33°F (1°C). The computed thickness of undeformed first-year ice at the end of the winter season, 148 cm, decreased to zero during the 59-day period that began on that date and ended with the accumulation of 297 TDD on July 26th.

5. ***Coastal Flaw Lead:*** A narrow flaw lead that existed off the Chukchi Sea coast at the end of April expanded throughout May, evolving into a large expanse of open water that was approximately 15 nm (37 km) wide off Point Barrow and 85 nm (158 km) wide off Point Lay at month-end. It continued to expand in June and July.

"THIS INFORMATION IS DISTRIBUTED SOLELY FOR THE PURPOSE OF PRE-DISSEMINATION PEER REVIEW UNDER APPLICABLE INFORMATION QUALITY GUIDELINES. IT HAS NOT BEEN FORMALLY DISSEMINATED BY BSEE. IT DOES NOT REPRESENT AND SHOULD NOT BE CONSTRUED TO REPRESENT ANY BSEE DETERMINATION OR POLICY."

6. ***River Overflood:*** Of the seven rivers that discharge in or adjacent to the Chukchi Sea study area, the first began overflooding the sea ice on May 12th and the last on June 1st. Most of the flood water was contained in the receiving lagoons, with minimal penetration onto the landfast ice farther offshore.

7. ***Lagoon Ice:*** Break-up in the semi-protected lagoon areas began with South Kasegaluk Lagoon on May 23rd, continued with North Kasegaluk Lagoon and the Kuk River Entrance on June 10th, and concluded with Peard Bay on June 14th. Open water followed in South Kasegaluk Lagoon on June 20th, North Kasegaluk Lagoon on June 27th or 28th, the Kuk River Entrance between June 25th and 30th, and Peard Bay on July 7th.

8. ***Landfast Ice:*** Break-up of the landfast ice occurred on May 13th when an easterly storm dislodged a large piece from the region between Wainwright and Icy Cape, and smaller pieces from the region between Icy Cape and Point Lay. Intermittent losses followed during the remainder of May and first half of June, including a massive piece measuring 74 km long and 19 km wide that broke free from the region between Point Franklin and Utqiagvik. The rate of loss increased in mid-June in response to moderate northeasterly winds and warm air temperatures. At the beginning of July, the landfast ice that remained consisted of intermittent patches spanning the entire length of the study area. The last remnant, grounded off the base of the Point Franklin Spit, disappeared on July 16th or 17th.

9. ***Pack Ice:*** The pack ice retreated to the northwest at a relatively rapid rate in May, causing the southern edge to lie approximately 15 nm (37 km) off Point Barrow and 85 nm (158 km) off Point Lay at month-end. Although the retreat continued in June, it proceeded at a slower pace that reflected occasional reversals. The ice continued to dissipate in July, vacating the Siberian coast during the third week of the month. At the end of July, the southern edge trended northwest from the vicinity of Utqiagvik with the exception of a 50-nm (93-km) wide tongue that extended southwest as far as the Devil's Paw Prospects.

10. ***Ice Pile-Ups and Ride-Ups:*** Of the 57 ice pile-ups observed on the Chukchi Sea coast in late February, 53 were evident at the time of the break-up flights in mid-June. In addition to these relict features, five new pile-ups that had formed during break-up were identified. Two were located on the barrier islands between Point Lay and Icy Cape, while three were located on the mainland shore near the base of the Point Franklin Spit. The heights of the new pile-ups ranged from 2 to 5 m above sea level, the encroachment distances from 3 to 5 m onto the subaerial beach, and the alongshore lengths from 600 to 2,800 m.

"THIS INFORMATION IS DISTRIBUTED SOLELY FOR THE PURPOSE OF PRE-DISSEMINATION PEER REVIEW UNDER APPLICABLE INFORMATION QUALITY GUIDELINES. IT HAS NOT BEEN FORMALLY DISSEMINATED BY BSEE. IT DOES NOT REPRESENT AND SHOULD NOT BE CONSTRUED TO REPRESENT ANY BSEE DETERMINATION OR POLICY."

11. ***Multi-Year Ice:*** Multi-year ice was present in the Chukchi Sea study area throughout the break-up study period. At the beginning of May, relatively small floes were embedded in the landfast ice at concentrations ranging from negligible to 20%. The dispersal of these floes mirrored the break-up of the landfast ice, commencing in mid-May and continuing through mid-July. Multi-year ice also was present in the pack ice, at concentrations ranging from negligible to 30%. The maximum horizontal dimensions of these floes varied from less than 10 m to more than 10 km.

12. ***Ice Drift:*** Two drift buoys embedded in the pack ice attained monthly average speeds of 7.8 and 8.5 nm/day (14.5 and 15.8 km/day) in July. The highest daily average speed, 13.8 nm/day (25.6 km/day), occurred on July 8th.

Beaufort Sea

1. ***Air Temperatures:*** The daily average air temperatures at Deadhorse Airport tended to fall within the normal range throughout the three-month study period, rising above on ten occasions (11% frequency) and dropping below on four (4% frequency). When excursions outside the normal range did occur, they were of limited extent and duration.

2. ***Wind Regime:*** As in the case of the Chukchi, easterly winds predominated by a substantial margin in each of the three months from May through July. Over the entire period, they outnumbered westerlies by a margin of 79% to 21%. The average monthly speeds decreased from 13 kt (7 m/s) in May to 12 kt (6 m/s) in June and 9 kt (5 m/s) in July.

3. ***Storm Events:*** Only four storm events took place during the study period, all of which were easterlies. They produced 18 storm-days, resulting in an average duration of 4.5 days/event.

4. ***Ice Thickness:*** TDD began to accumulate on May 23rd, when the daily average air temperature reached 33°F (1°C) at Deadhorse Airport. The computed thickness of undeformed first-year ice at the end of the winter season, 162 cm, decreased to zero during the 47-day period that began on that date and ended with the accumulation of 319 TDD on July 8th.

5. ***River Overflood:*** The Canning and Sagavanirktok began overflooding the sea ice on May 19th, the Colville on May 22nd, the Kuparuk on May 27th, and the Ikpikpuk on May 29th. Most of the flood water remained in the receiving bays and lagoons. The sole exceptions consisted of the discharge of the Canning River onto the sea ice east of Brownlow Point, and small tongues of water from the Kuparuk that pushed past the barrier islands off Gwydyr Bay.

"THIS INFORMATION IS DISTRIBUTED SOLELY FOR THE PURPOSE OF PRE-DISSEMINATION PEER REVIEW UNDER APPLICABLE INFORMATION QUALITY GUIDELINES. IT HAS NOT BEEN FORMALLY DISSEMINATED BY BSEE. IT DOES NOT REPRESENT AND SHOULD NOT BE CONSTRUED TO REPRESENT ANY BSEE DETERMINATION OR POLICY."

6. ***Lagoon Ice:*** Break-up of the lagoon ice began on or about June 4th when flood water from the Sagavanirktok River melted through the ice in Prudhoe Bay. Through-ice melting followed in Stefansson Sound, South Harrison Bay, South Camden Bay, Gwydyr Bay, and Smith Bay between June 8th and 11th. In Simpson Lagoon, break-up took place on or about June 26th in response to the heat emanating from the mainland coast. Open water in the lagoon areas occurred over a period of several weeks that began with Gwydyr Bay between June 20th and 26th and ended with Stefansson Sound on July 10th. All of the lagoon sites were ice-free by the end of July.

7. ***Landfast Ice:*** Break-up of the landfast ice between Point Barrow and Cross Island occurred on May 23rd when a small loss occurred off Cape Halkett at the end of a six-day easterly storm. Farther east, between Cross Island and Barter Island, break-up began with modest losses off Stefansson Sound and Camden Bay on May 27th. In early June, the landfast ice edge tended to lie between the 18- and 11-m isobaths from Point Barrow to Flaxman Island, and to protrude seaward of the 18-m isobath in Camden Bay. In the absence of westerly storms, losses were minimal until the last week of the month. At that time, warm air temperatures, increased wind speeds, and warm sea surface temperatures resulting both from river overflood and from the arrival of warm-water plumes from the Alaska Coastal Current to the west and Mackenzie River to the east, caused substantial losses off Smith Bay and in Harrison and Camden Bays. The accelerated rate of deterioration continued during the first half of July. By mid-month, landfast ice was confined to a patch in Elson Lagoon, narrow strips on both sides of Smith Bay, small patches on the west side of Harrison Bay, and a narrow, discontinuous strip fronting the barrier islands from Cross to Flaxman. At the end of the month, small patches persisted between Pole and Flaxman Islands.

8. ***Pack Ice:*** The pack ice remained compact during the first three weeks of May. At month-end, however, warm water from the Alaska Coastal Current produced patches of open water adjacent to the landfast ice as far east as Harrison Bay. In analogous fashion, warm water from the Mackenzie River created a patch of open water adjacent to the landfast ice in Camden Bay. In June, unrelenting easterly winds propelled the Mackenzie plume to the west while impeding the easterly progress of the plume from the Alaska Coastal Current. During the final week, the pack ice concentrations in the nearshore region declined markedly in response to the westward progression of the Mackenzie plume to Harrison Bay and the eastern progression of the Alaska Coastal Current plume to Smith Bay. At the end of the month, the only two areas in which dense tongues of pack ice extended as far south as the landfast ice were located off western Harrison Bay and off Admiralty Bay. The deterioration continued in July, with the dense tongues dispersing by mid-month.

"THIS INFORMATION IS DISTRIBUTED SOLELY FOR THE PURPOSE OF PRE-DISSEMINATION PEER REVIEW UNDER APPLICABLE INFORMATION QUALITY GUIDELINES. IT HAS NOT BEEN FORMALLY DISSEMINATED BY BSEE. IT DOES NOT REPRESENT AND SHOULD NOT BE CONSTRUED TO REPRESENT ANY BSEE DETERMINATION OR POLICY."

9. ***Ice Pile-Ups and Ride-Ups:*** Of the 32 ice pile-ups observed in the central portion of the Alaskan Beaufort Sea in late February, 16 were evident at the time of the break-up flights in early July. In all cases, the dimensions of the relict pile-ups had been diminished by melting. No new pile-ups or ride-ups were discovered during the flights in July.

10. ***Multi-Year Ice:*** Multi-year ice was present in the Beaufort Sea study area throughout the break-up study period. At the beginning of May, the concentration tended to be less than 10% in the landfast ice and to range from less than 10% to 50% in the pack ice. The only region lacking multi-year ice was a tongue of first-year ice that extended from the U.S.-Canadian border to the eastern edge of Harrison Bay just offshore of the landfast ice. The multi-year ice embedded in the landfast ice remained in place until late May, when losses began to occur in conjunction with the disintegration of the latter. The dispersal of the embedded multi-year ice paralleled that of the landfast ice, which continued through the end of the study period. With the exception of the nearshore tongue of first-year ice, which closed during the first week in June, multi-year ice remained omnipresent in the pack ice through the end of July. The concentrations ranged from less than 10% to a maximum of 70%. The floe sizes varied over a wide range, from brash ice to maximum horizontal dimensions exceeding 25 km.

11. ***Ice Drift:*** Drift buoys embedded in the pack ice attained monthly average speeds that averaged 5.4 nm/day (10.0 km/day) in May, 4.3 nm/day (8.0 km/day) in June, and 2.9 nm/day (5.4 km/day) in July. The highest daily average speed, 15.4 nm/day (28.5 km/day), occurred on both May 12th and July 28th.

Trends

1. ***Air Temperatures:*** Since the 1970s, progressively warmer break-up seasons have caused the number of accumulated thawing-degree days at Utqiagvik to increase at an average rate of 4.2 per year. The rate of warming has varied widely, however, on time scales ranging from interannual to interdecadal.

2. ***Storms:*** Since the early 1980s, the frequency of storm events during break-up has nearly doubled, from 3.2 to 5.8 storms per year.

3. ***River Overflood:*** The limited data available suggest that the initiation of river overflood onto the sea ice in the Chukchi and Beaufort Seas has been trending earlier at rates ranging from negligible to less than one day per year.

4. ***Timing of Break-Up in the Chukchi Sea:*** The occurrence of break-up appears to be trending earlier, but the rate of change cannot be quantified due to the variability inherent in the timing coupled with a paucity of both historical and recent data.

"THIS INFORMATION IS DISTRIBUTED SOLELY FOR THE PURPOSE OF PRE-DISSEMINATION PEER REVIEW UNDER APPLICABLE INFORMATION QUALITY GUIDELINES. IT HAS NOT BEEN FORMALLY DISSEMINATED BY BSEE. IT DOES NOT REPRESENT AND SHOULD NOT BE CONSTRUED TO REPRESENT ANY BSEE DETERMINATION OR POLICY."

5. ***Timing of Break-Up in the Beaufort Sea:*** The data acquired in 2017 and 2020, when compared with those from 1953 through 1975, suggest that both break-up and open water are trending earlier, with the occurrence of open water advancing more rapidly than that of break-up. As a result, the duration of the break-up season appears to be decreasing. The rates of change in the timing of break-up and open water appear to be highest for pack ice, intermediate for landfast ice, and insignificant for lagoon ice. It is cautioned, however, that additional data will be required to substantiate and refine these preliminary findings.

6. ***Length of Open-Water Season:*** Trends toward an earlier occurrence of break-up and a later occurrence of freeze-up are causing the length of the open-water season to increase at rapid rates in both the Chukchi and Beaufort Seas.

7. ***Multi-Year Ice:*** The probability of multi-year ice residing in the Chukchi Sea and nearshore portion of the Beaufort Sea during break-up appears to have decreased since the 1980s. Nevertheless, the possibility of encountering such ice cannot be dismissed.

"THIS INFORMATION IS DISTRIBUTED SOLELY FOR THE PURPOSE OF PRE-DISSEMINATION PEER REVIEW UNDER APPLICABLE INFORMATION QUALITY GUIDELINES. IT HAS NOT BEEN FORMALLY DISSEMINATED BY BSEE. IT DOES NOT REPRESENT AND SHOULD NOT BE CONSTRUED TO REPRESENT ANY BSEE DETERMINATION OR POLICY."

10. REFERENCES

Arguez, A., I. Durre, S. Applequist, M. Squires, R. Vose, X. Yin, and R. Bilotta, 2010, "NOAA's U.S. Climate Normals (1981-2010)", NOAA National Climatic Data Center, 2015, http://www.ncdc.noaa.gov/cdo-web/datatools/normals.

Bailey, A., 2012, "Starting and stopping Shell begins Chukchi drilling, then suspends operation because of ice floe", Petroleum News, vol. 1, no. 38, http://www.petroleumnews.com/pntruncate/892105677.shtml.

Burris, J., 2020, personal communication, Hilcorp North Slope, LLC, Prudhoe Bay, Alaska.

Barrett, S.A. and W.J. Stringer, 1978, "Growth Mechanisms of Katie's Floeberg", *Arctic and Alpine Research*, Vol. 10, No. 4, pp.775-783.

Barry, R.G., R.E. Moritz, and J.C. Rogers, 1979, "The Fast Ice Regimes of the Beaufort and Chukchi Sea Coasts", *Cold Regions Science and Technology*, Vol. 1, pp. 129-152.

Bilello, M., 1960, "Formation, Growth, and Decay of Sea Ice in the Canadian Arctic Archipelago", SIPRE Research Report 65, Hanover, New Hampshire.

Bilello, M., 1980, "Formation, Growth, and Decay of Lake, River, and Fast Sea Ice in Canada and Alaska", CRREL Report 80-6, Hanover, New Hampshire.

Bureau of Ocean Energy Management, 2020, Environmental Studies Program: Ongoing Study, "Landfast Ice Climatology within the Arctic OCS (AK-19-03)", https://www.boem.gov/sites/default/files/documents/newsroom/PO_AK-19-03_1.pdf.

Canadian Ice Service, 2020, Ice Forecast and Observations, https://www.canada.ca/en/environment-climate-change/services/ice-forecasts-observations.html.

Coastal Frontiers Corporation, 2011, "2011 River Overflood and Ice Encroachment in the Northeast Chukchi Sea", report prepared for Shell Offshore, Inc., Chatsworth, California, 26 pp. + appen.

Coastal Frontiers Corporation, 2014, "2014 Chukchi Sea River Overflood Mapping", Memorandum from Greg Hearon to Michael Coyne, Shell Exploration and Production Company, Chatsworth, California, 14 pp.

Coastal Frontiers Corporation, 2015, "Northstar Development 2014 Pipeline Route Monitoring Program", report prepared for BP Exploration (Alaska) Inc., Moorpark, California, 64 pp. + appen.

"THIS INFORMATION IS DISTRIBUTED SOLELY FOR THE PURPOSE OF PRE-DISSEMINATION PEER REVIEW UNDER APPLICABLE INFORMATION QUALITY GUIDELINES. IT HAS NOT BEEN FORMALLY DISSEMINATED BY BSEE. IT DOES NOT REPRESENT AND SHOULD NOT BE CONSTRUED TO REPRESENT ANY BSEE DETERMINATION OR POLICY."

Coastal Frontiers Corporation and Vaudrey and Associates, Inc., 2010, "2009-10 Freeze-Up Study of the Alaskan Beaufort and Chukchi Seas", Joint Industry Project performed for Shell International Exploration and Production, Inc., and the U.S. Minerals Management Service, Chatsworth, California, 100 pp. + appen.

Coastal Frontiers Corporation and Vaudrey and Associates, Inc., 2011, "2010-11 Freeze-Up Study of the Alaskan Beaufort and Chukchi Seas", Joint Industry Project performed for Shell Offshore, Inc., and Bureau of Ocean Energy Management, Regulation, and Enforcement, U.S. Dept. of the Interior, Chatsworth, California, 149 pp. + appen.

Coastal Frontiers Corporation and Vaudrey and Associates, Inc., 2012, "2011-12 Freeze-Up Study of the Alaskan Beaufort and Chukchi Seas", Joint Industry Project performed for Shell International Exploration and Production, Inc., and Bureau of Safety and Environmental Enforcement, U.S. Dept. of the Interior, Chatsworth, California, 182 pp. + appen.

Coastal Frontiers Corporation and Vaudrey and Associates, Inc., 2013 (revised January 2014), "2012-13 Freeze-Up Study of the Alaskan Beaufort and Chukchi Seas", Joint Industry Project performed for Shell Gulf of Mexico Inc. and Shell Offshore Inc., Statoil Petroleum AS, and Bureau of Safety and Environmental Enforcement, U.S. Dept. of the Interior, Moorpark, California, 175 pp. + appen.

Coastal Frontiers Corporation and Vaudrey and Associates, Inc., 2014, "2013-14 Freeze-Up Study of the Alaskan Beaufort and Chukchi Seas", Joint Industry Project performed for Shell Gulf of Mexico Inc. and Shell Offshore Inc., and Bureau of Safety and Environmental Enforcement, U.S. Dept. of the Interior, Moorpark, California, 185 pp. + appen.

Coastal Frontiers Corporation and Vaudrey and Associates, Inc., 2015, "2014-15 Freeze-Up Study of the Alaskan Beaufort and Chukchi Seas", Joint Industry Project performed for Shell Offshore Inc. and Bureau of Safety and Environmental Enforcement, U.S. Dept. of the Interior, Moorpark, California, 200 pp. + appen.

Coastal Frontiers Corporation and Vaudrey and Associates, Inc., 2016, "2015-16 Freeze-Up Study of the Alaskan Beaufort and Chukchi Seas", Joint Industry Project performed for Shell Offshore Inc. and Bureau of Safety and Environmental Enforcement, U.S. Dept. of the Interior, Moorpark, California, 203 pp. + appen.

Coastal Frontiers Corporation and Vaudrey and Associates, Inc., 2017, "2016-17 Freeze-Up Study of the Alaskan Beaufort and Chukchi Seas", report prepared for Bureau of Safety and Environmental Enforcement, U.S. Dept. of the Interior, Moorpark, California, 180 pp. + appen.

"THIS INFORMATION IS DISTRIBUTED SOLELY FOR THE PURPOSE OF PRE-DISSEMINATION PEER REVIEW UNDER APPLICABLE INFORMATION QUALITY GUIDELINES. IT HAS NOT BEEN FORMALLY DISSEMINATED BY BSEE. IT DOES NOT REPRESENT AND SHOULD NOT BE CONSTRUED TO REPRESENT ANY BSEE DETERMINATION OR POLICY."

Coastal Frontiers Corporation and Vaudrey and Associates, Inc., 2018, "2017 Break-Up Study of the Alaskan Beaufort and Chukchi Seas", report prepared for Bureau of Safety and Environmental Enforcement, U.S. Dept. of the Interior, Moorpark, California, 143 pp. + appen.

Coastal Frontiers Corporation and Vaudrey and Associates, Inc., 2020, "2019-20 Freeze-Up Study of the Alaskan Beaufort and Chukchi Seas", report prepared for Bureau of Safety and Environmental Enforcement, U.S. Dept. of the Interior, Moorpark, California, 194 pp. + appen.

Cox, G.F. and W.S. Dehn, 1981, "Summer Ice Conditions in the Prudhoe Bay Area, 1953-75", *Proc. Sixth International Conference on Port and Ocean Engineering under Arctic Conditions*, Vol. 2, Quebec, Canada, pp. 799-808.

Eicken, H., L. Shapiro, A. Gaylord, A. Mahoney, and P. Cotter, 2006, "Mapping and Characteristics of Recurring Spring Leads and Landfast Ice in the Beaufort and Chukchi Seas", OCS Study MMS 2005-068, U.S. Department of the Interior, Mineral Management Service, Alaska Outer Continental Shelf Region, Anchorage, Alaska.

EC, 2020, Aviation, Marine, Ice and Other Weather Services, https://www.canada.ca/en/services/environment/weather/other-services.html.

GINA, 2020, GINA Alaska Direct Broadcast Satellite Data Portal, feeder.gina.alaska.edu.

Hearon, G., D. Dickins, K. Ambrosius, and K. Morris, 2009, "Mapping Sea Ice Overflood Using Remote Sensing: Smith Bay to Camden Bay", report prepared by DF Dickins Associates, Coastal Frontiers Corporation, Aerometric, and The Geophysical Institute, University of Alaska for US Department of Interior, Minerals Management Service, Alaska OCS Region under Contract M06PC00034.

Kovacs, A., 1996, "Sea Ice: Part I. Bulk Salinity Versus Ice Floe Thickness", CRREL Report 96-7, Hanover, New Hampshire, 16 pp.

JAMSTEC, 2020, Institute of Arctic Climate and Environment Research (IACE), http://www.jamstec.go.jp/iace/e/.

Kovacs, A., A. Gow, and W. Dehn, 1976, "Islands of Grounded Sea Ice", CRREL Report 76-4, Hanover, New Hampshire.

Krishfield, R., J. Toole, A. Proshutinsky, and M.-L. Timmermans, 2008, "Automated Ice-Tethered Profilers for Seawater Observations under Pack Ice in All Seasons", *Journal of Atmospheric and Oceanic Technology*, Vol. 25, November 2008, pp. 2091-2105.

"THIS INFORMATION IS DISTRIBUTED SOLELY FOR THE PURPOSE OF PRE-DISSEMINATION PEER REVIEW UNDER APPLICABLE INFORMATION QUALITY GUIDELINES. IT HAS NOT BEEN FORMALLY DISSEMINATED BY BSEE. IT DOES NOT REPRESENT AND SHOULD NOT BE CONSTRUED TO REPRESENT ANY BSEE DETERMINATION OR POLICY."

Leidersdorf, C.B., G.E. Hearon, K.D. Vaudrey, and G. Swank, 2007, "Strudel Scour Formation off Arctic River Deltas", *Proc., 30th International Conference on Coastal Engineering*, Vol. 5, ASCE, World Scientific, Hackensack, New Jersey, p. 5312-5324.

MacDonald, Dettwiler and Associates, Ltd., 2020, https://mdacorporation.com/docs/default-source/brochures/isg/surveillance-and-intelligence/space-missions/radar/radarsat-2-information-products.pdf?sfvrsn=6.

Mahoney, A., H. Eicken, A. Gaylord, and L. Shapiro, 2007, "Alaska Landfast Sea Ice: Links with Bathymetry and Atmospheric Circulation", *Journal of Geophysical Research*, Vol. 112, C02001.

Mahoney, A., H. Eicken, L. Shapiro, R. Gens, T. Heinrichs, F. Meyer, and A. Graves, 2012, "Mapping and Characterization of Recurring Spring Leads and Landfast Ice in the Beaufort and Chukchi Seas", Final Report, OCS Study BOEM 2012-067, University of Alaska Fairbanks, Fairbanks, Alaska, 154 pp.

MDA Geospatial Services, Inc., 2020, "RADARSAT-2 Single User License", LI-11525-34 V1.11, Richmond, B.C., Canada, 3 pp.

NASA, 2020a, Worldview Snapshots, https://wvs.earthdata.nasa.gov.

NASA, 2020b, Earth Observatory, https://earthobservatory.nasa.gov/images/146471/sea-ice-below-normal-despite-a-seasonal-bump.

National Ice Center, 2020, https://www.natice.noaa.gov/Main_Products.htm.

National Ocean Service, 2020, http://tidesandcurrents.noaa.gov.

National Snow and Ice Data Center, 2020, "Monthly Archives: April 2020", http://nsidc.org/arcticseaicenews/2020/04/

National Snow and Ice Data Center, 2019, "Falling up", Arctic Sea Ice News and Analysis, October 3, 2019, http://nsidc.org/arcticseaicenews/2019/10/falling-up/.

National Weather Service, 2020, Alaska Region Headquarters, https://www.weather.gov/afc/ice.

NOAA, 2020, NOAA's Local Climatological Data, https://www.ncdc.noaa.gov/cdo-web/datatools/lcd.

Perovich, D., S. Gerland, S. Hendricks, W. Meier, M. Nicolaus, J. Richter-Menge, and M. Tschudi, 2013, "Arctic Report Card, Update for 2013", Sea Ice, NOAA, http://www.arctic.noaa.gov/reportcard/sea_ice.html.

"THIS INFORMATION IS DISTRIBUTED SOLELY FOR THE PURPOSE OF PRE-DISSEMINATION PEER REVIEW UNDER APPLICABLE INFORMATION QUALITY GUIDELINES. IT HAS NOT BEEN FORMALLY DISSEMINATED BY BSEE. IT DOES NOT REPRESENT AND SHOULD NOT BE CONSTRUED TO REPRESENT ANY BSEE DETERMINATION OR POLICY."

Polar Science Center, 2020, "International Arctic Buoy Programme", Applied Physics Laboratory, University of Washington, http://iabp.apl.washington.edu.

Regional and Mesoscale Meteorology Branch, 2020, National Oceanic and Atmospheric Administration, rammb.cira.colostate.edu.

Reimnitz, E., C. Roderick, and S. Wolf, 1974, "Strudel Scour: A Unique Arctic Marine Geologic Phenomenon", *Journal of Sedimentary Petrology*, vol. 44, no. 2, p. 409-420.

Rigor, I. G., 2020 (compiled by Polar Science Center), *IABP Drifting Buoy Pressure, Temperature, Position, and Interpolated Ice Velocity, Version 1*. Boulder, Colorado, doi: http://dx.doi.org/10.7265/N53X84K7.

Rodrigues, J., 2009, "The Increase in the Length of the Ice-Free Season in the Arctic", *Cold Regions Science and Technology*, Vol. 59, pp. 78-101.

Serreze, M.C., J.E. Walsh, F.S. Chapman III, T. Osterkamp, M. Dyurgerov, V. Romanovsky, W.C. Oechel, J. Morison, T. Zhang, and R.G. Barry, 2000, "Observational Evidence of Recent Change in the Northern High-Latitude Environment", *Climate Change*, Vol. 46, pp.159-207.

Stringer, W. and S. Barrett, 1975, "Ice Motion in the Vicinity of a Grounded Floeberg", *Proceedings POAC-75*, Fairbanks, Alaska.

Toimil, L. and A. Grantz, 1976, "Origin of a Bergfield in the Northeastern Chukchi Sea and its Influence on the Sedimentary Environment", *AIDJEX Bulletin 34*, December, 1976.

Toole, J.M., R. A. Krishfeld, M.-L. Timmermans, and A. Proshutinsky, 2011, "The Ice-Tethered Profiler: Argo of the Arctic", *Oceanography*, Vol. 23, No. 3, pp. 126-135, http://dx.doi.org/10.5670/oceanog.2011.64.

Vaudrey, K.D., 1982, "1981 Breakup Study of the Barrier Island Chain and Harrison Bay", AOGA Project No. 148, Vaudrey & Associates, Inc., Missouri City, Texas, 28 pp. + appen.

Vaudrey, K.D., 1983, "1982 Breakup Study of the Barrier Island Chain and Harrison-Smith Bays", AOGA Project No. 191, Vaudrey & Associates, Inc., San Luis Obispo, California, 35 pp. + appen.

Vaudrey, K.D., 1984a, "1983 Breakup Study of the Alaskan Beaufort and Upper Chukchi Seas", AOGA Project No. 224, Vaudrey & Associates, Inc., San Luis Obispo, California, 34 pp. + appen.

"THIS INFORMATION IS DISTRIBUTED SOLELY FOR THE PURPOSE OF PRE-DISSEMINATION PEER REVIEW UNDER APPLICABLE INFORMATION QUALITY GUIDELINES. IT HAS NOT BEEN FORMALLY DISSEMINATED BY BSEE. IT DOES NOT REPRESENT AND SHOULD NOT BE CONSTRUED TO REPRESENT ANY BSEE DETERMINATION OR POLICY."

Vaudrey, K.D., 1984b, "1983 Breakup Study of the Western Beaufort Sea and Upper Chukchi Sea", AOGA Project No. 225, Vaudrey & Associates, Inc., San Luis Obispo, California, 32 pp. + appen.

Vaudrey, K.D., 1985a, "Historical Summary of the 1980-82 Freeze-Up Seasons and 1981-83 Breakup seasons, AOGA Project No. 275, Vaudrey & Associates, Inc., San Luis Obispo, California, 79 pp. + appen. (2 volumes).

Vaudrey, K.D., 1985b, "1984 Breakup Study of the Alaskan Beaufort and Upper Chukchi Seas", AOGA Project No. 274, Vaudrey & Associates, Inc., San Luis Obispo, California, 49 pp. + appen.

Vaudrey, K.D., 1986, "1985 Breakup Study of the Beaufort and Upper Chukchi Seas", AOGA Project No. 319, Vaudrey & Associates, Inc., San Luis Obispo, California, 48 pp. + appen.

Vaudrey, K., 1988, "1987 Summer and Freeze-Up Ice Conditions in the Beaufort and Chukchi Seas Developed from Satellite Imagery", AOGA Project No. 360, Vaudrey & Associates, Inc., San Luis Obispo, California.

Vaudrey, K.D., 1989, "1988 Summer and Freeze-Up Ice Conditions in the Beaufort and Chukchi Seas Developed from Satellite Imagery", AOGA Project No. 370, Vaudrey & Associates, Inc., San Luis Obispo, California.

Vaudrey, K.D., 1990, "1989 Summer and Freeze-Up Ice Conditions in the Beaufort and Chukchi Seas Developed from Satellite Imagery", AOGA Project No. 372, Vaudrey & Associates, Inc., San Luis Obispo, California.

Vaudrey, K.D., 1991, "1990 Summer and Freeze-Up Ice Conditions in the Beaufort and Chukchi Seas Developed from Satellite Imagery", AOGA Project No. 381, Vaudrey & Associates, Inc., San Luis Obispo, California.

Vaudrey, K.D., 1992, "1991 Summer and Freeze-Up Ice Conditions in the Beaufort and Chukchi Seas Developed from Satellite Imagery", AOGA Project No. 386, Vaudrey & Associates, Inc., San Luis Obispo, California.

Vaudrey, K. and B. Thomas, 1981, "Katie's Floeberg – 1980", report prepared for the Kopanoar Partners by Gulf Research and Development Company, Houston, Texas.

Visser, N., 2020, personal communication, ConocoPhillips Alaska, Inc., Kuparuk, Alaska.

World Meteorological Organization, 2014, "Sea Ice Nomenclature", WMO Pub. No. 259 by Joint Technical Commission for Oceanography and Marine Meteorology (JCOMM), 3 vols.